FUNCTIONAL ASPECTS OF MESOSCOPIC BRAIN OSCILLATIONS: INSIGHTS FROM *IN VIVO* AND *IN VITRO* STUDIES

EDITED BY: Gürsel Caliskan, Sanja Mikulovic and Gabrielle Girardeau
PUBLISHED IN: Frontiers in Neural Circuits and
Frontiers in Behavioral Neuroscience

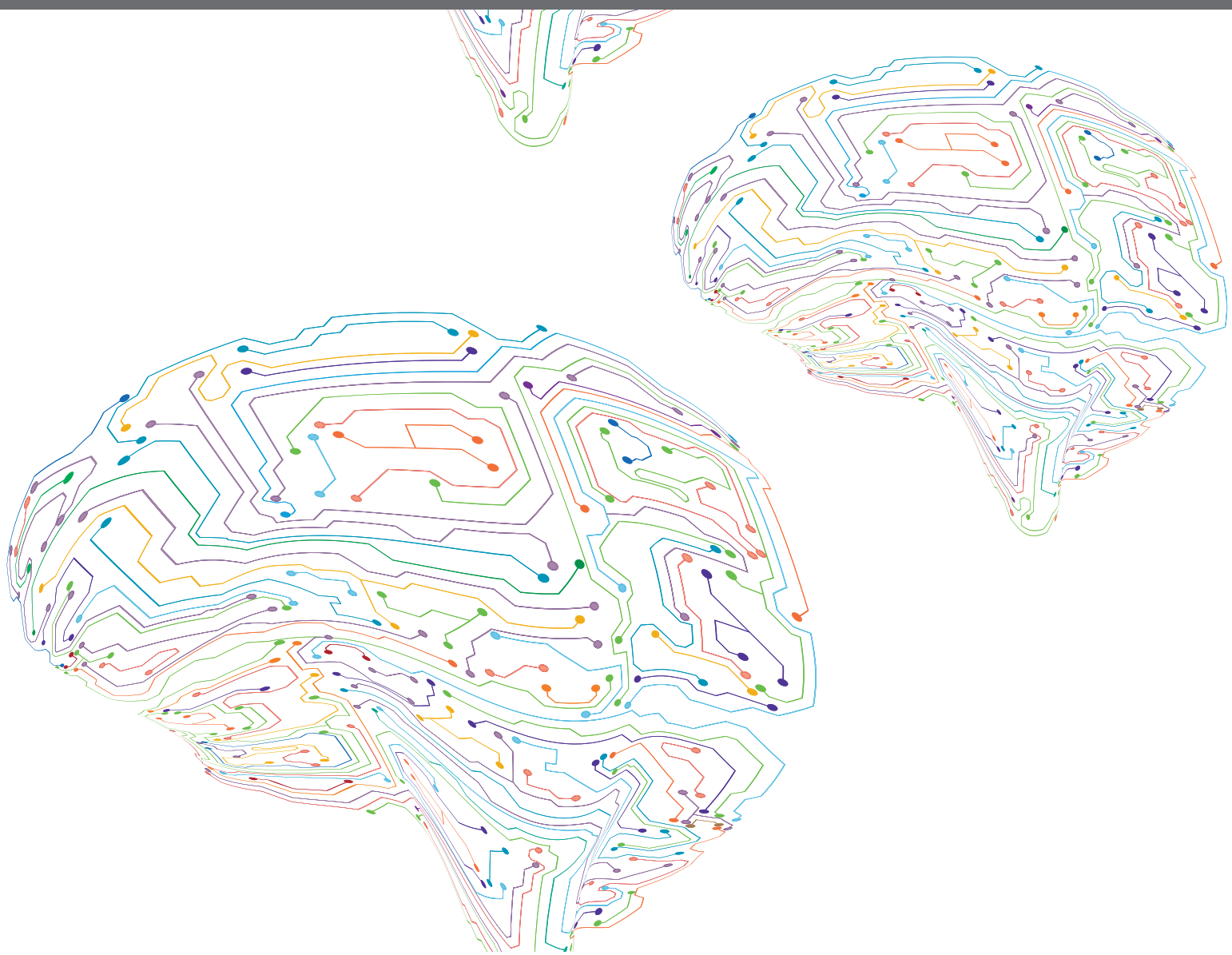

frontiers Research Topics

ISSN 1664-8714
ISBN 978-2-88976-668-0
DOI 10.3389/978-2-88976-668-0

About Frontiers

Frontiers is more than just an open-access publisher of scholarly articles: it is a pioneering approach to the world of academia, radically improving the way scholarly research is managed. The grand vision of Frontiers is a world where all people have an equal opportunity to seek, share and generate knowledge. Frontiers provides immediate and permanent online open access to all its publications, but this alone is not enough to realize our grand goals.

Frontiers Journal Series

The Frontiers Journal Series is a multi-tier and interdisciplinary set of open-access, online journals, promising a paradigm shift from the current review, selection and dissemination processes in academic publishing. All Frontiers journals are driven by researchers for researchers; therefore, they constitute a service to the scholarly community. At the same time, the Frontiers Journal Series operates on a revolutionary invention, the tiered publishing system, initially addressing specific communities of scholars, and gradually climbing up to broader public understanding, thus serving the interests of the lay society, too.

Dedication to Quality

Each Frontiers article is a landmark of the highest quality, thanks to genuinely collaborative interactions between authors and review editors, who include some of the world's best academicians. Research must be certified by peers before entering a stream of knowledge that may eventually reach the public - and shape society; therefore, Frontiers only applies the most rigorous and unbiased reviews.
Frontiers revolutionizes research publishing by freely delivering the most outstanding research, evaluated with no bias from both the academic and social point of view. By applying the most advanced information technologies, Frontiers is catapulting scholarly publishing into a new generation.

What are Frontiers Research Topics?

Frontiers Research Topics are very popular trademarks of the Frontiers Journals Series: they are collections of at least ten articles, all centered on a particular subject. With their unique mix of varied contributions from Original Research to Review Articles, Frontiers Research Topics unify the most influential researchers, the latest key findings and historical advances in a hot research area! Find out more on how to host your own Frontiers Research Topic or contribute to one as an author by contacting the Frontiers Editorial Office: frontiersin.org/about/contact

FUNCTIONAL ASPECTS OF MESOSCOPIC BRAIN OSCILLATIONS: INSIGHTS FROM *IN VIVO* AND *IN VITRO* STUDIES

Topic Editors:
Gürsel Caliskan, Otto von Guericke University Magdeburg, Germany
Sanja Mikulovic, Leibniz Institute for Neurobiology (LG), Germany
Gabrielle Girardeau, INSERM U839 Institut du Fer à Moulin (IFM), France

Citation: Caliskan, G., Mikulovic, S., Girardeau, G., eds. (2022). Functional Aspects of Mesoscopic Brain Oscillations: Insights From *in Vivo* and *in Vitro* Studies. Lausanne: Frontiers Media SA. doi: 10.3389/978-2-88976-668-0

Table of Contents

frontiers | Frontiers in Neural Circuits

EDITORIAL
published: 04 July 2022
doi: 10.3389/fncir.2022.960157

Editorial: Functional Aspects of Mesoscopic Brain Oscillations: Insights From *in vivo* and *in vitro* Studies

Gürsel Çalışkan [1,2], Sanja Mikulovic [3]* and Gabrielle Girardeau [4]**

[1] Department of Genetics and Molecular Neurobiology, Institute of Biology, Otto-von-Guericke-University Magdeburg, Magdeburg, Germany, [2] Center for Behavioral Brain Sciences, Magdeburg, Germany, [3] Research Group Cognition and Emotion, Leibniz Institute for Neurobiology, Magdeburg, Germany, [4] Research Group Sleep and Emotional Memory, Institut du Fer a Moulin, UMR-S 1270 INSERM and Sorbonne Université, Paris, France

Keywords: neural oscillations, cognition, innate and emotional behavior, memory, animal models

Editorial on the Research Topic

Functional Aspects of Mesoscopic Brain Oscillations: Insights From *in vivo* and *in vitro* Studies

Oscillatory activity is considered a major way for the brain to convey information within and across structures. These patterns range from slow (<1 Hz) to fast oscillations (>200 Hz) in a brain-state- and circuit-dependent manner (Buzsáki and Draguhn, 2004). From a functional perspective, a major challenge is to elucidate how a given frequency in a given brain circuit is associated with a specific behavior and try to understand how the identified oscillations sustain the cognitive processes associated with this state or behavior (Lee and Dan, 2012). In recent years, there has been a major leap in deciphering the mechanisms of distinct mesoscopic brain rhythms and their utilization for treatment of diseased brain states associated with aberrant emotional and cognitive behavior. In this Research Topic, we present a collection of 10 articles (3 Original Research, 1 Methods, 4 Reviews, 1 Mini Review, and 1 Perspective) that highlight recent advances on mechanisms underlying mesoscopic brain rhythms and their function in health and disease.

In their perspective article, Nokia and Pentonnen discuss the foundational and more recent work that led to the classical trio of brain oscillations for episodic memory consolidation: ripples, spindles and slow oscillation (SO). They underline the importance of two additional patterns that have recently emerged as strong modulators memory consolidation mediated by ripple-spindle-SO coordination: the historically understudied hippocampal dentate spike and breathing. The latter highlights the recent and growing body of evidence linking bodily parameters such as breathing and heart rate to cognitive processes.

In this line, Folschweiller and Sauer elaborate on the generation mechanisms and function of respiration-driven brain activity with a particular attention to its role in emotional cognition (e.g., fear, reward, despair) across species. They further discuss how breathing can impact cognition *via* modulation of specific oscillatory patterns [e.g., gamma (γ) oscillations and ripples] and underlying neuronal ensembles.

Aguilera et al. mini review addresses hippocampal theta (θ)-γ dynamics and suggests that the current model, focusing on discrete subtypes of γ activity, does not capture its full complexity. The authors refer to the recent studies showing that many θ cycles contain multiple γ bouts of various frequencies and propose application of novel methods, such as machine learning approaches, in order to extract the meaningful behavior-relevant information, without relying on pre-defined γ subtypes.

OPEN ACCESS

Edited and reviewed by:
Edward S. Ruthazer, McGill University, Canada

Correspondence:
Gürsel Çalışkan
guersel.caliskan@ovgu.de; caliskan.gursel@gmail.com
Sanja Mikulovic
sanja.mikulovic@lin-magdeburg.de
Gabrielle Girardeau
gabrielle.girardeau@inserm.fr

Received: *02 June 2022*
Accepted: *20 June 2022*
Published: *04 July 2022*

Citation:
Çalışkan G, Mikulovic S and Girardeau G (2022) Editorial: Functional Aspects of Mesoscopic Brain Oscillations: Insights From in vivo and in vitro Studies. Front. Neural Circuits 16:960157. doi: 10.3389/fncir.2022.960157

In their review article, Ibarra-Lecue et al. take a very broad perspective on brain rhythms and retrace the history of the study of brain oscillations up to the most recent findings. They illustrate a gradual shift from correlational studies to causal ones with the advent of new technologies such as optogenetics, while highlighting both the promises and limitations of these approaches to circuit and function dissection.

Földi et al. focuses on the neural mechanisms giving rise to "oscillopathies," with a particular focus on epileptic seizures. They discuss the importance of designing reliable seizure-predicting algorithms and devices capable of predicting and preventing seizures from happening. In particular, they put forward the idea of applying closed-loop techniques for "oscillotherapeutics" and refer, among others, to their own recent work in which closed-loop stimulation of the medial septum was used to successfully terminate epileptic seizures in rats.

The article by Speers and Bilkey reviews the vast literature on the abnormalities observed in θ, γ, and ripple oscillations in animal models of schizophrenia and discusses these findings with respect to studies in human subjects. They particularly focus on the disruption of hippocampal θ-phase precession, an important phenomenon for the sequential activation and reactivation of place cells, as a potential mechanism underlying cognitive deficits in schizophrenia.

Of note, specific oscillatory frequency ranges are used for the automatic classification of brain states or behaviors, together with the movement information (muscular activity and/or velocity). However, some behaviors are associated with oscillatory bands that overlap with each other. Notably, freezing and resting epochs including REM (Rapid Eye Movement) sleep, Non-REM sleep and quiet wakefulness are all characterized by immobility and overlapping oscillations. In their method paper, Pompili and Todorova establish that classical methods fail to discriminate between freezing and rest, and propose a novel tool using cortical spindles, that can be recorded with a simple EEG surface electrode, to reliable disambiguate freezing from non-REM sleep. This can be especially useful for studies using fear conditioning and extinction to study memory formation.

Neuromodulation is classically associated with long time scales. In their original article, Jelitai et al. however describe an inhibitory subpopulation in the serotoninergic median raphe region whose activity is coupled to hippocampal theta oscillations and ripples. These neurons synchronize ascending serotonergic and glutamatergic modulation with hippocampal activity on a subsecond timescale. The authors suggest that short and long timescale modulation are controlled by different mechanisms and open space for future studies investigating modulation with high temporospatial resolution.

Two original research articles use *in vitro* oscillation models in rodent hippocampal slice preparations. Such *in vitro* models provide robust tools for interrogating underlying cellular mechanisms and pharmacology of network oscillations. Landeck et al. demonstrate that enriched environments reduce inhibition during spontaneous hippocampal sharp wave ripples (SWR), leading to enhanced but disorganized neuronal activity during SWR. These observations suggest that *in vitro* oscillations are sensitive to behavioral manipulations and can be used as proxies for metaplasticity in the hippocampal sub-circuits. On the other hand, Klemz et al. perform pharmacological experiments on cholinergic-induced gamma oscillations using blockers or activators of several channels important for modulation of intrinsic cellular excitability. They show specific changes in gamma oscillation power upon modulation of voltage- and calcium-activated ion channels, highlighting their potential use against cognitive impairment.

With this Research Topic, we have aimed to catalyze the collective effort on identification of functional aspects of brain oscillatory activities and promote the use of these rhythms as biomarkers. We believe that the development of "oscillotherapeutics" will help correcting circuit dysfunctions underlying with disturbed emotional and cognitive functions in various psychiatric diseases.

AUTHOR CONTRIBUTIONS

GÇ, SM, and GG prepared and discussed a list of guests-authors, invited them, revised their manuscripts, and handled their revisions. The Editorial was written by all authors. All authors contributed to the article and approved the submitted version.

REFERENCES

Buzsáki, G., and Draguhn, A. (2004). Neuronal oscillations in cortical networks. *Science* 304, 1926–1929. doi: 10.1126/science.1099745

Lee, S.-H., and Dan, Y. (2012). Neuromodulation of brain states. *Neuron* 76, 209–222. doi: 10.1016/j.neuron.2012.09.012

Conflict of Interest: The authors declare that the research was conducted in the absence of any commercial or financial relationships that could be construed as a potential conflict of interest.

frontiers in Neural Circuits

REVIEW
published: 05 October 2021
doi: 10.3389/fncir.2021.741767

Disorganization of Oscillatory Activity in Animal Models of Schizophrenia

*Lucinda J. Speers and David K. Bilkey**

Department of Psychology, Otago University, Dunedin, New Zealand

Schizophrenia is a chronic, debilitating disorder with diverse symptomatology, including disorganized cognition and behavior. Despite considerable research effort, we have only a limited understanding of the underlying brain dysfunction. In this article, we review the potential role of oscillatory circuits in the disorder with a particular focus on the hippocampus, a region that encodes sequential information across time and space, as well as the frontal cortex. Several mechanistic explanations of schizophrenia propose that a loss of oscillatory synchrony between and within these brain regions may underlie some of the symptoms of the disorder. We describe how these oscillations are affected in several animal models of schizophrenia, including models of genetic risk, maternal immune activation (MIA) models, and models of NMDA receptor hypofunction. We then critically discuss the evidence for disorganized oscillatory activity in these models, with a focus on gamma, sharp wave ripple, and theta activity, including the role of cross-frequency coupling as a synchronizing mechanism. Finally, we focus on phase precession, which is an oscillatory phenomenon whereby individual hippocampal place cells systematically advance their firing phase against the background theta oscillation. Phase precession is important because it allows sequential experience to be compressed into a single 120 ms theta cycle (known as a 'theta sequence'). This time window is appropriate for the induction of synaptic plasticity. We describe how disruption of phase precession could disorganize sequential processing, and thereby disrupt the ordered storage of information. A similar dysfunction in schizophrenia may contribute to cognitive symptoms, including deficits in episodic memory, working memory, and future planning.

Keywords: oscillations, schizophrenia, hippocampus, prefrontal cortex, synchrony, theta, gamma, phase precession

OPEN ACCESS

Edited by:
Gürsel Caliskan,
Otto von Guericke University
Magdeburg, Germany

Reviewed by:
Guillermo Gonzalez-Burgos,
University of Pittsburgh,
United States
Zoltan Gerevich,
Charité—Universitätsmedizin Berlin,
Germany

***Correspondence:**
David K. Bilkey
david.bilkey@otago.ac.nz

Received: *15 July 2021*
Accepted: *16 September 2021*
Published: *05 October 2021*

Citation:
Speers LJ and Bilkey DK (2021) Disorganization of Oscillatory Activity in Animal Models of Schizophrenia. Front. Neural Circuits 15:741767. doi: 10.3389/fncir.2021.741767

INTRODUCTION

Schizophrenia is a complex neurological disorder that affects approximately one percent of the population worldwide (Jablensky, 2000; McGrath et al., 2008), and is a leading contributor of the global disease burden (Lopez et al., 2006). It is characterized by a heterogenous constellation of aetiological risk factors, pathophysiological mechanisms, and symptoms. These include positive symptoms, such as hallucinations and delusions, negative symptoms, such as flattened affect and avolition, and broad cognitive disturbances including episodic and working memory, attention, and executive function (Insel, 2010; Barch and Ceaser, 2012; Fusar-Poli et al., 2012; Cannon, 2015). Although the positive and negative symptoms of the disorder have historically received more attention, a growing number of studies investigating cognitive dysfunction in schizophrenia have provided evidence that these impairments are not only a critical factor in

predicting poor functional outcomes (Green, 1996), but that they also precede the onset of positive symptoms by almost a decade (Kahn and Keefe, 2013). These findings have prompted some to argue that schizophrenia should be recognized as primarily a cognitive disorder and that the development of new diagnostic tools and treatments has been hampered by the continued focus on psychotic symptoms at the expense of the underlying cognitive disturbances that generally precede them (Elvevag and Goldberg, 2000; Lesh et al., 2011; Kahn and Keefe, 2013).

One feature of schizophrenia is an inability to organize the elements of cognition into a cohesive whole (Javitt, 2009; Fornito and Bullmore, 2015; Friston et al., 2016). In line with this proposal, a growing number of studies have begun to focus on the disorganization of cognitive processes (König et al., 2001; Olypher et al., 2006; Minor and Lysaker, 2014). In particular, complex cognitive operations such as episodic memory and executive function require the dynamic integration of diverse information streams, including both top-down information about beliefs and expectations based on prior experience, as well as lower-level sensory, emotional, and motor information (Engel et al., 2001; Jardri and Denève, 2013). How distributed networks manage the appropriate integration, segregation and sequential ordering of such information remains an open question, although it has become increasingly clear that phase coding mechanisms, in which the temporal spiking of single cells is organized relative to synchronous oscillatory activity occurring at the network level, is likely to play a critical role (Gray et al., 1989; Lisman and Buzsáki, 2008; Buzsáki, 2010).

There is now a large body of literature demonstrating that disturbed oscillatory activity in schizophrenia is often correlated with broad cognitive impairments (Spencer et al., 2004; Schmiedt et al., 2005; Cho et al., 2006; Light et al., 2006; Basar-Eroglu et al., 2007; Haenschel et al., 2009; Uhlhaas and Singer, 2010; Kirihara et al., 2012; Senkowski and Gallinat, 2015; Barr et al., 2017; Adams et al., 2020). Post-mortem studies from individuals with schizophrenia have also provided vital information about basic-level disturbances that occur in schizophrenia, including specific disruptions at the site of N-methyl-D-aspartate (NMDA) receptors (Catts et al., 2016), as well as several GABA disturbances, particularly in regards to glutamic acid decarboxylase 67 (GAD67) and parvalbumin (PV+) expression (Akbarian and Huang, 2006; Fung et al., 2010; Gonzalez-Burgos et al., 2015; Kaar et al., 2019). These findings have led to promising hypotheses that schizophrenia may result from an imbalance of excitation/inhibition in key regions associated with schizophrenia pathology, including the prefrontal cortex (PFC) and the hippocampus (Lewis et al., 2005; Uhlhaas, 2013; Starc et al., 2017). However, direct evidence of how the structural, cellular, and molecular disturbances that are frequently observed in schizophrenia are causally linked to cognitive dysfunction has been more difficult to obtain (Wright et al., 2000; Heckers and Konradi, 2002; Harrison, 2004; Moghaddam and Javitt, 2012; Haijma et al., 2013; Van Den Heuvel and Fornito, 2014; Forsyth and Lewis, 2017). This is known as the problem of the "missing middle," in which the mesoscopic network processes that bridge the gap between microscopic disturbances and macroscopic behavioral outcomes have remained relatively opaque (Laughlin et al., 2000; Kao et al., 2017).

Bridging this gap is difficult with human subjects, as current non-invasive imaging tools do not provide adequate resolution to determine how basic level disturbances occurring at the cellular level manifest into disorganized network activity and consequent cognitive impairments. The refocusing of research on cognitive disturbances has thus provided an important opening for research involving animal models of schizophrenia, as cognitive disturbances can be more readily measured in animals, unlike the more subjective symptoms of psychosis. Animal models of schizophrenia also provide better access to biological and network mechanisms, as well as providing the opportunity for more targeted manipulations. Such models are, therefore, likely to provide a crucial step in bridging the missing "middle," as well as providing important information about both primary etiological causes and developmental trajectories.

This review will critically outline the current state of studies that have investigated disorganized oscillatory activity in animal models of schizophrenia, with a specific focus on the hippocampus. The first section will provide the rationale for investigating disorganized oscillatory activity in schizophrenia, as well as a brief overview of the findings and limitations of such studies in humans (for a more detailed review of disturbed oscillatory activity in individuals with schizophrenia, readers are referred to the review by Uhlhaas and Singer, 2010). The main body of the review will then focus on evidence accumulating from animal models of the disorder, including models of genetic risk, maternal immune activation (MIA), and models of NMDA receptor (NMDAR) hypofunction. We will present a critical analysis of these findings in relation to gamma and theta frequency oscillations, sharp-wave ripples (SPW-Rs), and theta phase precession, including the functional implications of disorganized oscillatory activity for cognitive processes that have been associated with these phenomena.

EEG AND MEG STUDIES IN INDIVIDUALS WITH SCHIZOPHRENIA

According to the dysconnection hypothesis, the core symptoms of schizophrenia proceed from the functional disintegration of specialized systems within the brain, including both the intrinsic connections within a local cell assembly and long-range connectivity between distinct brain regions (Friston, 1998; Friston et al., 2016). Robust evidence of functional dysconnectivity in schizophrenia has been provided by a range of non-invasive techniques such as functional magnetic resonance imaging (fMRI), magnetoencephalography (MEG), and electroencephalography (König et al., 2001; Liang et al., 2006; Hinkley et al., 2010; Pettersson-Yeo et al., 2011; Fornito et al., 2012; Di Lorenzo et al., 2015). In particular, MEG and EEG imaging techniques have provided valuable information about the amplitude, frequency, and coherence of rhythmic network activity at high temporal resolutions. These techniques have routinely demonstrated abnormal activity in both schizophrenia patients and their first-degree relatives in the theta (∼2–10 Hz),

beta (∼12–30 Hz), and gamma (∼30–90 Hz) frequency bands. These findings suggest that disorganized activity in these bands could be a potential endophenotype of the disorder (Uhlhaas and Singer, 2010; Williams and Boksa, 2010; Moran and Hong, 2011; Kirihara et al., 2012; Berger et al., 2016; Adams et al., 2020). Changes in oscillatory activity may either reflect or underlie a failure of coordinated network synchrony within and across several brain regions, consistent with the proposals that schizophrenia is predominantly a disorder of distributed neural dynamics rather than localized deficits (von der Malsburg et al., 2010; Uhlhaas and Singer, 2015).

Although these previous studies have provided critical evidence that oscillatory activity across several frequency bands is disorganized in schizophrenia, the non-invasive MEG and EEG techniques that are used in these studies are inherently limited in several respects. For example, the spatial resolution of these techniques is relatively low, and despite numerous technological advances that have improved the quality of source localization, the issue of field spread means that precise spatial localization of signal sources must be interpreted cautiously (Schoffelen and Gross, 2009). This issue is particularly important in regards to oscillatory activity that is generated in deeper brain regions, such as the hippocampus, where signals are more prone to distortion. Such issues are not fully resolved using invasive recording techniques, but a comparison of simultaneously obtained invasive and non-invasive EEG recordings in humans has demonstrated that the signal quality of invasive EEG recordings is ∼20–100 times better than non-invasive recordings (Ball et al., 2009).

Recent findings in animal models have also demonstrated that the precise temporal spiking of single cells in relation to background local field potential (LFP) oscillations is likely to be functionally important for both low-level plasticity-related processes and for high-level cognition that depends on sequential processing mechanisms (Buzsáki, 2015; Buzsáki and Tingley, 2018; Drieu and Zugaro, 2019). While these synchronizing phenomena appear to occur in humans (Liu et al., 2019; Qasim et al., 2020) they cannot readily be investigated with non-invasive techniques. Thus, although MEG and EEG studies provide important correlational evidence that disturbed network synchrony is likely associated with poor performance across a range of cognitive domains, direct evidence that these phenomena are causally linked is difficult to obtain with these techniques alone. Similar difficulties are apparent in regards to the cellular and molecular basis of oscillatory disorganization. Although a number of basic-level studies have begun to uncover the biological mechanisms of coordinated oscillatory activity (Buzsáki and Draguhn, 2004; Buzsáki and Wang, 2012; Colgin, 2013; Buzsáki, 2015; Drieu and Zugaro, 2019), it remains unclear how the complex aetiological and developmental processes associated with schizophrenia manifest into disorganized oscillatory activity at critical stages of disease progression. Animal models of schizophrenia provide a unique opportunity to resolve some of these issues, and given that the scaling and hierarchical organization of oscillatory activity is evolutionarily preserved across several species (Buzsáki et al., 2013), animal models may be able to provide important translational data across all levels of micro- meso and macroscopic dysfunction.

ANIMAL MODELS OF SCHIZOPHRENIA

Over the past few decades, several animal models of schizophrenia-risk have been developed, including genetic, developmental, lesion, and drug-induced models (Jones et al., 2011; Rapoport et al., 2012; Brown and Meyer, 2018; Lee and Zhou, 2019). This diversity reflects the heterogenous range of aetiological factors and pathophysiological mechanisms linked to schizophrenia. The specific disruptions associated with each model provide valuable information about the fundamental biological mechanisms of schizophrenia and allow for investigations of both the acute and longitudinal effects of known risk factors in isolation, and with greater control over the confounding effects of environment and medication. However, these advantages come at a cost, providing a simplified account of schizophrenia pathophysiology that is unlikely to capture the full complexity of the disorder. For example, current evidence suggests that schizophrenia does not emerge from a single genetic, biological or environmental cause, but rather through the complex interplay of these factors, including epigenetic mechanisms that converge on shared pathways of molecular dysfunction (Fatemi and Folsom, 2009; Horváth and Mirnics, 2015). One of the challenges of working with animal models is, therefore, to integrate the findings from these diverse models into a broader understanding of schizophrenia pathology.

Several recent reviews have begun to identify some of the common network disturbances observed in pre-clinical models, although most of these reviews have focused predominantly on the gamma frequency band (Uhlhaas and Singer, 2015), and models of NMDAR hypofunction have been more extensively reviewed than models of genetic and environmental risk factors (Jadi et al., 2016; Cadinu et al., 2018; Krajcovic et al., 2019; Bianciardi and Uhlhaas, 2021). The following section will briefly outline three types of animal models that have been used to investigate network disturbances associated with schizophrenia—models of NMDA hypofunction, genetic risk models, and maternal immune activation (MIA) models, with a focus on how the basic cellular disturbances associated with these models could contribute to the disorganized oscillatory activity.

NMDAR Hypofunction Models

Considerable evidence points to abnormal glutamate signaling in schizophrenia, particularly at the site of the NMDA subtype of glutamate receptors (Moghaddam and Javitt, 2012; Balu, 2016; Nakazawa and Sapkota, 2020). A transient induction of schizophrenia-like psychosis can also occur in humans following administration of NMDAR antagonists, leading to proposals that changes in glutamate signaling are fundamental to the disorder (Krystal et al., 1994; Umbricht et al., 2000; Moghaddam and Javitt, 2012). Several different animal models of NMDAR dysfunction have thus been developed to determine how NMDAR hypofunction contributes to schizophrenia pathophysiology, including those relying on the acute administration of the antagonist ketamine or MK-801, as

well as various NMDAR knockout models that allow researchers to examine the more chronic effects of disturbed NMDAR transmission during early development (Olney et al., 1999; Lee and Zhou, 2019). Since NMDA receptors occur on both principal cells and inhibitory interneurons, a disturbance in these systems has the potential to disrupt the excitatory/inhibitory balance within a network, as well as to modify the oscillatory function that depends on feedback inhibition in order to produce cycles of activity. Theoretically, this could have profound implications for the development and temporal coordination of complex neural circuits, and experimental evidence has confirmed that fast-spiking interneurons, including PV+ cells, are critical for organized oscillatory activity in both the gamma and theta frequency ranges (Cobb et al., 1995; Sohal et al., 2009; Wulff et al., 2009; Stark et al., 2013; Amilhon et al., 2015).

Both acute and chronic NMDA hypofunction have been shown to affect oscillatory activity in NMDAR antagonist models across a range of frequency bands, and these studies are discussed in greater detail in the relevant sections below. Broadly speaking, these studies have provided robust evidence that disrupted NMDAR signaling leads to disturbed oscillatory activity in a number of brain regions (Ma and Leung, 2000; Cunningham et al., 2006; Pinault, 2008; Dzirasa et al., 2009; Hakami et al., 2009; Belforte et al., 2010; Carlén et al., 2012; Kittelberger et al., 2012; Kocsis, 2012; Caixeta et al., 2013; Kalweit et al., 2017; Aguilar et al., 2021). There is also evidence that disturbed oscillatory activity in NMDAR hypofunction models is mediated by abnormal synaptic inhibition, particularly by PV+ interneurons (Carlén et al., 2012; Kittelberger et al., 2012). It remains unclear however whether NMDA hypofunction and other GABAergic disturbances arise independently (Coyle, 2004; Gonzalez-Burgos and Lewis, 2012), although current evidence suggests that the timing of NMDAR manipulations is critical for the development of inhibitory circuits (Wang and Gao, 2009; Belforte et al., 2010). In line with this proposal, one study has demonstrated that the selective deletion of NMDA receptors from predominantly PV+ interneurons during early development triggers several molecular, physiological, and behavioral phenotypes reminiscent of schizophrenia, including spatial working memory impairments, social withdrawal, and reduced pre-pulse inhibition, as well as reduced network synchrony in the somatosensory cortex. The same manipulation had no effect however when performed on post-adolescent mice (Belforte et al., 2010).

Genetic Risk Models

Although models of NMDAR hypofunction provide important information about how NMDAR signaling contributes to abnormal oscillatory activity, such models may be lacking in ecological validity. Models based on either genetic or environmental risk factors can address this issue to some extent, although the specific biological mechanisms that contribute to abnormal oscillatory activity are more difficult to identify.

Numerous studies indicate that schizophrenia is likely to have a substantial hereditary component (Cardno et al., 1999; Sullivan et al., 2003; Lichtenstein et al., 2009; Harrison, 2015). A number of genomic regions that may confer an increased risk of developing schizophrenia have been identified, although most genetic variants associated with the disorder involve non-coding regions of DNA, indicating that they are predominantly involved in regulating gene expression, such as the timing, abundance, and location of transcription events, rather than encoding for protein sequences themselves (Harrison, 2015; Kahn et al., 2015). Consistent with proposals that schizophrenia is predominantly a neurodevelopmental disorder (Bullmore et al., 1997; Fatemi and Folsom, 2009), several risk variants are also preferentially expressed during fetal development, suggesting that the normal developmental processes of neuronal proliferation, differentiation, and migration may be disrupted during this critical period (Walsh et al., 2008; Birnbaum and Weinberger, 2017).

In particular, genes associated with neuregulin signaling have often been implicated in schizophrenia, and neuregulin is known to play an important role in the development of inhibitory circuits, synaptic plasticity, and axon myelination during critical stages of development (Stefansson et al., 2002; Brinkmann et al., 2008; Mei and Xiong, 2008; Neddens et al., 2011; Ting et al., 2011). Other genes that are involved in early neurodevelopment and maturational processes, such as the Disrupted-in-Schizophrenia 1 (DISC1) gene, appear to exert delayed behavioral and neurochemical effects following pre- and perinatal insults in mice, with measurable effects only appearing after puberty, clearly mirroring the developmental trajectory of schizophrenia in humans (Niwa et al., 2010). Both DISC1 and neuregulin have also been associated with disturbed parvalbumin (PV+) expression in the hippocampus and the PFC (Hikida et al., 2007; Shen et al., 2008; Fazzari et al., 2010), as well as diminished complexity of dendritic spines in hippocampal regions, attenuated synaptic plasticity, and several cognitive phenotypes associated with the disorder (Li et al., 2007; Kvajo et al., 2008; Shamir et al., 2012). Similar neurodevelopmental disturbances have been observed in mouse models of 22q11 microdeletion (Paylor et al., 2001; Mukai et al., 2008, 2015). Taken together, these studies suggest that a range of genetic risk factors disrupt the development of neural circuits, with the most prominent effects emerging after adolescence.

Maternal Immune Activation (MIA) Models

A number of epidemiological studies indicate that maternal infection during the first and second trimesters is associated with an increased risk of developing schizophrenia in affected offspring (Mednick et al., 1994; Susser et al., 1996; Brown and Derkits, 2010; Selemon and Zecevic, 2015). Subsequent studies have revealed that exposure to proinflammatory cytokines at critical stages of neurodevelopment affects neuronal proliferation and synaptogenesis, which could potentially have profound consequences for the development of neural circuits (Gilmore and Jarskog, 1997; Meyer et al., 2009a,b; Watanabe et al., 2010; Selemon and Zecevic, 2015).

MIA has been extensively modeled in rodents using a variety of induction protocols, including exposure to polyriboinosinic: polyribocytidilic acid (PolyI:C), a synthetic analog of double-stranded RNA that regulates acute responses to viral pathogens (Meyer et al., 2009a,b; Boksa, 2010; Wolff and Bilkey, 2010;

Brown and Meyer, 2018; Kentner et al., 2019). The PolyI:C model has been shown to trigger a range of biophysical and molecular abnormalities consistent with schizophrenia, including decreases in hippocampal volume (Zuckerman et al., 2003; Piontkewitz et al., 2011; Crum et al., 2017), altered GAD and PV+ expression (Piontkewitz et al., 2012; Dickerson et al., 2014; Canetta et al., 2016; Cassella et al., 2016; Steullet et al., 2017), reduced inhibition (Zhang and van Praag, 2015), an increased glutamate/GABA ratio in the hippocampus (Patrich et al., 2016), abnormal synaptic plasticity (Savanthrapadian et al., 2013), and dopaminergic dysfunction (Zuckerman et al., 2003; Ozawa et al., 2006; Luchicchi et al., 2016).

A range of behavioral abnormalities that match the symptomatic profile of schizophrenia have also been observed, including several cognitive deficits that have also been associated with disorganized oscillatory activity (Fatemi and Folsom, 2009; Meyer et al., 2009a,b; Brown and Derkits, 2010), These include reduced PPI (Ozawa et al., 2006; Wolff and Bilkey, 2010; Howland et al., 2012; Zhang and van Praag, 2015; Luchicchi et al., 2016), reduced behavioral flexibility (Zuckerman and Weiner, 2005; Bitanihirwe et al., 2010; Savanthrapadian et al., 2013; Ballendine et al., 2015; Kleinmans and Bilkey, 2018), temporal processing disturbances (Deane et al., 2017), and spatial memory impairments (Meyer et al., 2008; Wolff et al., 2011; Murray et al., 2017).

THE IMPORTANCE OF HIPPOCAMPAL AND PREFRONTAL OSCILLATIONS FOR COGNITIVE PROCESSES, AND IMPLICATIONS FOR SCHIZOPHRENIA

Disorganized oscillatory activity has been documented throughout several brain regions in individuals with schizophrenia (Uhlhaas and Singer, 2010), and this current review is not exhaustive. Instead, we have chosen to focus on disorganized activity that occurs in hippocampal and frontal regions in the gamma, theta, and sharp-wave ripple bands. We also discuss how this may influence hippocampal-prefrontal functional connectivity.

Considerable evidence suggests that the temporal coordination of hippocampal activity is critically important for a range of cognitive processes, including episodic, relational, spatial, and working forms of memory, as well as flexible decision making (Buzsáki and Moser, 2013; Colgin, 2016; Drieu and Zugaro, 2019). The laminar organization of pyramidal cells in the hippocampus proper, as well as the predominantly unidirectional flow of information, produces a uniquely robust LFP signal that can be readily observed in animal models. This robust signal can be used to infer synchronous LFP activity with a relatively high degree of precision, as well as providing a reference point from which to investigate phase coding. As a result, a large body of work has focused on network synchrony and phase coding in relation to hippocampal LFPs, and the properties and mechanisms of these phenomena are relatively well characterized in comparison to other regions (Colgin, 2016; Drieu and Zugaro, 2019).

In humans, the hippocampus has predominantly been associated with episodic memory (Scoville and Milner, 1957; Vargha-Khadem et al., 1997), and recent evidence also suggests that prospective memory, such as the simulation of prospective episodes based on prior experience, is also hippocampus-dependent (Schacter et al., 2017). One defining characteristic of episodic memory is that it is anchored to a spatio-temporal context (Tulving, 1993). Thus, episodic memory typically includes details about where an event took place, and how the discrete components that comprise such events are ordered chronologically within the event space. Several aspects of hippocampal processing are ideally suited for the construction of episodic memory. For example, principal hippocampal cells, known as "place cells," are known to encode information about the spatial location as an animal moves through physical space (O'Keefe and Dostrovsky, 1971), and spatial cognition has been linked to memory performance across a number of experimental paradigms in both animals and humans (Eichenbaum et al., 1999; Smith and Mizumori, 2006; Eichenbaum, 2017b). The hippocampus also plays an important role in temporal processing (Meck et al., 2013; Eichenbaum, 2014) including temporal pattern separation (Jacobs et al., 2013) and sequence generation (Buzsáki and Tingley, 2018). Importantly, both spatial and temporal sequencing mechanisms are known to require the synchronized coordination of oscillatory activity in the theta, gamma, and sharp-wave ripple bands (Buzsáki, 2006).

Schizophrenia has been associated with structural, neurochemical, and functional abnormalities of the hippocampal formation at all stages of disease progression (Heckers, 2001; Heckers and Konradi, 2002; Harrison, 2004). This includes decreases in synapse expression (Heckers, 2001; Harrison, 2004) and altered GABAergic signaling (Benes et al., 1998; Zhang and Reynolds, 2002) that are consistent with disturbed oscillatory activity. At the macroscopic level, episodic memory impairments have frequently been observed in individuals with schizophrenia (Rushe et al., 1999; Toulopoulou et al., 2003; Danion et al., 2005, 2007; Leavitt and Goldberg, 2009; Berna et al., 2016), and one study has also shown disturbed hippocampal activation in patients as they imagine future scenarios (D'Argembeau et al., 2008). These complex cognitive operations are difficult to measure in animals, but the more fundamental aspects that are thought to underlie episodic memory construction, such as place cells and sequential processing, can readily be investigated in preclinical models. Importantly, schizophrenia has also been associated with spatial memory impairments (Park and Holzman, 1992; Park et al., 1995; Glahn et al., 2003; Hanlon et al., 2006; Weniger and Irle, 2008; Fajnerová et al., 2014), and sequential processing deficits have also been observed in patients and first-degree relatives (Dickinson et al., 2007; Siegert et al., 2008; Nour et al., 2021).

The prefrontal cortex has been frequently implicated in schizophrenia pathophysiology (Selemon and Zecevic, 2015; Caballero et al., 2016), and it is known to have an important role in several cognitive processes that are disrupted in patients, such as working memory, executive control, and adaptive behavioral responses (Perlstein et al., 2001; Forbes et al., 2009; Eisenberg and Berman, 2010; Narayanan et al., 2013; Senkowski and Gallinat,

2015). In particular, dysfunction across the hippocampus-PFC pathway is correlated with a range of cognitive deficits in schizophrenia (Pantelis et al., 2003; Ziermans et al., 2012; Godsil et al., 2013; Cannon et al., 2015). Interactions between these regions are also thought to play a critical role in the consolidation of long-term episodic memory, spatial decision making, and the assimilation of new memories within pre-existing knowledge frameworks, or schema (Preston and Eichenbaum, 2013; Squire et al., 2015; Sigurdsson and Duvarci, 2016).

GAMMA FREQUENCY OSCILLATIONS IN THE HIPPOCAMPUS AND PREFRONTAL CORTEX

Disturbed gamma activity appears to be particularly pronounced in individuals with schizophrenia, and such disruptions have been observed during both cognitive task performance (Cho et al., 2006; Basar-Eroglu et al., 2007; Haenschel et al., 2009; Barr et al., 2010; Senkowski and Gallinat, 2015; Barr et al., 2017) and at rest (Andreou et al., 2015; Grent et al., 2018). Gamma frequency disturbances have also been observed in unmedicated, first episode patients and first-degree relatives, suggesting that it may be an endophenotype of the disorder (Uhlhaas and Singer, 2010; Williams and Boksa, 2010). Such disturbances have also been linked to a dysregulation of E/I balance in patients at several stages of illness progression (Grent et al., 2018).

The integrity of gamma activity has been associated with successful working memory performance, spatial cognition, selective attention, sensory gating, and the perceptual "binding" of discrete components into an integrated whole (Gray et al., 1989; Fell et al., 2003; Haenschel et al., 2009; Nyhus and Curran, 2010; Williams and Boksa, 2010; Nguyen et al., 2020). Current evidence also suggests that gamma activity is important for the temporal organization of information within local circuits (Von Stein and Sarnthein, 2000; Siegel et al., 2009; Moran and Hong, 2011), and for suppressing irrelevant circuit noise in control animals (Sohal et al., 2009). PV+ interneurons in particular have been identified as a critical component in this latter process (Sohal et al., 2009), consistent with proposals that widespread GABAergic disturbances in schizophrenia contribute to gamma-mediated working memory impairments (Lewis et al., 2005). Recent studies have also shown that dopamine modulation coordinates gamma activity in prefrontal regions (Lohani et al., 2019), again consistent with schizophrenia pathophysiology (Howes and Kapur, 2009).

In line with human studies, gamma disturbances have consistently been observed in a number of different animal models, including models of genetic risk (Fisahn et al., 2009; Deakin et al., 2012; Fejgin et al., 2014; Sauer et al., 2015; Zhao et al., 2021), neurodevelopmental models such as MIA (Dickerson et al., 2010, 2014; Nakamura et al., 2019; Schroeder et al., 2019; Lippmann et al., 2021) and MAM (Lodge et al., 2009) as well as a large number of NMDAR hypofunction models (Cunningham et al., 2006; Pinault, 2008; Dzirasa et al., 2009; Hakami et al., 2009; Lodge et al., 2009; Dickerson et al., 2010; Kittelberger et al., 2012; Caixeta et al., 2013). Taken together, such studies suggest that the integrity of gamma oscillations may be particularly sensitive to a diverse range of cellular and molecular disturbances, and may therefore represent a common physiological outcome of these disturbances at the network level. In general, the majority of these studies have shown evidence of increased gamma power at baseline, particularly among NMDAR hypofunction models (Bianciardi and Uhlhaas, 2021). This is consistent with studies showing excessive gamma activity in individuals with schizophrenia during working memory tasks (Barr et al., 2010).

In particular, within-animal studies of NMDAR blockade by either ketamine or MK-801 have provided more causal evidence that NMDAR disruptions alter cortical gamma activity. *In vivo* studies of acute NMDAR blockade have generally found a consistent pattern of results in hippocampal regions, with increased gamma power being reported as well as hyperactive behaviors as rats freely roamed around a familiar environment (Ma and Leung, 2000, 2007; Kittelberger et al., 2012; Caixeta et al., 2013; Ji et al., 2013; Nagy et al., 2016; Kealy et al., 2017; Lee et al., 2017; Sampaio et al., 2018). However, increases in hippocampal gamma power have been shown to occur independently of locomotor hyperactivity, indicating that elevated gamma power is not simply a reflection of hyperactivity (Lazarewicz et al., 2010; Caixeta et al., 2013). Furthermore, although administration of ketamine has also been shown to increase baseline, evoked, and induced gamma power in the hippocampus, the relative power of induced gamma, when compared to baseline recordings, was decreased (Lazarewicz et al., 2010). Similar increases in sound-evoked gamma oscillations were observed from LFP electrodes located in the CA1 region (Sullivan et al., 2015). Importantly, the same study obtained similar results from both surface EEG recordings and LFP probes, providing verification that in this case, non-invasive recording techniques reflected findings obtained from more invasive methods, a critical step in assessing the translatability of animal studies to humans (Sullivan et al., 2015).

Increases in cortical gamma power following acute NMDAR antagonism have also been observed in a number of *in vivo* studies (Pinault, 2008; Hakami et al., 2009; Kocsis, 2012; Kulikova et al., 2012; Phillips et al., 2012b; Jones et al., 2014; Molina et al., 2014; Lee et al., 2017; Hansen et al., 2019; Aguilar et al., 2021). In one study, however, the effects were dose-dependent, with the highest doses leading to decreased gamma power (Hiyoshi et al., 2014). Furthermore, although ongoing gamma was elevated in another study, both stimulus-evoked gamma and PPI were reduced, suggesting that sensory gating abnormalities associated with schizophrenia may be linked to a diminished ability to modulate gamma activity accordingly (Jones et al., 2014). Pre-treatment with antipsychotics has also been shown to reduce baseline gamma power in cortical regions, although only chronic pre-treatment attenuated increased gamma power following exposure to ketamine (Anderson et al., 2014), whereas acute doses had no effect (Jones et al., 2012). However, in a follow-up study, both ketamine and MK-801 administration resulted in a reduction of evoked gamma power in response to a pre-pulse stimulus. This effect was attenuated *via* administration of clozapine only, indicating that the distinct mechanisms of

action associated with these antipsychotics have specific effects on either ongoing or evoked gamma activity (Hudson et al., 2016).

Studies conducted *in vitro* have also reported increases in induced gamma power in both hippocampal and prefrontal slices following systemic exposure to MK-801 (Kehrer et al., 2007; Lemercier et al., 2017), although there was no difference in spontaneous gamma activity (Lemercier et al., 2017). These effects were attenuated in a follow-up study *via* pre-treatment with the antipsychotic cariprazine (Meier et al., 2020).

Other important factors to consider are the time course of drug action, the effects of downstream signaling cascades, and other compensatory or homeostatic processes that may not be captured by acute NMDAR blockade. For example, one study has reported that hippocampal gamma was unaffected following acute administration of MK-801 (Kalweit et al., 2017), in contrast to several studies showing elevated gamma activity (Ma and Leung, 2000, 2007; Kittelberger et al., 2012; Caixeta et al., 2013; Ji et al., 2013; Nagy et al., 2016; Kealy et al., 2017; Lee et al., 2017; Sampaio et al., 2018). However, in the Kalweit et al. (2017) study, *in vivo* recordings were taken either 1 or 4 weeks after exposure to the drug, suggesting that acute NMDAR hypofunction only has transient effects on gamma activity. Interestingly, this manipulation still resulted in both reduced LTP and theta/gamma cross-coupling at both time-points, indicating that acute NMDAR hypofunction may have more long–term effects on cross-frequency coupling. Studies of chronic exposure to NMDAR antagonists have reported a different pattern of results. For example, chronic administration of ketamine resulted in a steady decrease in hippocampal gamma power 2–4 weeks after treatment, and this coincided with decreased numbers of PV+ interneurons (Kittelberger et al., 2012). Paradoxically, however, animals with the greatest PV+ reductions had increased gamma power relative to animals with smaller PV+ reductions (Kittelberger et al., 2012). Reduced gamma power has been observed following chronic ketamine (but not MK-801) exposure in slices from the rodent prelimbic cortex, a region that is analogous to the human dorsolateral prefrontal cortex (McNally et al., 2013). Taken together, these studies indicate that chronic NMDAR hypofunction may result in a different pattern of gamma abnormalities when compared to more acute exposures, although more studies will be required to explore this possibility.

EEG and MEG studies of baseline gamma activity in patients with schizophrenia have reported mixed results, although acute administration of ketamine in healthy humans typically produces similar gamma increases to those observed in animal studies (for a systematic review see Bianciardi and Uhlhaas, 2021). It might therefore be expected that selective NMDAR knockout models may show a more similar pattern to schizophrenia patients, although surprisingly, such models have tended to show increased baseline gamma activity in hippocampal regions (Korotkova et al., 2010; Carlén et al., 2012; Tatard-Leitman et al., 2015), more in line with acute NMDAR blockade. These models did however manifest a range of cognitive and behavioral abnormalities that reflect schizophrenia symptoms, and auditory-evoked gamma was also reduced in the study by Tatard-Leitman et al. (2015). Induced gamma was also reduced in hippocampal slices from a mutant model lacking certain AMPA receptors subunits on PV+ interneurons, and this result appeared to proceed from imprecise spike timing (Fuchs et al., 2007).

MIA studies have shown that hippocampal gamma power at baseline was unaffected in both familiar and novel environments, but acoustic-evoked gamma and PPI were both reduced (Nakamura et al., 2019). Reduced gamma power has also been observed in an MIA model during decision making and memory tasks, although this reduction was only observed in female offspring (Schroeder et al., 2019). Reduced gamma coherence between the PFC and hippocampus has also been associated with diminished PPI, although gamma power was unaffected (Dickerson et al., 2010, 2014). The temporal spiking of neurons in relation to gamma oscillations was also disturbed in the MIA model (Dickerson et al., 2010). Similar reductions of gamma coherence were observed in MIA animals prior to repetitive transcranial magnetic stimulation (rTMS), although this effect was partially attenuated following the rTMS protocol, suggesting that this may be a viable treatment option (Lippmann et al., 2021). Taken together, these studies suggest that MIA leads to reductions in either gamma power or coherence during specific tasks, and these disruptions may have important functional implications, for sensory gating in particular.

In another neurodevelopmental model, exposure to MAM on GD 17 has also been shown to decrease stimulus-evoked gamma power in offspring during a latent inhibition paradigm, and this was correlated with decreased numbers of PV+ interneurons in hippocampal and prefrontal regions (Lodge et al., 2009).

Models of genetic risk have also shown abnormal gamma activity. Gamma power during active exploration was increased in a *Df(h15q13)/+* model, although relative evoked gamma power in response to auditory stimulation was reduced (Fejgin et al., 2014), a pattern that reflects aberrant gamma activity frequently observed in schizophrenia patients (Light et al., 2006; Spencer et al., 2008; Brenner et al., 2009). Reductions of gamma power have also been observed in hippocampal slices from a dysbindin-1 model (Zhao et al., 2021). However, in another *in vitro* study, hippocampal gamma was indistinguishable from controls in a model of LPA-1 deficiency, although gamma power in superficial layers of the entorhinal cortex was significantly increased (Cunningham et al., 2006). There are a number of potential explanations for these different results, but the most likely is that the regulation of gamma activity in hippocampal regions may be affected by network activity that originates outside the hippocampus proper and that these more complex mechanisms are not captured in isolated slices (Cunningham et al., 2006). In support of this proposal, emerging evidence that entorhinal cortex-hippocampus pathways are critical for the organization of information transfer at gamma frequencies suggests that the integrity of EC transmission is likely to exert important effects on hippocampal gamma power and synchrony (Fernández-Ruiz et al., 2017, 2021).

Models targeting neuregulin signaling have also shown a range of induced gamma abnormalities, including reduced gamma frequency (Deakin et al., 2012) and power (Fisahn et al., 2009) in hippocampal slices. Neuregulin signaling has

been shown to be important for the synchronization of network activity in the prefrontal cortex *in vivo* (Hou et al., 2014; Barz et al., 2016), and increases of induced gamma power that occur in wildtype animals were absent in mutant mice lacking ErbB4 receptors on interneurons located in frontal regions (Hou et al., 2014). Stimulus-evoked gamma is also reduced in mice with the Neurogulin-1 genetic susceptibility (Barz et al., 2016). DISC-1 models have shown disturbed synchrony in the gamma range that was associated with disrupted PV+ interneurons (Sauer et al., 2015), and recent dual-hit models (DISC1 and MIA) have also shown disorganized temporal spiking in relation to oscillatory activity in the gamma range (Hartung et al., 2016; Chini et al., 2020).

Several studies using animal models have also demonstrated that the familiarity of the task or recording environment is likely to exert important effects on gamma activity, suggesting that gamma frequency oscillations may play an important role in the reallocation of attentional resources in response to novelty. For example, a reduced shift in the preferred gamma firing phase of single cells located in the CA1 region in response to novelty has been observed in a DISC-1 model of genetic risk, and principal cells were more strongly phase- locked to both gamma and theta oscillations, specifically in novel environments (Kaefer et al., 2019). Novelty-induced irregularities were also observed in a genetic model of NMDA hypofunction (SRKO), in which the power of background gamma oscillations in frontal regions was increased prior to a social recognition task. When another animal was introduced to the testing arena, however, there was an attenuated increase in gamma power relative to controls, associated with reduced social recognition (Aguilar et al., 2021). These disruptions may be due to neuregulin-induced increases in dopamine signaling, as D4 dopamine receptor agonists increased gamma activity in hippocampal slices, and both NRG-1 and D4 receptor types are co-expressed on PV+ interneurons (Andersson et al., 2012). In another study that compared hippocampal-PFC gamma synchrony between wildtype and hyperdopaminergic (DAT-KO) mice in both novel and familiar environments, gamma synchrony between the hippocampus and PFC was initially high in both groups in the home environment. This was attenuated in the control group when animals subsequently explored a novel environment, resulting in elevated inter-regional gamma synchrony in the mutant group when compared to controls (Dzirasa et al., 2009). Although these studies are inconsistent in regards to the enhancement or attenuation of gamma activity in response to novelty, they all suggest that abnormal gamma activity during rest is likely to be an important factor when interpreting such results. Further support for this idea has been provided by studies demonstrating elevated CA1 gamma activity in a ketamine model when animals are well habituated to the environment (Caixeta et al., 2013). Increased hippocampal gamma activity reminiscent of REM sleep has also been observed in a DAT-KO model as animals explored a novel environment, an effect that was normalized *via* treatment with the antipsychotic haloperidol (Dzirasa et al., 2006). Taken together, these studies suggest that schizophrenia may be associated with inappropriate state-dependent gamma processing, which may disrupt the facilitation of long term potentiation (LTP) in response to novelty when learning is likely to be most beneficial (Li et al., 2003).

Overall, the evidence from animal models is largely consistent with human studies showing that gamma activity is disturbed in individuals with schizophrenia. The majority of studies have shown evidence of increased baseline gamma, whereas stimulus-evoked and induced gamma were more frequently, but not always, reduced. This suggests that abnormal gamma activity in response to changing environmental and task demands may underlie at least some of the sensory gating and task switching disturbances that have been associated with the disorder.

SHARP WAVE RIPPLES AND REPLAY

Sharp wave ripples (SPW-Rs) involve an irregular pattern of large amplitude waves that are typically present in hippocampal regions during slow-wave sleep, or when animals are awake but immobile (Buzsáki, 1986, 2015). These sharp wave events typically last for around 40–100 ms and are accompanied by a "ripple" oscillation that occurs above the gamma frequency range, between 100 and 200 Hz. The SPW-R is the LFP event that co-occurs with a neuron-level phenomenon known as a replay, whereby sequences of place field activity that has previously occurred during active exploration are reactivated (Pavlides and Winson, 1989; Wilson and McNaughton, 1994; Lee and Wilson, 2002). The reactivation of sequential spiking activity that occurs during SPW-Rs occurs in a time-compressed manner such that the representation of events occurs in a timeframe that is suitable for the induction of synaptic plasticity (Davidson et al., 2009). These reactivation patterns are most prominent during the first few hours after learning, and they are thought to contribute to the consolidation of newly acquired information and the subsequent transfer of memory from the hippocampus to more permanent storage in neocortical regions. Consistent with this proposal, perturbation of SPW-R activity during post-learning sleep in rodents has been shown to impair performance on spatial memory tasks (Girardeau et al., 2009; Ego-Stengel and Wilson, 2010). Similarly, stimulation of reward regions in response to SPW-R related place cell activity during sleep has been shown to induce an artificial place/reward association, providing compelling evidence that replay during sleep is functionally important for goal-related spatial memory (De Lavilléon et al., 2015). Replay events have also been shown to predict future trajectories (preplay) and so they may also have a role in planning (Pfeiffer and Foster, 2013).

Disordered ripple events have been observed in both a methylazoxymethanol acetate (MAM) neurodevelopmental model (Phillips et al., 2012a), and a DISC-1 genetic model (Altimus et al., 2015). Other studies, using a genetically modified calcineurin animal model which has been shown to reproduce several phenotypes associated with schizophrenia (Miyakawa et al., 2003), have also demonstrated a substantial increase in hippocampal SPW-R events in mutant animals during awake rest, as well the elimination of sequential replay (Suh et al., 2013). Furthermore, in a recent *in vitro* study, the temporal structure of SPW-R events was shown to be altered in hippocampal slices obtained from MIA animals (Gao et al., 2019). These

findings are all consistent with the hypothesis that pathological ripple activity could be involved in schizophrenia (Buzsáki, 2015). Recent advances have also made it possible to investigate SPW-R events in humans (Liu et al., 2019), and early evidence from schizophrenia patients indicates that replay is diminished, although ripple activity is enhanced relative to control subjects. in schizophrenia patients (Nour et al., 2021). These findings are consistent with the animal literature, although further work will be required to determine how these changes affect processes such as memory consolidation and planning. Furthermore, it is not clear what underlying changes produce the alterations in SPW-R events that are described here. For example, do they reflect subtle changes in circuitry or functional connectivity, or are they simply a response to a general loss of inhibition?

THETA FREQUENCY OSCILLATIONS IN THE HIPPOCAMPUS AND PFC

Although early studies of disturbed oscillatory activity in individuals with schizophrenia have focused predominantly on higher-frequency oscillations (Uhlhaas and Singer, 2010), more recent work has demonstrated that disturbances in the lower-frequency theta band are also common (Schmiedt et al., 2005; Siekmeier and Stufflebeam, 2010; Kirihara et al., 2012; Frantseva et al., 2014; Griesmayr et al., 2014; Andreou et al., 2015; Cousijn et al., 2015; Di Lorenzo et al., 2015; Garakh et al., 2015; Kim et al., 2015; Javitt et al., 2018; Ryman et al., 2018; Adams et al., 2020). Theta oscillations are thought to coordinate long-range communication across regions (Von Stein and Sarnthein, 2000; Moran and Hong, 2011) and theta frequency disturbances are therefore likely to be critical for a wide range of complex cognitive processes that require the integration of both higher and lower order processes across distributed networks. Theta oscillations in hippocampal and prefrontal regions have been extensively studied in both humans and non-clinical animal models, and theta activity in these regions has been associated with an exceptionally diverse range of cognitive operations, including episodic, spatial, and working forms of memory, sequential processing, adaptive learning, error monitoring, relational binding, social cognition, and flexible decision making. These studies have been comprehensively reviewed elsewhere (Hasselmo, 2005; Nyhus and Curran, 2010; Buzsáki and Moser, 2013; Colgin, 2013, 2016; Cavanagh and Frank, 2014; Hasselmo and Stern, 2014; Buzsáki and Tingley, 2018; Herweg et al., 2020; Karakaş, 2020).

The biophysical mechanisms underlying theta oscillations have also been extensively studied in non-clinical animal models, and such studies have provided a framework from which to understand the likely role of schizophrenia pathophysiology in disturbed oscillatory activity (Lisman and Buzsáki, 2008). For example, the generation and maintenance of the hippocampal theta rhythm involve several neurotransmitter systems that are known to be disturbed in schizophrenia, including the glutamate, GABA, dopamine, and acetylcholine systems (Freund and Antal, 1988; Stewart and Fox, 1990; Howes and Kapur, 2009; Losonczy et al., 2010; Moghaddam and Javitt, 2012; Nakazawa et al., 2012; Gonzalez-Burgos et al., 2015; Drieu and Zugaro, 2019; Caton et al., 2020). Furthermore, the regulation of local inhibitory networks has also been shown to exert profound effects on theta synchrony (Cobb et al., 1995; Kamondi et al., 1998; Goutagny et al., 2009). In particular, PV+ interneurons that target the peri-somatic regions of principal cells appear to play an important role in the temporal coordination of rhythmic LFPs within the theta range, as well as the temporal spiking profile of single cells relative to distinct theta phases of the theta cycle (Wulff et al., 2009; Stark et al., 2013; Amilhon et al., 2015). Findings from animal models of schizophrenia risk are generally consistent with these findings, indicating that theta disturbances frequently co-occur with disturbed GABAergic signaling, particularly at the site of PV+ interneurons (Lodge et al., 2009; Korotkova et al., 2010; Ducharme et al., 2012; Del Pino et al., 2013; Dickerson et al., 2014; Sauer et al., 2015; Nakamura et al., 2019).

To date, a broad range of abnormalities in theta activity in hippocampal and prefrontal regions have been described in animal models of schizophrenia, with evidence of both enhanced and reduced theta power, coherence, and synchrony. Models of NMDAR hypofunction, including both acute exposure and selective knockout models, have shown evidence of decreased baseline theta power in hippocampal regions (Korotkova et al., 2010; Lazarewicz et al., 2010; Kalweit et al., 2017). Event-related theta power in the hippocampus was also significantly reduced following sub-chronic exposure to ketamine when animals were tested 6 months after cessation of the drug exposure protocol, suggesting that chronic NMDAR hypofunction over a discrete time period can exert more permanent effects on circuitry (Featherstone et al., 2012). Acute administration of ketamine, however, led to layer-specific modulation of theta power in CA1 as animals freely moved around the recording apparatus (Caixeta et al., 2013). These latter data are consistent with evidence that theta properties vary systematically according to the precise location of recording electrodes in the hippocampus (Buzsáki et al., 1985; Brankačk et al., 1993; Lubenov and Siapas, 2009), and suggest that quite small changes in experimental procedures could influence the results. Increased theta power has also been observed in a genetic model of the disorder that knocks out a neuregulin receptor (ERBb4), a critical receptor for the integrity of fast-spiking interneurons. This increase in theta power co-occurred with increased intra-regional coherence across the hippocampal circuit but decreased theta synchrony between the hippocampus and PFC (Del Pino et al., 2013).

Disrupted phase-locking of single cells located in either the PFC or the hippocampus to the hippocampal theta rhythm has also been observed in both a DISC1 and a 22q11 deletion *(Df(16)$^{A+/-}$)* model, including decreases in both the phase-locking strength of individual cells, as well as the synchronization of preferred locking phase at the network level (Sigurdsson et al., 2010; Kaefer et al., 2019). In the *Df(16)$^{A+/-}$* model, these disturbances were also associated with reduced LFP coherence between the hippocampus and the PFC, as well as working memory impairments (Sigurdsson et al., 2010). Similar reductions were observed in an alternative model targeting the 22q11.2 deletion, in which the deficiencies at the site of the

ZDHHC8 gene resulted in reduced axonal growth during early development (Mukai et al., 2015).

Prelimbic theta synchrony has also been shown to be reduced in a DISC-1 model, although this effect appeared to be driven by reduced theta power in the hippocampus, although coherence was unaffected (Sauer et al., 2015). Disorganized hippocampal theta oscillations and reduced hippocampal/PFC theta synchrony have recently been observed in neonates exposed to a dual-hit procedure (DISC-1 and MIA). However, theta synchrony was subsequently augmented in pre-juveniles, suggesting that theta activity is likely to be sensitive to ongoing developmental processes (Hartung et al., 2016). Furthermore, unlike the single-hit genetic model (DISC1), MIA did not affect synchrony on its own, suggesting that the time-course of disruptions associated with each model is different and that such disruptions interact with each other in a complex fashion (Hartung et al., 2016). Interestingly, MIA has also been shown to delay the maturation of GABAergic transmission from predominantly depolarizing to hyperpolarizing (Corradini et al., 2018; Fernandez et al., 2018), which suggests that the precise time-course of such developmental shifts could potentially play a crucial role in the emergence of coordinated network synchrony later in life.

Single hit MIA models have generally shown a number of theta frequency disturbances once offspring reach maturity, including increased theta power at baseline, but reductions in evoked theta power (Nakamura et al., 2019). Increased theta power has been observed to occur in conjunction with diminished synaptic inhibition in hippocampal slices following an MIA manipulation (Ducharme et al., 2012). Decreased coupling between hippocampal and prefrontal regions has also been observed in an anesthetized MIA model, although coherence was similar to controls (Lippmann et al., 2021). However, theta coherence and the phase locking of PFC cells to hippocampal theta have been shown to be disturbed in an MIA model during waking behaviors (Dickerson et al., 2010, 2014), similar to findings reported in genetic-risk models (Sigurdsson et al., 2010). Furthermore, abnormal theta synchrony between these regions was attenuated in the MIA model following administration of the antipsychotic clozapine, although local increases in theta power were only observed in the PFC, suggesting that long-range coherence was more likely to be mediated by increased PFC theta synchrony than local changes in the hippocampus (Dickerson et al., 2012).

Reductions in PFC theta activity have also been reported in the MAM model of schizophrenia during a fear conditioning paradigm, while theta activity in the hippocampus was unchanged, again suggesting that theta disruptions in the PFC may be driving the functional dysconnectivity between these regions (Lodge et al., 2009). The same MAM model has previously been shown to produce both hippocampal hyperactivity and a subsequent hyperdopaminergic state that could be attenuated *via* inactivation of the ventral hippocampus, suggesting that hippocampal signaling may exert important effects on theta activity in downstream regions *via* dopamine modulation (Lodge and Grace, 2007, 2008). This is consistent with proposals that GABAergic disturbances in hippocampal regions are likely to have important effects on downstream dopamine signaling (Sonnenschein et al., 2020). However, theta phase synchrony between the hippocampus and PFC was not disrupted in a hyperdopaminergic model of the disorder created by knocking out a key dopamine transporter gene, suggesting that dopamine irregularities are not likely to be the primary mechanism of dysfunctional theta activity between these regions (Dzirasa et al., 2009).

Interestingly, infusion of dopamine into the PFC of naïve, anesthetized rats initiated similar increases in theta phase coherence and synchrony between the PFC and hippocampus to those observed during successful rule learning (Benchenane et al., 2010). This suggests that dopamine signaling in response to salient stimuli and prediction error may play a critical role in coordinating phase synchrony between the hippocampus and PFC and that such synchrony supports adaptive learning. Further support for this hypothesis has been provided by both human and rodent studies showing that lower frequency oscillations (<12 Hz) are important for adaptive behavioral adjustments in response to error detection (Narayanan et al., 2013). Hyperdopaminergic activity in schizophrenia may, therefore, contribute to inefficient cognitive task switching in response to current environmental and motivational demands.

In support of this hypothesis, a reduced novelty-induced shift in the preferred theta phase of CA1 cells has been observed in a DISC-1 model, accompanied by disturbed theta coordination at the network level during exploration (Kaefer et al., 2019). The DISC-1 model has also been associated with a number of dopamine signaling abnormalities (Trossbach et al., 2016). It has been proposed that hippocampal-PFC theta coherence may reflect sustained attention rather than working memory, as impaired spatial working memory performance could be predicted by either low gamma or beta coherence in a genetic risk model (gria1$^{-/-}$), while theta coherence was only disturbed in a novelty recognition paradigm (Bygrave et al., 2019). Given that several studies have also documented abnormal theta activity during resting states in both patients with schizophrenia and animal models of the disorder (Karbasforoushan and Woodward, 2012; Del Pino et al., 2013; Kaefer et al., 2019), these findings indicate that the dynamic modulation of theta activity in response to salient changes in either contextual cues or task demands may be a more critical component of schizophrenia pathology than simple hypo- or hypersynchrony within and between these regions.

In human studies, reduced theta power and diminished theta phase coupling between the mPFC and the medial temporal lobe have been observed in individuals with schizophrenia, and this was correlated with both memory performance and abnormal $GABA_A$ receptor expression in the schizophrenia group (Adams et al., 2020). Both the coherence of theta oscillations between hippocampal and prefrontal regions and the synchronous phase locking of PFC neurons to the hippocampal theta rhythm have been associated with spatial and working memory performance (Zielinski et al., 2019) as well as successful rule learning (Benchenane et al., 2010) in non-clinical rodent models. Tests of animal models of schizophrenia that have included a cognitive task have generally been consistent with these

findings, demonstrating that reduced theta coupling between the hippocampus and PFC is correlated with both spatial working memory deficits (Dzirasa et al., 2009; Sigurdsson et al., 2010; Del Pino et al., 2013) and reduced pre-pulse inhibition (Dickerson et al., 2010). Reductions in hippocampal theta power (Korotkova et al., 2010) and frequency (Fejgin et al., 2014) have also been associated with spatial memory deficits in animal models. In one model, however, impaired recognition memory was correlated with enhanced hippocampal/PFC coupling, although in that study, LFP activity was recorded while animals were under-anesthesia, which is unlikely to reflect theta activity that is directly associated with the cognitive task (Hartung et al., 2016). Additional studies will be required to clarify some of these outstanding issues, although in general, these studies suggest that targeting theta activity in hippocampal and prefrontal regions may be a promising avenue for future research into cognitive disorganization in schizophrenia.

Intriguingly, another study using a neurodevelopmental model of schizophrenia has demonstrated that targeted cognitive training during adolescence can normalize theta synchrony within hippocampal regions and that this normalization coincided with a rescue of the cognitive deficits that typically emerge post-adolescence (Lee et al., 2012). This suggests that targeting basic level mechanisms that support learning and memory during critical developmental periods is a viable strategy for preventing the development of schizophrenia in high-risk individuals, although it remains unclear whether directly enhancing theta coupling between hippocampal and prefrontal regions can also prevent pathological trajectories. In this vein, however, a recent study has shown that non-invasive electrical stimulation to frontal regions can promote theta synchrony in schizophrenia patients and that this effect was accompanied by improved cognitive control (Reinhart et al., 2015).

Overall, the evidence from animal models supports the proposal that disturbed theta activity may be related to several cognitive deficits observed in the disorder, although the pattern is complex. While NMDAR hypofunction models have generally shown evidence of reduced theta power, models of both genetic and environmental insults during early neurodevelopment have produced more variable results. This aside, coordinated synchrony between the hippocampus and PFC and abnormal phase-locking of single cells to the theta rhythm has been consistently observed across several studies suggesting that these processes may be a viable target for novel interventions.

THETA/GAMMA CROSS-COUPLING

LFP oscillations at gamma frequencies are often nested within the slower theta rhythm during specific behaviors, with higher gamma amplitudes typically coupled to the peak of the theta oscillation (Csicsvari et al., 2003; Belluscio et al., 2012; Colgin, 2016). This phenomenon, known as cross-frequency coupling, is thought to play an important role in the temporal organization of information during working and episodic memory processes (Lisman and Idiart, 1995; Lisman, 2005; Lisman and Buzsáki, 2008; Lisman and Jensen, 2013). Support for this hypothesis has been obtained in a number of studies showing that the strength of theta/gamma cross-coupling is increased during successful memory performance in rodents (Tort et al., 2009; Shirvalkar et al., 2010), monkeys (Jutras et al., 2009), and humans (Sederberg et al., 2006; Axmacher et al., 2010; Maris et al., 2011; Heusser et al., 2016).

It has also been proposed that the theta/gamma neural code may function as a neural syntax, with each gamma oscillation representing a single "word," while the theta oscillation works to organize the sequential order of such "words" into meaningful sentences (Lisman and Buzsáki, 2008; Buzsáki, 2010). Disturbed cross-frequency coupling has thus been linked to cognitive disorganization in schizophrenia (Lisman and Buzsáki, 2008), although experimental evidence for this proposal has been challenging to obtain. For example, no differences in cross-frequency coupling were observed when patients performed a simple auditory processing task (Kirihara et al., 2012), and although global theta/gamma cross-coupling was diminished in another study, it was actually enhanced for patients across electrodes located specifically in frontal temporal regions (Allen et al., 2011). More recently however, impaired theta/gamma cross-coupling in the PFC has been observed in patients while they performed a working memory task, and this was associated with poor task performance when compared to control subjects (Barr et al., 2017). Interestingly, peak gamma power for individual items within a sequence has also been shown to be organized sequentially according to distinct theta phases in healthy humans (Heusser et al., 2016), suggesting that disturbed phase coupling could be involved in the disorganization of temporal sequencing.

Hippocampal theta/gamma coupling has been investigated in several animal models of the disorder. In general, coupling deficits have been reported with the hippocampus itself (Caixeta et al., 2013; Kalweit et al., 2017). Administration of ketamine has been shown to alter hippocampal theta/gamma cross-coupling in a dose-dependant manner, with increased coupling evident for the lowest dose (25 mg/kg), but diminished coupling at the highest dose (75 mg/kg; Caixeta et al., 2013). In another study that used an alternative NMDA antagonist model (MK801), hippocampal theta/gamma cross-coupling was transiently disrupted during a high-frequency stimulation protocol designed to induce LTP, and this uncoupling co-occurred with diminished theta power, whereas gamma activity remained uninterrupted (Kalweit et al., 2017). Previous studies have demonstrated that theta/gamma coupling is highly correlated with LTP induction (Bikbaev and Manahan-Vaughan, 2007, 2008), and given that hippocampal LTP was also profoundly diminished following the transient NMDA blockade, it is possible that disrupted cross-frequency coupling reflects aberrant plasticity processes (Kalweit et al., 2017). However, it remains unclear whether disturbed coupling is a cause or effect of impaired synaptic plasticity, or whether reduced coupling in these models is associated with cognitive deficits.

Diminished theta/gamma phase coupling within both the hippocampus and prefrontal cortex has also been observed in an NMDA hypofunction model (NR1 KD) as animals explored a novel environment, although inter-regional phase coupling was enhanced, suggesting that hyper-coupling between these

regions could also be involved in pathological outcomes (Dzirasa et al., 2009). Enhanced cross-coupling between these regions was also observed in a dual-hit model (DISC-1 and MIA) under anesthesia, and although no differences were observed in either single-hit models in that study (Hartung et al., 2016), enhanced coupling was observed in another single-hit MIA model (Lippmann et al., 2021). This enhanced coupling furthermore was attenuated when animals were pre-treated with an rTMS protocol (Lippmann et al., 2021). The enhanced coupling has also been observed in naïve animals following stimulation of dopamine cells in the VTA (Lohani et al., 2019), suggesting that hyperdopaminergic activity in schizophrenia may also play a role.

Although the gamma rhythm has historically been conceptualized as a singular rhythm that encompasses a broad frequency range, recent reports suggest that gamma frequencies may be better conceptualized as two distinct frequency bands, with low gamma activity occurring at frequencies between 30 and 60 Hz, whereas high gamma occurs between 60 and 100 Hz (Colgin et al., 2009). These distinct bands are thought to have complementary functions in the hippocampus and may allow for the integrated organization of internally and externally generated information arriving from different sources. Thus, high gamma activity frequently occurs around the peak of the theta oscillation, and is thought to play an important role in the encoding of sensory information arriving from the EC, while low gamma tends to occur during the descending phases of the theta oscillation, and has been predominantly associated with memory retrieval processes originating in CA3 (Colgin et al., 2009; Schomburg et al., 2014). CA1 low gamma also predominantly co-occurs with sequential processing that sweeps ahead of the animal's current location, suggesting that it is preferentially involved in the prospective coding of future locations, whereas high gamma appears to represent the animal's current location in real time (Senior et al., 2008; Zheng et al., 2016), as well as during retrospective encoding of recently visited locations (Bieri et al., 2014). Although it currently remains unclear whether low and high gamma typically co-occur during a single theta cycle, or whether separate theta cycles preferentially represent either future and present locations depending on the animal's current situation and goals (Colgin et al., 2009; Zheng et al., 2016), these findings suggest that cross-coupling may be important for the organized integration of new information within existing schemas. This coding scheme could also have important implications for aberrant source monitoring in schizophrenia (Brébion et al., 2000; Martin et al., 2014), potentially shifting the emphasis from externally generated sensory information to internally generated representations, and *vice versa*. At the present time, however, it is unclear how the high/low gamma relationship is influenced by schizophrenia or is affected in animal models of the disorder.

HIPPOCAMPAL PHASE PRECESSION AND THETA SEQUENCES

The theta rhythm is not only an indicator of synchronous neural activity, but it also serves as a reference signal against which temporal, or phase coding of information can occur. Theta phase precession is a form of temporal coding that was first observed in CA1 place cells as animals moved along a linear track. In addition to spatial rate coding, which produces localized "place fields", it was noticed that the firing phase of these cells, referenced to the underlying theta-frequency LFP oscillation, changed systematically from a later to earlier phases of successive theta cycles as an animal advanced across a place field (O'Keefe and Recce, 1993; Skaggs et al., 1996). As a result, the firing phase of a cell provides information about where the animal is located within a place field, over and above that of the conventional rate code, and several studies have confirmed that this phase code is a more robust predictor of an animal's current location than the rate code alone (Jensen and Lisman, 2000; Huxter et al., 2003; Tingley and Buzsáki, 2018).

While phase precession describes location-dependent changes in the spiking activity of single cells, it also has important implications for sequential processing at the network level. When several cells with overlapping place fields are co-active, the phase precession of individual cells produces an emergent phenomenon known as a "theta sequence" (Foster and Wilson, 2007), wherein recently experienced event sequences occurring at behavioral timescales are preserved and compressed within a single theta cycle (∼120 ms), a timescale that is suitable for the induction of synaptic plasticity (Skaggs et al., 1996; Bi and Poo, 1998; Dan and Poo, 2004). Theta sequences have thus garnered considerable interest as a mechanism of sequential memory encoding and storage (Skaggs et al., 1996; Dragoi and Buzsáki, 2006; Jaramillo and Kempter, 2017; Buzsáki and Tingley, 2018; Drieu and Zugaro, 2019). Several studies have now confirmed that theta sequences rapidly emerge during active exploration of an environment, although additional network synchronization is required to ensure that critical phase precession properties, such as the starting phase and slope of precession, are relatively coherent across co-active cells (Foster and Wilson, 2007; Schmidt et al., 2009; Feng et al., 2015).

Both phase precession and theta sequences have now been observed in a range of experimental conditions, including tasks that require goal-planning and decision-making (Johnson and Redish, 2007; Gupta et al., 2012; Wikenheiser and Redish, 2015), as well as several paradigms that don't include a spatial component (Lenck-Santini et al., 2008; Pastalkova et al., 2008; Royer et al., 2012; Cei et al., 2014). Importantly, hippocampal phase coding has also been associated with the sequential integration of sound and odor cues (Terada et al., 2017), as well as internally generated states (Takahashi et al., 2014; Wang et al., 2015). These findings suggest that theta sequences are involved in the complex construction of mental maps, an important component of both episodic memory and decision making (Kaplan et al., 2017). Interestingly, the developmental emergence of theta sequences has recently been shown to coincide with the maturation of hippocampal memory in rodents (Muessig et al., 2019), providing compelling evidence that theta sequences may serve as a neural substrate for episodic memory traces more generally. Recent studies have also demonstrated that theta sequences are associated with episodic memory and sequential planning in humans (Heusser et al., 2016; Kaplan et al., 2020),

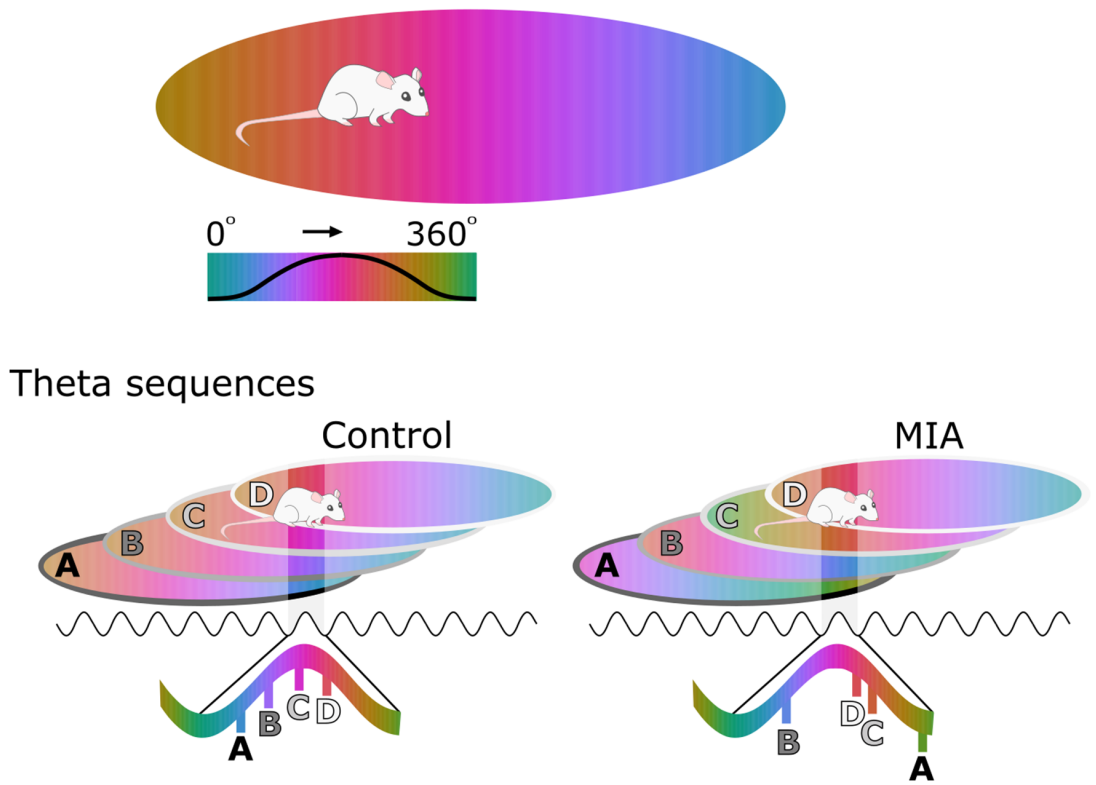

FIGURE 1 | Disorganized phase coding of hippocampal place cells produces disordered theta sequences in maternal immune activation (MIA) animals. The upper cartoon illustrates phase coding occurring as an animal crosses a place field, with phase color-coded. As the animal enters the place field, the cell spikes at late phases of the theta cycle, but spiking processes towards earlier phases as the animal traverses the field. The lower cartoon demonstrates how theta sequences emerge as a result of phase precession in several cells with overlapping place fields. In the control example, the starting phase of precession is coordinated at the network level, resulting in ordered theta sequences that are concentrated along a portion of a theta cycle. Here cell A fires first during the theta cycle because the animal is exiting this place field. In contrast Cell D fires last, because the animal is entering this field. In the MIA example, starting phase varies from cell to cell, resulting in disordered sequences that are also spread further across the theta cycle.

and direct evidence of phase precession has also been confirmed in single cell recordings from human subjects performing a virtual reality navigation task (Qasim et al., 2020).

Hippocampal phase precession has only recently been investigated in a model of schizophrenia risk. In this study, the firing of individual pyramidal cells in the CA1 region of MIA animals displayed what appeared to be normal phase precession as these animals moved through that cell's place field. On closer examination, however, the starting phase of this precession as an animal enters a new place field was considerably more variable between-cells in MIA animals than in controls (Speers et al., 2021). An important theoretical consequence of this variability is that the sequence of place fields (or other experiences) that an animal encounters would be replayed in a disordered manner during each theta sequence (**Figure 1**). To test this hypothesis, the correlations between the spike time difference of simultaneously recorded cell pairs and the distance between their respective place fields were determined. Results showed that there was a significant positive correlation between these two measures in the control cells, as would be expected if theta sequences are functioning normally. In contrast, there was no such relationship in the MIA cells indicating that theta sequences were disordered in the MIA group (Speers et al., 2021). To illustrate the effect of this change, in MIA animals a sequence experienced in the order ABCD would be encoded and recalled in a disordered fashion, for example as BDCA.

In addition to disordered theta sequences, increased starting phase variability should result in reduced clustering of sequential spiking within each consecutive theta cycle, provided that individual cells do not precess a full 360 degrees (Schmidt et al., 2009). This could potentially allow spikes from one cycle to become erroneously associated with those in the next cycle, further corrupting the sequential order of experience, as well as distorting the segmentation of experience into discrete events (Gupta et al., 2012). An analogy for this phenomenon is that the pause in firing that normally occurs between cycles serves as "punctuation" by separating out units of meaningful information. This lack of "punctuation," if it occurs in schizophrenia, may contribute to a disintegration of event boundaries (Lisman and Buzsáki, 2008; Richmond et al., 2017),

consistent with evidence that event segmentation is disrupted at both lower and higher order levels among individuals with schizophrenia (Zalla et al., 2004; Coffman et al., 2016).

Two previous studies have also provided indirect evidence that the phase coding may be disrupted in other animal models of schizophrenia, although phase precession itself was not explicitly investigated. In one study, the phase-locking preference of CA1 cells to theta was more variable in a DISC-1 model (Kaefer et al., 2019), which would be a logical consequence of a more variable starting phase. Another study has demonstrated that administration of PCP, which has been shown to induce transient schizophrenia-like symptoms in healthy individuals and to exacerbate symptoms in patients, disrupts the precise spike timing of place cell pairs relative to the theta rhythm without disrupting other place field properties (Kao et al., 2017). Both of these studies are consistent with the findings outlined in Speers et al. (2021), suggesting that disorganized phase coding mechanisms potentially occur in other models of schizophrenia. Furthermore, although the precise mechanisms of phase precession and theta sequences remain to be elucidated, several animal models of schizophrenia have shown evidence of basic-level disturbances that are consistent with a discoordination of phasic spiking, with current evidence pointing towards PV+ interneurons as a critical factor (Lodge et al., 2009; Ducharme et al., 2012; Royer et al., 2012; Del Pino et al., 2013; Dickerson et al., 2014; Drieu and Zugaro, 2019).

Phase precession has been shown to occur in regions outside of the hippocampus, suggesting that phase coding mechanisms could be important across a wider distributed network. For example, phase precession has been documented in the prefrontal cortex (Jones and Wilson, 2005), as well as in subcortical areas that are likely to be important for dopamine regulation, such as the lateral septum, the striatum, and the ventral tegmental area (Lansink et al., 2009; Luo et al., 2011; van der Meer and Redish, 2011; Tingley and Buzsáki, 2018). In turn, striatal dopaminergic concentrations have been shown to be strongly influenced by the synchronization of GABAergic micro-circuits in a computational model, suggesting that dopamine might have a wider modulatory role in the coordination of phasic spiking at the network level (Humphries et al., 2009).

Finally, if theta sequences provide the biophysical scaffolding that supports the encoding and storage of temporally extended memories, then a disruption of this system could have profound implications for learning and memory processes, as well as the disorganization of thought that occurs in the disorder (Lisman and Buzsáki, 2008). Sequential processing deficits have frequently been documented in schizophrenia patients, their first-degree relatives, and other at-risk individuals, including disturbances of temporal order judgment and impaired sequence learning (Dickinson et al., 2007; Lisman and Buzsáki, 2008; Pedersen et al., 2008; Siegert et al., 2008; Meck et al., 2013; Ciullo et al., 2016; Eichenbaum, 2017a; Thoenes and Oberfeld, 2017). Such deficits also appear to be independent of other cognitive impairments (Ciullo et al., 2016), suggesting that they may be a primary feature of the disorder and a potential trait marker (Andreasen et al., 1999). A fundamental disorganization of sequential processing mechanisms could furthermore affect a wide range of cognitive processes that have been shown to be disturbed in schizophrenia (Barch and Ceaser, 2012; Thoenes and Oberfeld, 2017), and which can be effectively modeled in animals. Additional studies will be required to establish a more direct link between disrupted phase coding and these specific cognitive deficits, and this is a promising area for further research.

DISCUSSION

In summary, we have described how oscillations in neural systems may serve as a scaffold upon which coherence and communication can be achieved within and between brain regions. We have also discussed how disruptions in these oscillatory mechanisms could lead to the kind of disorganized processing and functional disintegration that is observed in schizophrenia, to the degree that it might underlie some of the core features of the disorder, particularly the disruption of episodic memory and planning processes. While dysfunction in a number of different brain regions is likely to occur in schizophrenia, we have chosen to focus on the hippocampus because of its role in encoding sequential information across time and space. The use of animal models has allowed for a detailed examination of the biological mechanisms that might underlie these processes, with current evidence pointing to local GABAergic circuits as a critical component of coordinated spiking activity, as well as network synchrony within and between the hippocampus and PFC. A graphical overview of these disruptions as they occur at the microscopic, mesoscopic, and macroscopic levels is provided in **Figure 2**.

In particular, we have focussed on phase precession and theta sequences because of their potential to underlie certain types of sequence learning, and have described how a disruption of phase precession, as observed in the MIA model, could result in a fundamental disorganization of sequential information processing. If a similar dysfunction occurs in schizophrenia, it may contribute to several symptoms of cognitive disorganization that have been documented in schizophrenia, such as and impaired episodic and working memory, diminished future planning, thought disorder, and misattributions of agency and control. Taken together with the large body of evidence documenting sequential processing and episodic memory deficits in schizophrenia, these findings suggest that investigating disorganized phase coding in different animal models of the disorder is a promising area for future research.

Correlational evidence linking disturbed oscillatory processes to cognitive dysfunction has been provided across a number of animal models of the disorder, although this work is still in its early stages. In particular, more direct manipulations that target oscillatory activity within specific frequency ranges are still required to confirm that these phenomena are causally linked. Such studies are currently difficult due to the complex nature of the oscillatory activity that occurs across distributed networks, but emerging evidence describing the basic level mechanisms of coordinated network synchrony and phase coding, in addition to technological advances, is

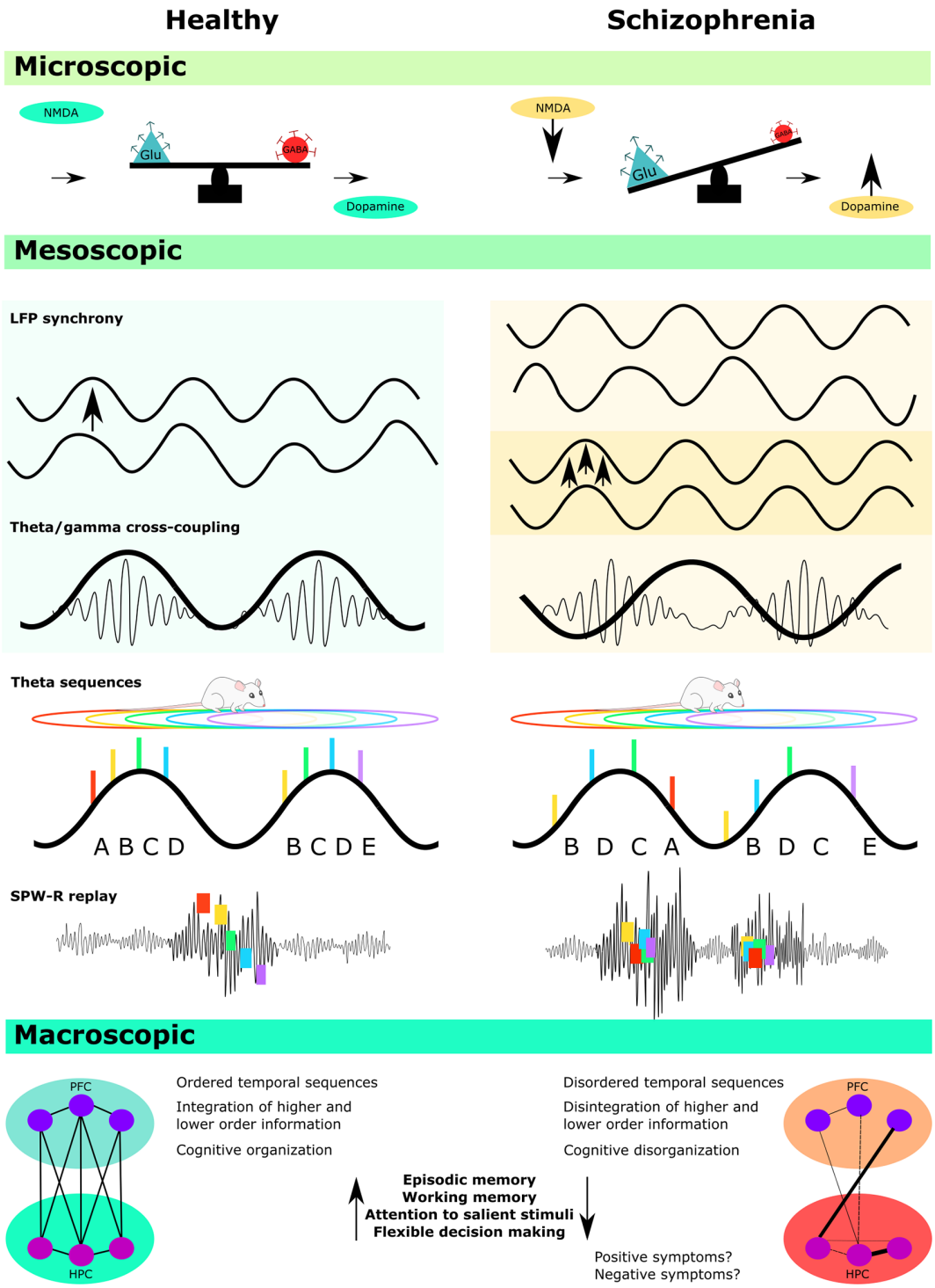

FIGURE 2 | Disorganized oscillatory activity provides the mesoscopic link between microscopic disruptions at the cellular and molecular level, and macroscopic outcomes for impaired cognition in schizophrenia. At the microscopic level, hypofunction at the site of NMDA receptors leads to an imbalance of excitatory/inhibitory regulation in schizophrenia. This in turn is thought to lead to dysregulation of dopamine transmission, with hyperdopaminergic activity predominant in sub-cortical regions. At the mesoscopic level, local field potential (LFP) synchrony is disturbed across several frequency bands, including theta and gamma. This can manifest as a desynchronized activity within and between hippocampal and prefrontal regions, and disturbed theta/gamma cross coupling. A failure to coordinate the spiking of single cells relative to the hippocampal theta rhythm also leads to disordered theta sequences and diminished neural syntax across multiple theta cycles, as well as a loss of structured replay activity during sharp-wave ripples. Finally, at the macroscopic level, these disturbances are thought to contribute to functional dysconnectivity across distributed networks. At the cognitive and behavioral levels, this manifests as diminished performance across a range of tasks.

likely to open up new pathways for animal research in this domain.

Finally, animal models of the disorder with good construct, face, and predictive validity have the potential to allow for the complex aetiological and developmental processes associated with schizophrenia to be unpacked, including the pathological trajectories that contribute to disorganized oscillatory at critical stages of neural development and maturation. At the present time, however, a number of research questions addressing these issues remain unanswered. Future studies that attempt to attenuate abnormal network synchrony and phase coding disturbances in animal models *via* administration of either antipsychotics or drugs that specifically target dysfunctional inhibitory networks, will help to clarify whether the disorganized oscillatory activity may be a viable target for preclinical interventions, as well as the development of novel treatments.

AUTHOR CONTRIBUTIONS

These authors have contributed equally to this work. All authors contributed to the article and approved the submitted version.

FUNDING

This work was supported through funding from the Health Research Council of New Zealand (grant number 19/044), the Neurological Foundation of New Zealand (grant number 1820-SPG), and the psychology department at the University of Otago.

ACKNOWLEDGMENTS

We would like to acknowledge our support team in the psychology department at the University of Otago.

REFERENCES

Adams, R. A., Bush, D., Zheng, F., Meyer, S. S., Kaplan, R., Orfanos, S., et al. (2020). Impaired theta phase coupling underlies frontotemporal dysconnectivity in schizophrenia. *Brain* 143, 1261–1277. doi: 10.1093/brain/awaa035

Aguilar, D. D., Radzik, L. K., Schiffino, F. L., Folorunso, O. O., Zielinski, M. R., Coyle, J. T., et al. (2021). Altered neural oscillations and behavior in a genetic mouse model of NMDA receptor hypofunction. *Sci. Rep.* 11:9031. doi: 10.1038/s41598-021-88428-9

Akbarian, S., and Huang, H.-S. (2006). Molecular and cellular mechanisms of altered GAD1/GAD67 expression in schizophrenia and related disorders. *Brain Res. Rev.* 52, 293–304. doi: 10.1016/j.brainresrev.2006.04.001

Allen, E. A., Liu, J., Kiehl, K. A., Gelernter, J., Pearlson, G. D., Perrone-Bizzozero, N. I., et al. (2011). Components of cross-frequency modulation in health and disease. *Front. Syst. Neurosci.* 5:59. doi: 10.3389/fnsys.2011.00059

Altimus, C., Harrold, J., Jaaro-Peled, H., Sawa, A., and Foster, D. J. (2015). Disordered ripples are a common feature of genetically distinct mouse models relevant to schizophrenia. *Mol. Neuropsychiatry* 1, 52–59. doi: 10.1159/000380765

Amilhon, B., Huh, C. Y., Manseau, F., Ducharme, G., Nichol, H., Adamantidis, A., et al. (2015). Parvalbumin interneurons of hippocampus tune population activity at theta frequency. *Neuron* 86, 1277–1289. doi: 10.1016/j.neuron.2015.05.027

Andersson, R. H., Johnston, A., Herman, P. A., Winzer-Serhan, U. H., Karavanova, I., Vullhorst, D., et al. (2012). Neuregulin and dopamine modulation of hippocampal gamma oscillations is dependent on dopamine D4 receptors. *Proc. Natl. Acad. Sci. U S A* 109, 13118–13123. doi: 10.1073/pnas.1201011109

Anderson, P. M., Pinault, D., O'Brien, T. J., and Jones, N. C. (2014). Chronic administration of antipsychotics attenuates ongoing and ketamine-induced increases in cortical γ oscillations. *Int. J. Neuropsychopharmacol.* 17, 1895–1904. doi: 10.1017/S1461145714000959

Andreasen, N. C., Nopoulos, P., O'Leary, D. S., Miller, D. D., Wassink, T., and Flaum, M. (1999). Defining the phenotype of schizophrenia: cognitive dysmetria and its neural mechanisms. *Biol. Psychiatry* 46, 908–920. doi: 10.1016/s0006-3223(99)00152-3

Andreou, C., Leicht, G., Nolte, G., Polomac, N., Moritz, S., Karow, A., et al. (2015). Resting-state theta-band connectivity and verbal memory in schizophrenia and in the high-risk state. *Schizophr. Res.* 161, 299–307. doi: 10.1016/j.schres.2014.12.018

Axmacher, N., Henseler, M. M., Jensen, O., Weinreich, I., Elger, C. E., and Fell, J. (2010). Cross-frequency coupling supports multi-item working memory in the human hippocampus. *Proc. Natl. Acad. Sci. U S A* 107, 3228–3233. doi: 10.1073/pnas.0911531107

Ball, T., Kern, M., Mutschler, I., Aertsen, A., and Schulze-Bonhage, A. (2009). Signal quality of simultaneously recorded invasive and non-invasive EEG. *NeuroImage* 46, 708–716. doi: 10.1016/j.neuroimage.2009.02.028

Ballendine, S. A., Greba, Q., Dawicki, W., Zhang, X., Gordon, J. R., and Howland, J. G. (2015). Behavioral alterations in rat offspring following maternal immune activation and ELR-CXC chemokine receptor antagonism during pregnancy: implications for neurodevelopmental psychiatric disorders. *Prog. Neuropsychopharmacol. Biol. Psychiatry* 57, 155–165. doi: 10.1016/j.pnpbp.2014.11.002

Balu, D. T. (2016). The NMDA receptor and schizophrenia: from pathophysiology to treatment. *Adv. Pharmacol.* 76, 351–382. doi: 10.1016/bs.apha.2016.01.006

Barch, D. M., and Ceaser, A. (2012). Cognition in schizophrenia: core psychological and neural mechanisms. *Trends Cogn. Sci.* 16, 27–34. doi: 10.1016/j.tics.2011.11.015

Barr, M., Farzan, F., Tran, L. C., Chen, R., Fitzgerald, P., and Daskalakis, Z. (2010). Evidence for excessive frontal evoked gamma oscillatory activity in schizophrenia during working memory. *Schizophr. Res.* 121, 146–152. doi: 10.1016/j.schres.2010.05.023

Barr, M. S., Rajji, T. K., Zomorrodi, R., Radhu, N., George, T. P., Blumberger, D. M., et al. (2017). Impaired theta-gamma coupling during working memory performance in schizophrenia. *Schizophr. Res.* 189, 104–110. doi: 10.1016/j.schres.2017.01.044

Barz, C. S., Bessaih, T., Abel, T., Feldmeyer, D., and Contreras, D. (2016). Sensory encoding in Neuregulin 1 mutants. *Brain Struct. Funct.* 221, 1067–1081. doi: 10.1007/s00429-014-0955-x

Basar-Eroglu, C., Brand, A., Hildebrandt, H., Kedzior, K. K., Mathes, B., and Schmiedt, C. (2007). Working memory related gamma oscillations in schizophrenia patients. *Int. J. Psychophysiol.* 64, 39–45. doi: 10.1016/j.ijpsycho.2006.07.007

Belforte, J. E., Zsiros, V., Sklar, E. R., Jiang, Z., Yu, G., Li, Y., et al. (2010). Postnatal NMDA receptor ablation in corticolimbic interneurons confers schizophrenia-like phenotypes. *Nat. Neurosci.* 13, 76–83. doi: 10.1038/nn.2447

Belluscio, M. A., Mizuseki, K., Schmidt, R., Kempter, R., and Buzsáki, G. (2012). Cross-frequency phase-phase coupling between theta and gamma oscillations in the hippocampus. *J. Neurosci.* 32, 423–435. doi: 10.1523/JNEUROSCI.4122-11.2012

Benchenane, K., Peyrache, A., Khamassi, M., Tierney, P. L., Gioanni, Y., Battaglia, F. P., et al. (2010). Coherent theta oscillations and reorganization of spike timing in the hippocampal-prefrontal network upon learning. *Neuron* 66, 921–936. doi: 10.1016/j.neuron.2010.05.013

Benes, F. M., Kwok, E. W., Vincent, S. L., and Todtenkopf, M. S. (1998). A reduction of nonpyramidal cells in sector CA2 of schizophrenics and manic depressives. *Biol. Psychiatry* 44, 88–97. doi: 10.1016/s0006-3223(98)00138-3

Berger, B., Minarik, T., Griesmayr, B., Stelzig-Schoeler, R., Aichhorn, W., and Sauseng, P. (2016). Brain oscillatory correlates of altered executive functioning

in positive and negative symptomatic schizophrenia patients and healthy controls. *Front. Psychol.* 7:705. doi: 10.3389/fpsyg.2016.00705

Berna, F., Potheegadoo, J., Aouadi, I., Ricarte, J. J., Alle, M. C., Coutelle, R., et al. (2016). A meta-analysis of autobiographical memory studies in schizophrenia spectrum disorder. *Schizophr. Bull.* 42, 56–66. doi: 10.1093/schbul/sbv099

Bi, G.-Q., and Poo, M.-M. (1998). Synaptic modifications in cultured hippocampal neurons: dependence on spike timing, synaptic strength and postsynaptic cell type. *J. Neurosci.* 18, 10464–10472. doi: 10.1523/JNEUROSCI.18-24-10464.1998

Bianciardi, B., and Uhlhaas, P. J. (2021). Do NMDA-R antagonists re-create patterns of spontaneous gamma-band activity in schizophrenia? A systematic review and perspective. *Neurosci. Biobehav. Rev.* 124, 308–323. doi: 10.1016/j.neubiorev.2021.02.005

Bieri, K. W., Bobbitt, K. N., and Colgin, L. L. (2014). Slow and fast gamma rhythms coordinate different spatial coding modes in hippocampal place cells. *Neuron* 82, 670–681. doi: 10.1016/j.neuron.2014.03.013

Bikbaev, A., and Manahan-Vaughan, D. (2007). Hippocampal network activity is transiently altered by induction of long-term potentiation in the dentate gyrus of freely behaving rats. *Front. Behav. Neurosci.* 1:7. doi: 10.3389/neuro.08.007.2007

Bikbaev, A., and Manahan-Vaughan, D. (2008). Relationship of hippocampal theta and gamma oscillations to potentiation of synaptic transmission. *Front. Neurosci.* 2, 56–63. doi: 10.3389/neuro.01.010.2008

Birnbaum, R., and Weinberger, D. R. (2017). Genetic insights into the neurodevelopmental origins of schizophrenia. *Nat. Rev. Neurosci.* 18, 727–740. doi: 10.1038/nrn.2017.125

Bitanihirwe, B. K., Peleg-Raibstein, D., Mouttet, F., Feldon, J., and Meyer, U. (2010). Late prenatal immune activation in mice leads to behavioral and neurochemical abnormalities relevant to the negative symptoms of schizophrenia. *Neuropsychopharmacology* 35, 2462–2478. doi: 10.1038/npp.2010.129

Boksa, P. (2010). Effects of prenatal infection on brain development and behavior: a review of findings from animal models. *Brain Behav. Immun.* 24, 881–897. doi: 10.1016/j.bbi.2010.03.005

Brankačk, J., Stewart, M., and Fox, S. E. (1993). Current source density analysis of the hippocampal theta rhythm: associated sustained potentials and candidate synaptic generators. *Brain Res.* 615, 310–327. doi: 10.1016/0006-8993(93)90043-m

Brébion, G., Amador, X., David, A., Malaspina, D., Sharif, Z., and Gorman, J. M. (2000). Positive symptomatology and source-monitoring failure in schizophrenia—an analysis of symptom-specific effects. *Psychiatry Res.* 95, 119–131. doi: 10.1016/s0165-1781(00)00174-8

Brenner, C. A., Krishnan, G. P., Vohs, J. L., Ahn, W.-Y., Hetrick, W. P., Morzorati, S. L., et al. (2009). Steady state responses: electrophysiological assessment of sensory function in schizophrenia. *Schizophr. Bull.* 35, 1065–1077. doi: 10.1093/schbul/sbp091

Brinkmann, B. G., Agarwal, A., Sereda, M. W., Garratt, A. N., Müller, T., Wende, H., et al. (2008). Neuregulin-1/ErbB signaling serves distinct functions in myelination of the peripheral and central nervous system. *Neuron* 59, 581–595. doi: 10.1016/j.neuron.2008.06.028

Brown, A. S., and Derkits, E. J. (2010). Prenatal infection and schizophrenia: a review of epidemiologic and translational studies. *Am. J. Psychiatry* 167, 261–280. doi: 10.1176/appi.ajp.2009.09030361

Brown, A. S., and Meyer, U. (2018). Maternal immune activation and neuropsychiatric illness: a translational research perspective. *Am. J. Psychiatry* 175, 1073–1083. doi: 10.1176/appi.ajp.2018.17121311

Bullmore, E., Frangou, S., and Murray, R. (1997). The dysplastic net hypothesis: an integration of developmental and dysconnectivity theories of schizophrenia. *Schizophr. Res.* 28, 143–156. doi: 10.1016/s0920-9964(97)00114-x

Buzsáki, G. (1986). Hippocampal sharp waves: their origin and significance. *Brain Res.* 398, 242–252. doi: 10.1016/0006-8993(86)91483-6

Buzsáki, G. (2006). *Rhythms of the Brain.* New York, NY: Oxford University Press.

Buzsáki, G. (2010). Neural syntax: cell assemblies, synapsembles, and readers. *Neuron* 68, 362–385. doi: 10.1016/j.neuron.2010.09.023

Buzsáki, G. (2015). Hippocampal sharp wave-ripple: a cognitive biomarker for episodic memory and planning. *Hippocampus* 25, 1073–1188. doi: 10.1002/hipo.22488

Buzsáki, G., and Draguhn, A. (2004). Neuronal oscillations in cortical networks. *Science* 304, 1926–1929. doi: 10.1126/science.1099745

Buzsáki, G., Logothetis, N., and Singer, W. (2013). Scaling brain size, keeping timing: evolutionary preservation of brain rhythms. *Neuron* 80, 751–764. doi: 10.1016/j.neuron.2013.10.002

Buzsáki, G., and Moser, E. I. (2013). Memory, navigation and theta rhythm in the hippocampal-entorhinal system. *Nat. Neurosci.* 16, 130–138. doi: 10.1038/nn.3304

Buzsáki, G., Rappelsberger, P., and Kellényi, L. (1985). Depth profiles of hippocampal rhythmic slow activity ('theta rhythm') depend on behaviour. *Electroencephalogr. Clin. Neurophysiol.* 61, 77–88. doi: 10.1016/0013-4694(85)91075-2

Buzsáki, G., and Tingley, D. (2018). Space and time: the hippocampus as a sequence generator. *Trends Cogn. Sci.* 22, 853–869. doi: 10.1016/j.tics.2018.07.006

Buzsáki, G., and Wang, X.-J. (2012). Mechanisms of gamma oscillations. *Annu. Rev. Neurosci.* 35, 203–225. doi: 10.1146/annurev-neuro-062111-150444

Bygrave, A. M., Jahans-Price, T., Wolff, A. R., Sprengel, R., Kullmann, D. M., Bannerman, D. M., et al. (2019). Hippocampal-prefrontal coherence mediates working memory and selective attention at distinct frequency bands and provides a causal link between schizophrenia and its risk gene GRIA1. *Transl. Psychiatry* 9:142. doi: 10.1038/s41398-019-0471-0

Caballero, A., Granberg, R., and Tseng, K. Y. (2016). Mechanisms contributing to prefrontal cortex maturation during adolescence. *Neurosci. Biobehav. Rev.* 70, 4–12. doi: 10.1016/j.neubiorev.2016.05.013

Cadinu, D., Grayson, B., Podda, G., Harte, M. K., Doostdar, N., and Neill, J. C. (2018). NMDA receptor antagonist rodent models for cognition in schizophrenia and identification of novel drug treatments, an update. *Neuropharmacology* 142, 41–62. doi: 10.1016/j.neuropharm.2017.11.045

Caixeta, F. V., Cornélio, A. M., Scheffer-Teixeira, R., Ribeiro, S., and Tort, A. B. (2013). Ketamine alters oscillatory coupling in the hippocampus. *Sci. Rep.* 3:2348. doi: 10.1038/srep02348

Canetta, S., Bolkan, S., Padilla-Coreano, N., Song, L., Sahn, R., Harrison, N., et al. (2016). Maternal immune activation leads to selective functional deficits in offspring parvalbumin interneurons. *Mol. Psychiatry* 21, 956–968. doi: 10.1038/mp.2015.222

Cannon, T. D. (2015). How schizophrenia develops: cognitive and brain mechanisms underlying onset of psychosis. *Trends Cogn. Sci.* 19, 744–756. doi: 10.1016/j.tics.2015.09.009

Cannon, T. D., Chung, Y., He, G., Sun, D., Jacobson, A., van Erp, T. G., et al. (2015). Progressive reduction in cortical thickness as psychosis develops: a multisite longitudinal neuroimaging study of youth at elevated clinical risk. *Biol. Psychiatry* 77, 147–157. doi: 10.1016/j.biopsych.2014.05.023

Cardno, A. G., Marshall, E. J., Coid, B., Macdonald, A. M., Ribchester, T. R., Davies, N. J., et al. (1999). Heritability estimates for psychotic disorders: the Maudsley twin psychosis series. *Arch. Gen. Psychiatry* 56, 162–168. doi: 10.1001/archpsyc.56.2.162

Carlén, M., Meletis, K., Siegle, J., Cardin, J., Futai, K., Vierling-Claassen, D., et al. (2012). A critical role for NMDA receptors in parvalbumin interneurons for gamma rhythm induction and behavior. *Mol. Psychiatry* 17, 537–548. doi: 10.1038/mp.2011.31

Cassella, S. N., Hemmerle, A. M., Lundgren, K. H., Kyser, T. L., Ahlbrand, R., Bronson, S. L., et al. (2016). Maternal immune activation alters glutamic acid decarboxylase-67 expression in the brains of adult rat offspring. *Schizophr. Res.* 171, 195–199. doi: 10.1016/j.schres.2016.01.041

Caton, M., Ochoa, E. L., and Barrantes, F. J. (2020). The role of nicotinic cholinergic neurotransmission in delusional thinking. *NPJ Schizophr.* 6:16. doi: 10.1038/s41537-020-0105-9

Catts, V. S., Lai, Y. L., Weickert, C. S., Weickert, T. W., and Catts, S. V. (2016). A quantitative review of the postmortem evidence for decreased cortical N-methyl-d-aspartate receptor expression levels in schizophrenia: how can we link molecular abnormalities to mismatch negativity deficits? *Biol. Psychol.* 116, 57–67. doi: 10.1016/j.biopsycho.2015.10.013

Cavanagh, J. F., and Frank, M. J. (2014). Frontal theta as a mechanism for cognitive control. *Trends Cogn. Sci.* 18, 414–421. doi: 10.1016/j.tics.2014.04.012

Cei, A., Girardeau, G., Drieu, C., El Kanbi, K., and Zugaro, M. (2014). Reversed theta sequences of hippocampal cell assemblies during backward travel. *Nat. Neurosci.* 17, 719–724. doi: 10.1038/nn.3698

Chini, M., Pöpplau, J. A., Lindemann, C., Carol-Perdiguer, L., Hnida, M., Oberländer, V., et al. (2020). Resolving and rescuing developmental miswiring in a mouse model of cognitive impairment. *Neuron* 105, 60–74.e7. doi: 10.1016/j.neuron.2019.09.042

Cho, R., Konecky, R., and Carter, C. S. (2006). Impairments in frontal cortical γ synchrony and cognitive control in schizophrenia. *Proc. Natl. Acad. Sci. U S A* 103, 19878–19883. doi: 10.1073/pnas.0609440103

Ciullo, V., Spalletta, G., Caltagirone, C., Jorge, R. E., and Piras, F. (2016). Explicit time deficit in schizophrenia: systematic review and meta-analysis indicate it is primary and not domain specific. *Schizophr. Bull.* 42, 505–518. doi: 10.1093/schbul/sbv104

Cobb, S., Buhl, E., Halasy, K., Paulsen, O., and Somogyi, P. (1995). Synchronization of neuronal activity in hippocampus by individual GABAergic interneurons. *Nature* 378, 75–78. doi: 10.1038/378075a0

Coffman, B. A., Haigh, S. M., Murphy, T. K., and Salisbury, D. F. (2016). Event-related potentials demonstrate deficits in acoustic segmentation in schizophrenia. *Schizophr. Res.* 173, 109–115. doi: 10.1016/j.schres.2016.03.012

Colgin, L. L. (2013). Mechanisms and functions of theta rhythms. *Annu. Rev. Neurosci.* 36, 295–312. doi: 10.1146/annurev-neuro-062012-170330

Colgin, L. L. (2016). Rhythms of the hippocampal network. *Nat. Rev. Neurosci.* 17:239. doi: 10.1038/nrn.2016.21

Colgin, L. L., Denninger, T., Fyhn, M., Hafting, T., Bonnevie, T., Jensen, O., et al. (2009). Frequency of gamma oscillations routes flow of information in the hippocampus. *Nature* 462, 353–357. doi: 10.1038/nature08573

Corradini, I., Focchi, E., Rasile, M., Morini, R., Desiato, G., Tomasoni, R., et al. (2018). Maternal immune activation delays excitatory-to-inhibitory gamma-aminobutyric acid switch in offspring. *Biol. Psychiatry* 83, 680–691. doi: 10.1016/j.biopsych.2017.09.030

Cousijn, H., Tunbridge, E. M., Rolinski, M., Wallis, G., Colclough, G. L., Woolrich, M. W., et al. (2015). Modulation of hippocampal theta and hippocampal-prefrontal cortex function by a schizophrenia risk gene. *Hum. Brain Mapp.* 36, 2387–2395. doi: 10.1002/hbm.22778

Coyle, J. T. (2004). The GABA-glutamate connection in schizophrenia: which is the proximate cause? *Biochem. Pharmacol.* 68, 1507–1514. doi: 10.1016/j.bcp.2004.07.034

Crum, W. R., Sawiak, S. J., Chege, W., Cooper, J. D., Williams, S. C. R., and Vernon, A. C. (2017). Evolution of structural abnormalities in the rat brain following in utero exposure to maternal immune activation: a longitudinal *in vivo* MRI study. *Brain Behav. Immun.* 63, 50–59. doi: 10.1016/j.bbi.2016.12.008

Csicsvari, J., Jamieson, B., Wise, K. D., and Buzsáki, G. (2003). Mechanisms of gamma oscillations in the hippocampus of the behaving rat. *Neuron* 37, 311–322. doi: 10.1016/s0896-6273(02)01169-8

Cunningham, M. O., Hunt, J., Middleton, S., LeBeau, F. E., Gillies, M. G., Davies, C. H., et al. (2006). Region-specific reduction in entorhinal gamma oscillations and parvalbumin-immunoreactive neurons in animal models of psychiatric illness. *J. Neurosci.* 26, 2767–2776. doi: 10.1523/JNEUROSCI.5054-05.2006

Dan, Y., and Poo, M.-M. (2004). Spike timing-dependent plasticity of neural circuits. *Neuron* 44, 23–30. doi: 10.1016/j.neuron.2004.09.007

Danion, J.-M., Cuervo, C., Piolino, P., Huron, C., Riutort, M., Peretti, C. S., et al. (2005). Conscious recollection in autobiographical memory: an investigation in schizophrenia. *Conscious. Cogn.* 14, 535–547. doi: 10.1016/j.concog.2005.01.005

Danion, J.-M., Huron, C., Vidailhet, P., and Berna, F. (2007). Functional mechanisms of episodic memory impairment in schizophrenia. *Can. J. Psychiatry* 52, 693–701. doi: 10.1177/070674370705201103

D'Argembeau, A., Raffard, S., and Van der Linden, M. (2008). Remembering the past and imagining the future in schizophrenia. *J. Abnorm. Psychol.* 117, 247–251. doi: 10.1037/0021-843X.117.1.247

Davidson, T. J., Kloosterman, F., and Wilson, M. A. (2009). Hippocampal replay of extended experience. *Neuron* 63, 497–507. doi: 10.1016/j.neuron.2009.07.027

De Lavilléon, G., Lacroix, M. M., Rondi-Reig, L., and Benchenane, K. (2015). Explicit memory creation during sleep demonstrates a causal role of place cells in navigation. *Nat. Neurosci.* 18, 493–495. doi: 10.1038/nn.3970

Deakin, I. H., Nissen, W., Law, A. J., Lane, T., Kanso, R., Schwab, M. H., et al. (2012). Transgenic overexpression of the type I isoform of neuregulin 1 affects working memory and hippocampal oscillations but not long-term potentiation. *Cereb. Cortex* 22, 1520–1529. doi: 10.1093/cercor/bhr223

Deane, A. R., Millar, J., Bilkey, D. K., and Ward, R. D. (2017). Maternal immune activation in rats produces temporal perception impairments in adult offspring analogous to those observed in schizophrenia. *PLoS One* 12:e0187719. doi: 10.1371/journal.pone.0187719

Del Pino, I., García-Frigola, C., Dehorter, N., Brotons-Mas, J. R., Alvarez-Salvado, E., de Lagrán, M. M., et al. (2013). Erbb4 deletion from fast-spiking interneurons causes schizophrenia-like phenotypes. *Neuron* 79, 1152–1168. doi: 10.1016/j.neuron.2013.07.010

Di Lorenzo, G., Daverio, A., Ferrentino, F., Santarnecchi, E., Ciabattini, F., Monaco, L., et al. (2015). Altered resting-state EEG source functional connectivity in schizophrenia: the effect of illness duration. *Front. Hum. Neurosci.* 9:234. doi: 10.3389/fnhum.2015.00234

Dickerson, D., Overeem, K., Wolff, A., Williams, J., Abraham, W., and Bilkey, D. (2014). Association of aberrant neural synchrony and altered GAD67 expression following exposure to maternal immune activation, a risk factor for schizophrenia. *Transl. Psychiatry* 4:e418. doi: 10.1038/tp.2014.64

Dickinson, D., Ramsey, M. E., and Gold, J. M. (2007). Overlooking the obvious: a meta-analytic comparison of digit symbol coding tasks and other cognitive measures in schizophrenia. *Arch. Gen. Psychiatry* 64, 532–542. doi: 10.1001/archpsyc.64.5.532

Dickerson, D. D., Restieaux, A. M., and Bilkey, D. K. (2012). Clozapine administration ameliorates disrupted long-range synchrony in a neurodevelopmental animal model of schizophrenia. *Schizophr. Res.* 135, 112–115. doi: 10.1016/j.schres.2011.12.016

Dickerson, D. D., Wolff, A. R., and Bilkey, D. K. (2010). Abnormal long-range neural synchrony in a maternal immune activation animal model of schizophrenia. *J. Neurosci.* 30, 12424–12431. doi: 10.1523/JNEUROSCI.3046-10.2010

Dragoi, G., and Buzsáki, G. (2006). Temporal encoding of place sequences by hippocampal cell assemblies. *Neuron* 50, 145–157. doi: 10.1016/j.neuron.2006.02.023

Drieu, C., and Zugaro, M. (2019). Hippocampal sequences during exploration: mechanisms and functions. *Front. Cell. Neurosci.* 13:232. doi: 10.3389/fncel.2019.00232

Ducharme, G., Lowe, G. C., Goutagny, R., and Williams, S. (2012). Early alterations in hippocampal circuitry and theta rhythm generation in a mouse model of prenatal infection: implications for schizophrenia. *PLoS One* 7:e29754. doi: 10.1371/journal.pone.0029754

Dzirasa, K., Ramsey, A. J., Takahashi, D. Y., Stapleton, J., Potes, J. M., Williams, J. K., et al. (2009). Hyperdopaminergia and NMDA receptor hypofunction disrupt neural phase signaling. *J. Neurosci.* 29, 8215–8224. doi: 10.1523/JNEUROSCI.1773-09.2009

Dzirasa, K., Ribeiro, S., Costa, R., Santos, L. M., Lin, S.-C., Grosmark, A., et al. (2006). Dopaminergic control of sleep-wake states. *J. Neurosci.* 26, 10577–10589. doi: 10.1523/JNEUROSCI.1767-06.2006

Ego-Stengel, V., and Wilson, M. A. (2010). Disruption of ripple-associated hippocampal activity during rest impairs spatial learning in the rat. *Hippocampus* 20, 1–10. doi: 10.1002/hipo.20707

Eichenbaum, H. (2014). Time cells in the hippocampus: a new dimension for mapping memories. *Nat. Rev. Neurosci.* 15, 732–744. doi: 10.1038/nrn3827

Eichenbaum, H. (2017a). On the integration of space, time, and memory. *Neuron* 95, 1007–1018. doi: 10.1016/j.neuron.2017.06.036

Eichenbaum, H. (2017b). The role of the hippocampus in navigation is memory. *J. Neurophysiol.* 117, 1785–1796. doi: 10.1152/jn.00005.2017

Eichenbaum, H., Dudchenko, P., Wood, E., Shapiro, M., and Tanila, H. (1999). The hippocampus, memory and place cells: is it spatial memory or a memory space? *Neuron* 23, 209–226. doi: 10.1016/s0896-6273(00)80773-4

Eisenberg, D. P., and Berman, K. F. (2010). Executive function, neural circuitry and genetic mechanisms in schizophrenia. *Neuropsychopharmacology* 35, 258–277. doi: 10.1038/npp.2009.111

Elvevag, B., and Goldberg, T. E. (2000). Cognitive impairment in schizophrenia is the core of the disorder. *Crit. Rev. Neurobiol.* 14, 1–21. doi: 10.1615/CritRevNeurobiol.v14.i1.10

Engel, A. K., Fries, P., and Singer, W. (2001). Dynamic predictions: oscillations and synchrony in top-down processing. *Nat. Rev. Neurosci.* 2, 704–716. doi: 10.1038/35094565

Fajnerová, I., Rodriguez, M., Levčík, D., Konrádová, L., Mikoláš, P., Brom, C., et al. (2014). A virtual reality task based on animal research-spatial learning and memory in patients after the first episode of schizophrenia. *Front. Behav. Neurosci.* 8:157. doi: 10.3389/fnbeh.2014.00157

Fatemi, S. H., and Folsom, T. D. (2009). The neurodevelopmental hypothesis of schizophrenia, revisited. *Schizophr. Bull.* 35, 528–548. doi: 10.1093/schbul/sbn187

Fazzari, P., Paternain, A. V., Valiente, M., Pla, R., Luján, R., Lloyd, K., et al. (2010). Control of cortical GABA circuitry development by Nrg1 and ErbB4 signalling. *Nature* 464, 1376–1380. doi: 10.1038/nature08928

Featherstone, R. E., Liang, Y., Saunders, J. A., Tatard-Leitman, V. M., Ehrlichman, R. S., and Siegel, S. J. (2012). Subchronic ketamine treatment leads to permanent changes in EEG, cognition and the astrocytic glutamate transporter EAAT2 in mice. *Neurobiol. Dis.* 47, 338–346. doi: 10.1016/j.nbd.2012.05.003

Fejgin, K., Nielsen, J., Birknow, M. R., Bastlund, J. F., Nielsen, V., Lauridsen, J. B., et al. (2014). A mouse model that recapitulates cardinal features of the 15q13. 3 microdeletion syndrome including schizophrenia-and epilepsy-related alterations. *Biol. Psychiatry* 76, 128–137. doi: 10.1016/j.biopsych.2013.08.014

Fell, J., Fernandez, G., Klaver, P., Elger, C. E., and Fries, P. (2003). Is synchronized neuronal gamma activity relevant for selective attention? *Brain Res. Brain Res. Rev.* 42, 265–272. doi: 10.1016/s0165-0173(03)00178-4

Feng, T., Silva, D., and Foster, D. J. (2015). Dissociation between the experience-dependent development of hippocampal theta sequences and single-trial phase precession. *J. Neurosci.* 35, 4890–4902. doi: 10.1523/JNEUROSCI.2614-14.2015

Fernandez, A., Dumon, C., Guimond, D., Tyzio, R., Bonifazi, P., Lozovaya, N., et al. (2018). The GABA developmental shift is abolished by maternal immune activation already at birth. *Cereb. Cortex* 29, 3982–3992. doi: 10.1093/cercor/bhy279

Fernández-Ruiz, A., Oliva, A., Nagy, G. A., Maurer, A. P., Berényi, A., and Buzsáki, G. (2017). Entorhinal-CA3 dual-input control of spike timing in the hippocampus by theta-gamma coupling. *Neuron* 93, 1213–1226. doi: 10.1016/j.neuron.2017.02.017

Fernández-Ruiz, A., Oliva, A., Soula, M., Rocha-Almeida, F., Nagy, G. A., Martin-Vazquez, G., et al. (2021). Gamma rhythm communication between entorhinal cortex and dentate gyrus neuronal assemblies. *Science* 372:eabf3119. doi: 10.1126/science.abf3119

Fisahn, A., Neddens, J., Yan, L., and Buonanno, A. (2009). Neuregulin-1 modulates hippocampal gamma oscillations: implications for schizophrenia. *Cereb. Cortex* 19, 612–618. doi: 10.1093/cercor/bhn107

Forbes, N., Carrick, L., McIntosh, A., and Lawrie, S. (2009). Working memory in schizophrenia: a meta-analysis. *Psychol. Med.* 39, 889–905. doi: 10.1017/S0033291708004558

Fornito, A., and Bullmore, E. T. (2015). Reconciling abnormalities of brain network structure and function in schizophrenia. *Curr. Opin. Neurobiol.* 30, 44–50. doi: 10.1016/j.conb.2014.08.006

Fornito, A., Zalesky, A., Pantelis, C., and Bullmore, E. T. (2012). Schizophrenia, neuroimaging and connectomics. *NeuroImage* 62, 2296–2314. doi: 10.1016/j.neuroimage.2011.12.090

Forsyth, J. K., and Lewis, D. A. (2017). Mapping the consequences of impaired synaptic plasticity in schizophrenia through development: an integrative model for diverse clinical features. *Trends Cogn. Sci.* 21, 760–778. doi: 10.1016/j.tics.2017.06.006

Foster, D. J., and Wilson, M. A. (2007). Hippocampal theta sequences. *Hippocampus* 17, 1093–1099. doi: 10.1002/hipo.20345

Frantseva, M., Cui, J., Farzan, F., Chinta, L. V., Perez Velazquez, J. L., and Daskalakis, Z. J. (2014). Disrupted cortical conductivity in schizophrenia: TMS-EEG study. *Cereb. Cortex* 24, 211–221. doi: 10.1093/cercor/bhs304

Freund, T. F., and Antal, M. (1988). GABA-containing neurons in the septum control inhibitory interneurons in the hippocampus. *Nature* 336, 170–173. doi: 10.1038/336170a0

Friston, K. J. (1998). The disconnection hypothesis. *Schizophr. Res.* 30, 115–125. doi: 10.1016/s0920-9964(97)00140-0

Friston, K., Brown, H. R., Siemerkus, J., and Stephan, K. E. (2016). The dysconnection hypothesis (2016). *Schizophr. Res.* 176, 83–94. doi: 10.1016/j.schres.2016.07.014

Fuchs, E. C., Zivkovic, A. R., Cunningham, M. O., Middleton, S., LeBeau, F. E., Bannerman, D. M., et al. (2007). Recruitment of parvalbumin-positive interneurons determines hippocampal function and associated behavior. *Neuron* 53, 591–604. doi: 10.1016/j.neuron.2007.01.031

Fung, S. J., Webster, M. J., Sivagnanasundaram, S., Duncan, C., Elashoff, M., and Weickert, C. S. (2010). Expression of interneuron markers in the dorsolateral prefrontal cortex of the developing human and in schizophrenia. *Am. J. Psychiatry* 167, 1479–1488. doi: 10.1176/appi.ajp.2010.09060784

Fusar-Poli, P., Deste, G., Smieskova, R., Barlati, S., Yung, A. R., Howes, O., et al. (2012). Cognitive functioning in prodromal psychosis: a meta-analysis. *Arch. Gen. Psychiatry* 69, 562–571. doi: 10.1001/archgenpsychiatry.2011.1592

Gao, M., Orita, K., and Ikegaya, Y. (2019). Maternal immune activation in pregnant mice produces offspring with altered hippocampal ripples. *Biol. Pharm. Bull.* 42, 666–670. doi: 10.1248/bpb.b19-00028

Garakh, Z., Zaytseva, Y., Kapranova, A., Fiala, O., Horacek, J., Shmukler, A., et al. (2015). EEG correlates of a mental arithmetic task in patients with first episode schizophrenia and schizoaffective disorder. *Clin. Neurophysiol.* 126, 2090–2098. doi: 10.1016/j.clinph.2014.12.031

Gilmore, J. H., and Jarskog, L. F. (1997). Exposure to infection and brain development: cytokines in the pathogenesis of schizophrenia. *Schizophr. Res.* 24, 365–367. doi: 10.1016/s0920-9964(96)00123-5

Girardeau, G., Benchenane, K., Wiener, S. I., Buzsáki, G., and Zugaro, M. B. (2009). Selective suppression of hippocampal ripples impairs spatial memory. *Nat. Neurosci.* 12, 1222–1223. doi: 10.1038/nn.2384

Glahn, D. C., Therman, S., Manninen, M., Huttunen, M., Kaprio, J., Lönnqvist, J., et al. (2003). Spatial working memory as an endophenotype for schizophrenia. *Biol. Psychiatry* 53, 624–626. doi: 10.1016/s0006-3223(02)01641-4

Godsil, B. P., Kiss, J. P., Spedding, M., and Jay, T. M. (2013). The hippocampal-prefrontal pathway: the weak link in psychiatric disorders? *Eur. Neuropsychopharmacol.* 23, 1165–1181. doi: 10.1016/j.euroneuro.2012.10.018

Gonzalez-Burgos, G., Cho, R. Y., and Lewis, D. A. (2015). Alterations in cortical network oscillations and parvalbumin neurons in schizophrenia. *Biol. Psychiatry* 77, 1031–1040. doi: 10.1016/j.biopsych.2015.03.010

Gonzalez-Burgos, G., and Lewis, D. A. (2012). NMDA receptor hypofunction, parvalbumin-positive neurons and cortical gamma oscillations in schizophrenia. *Schizophr. Bull.* 38, 950–957. doi: 10.1093/schbul/sbs010

Goutagny, R., Jackson, J., and Williams, S. (2009). Self-generated theta oscillations in the hippocampus. *Nat. Neurosci.* 12, 1491–1493. doi: 10.1038/nn.2440

Gray, C. M., König, P., Engel, A. K., and Singer, W. (1989). Oscillatory responses in cat visual cortex exhibit inter-columnar synchronization which reflects global stimulus properties. *Nature* 338, 334–337. doi: 10.1038/338334a0

Green, M. F. (1996). What are the functional consequences of neurocognitive deficits in schizophrenia? *Am. J. Psychiatry* 153, 321–330. doi: 10.1176/ajp.153.3.321

Grent, T., Gross, J., Goense, J., Wibral, M., Gajwani, R., Gumley, A. I., et al. (2018). Resting-state gamma-band power alterations in schizophrenia reveal E/I-balance abnormalities across illness-stages. *eLife* 7:e37799. doi: 10.7554/eLife.37799

Griesmayr, B., Berger, B., Stelzig-Schoeler, R., Aichhorn, W., Bergmann, J., and Sauseng, P. (2014). EEG theta phase coupling during executive control of visual working memory investigated in individuals with schizophrenia and in healthy controls. *Cogn. Affect. Behav. Neurosci.* 14, 1340–1355. doi: 10.3758/s13415-014-0272-0

Gupta, A. S., Van Der Meer, M. A., Touretzky, D. S., and Redish, A. D. (2012). Segmentation of spatial experience by hippocampal theta sequences. *Nat. Neurosci.* 15, 1032–1039. doi: 10.1038/nn.3138

Haenschel, C., Bittner, R. A., Waltz, J., Haertling, F., Wibral, M., Singer, W., et al. (2009). Cortical oscillatory activity is critical for working memory as revealed by deficits in early-onset schizophrenia. *J. Neurosci.* 29, 9481–9489. doi: 10.1523/JNEUROSCI.1428-09.2009

Haijma, S. V., Van Haren, N., Cahn, W., Koolschijn, P. C. M., Hulshoff Pol, H. E., and Kahn, R. S. (2013). Brain volumes in schizophrenia: a meta-analysis in over 18 000 subjects. *Schizophr. Bull.* 39, 1129–1138. doi: 10.1093/schbul/sbs118

Hakami, T., Jones, N. C., Tolmacheva, E. A., Gaudias, J., Chaumont, J., Salzberg, M., et al. (2009). NMDA receptor hypofunction leads to generalized and persistent aberrant γ oscillations independent of hyperlocomotion and the state of consciousness. *PLoS One* 4:e6755. doi: 10.1371/journal.pone.0006755

Hanlon, F. M., Weisend, M. P., Hamilton, D. A., Jones, A. P., Thoma, R. J., Huang, M., et al. (2006). Impairment on the hippocampal-dependent virtual Morris water task in schizophrenia. *Schizophr. Res.* 87, 67–80. doi: 10.1016/j.schres.2006.05.021

Hansen, I. H., Agerskov, C., Arvastson, L., Bastlund, J. F., Sørensen, H. B., and Herrik, K. F. (2019). Pharmaco-electroencephalographic responses in the rat differ between active and inactive locomotor states. *Eur. J. Neurosci.* 50, 1948–1971. doi: 10.1111/ejn.14373

Harrison, P. J. (2004). The hippocampus in schizophrenia: a review of the neuropathological evidence and its pathophysiological implications. *Psychopharmacology* 174, 151–162. doi: 10.1007/s00213-003-1761-y

Harrison, P. J. (2015). Recent genetic findings in schizophrenia and their therapeutic relevance. *J. Psychopharmacol.* 29, 85–96. doi: 10.1177/0269881114553647

Hartung, H., Cichon, N., De Feo, V., Riemann, S., Schildt, S., Lindemann, C., et al. (2016). From shortage to surge: a developmental switch in hippocampal-prefrontal coupling in a gene-environment model of neuropsychiatric disorders. *Cereb. Cortex* 26, 4265–4281. doi: 10.1093/cercor/bhw274

Hasselmo, M. E. (2005). What is the function of hippocampal theta rhythm?—Linking behavioral data to phasic properties of field potential and unit recording data. *Hippocampus* 15, 936–949. doi: 10.1002/hipo.20116

Hasselmo, M. E., and Stern, C. E. (2014). Theta rhythm and the encoding and retrieval of space and time. *NeuroImage* 85, 656–666. doi: 10.1016/j.neuroimage.2013.06.022

Heckers, S. (2001). Neuroimaging studies of the hippocampus in schizophrenia. *Hippocampus* 11, 520–528. doi: 10.1002/hipo.1068

Heckers, S., and Konradi, C. (2002). Hippocampal neurons in schizophrenia. *J. Neural Transm.* 109, 891–905. doi: 10.1007/s007020200073

Herweg, N. A., Solomon, E. A., and Kahana, M. J. (2020). Theta oscillations in human memory. *Trends Cogn. Sci.* 24, 208–227. doi: 10.1016/j.tics.2019.12.006

Heusser, A. C., Poeppel, D., Ezzyat, Y., and Davachi, L. (2016). Episodic sequence memory is supported by a theta-gamma phase code. *Nat. Neurosci.* 19, 1374–1380. doi: 10.1038/nn.4374

Hikida, T., Jaaro-Peled, H., Seshadri, S., Oishi, K., Hookway, C., Kong, S., et al. (2007). Dominant-negative DISC1 transgenic mice display schizophrenia-associated phenotypes detected by measures translatable to humans. *Proc. Natl. Acad. Sci. U S A* 104, 14501–14506. doi: 10.1073/pnas.0704774104

Hinkley, L. B., Owen, J. P., Fisher, M., Findlay, A. M., Vinogradov, S., and Nagarajan, S. S. (2010). Cognitive impairments in schizophrenia as assessed through activation and connectivity measures of magnetoencephalography (MEG) data. *Front. Hum. Neurosci.* 3:73. doi: 10.3389/neuro.09.073.2009

Hiyoshi, T., Kambe, D., Karasawa, J.-I., and Chaki, S. (2014). Differential effects of NMDA receptor antagonists at lower and higher doses on basal gamma band oscillation power in rat cortical electroencephalograms. *Neuropharmacology* 85, 384–396. doi: 10.1016/j.neuropharm.2014.05.037

Horváth, S., and Mirnics, K. (2015). Schizophrenia as a disorder of molecular pathways. *Biol. Psychiatry* 77, 22–28. doi: 10.1016/j.biopsych.2014.01.001

Hou, X.-J., Ni, K.-M., Yang, J.-M., and Li, X.-M. (2014). Neuregulin 1/ErbB4 enhances synchronized oscillations of prefrontal cortex neurons *via* inhibitory synapses. *Neuroscience* 261, 107–117. doi: 10.1016/j.neuroscience.2013.12.040

Howes, O. D., and Kapur, S. (2009). The dopamine hypothesis of schizophrenia: version III—the final common pathway. *Schizophr. Bull.* 35, 549–562. doi: 10.1093/schbul/sbp006

Howland, J., Cazakoff, B., and Zhang, Y. (2012). Altered object-in-place recognition memory, prepulse inhibition and locomotor activity in the offspring of rats exposed to a viral mimetic during pregnancy. *Neuroscience* 201, 184–198. doi: 10.1016/j.neuroscience.2011.11.011

Hudson, M., Rind, G., O'Brien, T., and Jones, N. (2016). Reversal of evoked gamma oscillation deficits is predictive of antipsychotic activity with a unique profile for clozapine. *Transl. Psychiatry* 6:e784. doi: 10.1038/tp.2016.51

Humphries, M. D., Wood, R., and Gurney, K. (2009). Dopamine-modulated dynamic cell assemblies generated by the GABAergic striatal microcircuit. *Neural Netw.* 22, 1174–1188. doi: 10.1016/j.neunet.2009.07.018

Huxter, J., Burgess, N., and O'Keefe, J. (2003). Independent rate and temporal coding in hippocampal pyramidal cells. *Nature* 425, 828–832. doi: 10.1038/nature02058

Insel, T. R. (2010). Rethinking schizophrenia. *Nature* 468, 187–193. doi: 10.1038/nature09552

Jablensky, A. (2000). Epidemiology of schizophrenia: the global burden of disease and disability. *Eur. Arch. Psychiatry Clin. Neurosci.* 250, 274–285. doi: 10.1007/s004060070002

Jacobs, N. S., Allen, T. A., Nguyen, N., and Fortin, N. J. (2013). Critical role of the hippocampus in memory for elapsed time. *J. Neurosci.* 33, 13888–13893. doi: 10.1523/JNEUROSCI.1733-13.2013

Jadi, M. P., Behrens, M. M., and Sejnowski, T. J. (2016). Abnormal gamma oscillations in N-methyl-D-aspartate receptor hypofunction models of schizophrenia. *Biol. Psychiatry* 79, 716–726. doi: 10.1016/j.biopsych.2015.07.005

Jaramillo, J., and Kempter, R. (2017). Phase precession: a neural code underlying episodic memory? *Curr. Opin. Neurobiol.* 43, 130–138. doi: 10.1016/j.conb.2017.02.006

Jardri, R., and Denève, S. (2013). Circular inferences in schizophrenia. *Brain* 136, 3227–3241. doi: 10.1093/brain/awt257

Javitt, D. C. (2009). Sensory processing in schizophrenia: neither simple nor intact. *Schizophr. Bull.* 35, 1059–1064. doi: 10.1093/schbul/sbp110

Javitt, D. C., Lee, M., Kantrowitz, J. T., and Martinez, A. (2018). Mismatch negativity as a biomarker of theta band oscillatory dysfunction in schizophrenia. *Schizophr. Res.* 191, 51–60. doi: 10.1016/j.schres.2017.06.023

Jensen, O., and Lisman, J. E. (2000). Position reconstruction from an ensemble of hippocampal place cells: contribution of theta phase coding. *J. Neurophysiol.* 83, 2602–2609. doi: 10.1152/jn.2000.83.5.2602

Ji, B., Wang, X., Pinto-Duarte, A., Kim, M., Caldwell, S., Young, J. W., et al. (2013). Prolonged ketamine effects in Sp4 hypomorphic mice: mimicking phenotypes of schizophrenia. *PLoS One* 8:e66327. doi: 10.1371/journal.pone.0066327

Johnson, A., and Redish, A. D. (2007). Neural ensembles in CA3 transiently encode paths forward of the animal at a decision point. *J. Neurosci.* 27, 12176–12189. doi: 10.1523/JNEUROSCI.3761-07.2007

Jones, N. C., Anderson, P., Rind, G., Sullivan, C., Van Den Buuse, M., and O'Brien, T. J. (2014). Effects of aberrant gamma frequency oscillations on prepulse inhibition. *Int. J. Neuropsychopharmacol.* 17, 1671–1681. doi: 10.1017/S1461145714000492

Jones, N. C., Reddy, M., Anderson, P., Salzberg, M. R., O'Brien, T. J., and Pinault, D. (2012). Acute administration of typical and atypical antipsychotics reduces EEG gamma power, but only the preclinical compound LY379268 reduces the ketamine-induced rise in gamma power. *Int. J. Neuropsychopharmacol.* 15, 657–668. doi: 10.1017/S1461145711000848

Jones, C., Watson, D., and Fone, K. (2011). Animal models of schizophrenia. *Br. J. Pharmacol.* 164, 1162–1194. doi: 10.1111/j.1476-5381.2011.01386.x

Jones, M. W., and Wilson, M. A. (2005). Phase precession of medial prefrontal cortical activity relative to the hippocampal theta rhythm. *Hippocampus* 15, 867–873. doi: 10.1002/hipo.20119

Jutras, M. J., Fries, P., and Buffalo, E. A. (2009). Gamma-band synchronization in the macaque hippocampus and memory formation. *J. Neurosci.* 29, 12521–12531. doi: 10.1523/JNEUROSCI.0640-09.2009

Kaar, S. J., Angelescu, I., Marques, T. R., and Howes, O. D. (2019). Pre-frontal parvalbumin interneurons in schizophrenia: a meta-analysis of post-mortem studies. *J. Neural Transm.* 126, 1637–1651. doi: 10.1007/s00702-019-02080-2

Kaefer, K., Malagon-Vina, H., Dickerson, D. D., O'Neill, J., Trossbach, S. V., Korth, C., et al. (2019). Disrupted-in-schizophrenia 1 overexpression disrupts hippocampal coding and oscillatory synchronization. *Hippocampus* 29, 802–816. doi: 10.1002/hipo.23076

Kahn, R. S., and Keefe, R. S. (2013). Schizophrenia is a cognitive illness: time for a change in focus. *JAMA Psychiatry* 70, 1107–1112. doi: 10.1001/jamapsychiatry.2013.155

Kahn, R. S., Sommer, I. E., Murray, R. M., Meyer-Lindenberg, A., Weinberger, D. R., Cannon, T. D., et al. (2015). Schizophrenia. *Nat. Rev. Dis. Primers* 1:15067. doi: 10.1038/nrdp.2015.67

Kalweit, A. N., Amanpour-Gharaei, B., Colitti-Klausnitzer, J., and Manahan-Vaughan, D. (2017). Changes in neuronal oscillations accompany the loss of hippocampal LTP that occurs in an animal model of psychosis. *Front. Behav. Neurosci.* 11:36. doi: 10.3389/fnbeh.2017.00036

Kamondi, A., Acsády, L., Wang, X. J., and Buzsáki, G. (1998). Theta oscillations in somata and dendrites of hippocampal pyramidal cells *in vivo*: activity-dependent phase-precession of action potentials. *Hippocampus* 8, 244–261. doi: 10.1002/(SICI)1098-1063(1998)8:3<244::AID-HIPO7>3.0.CO;2-J

Kao, H.-Y., Dvořák, D., Park, E., Kenney, J., Kelemen, E., and Fenton, A. A. (2017). Phencyclidine discoordinates hippocampal network activity but not place fields. *J. Neurosci.* 37, 12031–12049. doi: 10.1523/JNEUROSCI.0630-17.2017

Kaplan, R., Schuck, N. W., and Doeller, C. F. (2017). The role of mental maps in decision-making. *Trends Neurosci.* 40, 256–259. doi: 10.1016/j.tins.2017.03.002

Kaplan, R., Tauste Campo, A., Bush, D., King, J., Principe, A., Koster, R., et al. (2020). Human hippocampal theta oscillations reflect sequential dependencies during spatial planning. *Cogn. Neurosci.* 11, 122–131. doi: 10.1080/17588928.2019.1676711

Karakaş, S. (2020). A review of theta oscillation and its functional correlates. *Int. J. Psychophysiol.* 157, 82–99. doi: 10.1016/j.ijpsycho.2020.04.008

Karbasforoushan, H., and Woodward, N. D. (2012). Resting-state networks in schizophrenia. *Curr. Top. Med. Chem.* 12, 2404–2414. doi: 10.2174/156802612805289863

Kealy, J., Commins, S., and Lowry, J. P. (2017). The effect of NMDA-R antagonism on simultaneously acquired local field potentials and tissue oxygen levels in the brains of freely-moving rats. *Neuropharmacology* 116, 343–350. doi: 10.1016/j.neuropharm.2017.01.006

Kehrer, C., Dugladze, T., Maziashvili, N., Wójtowicz, A., Schmitz, D., Heinemann, U., et al. (2007). Increased inhibitory input to CA1 pyramidal cells alters hippocampal gamma frequency oscillations in the MK-801 model of acute psychosis. *Neurobiol. Dis.* 25, 545–552. doi: 10.1016/j.nbd.2006.10.015

Kentner, A. C., Bilbo, S. D., Brown, A. S., Hsiao, E. Y., McAllister, A. K., Meyer, U., et al. (2019). Maternal immune activation: reporting guidelines to improve the rigor, reproducibility and transparency of the model. *Neuropsychopharmacology* 44, 245–258. doi: 10.1038/s41386-018-0185-7

Kim, J. W., Lee, Y. S., Han, D. H., Min, K. J., Lee, J., and Lee, K. (2015). Diagnostic utility of quantitative EEG in un-medicated schizophrenia. *Neurosci. Lett.* 589, 126–131. doi: 10.1016/j.neulet.2014.12.064

Kirihara, K., Rissling, A. J., Swerdlow, N. R., Braff, D. L., and Light, G. A. (2012). Hierarchical organization of gamma and theta oscillatory dynamics in schizophrenia. *Biol. Psychiatry* 71, 873–880. doi: 10.1016/j.biopsych.2012.01.016

Kittelberger, K., Hur, E. E., Sazegar, S., Keshavan, V., and Kocsis, B. (2012). Comparison of the effects of acute and chronic administration of ketamine on hippocampal oscillations: relevance for the NMDA receptor hypofunction model of schizophrenia. *Brain Struct. Funct.* 217, 395–409. doi: 10.1007/s00429-011-0351-8

Kleinmans, M., and Bilkey, D. K. (2018). Reversal learning impairments in the maternal immune activation rat model of schizophrenia. *Behav. Neurosci.* 132, 520 –525. doi: 10.1037/bne0000275

Kocsis, B. (2012). Differential role of NR2A and NR2B subunits in N-methyl-D-aspartate receptor antagonist-induced aberrant cortical gamma oscillations. *Biol. Psychiatry* 71, 987–995. doi: 10.1016/j.biopsych.2011.10.002

König, T., Lehmann, D., Saito, N., Kuginuki, T., Kinoshita, T., and Koukkou, M. (2001). Decreased functional connectivity of EEG theta-frequency activity in first-episode, neuroleptic-naıve patients with schizophrenia: preliminary results. *Schizophr. Res.* 50, 55–60. doi: 10.1016/s0920-9964(00)00154-7

Korotkova, T., Fuchs, E. C., Ponomarenko, A., von Engelhardt, J., and Monyer, H. (2010). NMDA receptor ablation on parvalbumin-positive interneurons impairs hippocampal synchrony, spatial representations and working memory. *Neuron* 68, 557–569. doi: 10.1016/j.neuron.2010.09.017

Krajcovic, B., Fajnerova, I., Horacek, J., Kelemen, E., Kubik, S., Svoboda, J., et al. (2019). Neural and neuronal discoordination in schizophrenia: from ensembles through networks to symptoms. *Acta Physiol.* 226:e13282. doi: 10.1111/apha.13282

Krystal, J. H., Karper, L. P., Seibyl, J. P., Freeman, G. K., Delaney, R., Bremner, J. D., et al. (1994). Subanesthetic effects of the noncompetitive NMDA antagonist, ketamine, in humans: psychotomimetic, perceptual, cognitive and neuroendocrine responses. *Arch. Gen. Psychiatry* 51, 199–214. doi: 10.1001/archpsyc.1994.03950030035004

Kulikova, S. P., Tolmacheva, E. A., Anderson, P., Gaudias, J., Adams, B. E., Zheng, T., et al. (2012). Opposite effects of ketamine and deep brain stimulation on rat thalamocortical information processing. *Eur. J. Neurosci.* 36, 3407–3419. doi: 10.1111/j.1460-9568.2012.08263.x

Kvajo, M., McKellar, H., Arguello, P. A., Drew, L. J., Moore, H., MacDermott, A. B., et al. (2008). A mutation in mouse Disc1 that models a schizophrenia risk allele leads to specific alterations in neuronal architecture and cognition. *Proc. Natl. Acad. Sci. U S A* 105, 7076–7081. doi: 10.1073/pnas.0802615105

Lansink, C. S., Goltstein, P. M., Lankelma, J. V., McNaughton, B. L., and Pennartz, C. M. (2009). Hippocampus leads ventral striatum in replay of place-reward information. *PLoS Biol.* 7:e1000173. doi: 10.1371/journal.pbio.1000173

Laughlin, R. B., Pines, D., Schmalian, J., Stojković, B. P., and Wolynes, P. (2000). The middle way. *Proc. Natl. Acad. Sci. U S A* 97, 32–37. doi: 10.1073/pnas.97.1.32

Lazarewicz, M. T., Ehrlichman, R. S., Maxwell, C. R., Gandal, M. J., Finkel, L. H., and Siegel, S. J. (2010). Ketamine modulates theta and gamma oscillations. *J. Cogn. Neurosci.* 22, 1452–1464. doi: 10.1162/jocn.2009.21305

Leavitt, V. M., and Goldberg, T. E. (2009). Episodic memory in schizophrenia. *Neuropsychol. Rev.* 19, 312–323. doi: 10.1007/s11065-009-9107-0

Lee, H., Dvorak, D., Kao, H.-Y., Duffy, Á. M., Scharfman, H. E., and Fenton, A. A. (2012). Early cognitive experience prevents adult deficits in a neurodevelopmental schizophrenia model. *Neuron* 75, 714–724. doi: 10.1016/j.neuron.2012.06.016

Lee, J., Hudson, M. R., O'Brien, T. J., Nithianantharajah, J., and Jones, N. C. (2017). Local NMDA receptor hypofunction evokes generalized effects on gamma and high-frequency oscillations and behavior. *Neuroscience* 358, 124–136. doi: 10.1016/j.neuroscience.2017.06.039

Lee, A. K., and Wilson, M. A. (2002). Memory of sequential experience in the hippocampus during slow wave sleep. *Neuron* 36, 1183–1194. doi: 10.1016/s0896-6273(02)01096-6

Lee, G., and Zhou, Y. (2019). NMDAR hypofunction animal models of schizophrenia. *Front. Mol. Neurosci.* 12:185. doi: 10.3389/fnmol.2019.00185

Lemercier, C. E., Holman, C., and Gerevich, Z. (2017). Aberrant alpha and gamma oscillations *ex vivo* after single application of the NMDA receptor antagonist MK-801. *Schizophr. Res.* 188, 118–124. doi: 10.1016/j.schres.2017.01.017

Lenck-Santini, P.-P., Fenton, A. A., and Muller, R. U. (2008). Discharge properties of hippocampal neurons during performance of a jump avoidance task. *J. Neurosci.* 28, 6773–6786. doi: 10.1523/JNEUROSCI.5329-07.2008

Lesh, T. A., Niendam, T. A., Minzenberg, M. J., and Carter, C. S. (2011). Cognitive control deficits in schizophrenia: mechanisms and meaning. *Neuropsychopharmacology* 36, 316–338. doi: 10.1038/npp.2010.156

Lewis, D. A., Hashimoto, T., and Volk, D. W. (2005). Cortical inhibitory neurons and schizophrenia. *Nat. Rev. Neurosci.* 6, 312–324. doi: 10.1038/nrn1648

Li, S., Cullen, W. K., Anwyl, R., and Rowan, M. J. (2003). Dopamine-dependent facilitation of LTP induction in hippocampal CA1 by exposure to spatial novelty. *Nat. Neurosci.* 6, 526–531. doi: 10.1038/nn1049

Li, W., Zhou, Y., Jentsch, J. D., Brown, R. A., Tian, X., Ehninger, D., et al. (2007). Specific developmental disruption of disrupted-in-schizophrenia-1 function results in schizophrenia-related phenotypes in mice. *Proc. Natl. Acad. Sci. U S A* 104, 18280–18285. doi: 10.1073/pnas.0706900104

Liang, M., Zhou, Y., Jiang, T., Liu, Z., Tian, L., Liu, H., et al. (2006). Widespread functional disconnectivity in schizophrenia with resting-state functional magnetic resonance imaging. *Neuroreport* 17, 209–213. doi: 10.1097/01.wnr.0000198434.06518.b8

Lichtenstein, P., Yip, B. H., Björk, C., Pawitan, Y., Cannon, T. D., Sullivan, P. F., et al. (2009). Common genetic determinants of schizophrenia and bipolar disorder in Swedish families: a population-based study. *Lancet* 373, 234–239. doi: 10.1016/S0140-6736(09)60072-6

Light, G. A., Hsu, J. L., Hsieh, M. H., Meyer-Gomes, K., Sprock, J., Swerdlow, N. R., et al. (2006). Gamma band oscillations reveal neural network cortical coherence dysfunction in schizophrenia patients. *Biol. Psychiatry* 60, 1231–1240. doi: 10.1016/j.biopsych.2006.03.055

Lippmann, B., Barmashenko, G., and Funke, K. (2021). Effects of repetitive transcranial magnetic and deep brain stimulation on long-range synchrony

of oscillatory activity in a rat model of developmental schizophrenia. *Eur. J. Neurosci.* 53, 2848–2869. doi: 10.1111/ejn.15125

Lisman, J. (2005). The theta/gamma discrete phase code occuring during the hippocampal phase precession may be a more general brain coding scheme. *Hippocampus* 15, 913–922. doi: 10.1002/hipo.20121

Lisman, J., and Buzsáki, G. (2008). A neural coding scheme formed by the combined function of gamma and theta oscillations. *Schizophr. Bull.* 34, 974–980. doi: 10.1093/schbul/sbn060

Lisman, J. E., and Idiart, M. A. (1995). Storage of 7+/-2 short-term memories in oscillatory subcycles. *Science* 267, 1512–1515. doi: 10.1126/science.7878473

Lisman, J. E., and Jensen, O. (2013). The theta-gamma neural code. *Neuron* 77, 1002–1016. doi: 10.1016/j.neuron.2013.03.007

Liu, Y., Dolan, R. J., Kurth-Nelson, Z., and Behrens, T. E. (2019). Human replay spontaneously reorganizes experience. *Cell* 178, 640.e614–652.e614. doi: 10.1016/j.cell.2019.06.012

Lodge, D. J., Behrens, M. M., and Grace, A. A. (2009). A loss of parvalbumin-containing interneurons is associated with diminished oscillatory activity in an animal model of schizophrenia. *J. Neurosci.* 29, 2344–2354. doi: 10.1523/JNEUROSCI.5419-08.2009

Lodge, D. J., and Grace, A. A. (2007). Aberrant hippocampal activity underlies the dopamine dysregulation in an animal model of schizophrenia. *J. Neurosci.* 27, 11424–11430. doi: 10.1523/JNEUROSCI.2847-07.2007

Lodge, D. J., and Grace, A. A. (2008). Hippocampal dysfunction and disruption of dopamine system regulation in an animal model of schizophrenia. *Neurotox. Res.* 14, 97–104. doi: 10.1007/BF03033801

Lohani, S., Martig, A. K., Deisseroth, K., Witten, I. B., and Moghaddam, B. (2019). Dopamine modulation of prefrontal cortex activity is manifold and operates at multiple temporal and spatial scales. *Cell Rep.* 27, P99–114.E6. doi: 10.1016/j.celrep.2019.03.012

Lopez, A. D., Mathers, C. D., Ezzati, M., Jamison, D. T., and Murray, C. J. (2006). *Global Burden of Disease and Risk Factors.* Washington, DC: The World Bank.

Losonczy, A., Zemelman, B. V., Vaziri, A., and Magee, J. C. (2010). Network mechanisms of theta related neuronal activity in hippocampal CA1 pyramidal neurons. *Nat. Neurosci.* 13, 967–972. doi: 10.1038/nn.2597

Lubenov, E. V., and Siapas, A. G. (2009). Hippocampal theta oscillations are travelling waves. *Nature* 459:534. doi: 10.1038/nature08010

Luchicchi, A., Lecca, S., Melis, M., De Felice, M., Cadeddu, F., Frau, R., et al. (2016). Maternal immune activation disrupts dopamine system in the offspring. *Int. J. Neuropsychopharmacol.* 19:pyw007. doi: 10.1093/ijnp/pyw007

Luo, A. H., Tahsili-Fahadan, P., Wise, R. A., Lupica, C. R., and Aston-Jones, G. (2011). Linking context with reward: a functional circuit from hippocampal CA3 to ventral tegmental area. *Science* 333, 353–357. doi: 10.1126/science.1204622

Ma, J., and Leung, L.-W. S. (2000). Relation between hippocampal γ waves and behavioral disturbances induced by phencyclidine and methamphetamine. *Behav. Brain Res.* 111, 1–11. doi: 10.1016/s0166-4328(00)00138-8

Ma, J., and Leung, L. S. (2007). The supramammillo-septal-hippocampal pathway mediates sensorimotor gating impairment and hyperlocomotion induced by MK-801 and ketamine in rats. *Psychopharmacology* 191, 961–974. doi: 10.1007/s00213-006-0667-x

Maris, E., van Vugt, M., and Kahana, M. (2011). Spatially distributed patterns of oscillatory coupling between high-frequency amplitudes and low-frequency phases in human iEEG. *NeuroImage* 54, 836–850. doi: 10.1016/j.neuroimage.2010.09.029

Martin, B., Wittmann, M., Franck, N., Cermolacce, M., Berna, F., and Giersch, A. (2014). Temporal structure of consciousness and minimal self in schizophrenia. *Front. Psychol.* 5:1175. doi: 10.3389/fpsyg.2014.01175

McGrath, J., Saha, S., Chant, D., and Welham, J. (2008). Schizophrenia: a concise overview of incidence, prevalence and mortality. *Epidemiol. Rev.* 30, 67–76. doi: 10.1093/epirev/mxn001

McNally, J. M., McCarley, R. W., and Brown, R. E. (2013). Chronic ketamine reduces the peak frequency of gamma oscillations in mouse prefrontal cortex *ex vivo*. *Front. Psychiatry* 4:106. doi: 10.3389/fpsyt.2013.00106

Meck, W. H., Church, R. M., and Matell, M. S. (2013). Hippocampus, time and memory—A retrospective analysis. *Behav. Neurosci.* 127:642. doi: 10.1037/a0034201

Mednick, S., Huttunen, M. O., and Machón, R. A. (1994). Prenatal influenza infections and adult schizophrenia. *Schizophr. Bull.* 20, 263–267. doi: 10.1093/schbul/20.2.263

Mei, L., and Xiong, W.-C. (2008). Neuregulin 1 in neural development, synaptic plasticity and schizophrenia. *Nat. Rev. Neurosci.* 9, 437–452. doi: 10.1038/nrn2392

Meier, M. A., Lemercier, C. E., Kulisch, C., Kiss, B., Lendvai, B., Adham, N., et al. (2020). The novel antipsychotic cariprazine stabilizes gamma oscillations in rat hippocampal slices. *Br J. Pharmacol.* 177, 1622–1634. doi: 10.1111/bph.14923

Meyer, U., Feldon, J., and Fatemi, S. H. (2009a). *in vivo* rodent models for the experimental investigation of prenatal immune activation effects in neurodevelopmental brain disorders. *Neurosci. Biobehav. Rev.* 33, 1061–1079. doi: 10.1016/j.neubiorev.2009.05.001

Meyer, U., Feldon, J., and Yee, B. K. (2009b). A review of the fetal brain cytokine imbalance hypothesis of schizophrenia. *Schizophr. Bull.* 35, 959–972. doi: 10.1093/schbul/sbn022

Meyer, U., Nyffeler, M., Yee, B. K., Knuesel, I., and Feldon, J. (2008). Adult brain and behavioral pathological markers of prenatal immune challenge during early/middle and late fetal development in mice. *Brain Behav. Immun.* 22, 469–486. doi: 10.1016/j.bbi.2007.09.012

Minor, K. S., and Lysaker, P. H. (2014). Necessary, but not sufficient: links between neurocognition, social cognition and metacognition in schizophrenia are moderated by disorganized symptoms. *Schizophr. Res.* 159, 198–204. doi: 10.1016/j.schres.2014.08.005

Miyakawa, T., Leiter, L. M., Gerber, D. J., Gainetdinov, R. R., Sotnikova, T. D., Zeng, H., et al. (2003). Conditional calcineurin knockout mice exhibit multiple abnormal behaviors related to schizophrenia. *Proc. Natl. Acad. Sci. U S A* 100, 8987–8992. doi: 10.1073/pnas.1432926100

Moghaddam, B., and Javitt, D. (2012). From revolution to evolution: the glutamate hypothesis of schizophrenia and its implication for treatment. *Neuropsychopharmacology* 37, 4–15. doi: 10.1038/npp.2011.181

Molina, L. A., Skelin, I., and Gruber, A. J. (2014). Acute NMDA receptor antagonism disrupts synchronization of action potential firing in rat prefrontal cortex. *PLoS One* 9:e85842. doi: 10.1371/journal.pone.0085842

Moran, L. V., and Hong, L. E. (2011). High vs low frequency neural oscillations in schizophrenia. *Schizophr. Bull.* 37, 659–663. doi: 10.1093/schbul/sbr056

Muessig, L., Lasek, M., Varsavsky, I., Cacucci, F., and Wills, T. J. (2019). Coordinated emergence of hippocampal replay and theta sequences during post-natal development. *Curr. Biol.* 29, 834.e834–840.e834. doi: 10.1016/j.cub.2019.01.005

Mukai, J., Dhilla, A., Drew, L. J., Stark, K. L., Cao, L., MacDermott, A. B., et al. (2008). Palmitoylation-dependent neurodevelopmental deficits in a mouse model of 22q11 microdeletion. *Nat. Neurosci.* 11:1302. doi: 10.1038/nn.2204

Mukai, J., Tamura, M., Fénelon, K., Rosen, A. M., Spellman, T. J., Kang, R., et al. (2015). Molecular substrates of altered axonal growth and brain connectivity in a mouse model of schizophrenia. *Neuron* 86, 680–695. doi: 10.1016/j.neuron.2015.04.003

Murray, B. G., Davies, D. A., Molder, J. J., and Howland, J. G. (2017). Maternal immune activation during pregnancy in rats impairs working memory capacity of the offspring. *Neurobiol. Learn. Mem.* 141, 150–156. doi: 10.1016/j.nlm.2017.04.005

Nagy, D., Stoiljkovic, M., Menniti, F. S., and Hajós, M. (2016). Differential effects of an NR2B NAM and ketamine on synaptic potentiation and gamma synchrony: relevance to rapid-onset antidepressant efficacy. *Neuropsychopharmacology* 41, 1486–1494. doi: 10.1038/npp.2015.298

Nakamura, J. P., Schroeder, A., Hudson, M., Jones, N., Gillespie, B., Du, X., et al. (2019). The maternal immune activation model uncovers a role for the Arx gene in GABAergic dysfunction in schizophrenia. *Brain Behav. Immun.* 81, 161–171. doi: 10.1016/j.bbi.2019.06.009

Nakazawa, K., and Sapkota, K. (2020). The origin of NMDA receptor hypofunction in schizophrenia. *Pharmacol. Ther.* 205:107426. doi: 10.1016/j.pharmthera.2019.107426

Nakazawa, K., Zsiros, V., Jiang, Z., Nakao, K., Kolata, S., Zhang, S., et al. (2012). GABAergic interneuron origin of schizophrenia pathophysiology. *Neuropharmacology* 62, 1574–1583. doi: 10.1016/j.neuropharm.2011.01.022

Narayanan, N. S., Cavanagh, J. F., Frank, M. J., and Laubach, M. (2013). Common medial frontal mechanisms of adaptive control in humans and rodents. *Nat. Neurosci.* 16, 1888–1895. doi: 10.1038/nn.3549

Neddens, J., Fish, K. N., Tricoire, L., Vullhorst, D., Shamir, A., Chung, W., et al. (2011). Conserved interneuron-specific ErbB4 expression in frontal cortex of rodents, monkeys and humans: implications for schizophrenia. *Biol. Psychiatry* 70, 636–645. doi: 10.1016/j.biopsych.2011.04.016

Nguyen, A. T., Hetrick, W. P., O'Donnell, B. F., and Brenner, C. A. (2020). Abnormal beta and gamma frequency neural oscillations mediate auditory sensory gating deficit in schizophrenia. *J. Psychiatr. Res.* 124, 13–21. doi: 10.1016/j.jpsychires.2020.01.014

Niwa, M., Kamiya, A., Murai, R., Kubo, K.-I., Gruber, A. J., Tomita, K., et al. (2010). Knockdown of DISC1 by in utero gene transfer disturbs postnatal dopaminergic maturation in the frontal cortex and leads to adult behavioral deficits. *Neuron* 65, 480–489. doi: 10.1016/j.neuron.2010.01.019

Nour, M. M., Liu, Y., Arumuham, A., Kurth-Nelson, Z., and Dolan, R. J. (2021). Impaired neural replay of inferred relationships in schizophrenia. *Cell* 184, P4315–4328.E17. doi: 10.1016/j.cell.2021.06.012

Nyhus, E., and Curran, T. (2010). Functional role of gamma and theta oscillations in episodic memory. *Neurosci. Biobehav. Rev.* 34, 1023–1035. doi: 10.1016/j.neubiorev.2009.12.014

O'Keefe, J., and Dostrovsky, J. (1971). The hippocampus as a spatial map: preliminary evidence from unit activity in the freely-moving rat. *Brain Res.* 34, 171–175. doi: 10.1016/0006-8993(71)90358-1

O'Keefe, J., and Recce, M. L. (1993). Phase relationship between hippocampal place units and the EEG theta rhythm. *Hippocampus* 3, 317–330. doi: 10.1002/hipo.450030307

Olney, J. W., Newcomer, J. W., and Farber, N. B. (1999). NMDA receptor hypofunction model of schizophrenia. *J. Psychiatr. Res.* 33, 523–533. doi: 10.1016/s0022-3956(99)00029-1

Olypher, A. V., Klement, D., and Fenton, A. A. (2006). Cognitive disorganization in hippocampus: a physiological model of the disorganization in psychosis. *J. Neurosci.* 26, 158–168. doi: 10.1523/JNEUROSCI.2064-05.2006

Ozawa, K., Hashimoto, K., Kishimoto, T., Shimizu, E., Ishikura, H., and Iyo, M. (2006). Immune activation during pregnancy in mice leads to dopaminergic hyperfunction and cognitive impairment in the offspring: a neurodevelopmental animal model of schizophrenia. *Biol. Psychiatry* 59, 546–554. doi: 10.1016/j.biopsych.2005.07.031

Pantelis, C., Velakoulis, D., McGorry, P. D., Wood, S. J., Suckling, J., Phillips, L. J., et al. (2003). Neuroanatomical abnormalities before and after onset of psychosis: a cross-sectional and longitudinal MRI comparison. *Lancet* 361, 281–288. doi: 10.1016/S0140-6736(03)12323-9

Park, S., and Holzman, P. S. (1992). Schizophrenics show spatial working memory deficits. *Arch. Gen. Psychiatry* 49, 975–982. doi: 10.1001/archpsyc.1992.01820120063009

Park, S., Holzman, P. S., and Goldman-Rakic, P. S. (1995). Spatial working memory deficits in the relatives of schizophrenic patients. *Arch. Gen. Psychiatry* 52, 821–828. doi: 10.1001/archpsyc.1995.03950220031007

Pastalkova, E., Itskov, V., Amarasingham, A., and Buzsáki, G. (2008). Internally generated cell assembly sequences in the rat hippocampus. *Science* 321, 1322–1327. doi: 10.1126/science.1159775

Patrich, E., Piontkewitz, Y., Peretz, A., Weiner, I., and Attali, B. (2016). Maternal immune activation produces neonatal excitability defects in offspring hippocampal neurons from pregnant rats treated with poly I: C. *Sci. Rep.* 6:19106. doi: 10.1038/srep19106

Pavlides, C., and Winson, J. (1989). Influences of hippocampal place cell firing in the awake state on the activity of these cells during subsequent sleep episodes. *J. Neurosci.* 9, 2907–2918. doi: 10.1523/JNEUROSCI.09-08-02907.1989

Paylor, R., McIlwain, K. L., McAninch, R., Nellis, A., Yuva-Paylor, L. A., Baldini, A., et al. (2001). Mice deleted for the DiGeorge/velocardiofacial syndrome region show abnormal sensorimotor gating and learning and memory impairments. *Hum. Mol. Genet.* 10, 2645–2650. doi: 10.1093/hmg/10.23.2645

Pedersen, A., Siegmund, A., Ohrmann, P., Rist, F., Rothermundt, M., Suslow, T., et al. (2008). Reduced implicit and explicit sequence learning in first-episode schizophrenia. *Neuropsychologia* 46, 186–195. doi: 10.1016/j.neuropsychologia.2007.07.021

Perlstein, W. M., Carter, C. S., Noll, D. C., and Cohen, J. D. (2001). Relation of prefrontal cortex dysfunction to working memory and symptoms in schizophrenia. *Am. J. Psychiatry* 158, 1105–1113. doi: 10.1176/appi.ajp.158.7.1105

Pettersson-Yeo, W., Allen, P., Benetti, S., McGuire, P., and Mechelli, A. (2011). Dysconnectivity in schizophrenia: where are we now. *Neurosci. Biobehav. Rev.* 35, 1110–1124. doi: 10.1016/j.neubiorev.2010.11.004

Pfeiffer, B. E., and Foster, D. J. (2013). Hippocampal place-cell sequences depict future paths to remembered goals. *Nature* 497, 74–79. doi: 10.1038/nature12112

Phillips, K. G., Bartsch, U., McCarthy, A. P., Edgar, D. M., Tricklebank, M. D., Wafford, K. A., et al. (2012a). Decoupling of sleep-dependent cortical and hippocampal interactions in a neurodevelopmental model of schizophrenia. *Neuron* 76, 526–533. doi: 10.1016/j.neuron.2012.09.016

Phillips, K., Cotel, M., McCarthy, A., Edgar, D., Tricklebank, M., O'Neill, M., et al. (2012b). Differential effects of NMDA antagonists on high frequency and gamma EEG oscillations in a neurodevelopmental model of schizophrenia. *Neuropharmacology* 62, 1359–1370. doi: 10.1016/j.neuropharm.2011.04.006

Pinault, D. (2008). N-methyl d-aspartate receptor antagonists ketamine and MK-801 induce wake-related aberrant γ oscillations in the rat neocortex. *Biol. Psychiatry* 63, 730–735. doi: 10.1016/j.biopsych.2007.10.006

Piontkewitz, Y., Arad, M., and Weiner, I. (2011). Abnormal trajectories of neurodevelopment and behavior following in utero insult in the rat. *Biol. Psychiatry* 70, 842–851. doi: 10.1016/j.biopsych.2011.06.007

Piontkewitz, Y., Bernstein, H.-G., Dobrowolny, H., Bogerts, B., Weiner, I., and Keilhoff, G. (2012). Effects of risperidone treatment in adolescence on hippocampal neurogenesis, parvalbumin expression and vascularization following prenatal immune activation in rats. *Brain Behav. Immun.* 26, 353–363. doi: 10.1016/j.bbi.2011.11.004

Preston, A. R., and Eichenbaum, H. (2013). Interplay of hippocampus and prefrontal cortex in memory. *Curr. Biol.* 23, R764–R773. doi: 10.1016/j.cub.2013.05.041

Qasim, S. E., Fried, I., and Jacobs, J. (2020). Phase precession in the human hippocampus and entorhinal cortex. *bioRxiv* [Preprint]. doi: 10.1101/2020.09.06.285320

Rapoport, J., Giedd, J., and Gogtay, N. (2012). Neurodevelopmental model of schizophrenia: update 2012. *Mol. Psychiatry* 17, 1228–1238. doi: 10.1038/mp.2012.23

Reinhart, R. M., Zhu, J., Park, S., and Woodman, G. F. (2015). Synchronizing theta oscillations with direct-current stimulation strengthens adaptive control in the human brain. *Proc. Natl. Acad. Sci. U S A* 112, 9448–9453. doi: 10.1073/pnas.1504196112

Richmond, L. L., Gold, D. A., and Zacks, J. M. (2017). Event perception: translations and applications. *J. Appl. Res. Mem. Cogn.* 6, 111–120. doi: 10.1016/j.jarmac.2016.11.002

Royer, S., Zemelman, B. V., Losonczy, A., Kim, J., Chance, F., Magee, J. C., et al. (2012). Control of timing, rate and bursts of hippocampal place cells by dendritic and somatic inhibition. *Nat. Neurosci.* 15:769. doi: 10.1038/nn.3077

Rushe, T., Woodruff, P., Murray, R., and Morris, R. (1999). Episodic memory and learning in patients with chronic schizophrenia. *Schizophr. Res.* 35, 85–96. doi: 10.1016/s0920-9964(98)00117-0

Ryman, S. G., Cavanagh, J. F., Wertz, C. J., Shaff, N. A., Dodd, A. B., Stevens, B., et al. (2018). Impaired midline theta power and connectivity during proactive cognitive control in schizophrenia. *Biol. Psychiatry* 84, 675–683. doi: 10.1016/j.biopsych.2018.04.021

Sampaio, L. R. L., Borges, L. T., Silva, J. M., de Andrade, F. R. O., Barbosa, T. M., Oliveira, T. Q., et al. (2018). Average spectral power changes at the hippocampal electroencephalogram in schizophrenia model induced by ketamine. *Fundam. Clin. Pharmacol.* 32, 60–68. doi: 10.1111/fcp.12319

Sauer, J.-F., Strüber, M., and Bartos, M. (2015). Impaired fast-spiking interneuron function in a genetic mouse model of depression. *eLife* 4:e04979. doi: 10.7554/eLife.04979

Savanthrapadian, S., Wolff, A. R., Logan, B. J., Eckert, M. J., Bilkey, D. K., and Abraham, W. C. (2013). Enhanced hippocampal neuronal excitability and LTP persistence associated with reduced behavioral flexibility in the maternal immune activation model of schizophrenia. *Hippocampus* 23, 1395–1409. doi: 10.1002/hipo.22193

Schacter, D. L., Addis, D. R., and Szpunar, K. K. (2017). "Escaping the past: contributions of the hippocampus to future thinking and imagination," in *The Hippocampus From Cells to Systems*, eds D. E. Hannula and M. C. Duff (New York, NY: Springer), 439–465.

Schmidt, R., Diba, K., Leibold, C., Schmitz, D., Buzsáki, G., and Kempter, R. (2009). Single-trial phase precession in the hippocampus. *J. Neurosci.* 29, 13232–13241. doi: 10.1523/JNEUROSCI.2270-09.2009

Schmiedt, C., Brand, A., Hildebrandt, H., and Basar-Eroglu, C. (2005). Event-related theta oscillations during working memory tasks in patients with schizophrenia and healthy controls. *Cogn. Brain Res. Brain Res.* 25, 936–947. doi: 10.1016/j.cogbrainres.2005.09.015

Schoffelen, J. M., and Gross, J. (2009). Source connectivity analysis with MEG and EEG. *Hum. Brain Mapp.* 30, 1857–1865. doi: 10.1002/hbm.20745

Schomburg, E. W., Fernández-Ruiz, A., Mizuseki, K., Berényi, A., Anastassiou, C. A., Koch, C., et al. (2014). Theta phase segregation of input-specific gamma patterns in entorhinal-hippocampal networks. *Neuron* 84, 470–485. doi: 10.1016/j.neuron.2014.08.051

Schroeder, A., Nakamura, J. P., Hudson, M., Jones, N. C., Du, X., Sundram, S., et al. (2019). Raloxifene recovers effects of prenatal immune activation on cognitive task-induced gamma power. *Psychoneuroendocrinology* 110:104448. doi: 10.1016/j.psyneuen.2019.104448

Scoville, W. B., and Milner, B. (1957). Loss of recent memory after bilateral hippocampal lesions. *J. Neurol. Neurosurg. Psychiatry* 20:11. doi: 10.1136/jnnp.20.1.11

Sederberg, P. B., Schulze-Bonhage, A., Madsen, J. R., Bromfield, E. B., McCarthy, D. C., Brandt, A., et al. (2006). Hippocampal and neocortical gamma oscillations predict memory formation in humans. *Cereb. Cortex* 17, 1190–1196. doi: 10.1093/cercor/bhl030

Selemon, L., and Zecevic, N. (2015). Schizophrenia: a tale of two critical periods for prefrontal cortical development. *Transl. Psychiatry* 5, e623–e623. doi: 10.1038/tp.2015.115

Senior, T. J., Huxter, J. R., Allen, K., O'Neill, J., and Csicsvari, J. (2008). Gamma oscillatory firing reveals distinct populations of pyramidal cells in the CA1 region of the hippocampus. *J. Neurosci.* 28, 2274–2286. doi: 10.1523/JNEUROSCI.4669-07.2008

Senkowski, D., and Gallinat, J. (2015). Dysfunctional prefrontal gamma-band oscillations reflect working memory and other cognitive deficits in schizophrenia. *Biol. Psychiatry* 77, 1010–1019. doi: 10.1016/j.biopsych.2015.02.034

Shamir, A., Kwon, O.-B., Karavanova, I., Vullhorst, D., Leiva-Salcedo, E., Janssen, M. J., et al. (2012). The importance of the NRG-1/ErbB4 pathway for synaptic plasticity and behaviors associated with psychiatric disorders. *J. Neurosci.* 32, 2988–2997. doi: 10.1523/JNEUROSCI.1899-11.2012

Shen, S., Lang, B., Nakamoto, C., Zhang, F., Pu, J., Kuan, S.-L., et al. (2008). Schizophrenia-related neural and behavioral phenotypes in transgenic mice expressing truncated Disc1. *J. Neurosci.* 28, 10893–10904. doi: 10.1523/JNEUROSCI.3299-08.2008

Shirvalkar, P. R., Rapp, P. R., and Shapiro, M. L. (2010). Bidirectional changes to hippocampal theta-gamma comodulation predict memory for recent spatial episodes. *Proc. Natl. Acad. Sci. U S A* 107, 7054–7059. doi: 10.1073/pnas.0911184107

Siegel, M., Warden, M. R., and Miller, E. K. (2009). Phase-dependent neuronal coding of objects in short-term memory. *Proc. Natl. Acad. Sci. U S A* 106, 21341–21346. doi: 10.1073/pnas.0908193106

Siegert, R. J., Weatherall, M., and Bell, E. M. (2008). Is implicit sequence learning impaired in schizophrenia? A meta-analysis. *Brain Cogn.* 67, 351–359. doi: 10.1016/j.bandc.2008.02.005

Siekmeier, P. J., and Stufflebeam, S. M. (2010). Patterns of spontaneous magnetoencephalographic activity in schizophrenic patients. *J. Clin. Neurophysiol.* 27:179. doi: 10.1097/WNP.0b013e3181e0b20a

Sigurdsson, T., and Duvarci, S. (2016). Hippocampal-prefrontal interactions in cognition, behavior and psychiatric disease. *Front. Syst. Neurosci.* 9:190. doi: 10.3389/fnsys.2015.00190

Sigurdsson, T., Stark, K. L., Karayiorgou, M., Gogos, J. A., and Gordon, J. A. (2010). Impaired hippocampal-prefrontal synchrony in a genetic mouse model of schizophrenia. *Nature* 464, 763–767. doi: 10.1038/nature08855

Skaggs, W. E., McNaughton, B. L., Wilson, M. A., and Barnes, C. A. (1996). Theta phase precession in hippocampal neuronal populations and the compression of temporal sequences. *Hippocampus* 6, 149–172. doi: 10.1002/(SICI)1098-1063(1996)6:2<149::AID-HIPO6>3.0.CO;2-K

Smith, D. M., and Mizumori, S. J. (2006). Hippocampal place cells, context and episodic memory. *Hippocampus* 16, 716–729. doi: 10.1002/hipo.20208

Sohal, V. S., Zhang, F., Yizhar, O., and Deisseroth, K. (2009). Parvalbumin neurons and gamma rhythms enhance cortical circuit performance. *Nature* 459, 698–702. doi: 10.1038/nature07991

Sonnenschein, S. F., Gomes, F. V., and Grace, A. A. (2020). Dysregulation of midbrain dopamine system and the pathophysiology of schizophrenia. *Front. Psychiatry* 11:613. doi: 10.3389/fpsyt.2020.00613

Speers, L. J., Cheyne, K. R., Cavani, E., Hayward, T., Schmidt, R., and Bilkey, D. K. (2021). Hippocampal sequencing mechanisms are disrupted in a maternal immune activation model of schizophrenia risk. *J. Neurosci.* 41, 6954–6965. doi: 10.1523/JNEUROSCI.0730-21.2021

Spencer, K. M., Nestor, P. G., Perlmutter, R., Niznikiewicz, M. A., Klump, M. C., Frumin, M., et al. (2004). Neural synchrony indexes disordered perception and cognition in schizophrenia. *Proc. Natl. Acad. Sci. U S A* 101, 17288–17293. doi: 10.1073/pnas.0406074101

Spencer, K. M., Salisbury, D. F., Shenton, M. E., and McCarley, R. W. (2008). γ-band auditory steady-state responses are impaired in first episode psychosis. *Biol. Psychiatry* 64, 369–375. doi: 10.1016/j.biopsych.2008.02.021

Squire, L. R., Genzel, L., Wixted, J. T., and Morris, R. G. (2015). Memory consolidation. *Cold Spring Harb. Perspect Biol.* 7:a021766. doi: 10.1101/cshperspect.a021766

Starc, M., Murray, J. D., Santamauro, N., Savic, A., Diehl, C., Cho, Y. T., et al. (2017). Schizophrenia is associated with a pattern of spatial working memory deficits consistent with cortical disinhibition. *Schizophr. Res.* 181, 107–116. doi: 10.1016/j.schres.2016.10.011

Stark, E., Eichler, R., Roux, L., Fujisawa, S., Rotstein, H. G., and Buzsáki, G. (2013). Inhibition-induced theta resonance in cortical circuits. *Neuron* 80, 1263–1276. doi: 10.1016/j.neuron.2013.09.033

Stefansson, H., Petursson, H., Sigurdsson, E., Steinthorsdottir, V., Bjornsdottir, S., Sigmundsson, T., et al. (2002). Neuregulin 1 and susceptibility to schizophrenia. *Am. J. Hum. Genet.* 71, 877–892. doi: 10.1086/342734

Steullet, P., Cabungcal, J., Coyle, J., Didriksen, M., Gill, K., Grace, A., et al. (2017). Oxidative stress-driven parvalbumin interneuron impairment as a common mechanism in models of schizophrenia. *Mol. Psychiatry* 22, 936–943. doi: 10.1038/mp.2017.47

Stewart, M., and Fox, S. E. (1990). Do septal neurons pace the hippocampal theta rhythm. *Trends Neurosci.* 13, 163–169. doi: 10.1016/0166-2236(90)90040-h

Suh, J., Foster, D. J., Davoudi, H., Wilson, M. A., and Tonegawa, S. (2013). Impaired hippocampal ripple-associated replay in a mouse model of schizophrenia. *Neuron* 80, 484–493. doi: 10.1016/j.neuron.2013.09.014

Sullivan, P. F., Kendler, K. S., and Neale, M. C. (2003). Schizophrenia as a complex trait: evidence from a meta-analysis of twin studies. *Arch. Gen. Psychiatry* 60, 1187–1192. doi: 10.1001/archpsyc.60.12.1187

Sullivan, E. M., Timi, P., Hong, L. E., and O'Donnell, P. (2015). Reverse translation of clinical electrophysiological biomarkers in behaving rodents under acute and chronic NMDA receptor antagonism. *Neuropsychopharmacology* 40, 719–727. doi: 10.1038/npp.2014.228

Susser, E., Neugebauer, R., Hoek, H. W., Brown, A. S., Lin, S., Labovitz, D., et al. (1996). Schizophrenia after prenatal famine: further evidence. *Arch. Gen. Psychiatry* 53, 25–31. doi: 10.1001/archpsyc.1996.01830010027005

Takahashi, M., Nishida, H., David Redish, A., and Lauwereyns, J. (2014). Theta phase shift in spike timing and modulation of gamma oscillation: a dynamic code for spatial alternation during fixation in rat hippocampal area CA1. *J. Neurophysiol.* 111, 1601–1614. doi: 10.1152/jn.00395.2013

Tatard-Leitman, V. M., Jutzeler, C. R., Suh, J., Saunders, J. A., Billingslea, E. N., Morita, S., et al. (2015). Pyramidal cell selective ablation of N-methyl-D-aspartate receptor 1 causes increase in cellular and network excitability. *Biol. Psychiatry* 77, 556–568. doi: 10.1016/j.biopsych.2014.06.026

Terada, S., Sakurai, Y., Nakahara, H., and Fujisawa, S. (2017). Temporal and rate coding for discrete event sequences in the hippocampus. *Neuron* 94, P1248–1262.E4. doi: 10.1016/j.neuron.2017.05.024

Thoenes, S., and Oberfeld, D. (2017). Meta-analysis of time perception and temporal processing in schizophrenia: differential effects on precision and accuracy. *Clin. Psychol. Rev.* 54, 44–64. doi: 10.1016/j.cpr.2017.03.007

Ting, A. K., Chen, Y., Wen, L., Yin, D.-M., Shen, C., Tao, Y., et al. (2011). Neuregulin 1 promotes excitatory synapse development and function in GABAergic interneurons. *J. Neurosci.* 31, 15–25. doi: 10.1523/JNEUROSCI.2538-10.2011

Tingley, D., and Buzsáki, G. (2018). Transformation of a spatial map across the hippocampal-lateral septal circuit. *Neuron* 98, 1229–1242. doi: 10.1016/j.neuron.2018.04.028

Tort, A. B., Komorowski, R. W., Manns, J. R., Kopell, N. J., and Eichenbaum, H. (2009). Theta-gamma coupling increases during the learning of item-context associations. *Proc. Natl. Acad. Sci. U S A* 106, 20942–20947. doi: 10.1073/pnas.0911331106

Toulopoulou, T., Rabe-Hesketh, S., King, H., Murray, R., and Morris, R. (2003). Episodic memory in schizophrenic patients and their relatives. *Schizophr. Res.* 63, 261–271. doi: 10.1016/s0920-9964(02)00324-9

Trossbach, S., Bader, V., Hecher, L., Pum, M., Masoud, S., Prikulis, I., et al. (2016). Misassembly of full-length Disrupted-in-Schizophrenia 1 protein is linked to altered dopamine homeostasis and behavioral deficits. *Mol. Psychiatry* 21, 1561–1572. doi: 10.1038/mp.2015.194

Tulving, E. (1993). What is episodic memory. *Curr. Direct. Psychol. Sci.* 2, 67–70.

Uhlhaas, P. J. (2013). Dysconnectivity, large-scale networks and neuronal dynamics in schizophrenia. *Curr. Opin. Neurobiol.* 23, 283–290. doi: 10.1016/j.conb.2012.11.004

Uhlhaas, P. J., and Singer, W. (2010). Abnormal neural oscillations and synchrony in schizophrenia. *Nat. Rev. Neurosci.* 11, 100–113. doi: 10.1038/nrn2774

Uhlhaas, P. J., and Singer, W. (2015). Oscillations and neuronal dynamics in schizophrenia: the search for basic symptoms and translational opportunities. *Biol. Psychiatry* 77, 1001–1009. doi: 10.1016/j.biopsych.2014.11.019

Umbricht, D., Schmid, L., Koller, R., Vollenweider, F. X., Hell, D., and Javitt, D. C. (2000). Ketamine-induced deficits in auditory and visual context-dependent processing in healthy volunteers: implications for models of cognitive deficits in schizophrenia. *Arch. Gen. Psychiatry* 57, 1139–1147. doi: 10.1001/archpsyc.57.12.1139

Van Den Heuvel, M. P., and Fornito, A. (2014). Brain networks in schizophrenia. *Neuropsychol. Rev.* 24, 32–48. doi: 10.1007/s11065-014-9248-7

van der Meer, M. A., and Redish, A. D. (2011). Theta phase precession in rat ventral striatum links place and reward information. *J. Neurosci.* 31, 2843–2854. doi: 10.1523/JNEUROSCI.4869-10.2011

Vargha-Khadem, F., Gadian, D. G., Watkins, K. E., Connelly, A., Van Paesschen, W., and Mishkin, M. (1997). Differential effects of early hippocampal pathology on episodic and semantic memory. *Science* 277, 376–380. doi: 10.1126/science.277.5324.376

von der Malsburg, C. E., Phillps, W. A., and Singer, W. E. (2010). *Dynamic Coordination in the Brain: From Neurons to Mind*. Cambridge, MA: MIT Press.

Von Stein, A., and Sarnthein, J. (2000). Different frequencies for different scales of cortical integration: from local gamma to long range alpha/theta synchronization. *Int. J. Psychophysiol.* 38, 301–313. doi: 10.1016/s0167-8760(00)00172-0

Walsh, T., McClellan, J. M., McCarthy, S. E., Addington, A. M., Pierce, S. B., Cooper, G. M., et al. (2008). Rare structural variants disrupt multiple genes in neurodevelopmental pathways in schizophrenia. *Science* 320, 539–543. doi: 10.1126/science.1155174

Wang, H.-X., and Gao, W.-J. (2009). Cell type-specific development of NMDA receptors in the interneurons of rat prefrontal cortex. *Neuropsychopharmacology* 34, 2028–2040. doi: 10.1038/npp.2009.20

Wang, Y., Romani, S., Lustig, B., Leonardo, A., and Pastalkova, E. (2015). Theta sequences are essential for internally generated hippocampal firing fields. *Nat. Neurosci.* 18, 282–288. doi: 10.1038/nn.3904

Watanabe, Y., Someya, T., and Nawa, H. (2010). Cytokine hypothesis of schizophrenia pathogenesis: evidence from human studies and animal models. *Psychiatry Clin. Neurosci.* 64, 217–230. doi: 10.1111/j.1440-1819.2010.02094.x

Weniger, G., and Irle, E. (2008). Allocentric memory impaired and egocentric memory intact as assessed by virtual reality in recent-onset schizophrenia. *Schizophr. Res.* 101, 201–209. doi: 10.1016/j.schres.2008.01.011

Wikenheiser, A. M., and Redish, A. D. (2015). Hippocampal theta sequences reflect current goals. *Nat. Neurosci.* 18, 289–294. doi: 10.1038/nn.3909

Williams, S., and Boksa, P. (2010). Gamma oscillations and schizophrenia. *J. Psychiatry Neurosci.* 35, 75–77. doi: 10.1503/jpn.100021

Wilson, M. A., and McNaughton, B. L. (1994). Reactivation of hippocampal ensemble memories during sleep. *Science* 265, 676–679. doi: 10.1126/science.8036517

Wolff, A. R., and Bilkey, D. K. (2010). The maternal immune activation (MIA) model of schizophrenia produces pre-pulse inhibition (PPI) deficits in both juvenile and adult rats but these effects are not associated with maternal weight loss. *Behav. Brain Res.* 213, 323–327. doi: 10.1016/j.bbr.2010.05.008

Wolff, A. R., Cheyne, K. R., and Bilkey, D. K. (2011). Behavioural deficits associated with maternal immune activation in the rat model of schizophrenia. *Behav. Brain Res.* 225, 382–387. doi: 10.1016/j.bbr.2011.07.033

Wright, I. C., Rabe-Hesketh, S., Woodruff, P. W., David, A. S., Murray, R. M., and Bullmore, E. T. (2000). Meta-analysis of regional brain volumes in schizophrenia. *Am. J. Psychiatry* 157, 16–25. doi: 10.1176/ajp.157.1.16

Wulff, P., Ponomarenko, A. A., Bartos, M., Korotkova, T. M., Fuchs, E. C., Bähner, F., et al. (2009). Hippocampal theta rhythm and its coupling with gamma oscillations require fast inhibition onto parvalbumin-positive interneurons. *Proc. Natl. Acad. Sci. U S A* 106, 3561–3566. doi: 10.1073/pnas.0813176106

Zalla, T., Verlut, I., Franck, N., Puzenat, D., and Sirigu, A. (2004). Perception of dynamic action in patients with schizophrenia. *Psychiatry Res.* 128, 39–51. doi: 10.1016/j.psychres.2003.12.026

Zhang, Z. J., and Reynolds, G. P. (2002). A selective decrease in the relative density of parvalbumin-immunoreactive neurons in the hippocampus in schizophrenia. *Schizophr. Res.* 55, 1–10. doi: 10.1016/s0920-9964(01)00188-8

Zhang, Z., and van Praag, H. (2015). Maternal immune activation differentially impacts mature and adult-born hippocampal neurons in male mice. *Brain Behav. Immun.* 45, 60–70. doi: 10.1016/j.bbi.2014.10.010

Zhao, J., Zhu, H., Duan, K., Petralia, R. S., Wang, Y.-X., Gu, Q., et al. (2021). Dysbindin-1 regulates mitochondrial fission and gamma oscillations. *Mol. Psychiatry* doi: 10.1038/s41380-021-01038-9. [Epub ahead of print].

Zheng, C., Bieri, K. W., Hsiao, Y.-T., and Colgin, L. L. (2016). Spatial sequence coding differs during slow and fast gamma rhythms in the hippocampus. *Neuron* 89, 398–408. doi: 10.1016/j.neuron.2015.12.005

Zielinski, M. C., Shin, J. D., and Jadhav, S. P. (2019). Coherent coding of spatial position mediated by theta oscillations in the hippocampus and prefrontal cortex. *J. Neurosci.* 39, 4550–4565. doi: 10.1523/JNEUROSCI.0106-19.2019

Ziermans, T. B., Schothorst, P. F., Schnack, H. G., Koolschijn, P. C. M., Kahn, R. S., van Engeland, H., et al. (2012). Progressive structural brain changes during development of psychosis. *Schizophr. Bull.* 38, 519–530. doi: 10.1093/schbul/sbq113

Zuckerman, L., Rehavi, M., Nachman, R., and Weiner, I. (2003). Immune activation during pregnancy in rats leads to a postpubertal emergence of disrupted latent inhibition, dopaminergic hyperfunction and altered limbic morphology in the offspring: a novel neurodevelopmental model of schizophrenia. *Neuropsychopharmacology* 28, 1778–1789. doi: 10.1038/sj.npp.1300248

Zuckerman, L., and Weiner, I. (2005). Maternal immune activation leads to behavioral and pharmacological changes in the adult offspring. *J. Psychiatr. Res.* 39, 311–323. doi: 10.1016/j.jpsychires.2004.08.008

Conflict of Interest: The authors declare that the research was conducted in the absence of any commercial or financial relationships that could be construed as a potential conflict of interest.

frontiers in Neural Circuits

REVIEW
published: 27 October 2021
doi: 10.3389/fncir.2021.761812

Respiration-Driven Brain Oscillations in Emotional Cognition

Shani Folschweiller[1,2] *and Jonas-Frederic Sauer*[1]*

[1]*Institute for Physiology I, University of Freiburg, Freiburg, Germany,* [2]*Faculty of Biology, University of Freiburg, Freiburg, Germany*

Respiration paces brain oscillations and the firing of individual neurons, revealing a profound impact of rhythmic breathing on brain activity. Intriguingly, respiration-driven entrainment of neural activity occurs in a variety of cortical areas, including those involved in higher cognitive functions such as associative neocortical regions and the hippocampus. Here we review recent findings of respiration-entrained brain activity with a particular focus on emotional cognition. We summarize studies from different brain areas involved in emotional behavior such as fear, despair, and motivation, and compile findings of respiration-driven activities across species. Furthermore, we discuss the proposed cellular and network mechanisms by which cortical circuits are entrained by respiration. The emerging synthesis from a large body of literature suggests that the impact of respiration on brain function is widespread across the brain and highly relevant for distinct cognitive functions. These intricate links between respiration and cognitive processes call for mechanistic studies of the role of rhythmic breathing as a timing signal for brain activity.

Keywords: network, emotion, respiration, oscillations, embodied cognition, neuronal synchronization, neuronal circuits, slow oscillation

OPEN ACCESS

Edited by:
Gabrielle Girardeau, INSERM U839 Institut du Fer à Moulin (IFM), France

Reviewed by:
Adriano B. L. Tort, Federal University of Rio Grande do Norte, Brazil
Sophie Bagur, Audition Institute, Pasteur Institute, France
Nikolaos Karalis, Friedrich Miescher Institute for Biomedical Research (FMI), Switzerland

***Correspondence:**
Jonas-Frederic Sauer
jonas.sauer@physiologie.uni-freiburg.de

Received: *20 August 2021*
Accepted: *05 October 2021*
Published: *27 October 2021*

Citation:
Folschweiller S and Sauer J-F (2021) Respiration-Driven Brain Oscillations in Emotional Cognition. Front. Neural Circuits 15:761812. doi: 10.3389/fncir.2021.761812

INTRODUCTION

Breathing ensures the constant supply of oxygen to the organism while eliminating CO_2 that is produced during metabolic processes. The perpetual sequence of inspiration and expiration is generated by an intricate network of excitatory and inhibitory cells in the brainstem, in particular in the ventral respiratory group (see Feldman and Del Negro, 2006 for a review on the network mechanisms underlying the generation of the breathing rhythm). However, viewing breathing as a one-way process going out of the central nervous system (CNS) gives an incomplete picture. Rather, rhythmic breathing exerts a backward influence on the brain in form of rhythmically entrained brain oscillations. More than six decades ago, Adrian found in seminal recordings from hedgehogs that the olfactory bulbs (OBs), the first relay station of the olfactory pathway, show respiration-synchronous oscillations in the local field potential (LFP, Adrian, 1942). Further experiments revealed that these oscillations are propagated to olfactory areas such as the piriform cortex, giving rise to the hypothesis that respiration-synchronous oscillations might aid the processing of olfactory inputs (Fontanini and Bower, 2006). In recent years, an increasing number of studies additionally reported respiration-synchronous brain oscillations in various brain regions, including higher-order areas involved in cognitive functions (**Figure 1**; Ito et al., 2014; Lockmann et al., 2016; Nguyen Chi et al., 2016; Biskamp et al., 2017; Zhong et al., 2017; Karalis and Sirota, 2018; Moberly et al., 2018; Bagur et al., 2021).

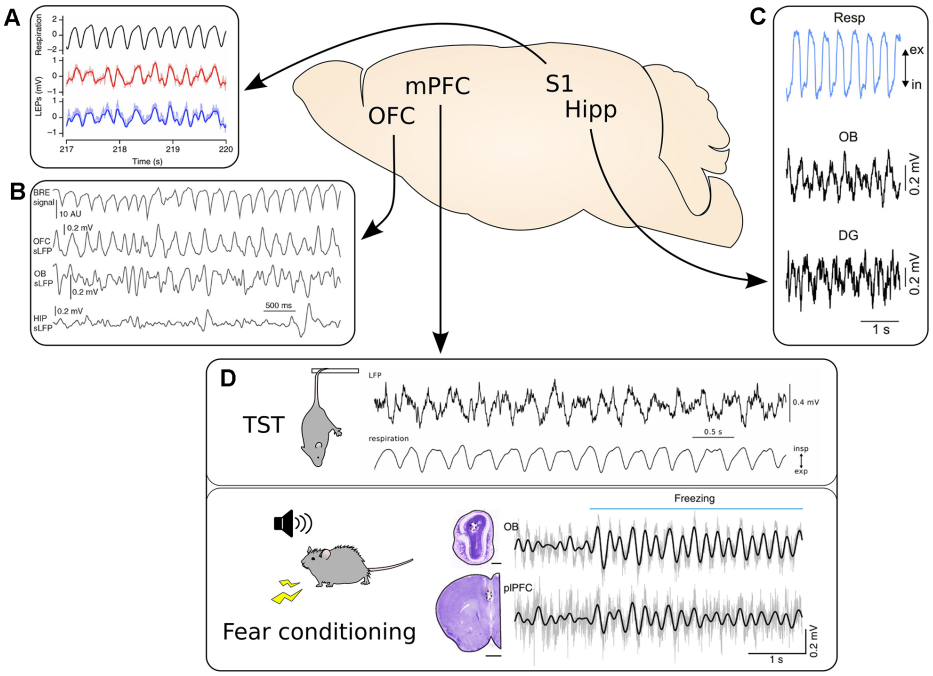

FIGURE 1 | Respiration-driven slow oscillations are widespread in the cortex. **(A)** Top, black: respiratory trace measured with a thermistor. Bottom, red/blue: LFP traces from two recording sites located 300 μm apart in the whisker barrel cortex during accelerated breathing induced by exposure to hypoxic air. Reprinted from Ito et al. (2014) under CC BY 4.0. **(B)** Video-based measuring of breathing (BRE signal, top) and simultaneous LFP recordings from OFC, OB, and hippocampus (HIP) during immobility. Reprinted from Kőszeghy et al. (2018) under CC BY 4.0. **(C)** Top, blue: respiration trace measured with a thermocouple. Middle and bottom, black: simultaneous LFP recordings from the OB and dentate gyrus (DG) of the hippocampus. Reprinted from Nguyen Chi et al. (2016) under CC BY 4.0. **(D)** The mPFC shows strong entrainment by respiration across a variety of behavioral states. Top: mPFC LFP recorded during immobility during the tail suspension test. Bottom: The simultaneous respiratory trace measured with a thermocouple. Adapted from Biskamp et al. (2017) under CC BY 4.0. Bottom: Synchronous LFP signal from the OB and prelimbic cortex (plPFC) recorded during auditory fear conditioning. Please note the increase in the amplitude of the 4 Hz rhythm in both LFP signals at freezing onset, indicated by the horizontal blue bar. Adapted from Moberly et al. (2018) under CC BY 4.0. *$p < 0.05$.

These data suggest that respiration-related oscillations [also called respiration rhythms (RRs)] might fulfill general functions in neuronal circuits that extend beyond the processing of olfactory inputs. In this review, we will discuss the relevance of RR for emotional cognition. We will start with the mechanism(s) giving rise to RR in the forebrain, describe where RR is found in networks involved in emotions, and focus then on the implications of these oscillations for cognitive processes. We will conclude with the most important points onto which further light should be shed.

MECHANISMS OF GENERATION OF RESPIRATION-DRIVEN BRAIN OSCILLATIONS

Building on the observations by Adrian, unit recording revealed that neurons in the OB are biased in their spiking by nasal airflow, irrespective of whether or not specific olfactory stimuli are presented (Macrides and Chorover, 1972). Calcium imaging from the axons of olfactory sensory neurons (OSNs) impinging on mitral cells, the main output neuron in the OB, furthermore showed that presynaptic activity is synchronized with nasal breathing, indicating that OSNs are receptive to air movement and transmit the air flow-induced activity to the OB (Carey et al., 2009). Direct recordings from OSNs indeed demonstrated that these neurons not only respond to specific odorants but are also mechanosensitive (Grosmaitre et al., 2007). Individual OSNs detect odorants through the expression of specific G-protein-coupled odorant receptors (Buck and Axel, 1991). Interestingly, the mechanosensitive properties of OSNs rely on the odorant receptors themselves (Connelly et al., 2015), with some but not all odorant receptor types being sensitive to nasal air movement. These data suggest that the RR activity in the OB is driven by airflow-induced spikes in a subset of OSNs.

Mitral and tufted cells in the OB synapse on neurons in the piriform cortex and other olfactory areas such as the anterior olfactory nucleus and entorhinal cortex (see Lane et al., 2020 for a review on olfactory sensory pathway), which connect to the neocortex. RR activity thus reaches the neocortex and hippocampus in a multi-synaptic pathway (Canning et al., 2000) and eventually gives rise to respiration-synchronized LFP oscillations, although the quantitative contributions of different anatomical routes remain to be established (**Figure 2**). There is indeed a causal relationship between nasal airflow, the OSN-OB system, and the occurrence of central RR: Tracheotomy, naris occlusion, chemical lesioning of OSNs with methimazole as well as removal or inactivation of the OB consistently eliminate RR oscillations in the neocortex and hippocampus (Ito et al., 2014;

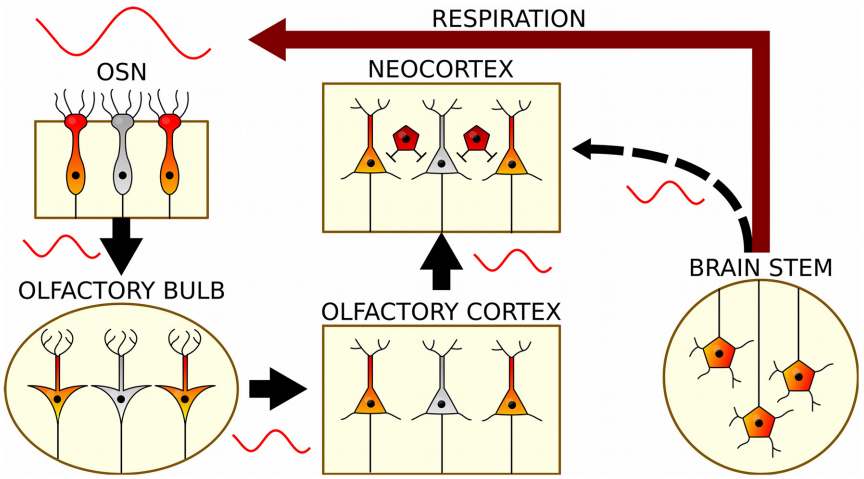

FIGURE 2 | The generation and propagation of respiration-related oscillations in the brain. Rhythmic breathing is generated in the brain stem and feeds back onto neocortical and hippocampal circuits *via* nasal airflow (red): Air movement through the nasal cavity excites OSNs, which transmit this rhythmic input to mitral and tufted cells of the OB. *Via* the olfactory cortex, RR reaches the neocortex and subcortical structures. In a presumed corollary discharge pathway, brain stem signals might in addition directly impose RR on cortical circuits (black).

Yanovsky et al., 2014; Biskamp et al., 2017; Moberly et al., 2018). In addition, respiration-synchronous cortical oscillations are absent when cats use oral instead of nasal breathing (Cavelli et al., 2020). Three lines of evidence support the notion that RR in the cortex reflects a "true" local signal rather than being volume-conducted from the OB. First, local neurons are modulated by ongoing RR. Both neocortical and hippocampal neurons discharge phase-coupled to RR (Yanovsky et al., 2014; Biskamp et al., 2017; Karalis and Sirota, 2018; Moberly et al., 2018; Bagur et al., 2021), and whole-cell recordings indicated respiration-synchronous subthreshold membrane oscillations in pyramidal neurons, initially in the piriform cortex (Fontanini et al., 2003) and more recently in the parietal cortex (Jung et al., 2019). Notably, these subthreshold oscillations are reduced when airflow through the nose is prevented by tracheotomy (Fontanini et al., 2003), further supporting the causal role of nasal airflow for cortical RRs. Second, current source density analysis identified respiration-synchronous current sinks in deep layers of the mPFC and in the hippocampal dentate gyrus (Lockmann et al., 2016; Karalis et al., 2016). Third, consistent with this result, Bagur et al. (2021) showed stronger coherence with the OB signal in deep than superficial layers of the mPFC.

While the origin and local nature of cortical RR LFP oscillations are thus well-validated, two key questions remain open: First, it is not entirely clear how the large-amplitude respiration-synchronous LFP is generated in the hippocampus and neocortex, or in other words how rhythmically oscillating discharges in axons from olfactory regions are translated into rhythmically active local populations ("translation problem"). A series of findings emphasize a central role of GABAergic interneurons in the generation of local RR: Single-unit recordings showed that a high proportion of GABAergic cells is phase-entrained by RR oscillations, and/or directly by rhythmic breathing, while the proportion of significantly coupled pyramidal cells is lower (Biskamp et al., 2017; Karalis and Sirota, 2018; Kőszeghy et al., 2018; Folschweiller and Sauer, 2021). Furthermore, subthreshold membrane oscillations in pyramidal cells of the parietal cortex seem to reflect inhibitory inputs, as they increase in amplitude when the holding potential is moved away from the reversal potential of GABAergic currents (Jung et al., 2019). It is thus possible that RR primarily relies on local interneurons, which might be rhythmically biased in their firing by long-range input from olfactory regions and impose the RR on the local pyramidal cell population. Silencing experiments and *in vivo* patch-clamp recordings from local interneurons should shed further light on that hypothesis in the future. Additionally, the neocortex of rodents responds best to specific frequencies of the respiration, with a peak correlation at 1.6 Hz in the barrel cortex of anesthetized animals (Ito et al., 2014), and a non linear entrainment of the mPFC LFP by optogenetic stimulation of the OB at a range of frequencies in sleeping mice (Bagur et al., 2021), suggesting that the resonance properties of the local cortical network might aid the broadcasting of the RR.

Second, it remains controversial to what extent nasal airflow-driven feedback contributes to the entrainment of cortical neurons. Ablation of OSNs by systemic application of methimazole (Bergman et al., 2002) has been reported to efficiently eliminate slow RR and RR-entrained fast gamma activities in the prefrontal cortex and hippocampus, but only partially affected the entrainment of local neurons to ongoing rhythmic breathing (Karalis and Sirota, 2018; Moberly et al., 2018). Karalis and Sirota (2018) suggested a corollary discharge or efference copy mechanism (Sperry, 1950; von Holst and Mittelstaedt, 1950) that transmits respiration-synchronous activity indirectly from the brainstem rhythm generator to the cortex (**Figure 2**). This mechanism might inform cortical circuits about the body movement caused by the act of

breathing to adjust proprioception accordingly. However, the anatomical underpinnings of the proposed corollary discharge mechanism are to date unknown. Neurons of the pre-Bötzinger complex, the primary site of generation of the RR, do not directly project to the neocortex (Yang and Feldman, 2017). Connections from pre-Bötzinger complex to the thalamus (Yang and Feldman, 2017), in particular the mediodorsal nucleus, and to the locus coeruleus (Yackle et al., 2017), which both project onwards to the forebrain, have been suggested as a potential anatomical substrate (Karalis and Sirota, 2018). Future work is needed to clarify the quantitative contribution of the presumed corollary discharge-induced entrainment of local circuits, ideally with methods that reversibly rather than chronically inactivate the OSN-OB-neocortex pathway.

THE ROLE OF RESPIRATION DRIVEN-OSCILLATIONS IN EMOTIONAL AND COGNITIVE CIRCUITS

The widespread occurrence of RR across the brain suggests an important role in the modulation of emotion and cognition. The breathing rhythm changes in frequency, regularity, and amplitude depending on emotional and arousal states, thus making it adapted to support cognition in different ways depending on the emotional context. Another hint of the importance of respiration in the forebrain is the highly conserved direct pathway to cortical areas of the olfactory system which, unlike other senses, bypasses the thalamus and is intricately connected with the limbic system. In the following segments, we will describe potential functions of RR for distinct states of emotional cognition.

The Role of RR in the Modulation of Fear Behavior

A particularly well-validated role of the RR in emotional cognition is its involvement in the regulation of fear behavior.

During auditory fear conditioning-induced freezing, the mPFC LFP and single units are strongly paced at the very regular 4 Hz frequency of the RR that mice exhibit in that state (**Figure 3A**; Karalis and Sirota, 2018; Moberly et al., 2018; Bagur et al., 2021), which seems to be the optimal breathing pattern to entrain cortical areas (Girin et al., 2021). Disrupting the olfactory sensorial afferences has been reported to increase the level of freezing (Moberly et al., 2018), to not affect freezing (Karalis and Sirota, 2018), or to decrease the length of freezing bouts, in the latter case highlighting a role of the RR in the maintenance of freezing (Bagur et al., 2021). These contradicting results on whether the RR supports or opposes freezing could be imputed to the fact that the mPFC, which is strongly entrained by RR during that behavior, can have bidirectional effects on the level of freezing (Sierra-Mercado et al., 2011). In addition, technical aspects might play a role: Bagur et al. (2021) recently showed that systemic application of methimazole, which was used to ablate OSNs in two studies reporting enhanced or unaltered levels of freezing (Moberly et al., 2018; Karalis and Sirota, 2018), results in enhanced freezing-like states in the absence of aversive foot shocks. These data suggest that unspecific behavioral alterations might confound the interpretation of OSN ablation on fear memory using this approach. In support of a role of the RR in the maintenance of freezing, previous work on putative RR in the mPFC, i.e., a 4 Hz rhythm entraining the mPFC LFP during freezing, showed that closed-loop optogenetic inhibition of the mPFC "in-phase" of the local 4 Hz rhythm disrupted freezing, while inhibition out of phase had the opposite effect (Dejean et al., 2016). Another study of the putative RR suggests it has a role in information flow from the mPFC to the basolateral amygdala (BLA; **Figure 3B**; Karalis et al., 2016). Interestingly, the part of the amygdala involved in conditioned fear, the BLA, and the PFC, do not receive direct projections from the OB. Nonetheless, the mPFC is likely entrained by the OB during freezing by a multisynaptic pathway (**Figure 3A**; Moberly et al., 2018; Bagur et al., 2021) as retrograde tracing from the mPFC did not reveal any direct projections from the OB, but optogenetic stimulation of the OB at different frequencies did result in entrainment of the mPFC LFP in a non-linear manner, implying an active propagation mechanism. So far, no simultaneous recording of the BLA LFP and respiration during freezing has been reported, but the respiration-paced BLA activity under neutral conditions (i.e., in the animal's home cage; **Figure 3C**; Karalis and Sirota, 2018) together with the high coherence with the mPFC LFP at 4 Hz during freezing strongly imply that the BLA is entrained by the RR during freezing. Altogether, these studies suggest a role of the RR in mediating communication between the mPFC and the BLA to control fear behavior.

The amygdala can be divided into several sub-regions with different connectivity and behavioral correlate. While the BLA, as mentioned above, does not receive direct input from the OB, the cortical amygdala (CoA) and the medial amygdala (MeA) are directly targeted by the main OB and involved in odor induced innate fear (Root et al., 2014; Isosaka et al., 2015). The projections from the main OB to the amygdala thus constitute a potential direct entry point for the RR to pace neuronal activity related to fear expression. Interestingly, the mPFC is also entrained by the RR during innate fear induced with odorants (Karalis and Sirota, 2018), and the IL cortex, which has the strongest entrainment by the RR, has direct projections to the CoA and MeA (Mcdonald et al., 1996). One could speculate that the IL synchronizes its activity *via* the RR to regulate the activity of the amygdala in innate fear behaviors in rodents as well.

So far, most of the studies about the role of the RR in fear were conducted on rodents, but the few experiments conducted on other species suggest that the entrainment of the amygdala by the RR is highly conserved in mammals. In cats, approximately 10% of the central amygdala cells fire respiration-synchronized in a neutral state (Zhang et al., 1986). In humans, the direct projections from the OB to the MeA and the CoA are also conserved (Lane et al., 2020), and faster brain oscillations have been shown to be phase-locked with the respiration in the amygdala during anticipation of an electric shock (Masaoka and Homma, 2000). Furthermore, it seems that breathing with a pattern characteristic of fear can generate feelings of fear, anxiety,

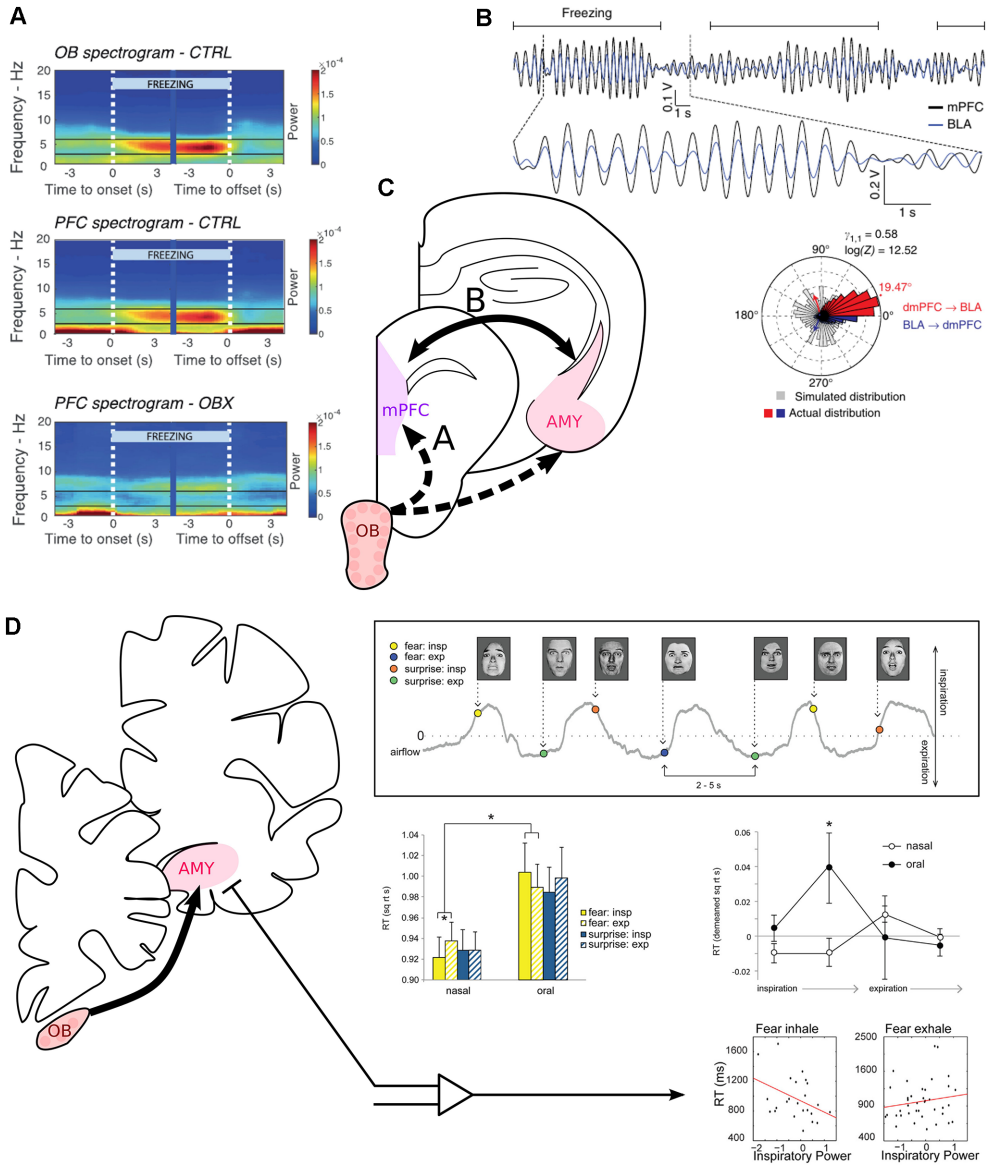

FIGURE 3 | Modulation of fear-related neural correlates and recognition of fearful faces by respiration. **(A)** The mPFC is entrained at 4 Hz by RR sensorial afferences during freezing. Spectrogram averaged across mice at freezing onset and offset, indicated by the white vertical dashed lines. Power spectra of the OB (top) and medial prefrontal cortex (PFC, middle) of control mice. Bottom: Power spectrum of the PFC of mice after bulbectomy. Reprinted from Bagur et al. (2021) under CC BY 4.0. **(B)** The mPFC and the basolateral amygdala (BLA) are highly coherent at 4 Hz during freezing. Top: Bandpass filtered 2–6 Hz LFP signals of the mPFC (black) and the simultaneously recorded BLA LFP (blue) during recall of conditioned fear. Freezing epochs are indicated by the horizontal black lines. Bottom: Phase difference between the mPFC and the amygdala (Red: above 0° of phase difference, mPFC phase precedes BLA phase. Blue: Below 360°, BLA phase precedes mPFC phase. Gray: simulated phase differences obtained by bootstrapping). Adapted by permission from Springer Nature, Nature Neuroscience, Karalis et al. (2016), copyright (2016). **(C)** The periamygdaloid cortex receives direct projection from the OB. BLA units are furthermore paced by RR in the home cage (Karalis and Sirota, 2018). **(D)** Inspiration facilitates the recognition of fearful faces. Top right, experimental paradigm: subjects had to discriminate between fearful or surprised faces presented at jittering interval of 2–5 s during nasal or oral breathing (gray line). Middle left: reaction time to recognize expressions for each emotion (yellow: fear, blue: surprise), depending on the phase of respiration (full: inspiration, dashed: expiration) and the breathing route. Middle right: Detrended reaction time for the recognition of fear for four phases of the breathing cycle. Oral breathing induced an increase in the reaction time during late inspiration. Bottom: Correlation between reaction time and the mean z-scored power in the delta band during the whole inspiration or expiration time window. On the left, "Fear inhale" shows the results for fearful faces presented during inspiration, and "Fear exhale" the results for fearful faces presented during expiration. Reprinted from Zelano et al. (2016) under CC BY 4.0. *$p < 0.05$.

and anger (Philippot et al., 2002), but it is still not known whether the activation of the direct projection from the OB to the amygdala, by odorants or airflow, is sufficient to trigger fear in humans. Nonetheless, sensorial reafferences coming from nasal breathing do influence another fear-related cognitive process, which is fear recognition.

The Role of the RR in Fear Recognition

In the amygdala, different sub-bands of the LFP, including delta, appear to be phase lock with inspiration during nasal breathing in humans (Zelano et al., 2016). Odors still play a facilitating role in visual fear recognition in humans (Kamiloglu et al., 2018), perhaps *via* direct projection from the OB onto the periamygdaloid cortex (Lane et al., 2020), which is involved in the recognition of fearful faces (Morris et al., 1996). But more interestingly, even in the absence of fear-related odorants, breathing in through the nose was also found to facilitate the recognition of fearful but not surprised faces (**Figure 3D**; Zelano et al., 2016). In one subject from whom the authors measured the amygdala LFP during the task, they observed that the patient was faster at the recognition of fear when the amygdala delta inspiratory power was higher. Importantly, the work of Zelano et al. (2016) shows that the RR influences the recognition of fear in humans in the absence of specific smells, potentially *via* an inspiration-triggered resetting of the local oscillations.

Overall, the sensorial afferences coming from the olfactory system can modulate fear-related behavior and cognition without carrying olfactory components, suggesting that the RR plays a role in different fear-related processes, potentially *via* the projection from the OB to the amygdala.

Potential Implications of RR in Other Emotional States

Despair

Besides fear, another strong negative emotional state paired with high arousal during which respiration seems to play a key role is despair-like behavioral responses to an unavoidable acute stress. Indeed, a very similar 4 Hz RR as during freezing recruits the mPFC LFP and single units during immobility in a tail suspension test (**Figure 1D**; Biskamp et al., 2017). As for freezing, the mPFC can also bidirectionally influence the response to challenging situations by promoting despair-like behavior or struggle (Warden et al., 2012), but the exact role of the RR in this behavior requires further investigation. Interestingly, bulbectomized rodents reliably show depressive-like behavior, including enhanced immobility during tail suspension (Song and Leonard, 2005). However, behavioral symptoms in bulbectomized animals start only around 2 weeks after bulbar ablation, arguing against an immediate effect of the loss of RR and/or olfactory inputs on the development of depressive symptoms. The congenital lack of olfactory sensorial afferences furthermore increases the prevalence of depression in humans (Croy et al., 2012). In addition, in the case of patients with chronic breathing disorders, where the RR is qualitatively disrupted, up to 80% of the patients show depression or anxiety disorders (Kunik et al., 2005). Unfortunately, it is currently not possible to deduce how much the reduced RR in the limbic network and the impaired olfactory inputs contribute to depressive symptoms in chronic breathing disorders and congenital anosmia.

Reward and Motivation

Recent publications have identified RR in several brain regions involved in reward, motivation, and addiction. One study described the RR entrainment of neurons in the ventral striatum (Karalis and Sirota, 2018). The ventral striatum is composed of the nucleus accumbens (NAcc) and the striatal part of the olfactory tubercle (OT). The OT is a direct target of the OB in rodents, monkey, and humans (Carmichael et al., 1994; Lane et al., 2020), thus providing a potential anatomical basis for the emergence of RR in the striatum. On the behavioral level, it has been shown that cocaine infusion in the OT but not in the NAcc nor the ventral pallidum induces place preference (Ikemoto, 2003). Moreover, rats learn to self-inject cocaine in their OT and NAcc shell, which is the dorsal extension of the OT, but not in the NAcc core, ventral pallidum, or dorsal striatum (Ikemoto, 2003). These results suggest that striatal regions with direct input from the OB are particularly important for the rewarding effects of the drug. It should be noted that the author observed a stronger rewarding effect in the medial OT, which is also receiving sparser inputs from the OB (Wesson and Wilson, 2011), suggesting a gradient between a lateral OT more involved in smell processing and a medial OT involved in reward. The OT sends projections to the orbitofrontal cortex, a prefrontal cortex area in which nearly all recorded single units are entrained by the RR in head-fixed animals (Kőszeghy et al., 2018), and which is thought to encode (among other things) reward expectation (Noonan et al., 2012).

There is additional evidence that neocortical inputs to the ventral striatum are more strongly paced by RR than inputs to the dorsal striatum. Karalis and Sirota (2018) observed a gradual decrease of the RR entrainment of the mPFC from ventral to dorsal. There is a medioventral to laterodorsal topography of connections between the mPFC and the striatum, with the IL being more connected to the OT, the PrL to the NAcc, and the ACC and motor cortices to the dorsal striatum (**Figure 4**; Voorn et al., 2004; Gabbott et al., 2005). These results demonstrate that interconnected brain regions involved in processing rewarding stimuli are paced by RR, raising the possibility that RR entrainment might support the encoding of reward-related information by synchronizing distant brain regions, similar to as it has been suggested for the coordination of mPFC and amygdala during the recall of fear memory. However, causal tests of such a potential function of RR remain to be performed.

To sum up, the RR rhythm has been recorded in multiple areas involved in emotion and higher-order cognitive functions in both rodents and humans. Behavioral performance is modulated by respiration (Zelano et al., 2016; Moberly et al., 2018; Bagur et al., 2021). Therefore, the role of RR in the brain is clearly broader than the support of olfactory processing. But it is important to note that the basic behaviors observed are not fully disrupted when the olfactory sensorial afferences are removed and the RR rhythm can have ambivalent effects on emotional cognition, possibly pointing toward a role in cognitive flexibility and emotion monitoring. In rodents, the RR oscillations might fulfill this role by synchronizing distant brain regions, neocortical areas such as the mPFC, with more ventral nuclei and paleocortices such as the amygdala and the OT that are strongly connected to the olfactory system. Additionally, the processing of smells is tightly linked to the RR, as well as whisking

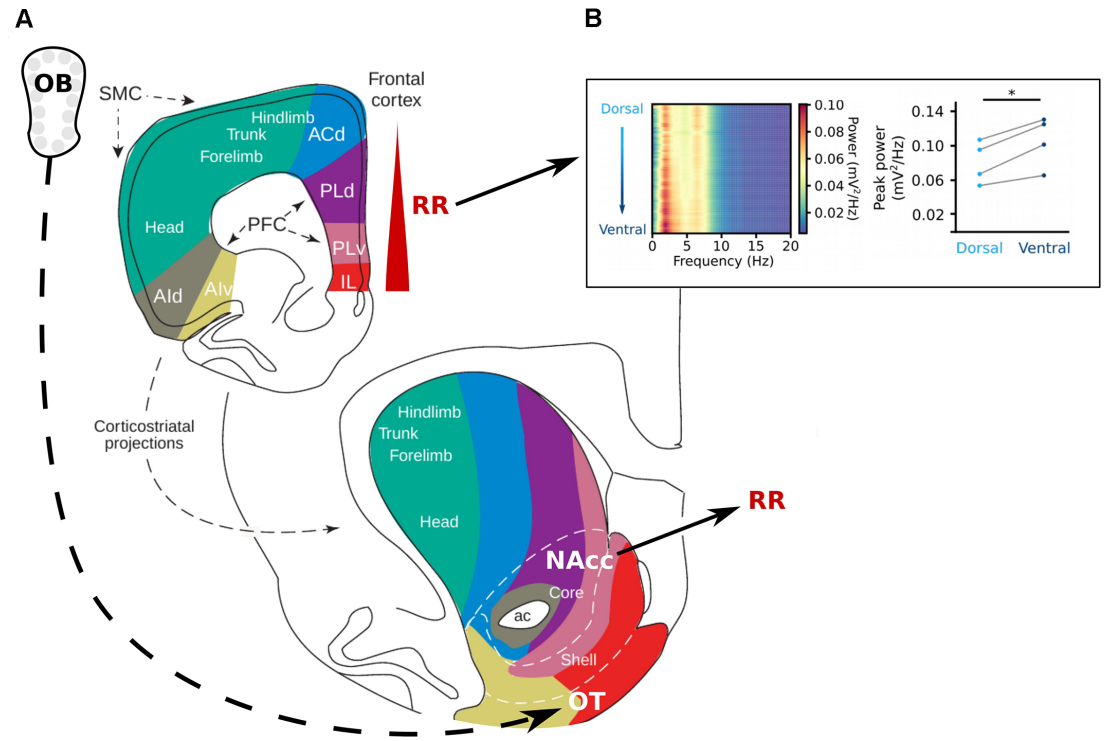

FIGURE 4 | The reward system and respiration-related oscillations. **(A)** Topography of the projections from the frontal cortex to the striatum. The olfactory tubercle (OT) receives direct projections from the OB and the nucleus accumbens (NAcc) has been shown to be strongly entrained by RR (Karalis and Sirota, 2018). In the prefrontal cortex, the RR power increases from dorsal to ventral (Karalis and Sirota, 2018; Folschweiller and Sauer, 2021). Adapted from Voorn et al. (2004); copyright (2004) Trends in Neurosciences, with permission from Elsevier. **(B)** Left: Power spectra of the mPFC along the dorsoventral axis, shows an increase in power at the frequency of respiration in the ventral direction. Left: Peak power for each mouse at 4 Hz at the most superficial recording site (light blue) and the deepest recording site (dark blue) of the mPFC. Reprinted from Folschweiller and Sauer (2021) under CC BY 4.0. *$p < 0.05$.

(**Figure 1A**; Ito et al., 2014), and respiration has been argued to be an important synchronization signal for sensorimotor integration (for review see Kleinfeld et al., 2014).

MECHANISMS OF HOW BREATHING MIGHT IMPACT COGNITION

Modulation of Gamma Oscillations

Brain activity is characterized by a vast family of oscillation patterns (see Buzsáki and Draguhn, 2004 for a review on different oscillations). Respiration might affect local circuit computation by modulating gamma oscillations (30–100 Hz). Gamma activities are strongly associated with cognitive functions: As mice perform a delayed non-match-to-place paradigm in a T-maze, hippocampal high-frequency gamma oscillations occur specifically during the decision phase as the mice approach the choice point in the maze (Yamamoto et al., 2014). Moreover, gamma oscillations are impaired in psychiatric disorders which present with cognitive disturbances (for review see Uhlhaas and Singer, 2010). Gamma oscillations occur nested in ongoing theta activities (for review see Colgin, 2015). This temporal organization of gamma oscillations by theta seems crucial for the behavioral functions. Tort et al. (2009) showed that theta-gamma coherence increased during learning of an item-context matching task. Similarly, another study demonstrated increasing 20–40 Hz gamma-theta coherence during learning of an odor-place association task (Igarashi et al., 2014). Furthermore, gamma oscillations in the neocortex are synchronized to hippocampal theta, suggesting that theta phase coupling might provide a general mechanism of information transfer across regions (Sirota et al., 2008).

Interestingly, recent work demonstrated that respiration-driven neocortical and hippocampal oscillations pace gamma activities. In the prefrontal cortex of mice, high-frequency gamma (80–100 Hz) is strongly entrained by RR (Biskamp et al., 2017; Zhong et al., 2017; Karalis and Sirota, 2018), while slow gamma (~40–80 Hz) and very high gamma (130–150 Hz) are entrained by theta oscillations (Biskamp et al., 2017; Zhong et al., 2017). This observation led to the hypothesis that theta and RR constitute two different channels of communication coupling to different gamma sub-bands (**Figure 5A**). In addition, gamma activities are synchronized with respiration across OB and wide areas of neocortex in the awake cats (Cavelli et al., 2020), suggesting that these principles apply to distinct species (it should be noted that 40 Hz gamma was entrained in cats, pointing to potential species-specific differences in modulated frequency that will require further investigation). Finally, recordings from the barrel cortex exhibited cross-

frequency coupling between respiration and ∼75 Hz gamma (Ito et al., 2014). These findings are supported by a different study reporting phase-coupling between regular ∼3 Hz OB potentials and high gamma activity in the hippocampus, motor, and sensory cortex (Rojas-Líbano et al., 2018), suggesting that the gamma-pacing effect of respiration might be a common principle across brain circuits.

It is likely that RR entrains hippocampal gamma oscillations *via* the entorhinal cortex (Nguyen Chi et al., 2016; Karalis and Sirota, 2018), which receives direct afferents from the OB (in monkeys, only a small rostral part of the entorhinal cortex receives direct inputs from the OB; Carmichael et al., 1994, which is also likely the case in humans; Insausti et al., 2002). RR synchronization of synaptic inputs from the medial entorhinal cortex (MEC) persists after olfactory deafferentiation, while respiration-rhythmic inputs from the lateral entorhinal cortex (LEC) are gone (Karalis and Sirota, 2018). The MEC has been argued to be important for "internal navigation" (using path integration), while the LEC might have a more prominent role in "external navigation" (using landmarks/cues; Connor and Knierim, 2017), suggesting that respiration might differentially affect afferents carrying distinct qualities of spatial information. Thus, the human hippocampus, in which delta oscillations are phase-locked to inspiration and depend on nasal breathing (Zelano et al., 2016), could be entrained by the means of sensorial afferences transmitted by the entorhinal cortex. On the behavioral level, it has indeed been demonstrated that encoding, consolidation, and recall of episodic memory can be modulated by respiration in humans (Zelano et al., 2016; Arshamian et al., 2018; Nakamura et al., 2018), with the discrete phase of the respiration affecting performance during encoding and recall, while the constant rhythmic airflow through the nasal cavity is relevant for consolidation. Importantly, experimentally disrupting the gamma range synchronization between the entorhinal cortex and the hippocampus impairs learning of spatial tasks in rodents (Fernández-Ruiz et al., 2021). Based on these results, it is possible that RR-nested gamma activities that are driven by entorhinal input support memory formation in the hippocampus.

Respiration might further impact gamma oscillations during sleep. In rapid eye movement (REM) sleep, during which theta-nested gamma oscillations are prevalent, the slow RR is found in the neocortex, with larger power in rostral areas such as the anterior cingulate cortex (Tort et al., 2018). RR frequency modulates the coupling between theta and gamma oscillations in the parietal cortex during REM sleep (Hammer et al., 2021). Changes in respiration frequency precede changes in slow gamma in the parietal cortex, but changes in parietal theta activity precede changes in breathing, suggesting a feedback loop interaction: The level of arousal during REM (equivalent to theta power) might change the breathing pattern, which in turn would modulate the parietal slow gamma oscillations (Tort et al., 2021). Taken together, these results emphasize multiple levels of control over gamma activities by respiration: Much like theta oscillations, RR defines time windows of preferred gamma activity in awake mice. Moreover, respiration controls theta-nested gamma oscillations during sleep.

Modulation of Ripples

Ripple oscillations are short bouts of high-frequency activity in CA1, which occur during offline states (sleep, immobility) and reflect highly synchronized firing of CA1 pyramidal neurons (O'Keefe, 1976, see Buzsáki, 2015 for review). Importantly, neuronal sequences related to visited places as well as upcoming trajectories are re- and pre-played, respectively, on compressed timescales during ripples (Lee and Wilson, 2002; Foster and Wilson, 2006; Diba and Buzsáki, 2007). These observations gave rise to the hypothesis that replay/preplay during ripples relates to the consolidation of learned behavioral sequences and the planning of future trajectories (Buzsáki, 2015). Experimentally suppressing ripples in rats during post-learning sleep indeed impaired learning in a spatial task, underscoring the relevance or ripples for memory formation (Girardeau et al., 2009). Moreover, ripples occur synchronously in higher-order neocortical areas and hippocampus in a learning-dependent manner, suggesting that they might aid the transfer of memory content to the neocortex (Khodagholy et al., 2017).

During awake immobility, when ripple frequency is high, RR seems ubiquitous in the forebrain. In mice, the RR occurs prominently in the mPFC, orbitofrontal cortex, and in the parietal cortex and hippocampus (Zhong et al., 2017; Kőszeghy et al., 2018). In humans, there is a global entrainment of neuronal activity at rest (Herrero et al., 2018; Kluger and Gross, 2020). It is worth noting that most of the areas entrained by respiration in humans belong to the default mode network (posterior cingulate cortex, angular gyrus, and the precuneus), the dorsal attention network (frontal eye fields, posterior and anterior intraparietal sulcus), and the salience network (anterior cingulate cortex, ventrolateral prefrontal cortex, and insula; Kluger and Gross, 2020). Interestingly, in recent work Liu et al. (2017) directly demonstrated that hippocampal ripples are entrained by respiration in rodents: They preferentially occur during early expiration (**Figure 5B**). Chemogenetically suppressing OB activity disrupted the respiration phase-locking of hippocampal ripples. In line with this observation, a different study found CA1 ripples to occur predominantly during the post-inspiratory phase (Karalis and Sirota, 2018). The synchronous activity of mPFC and NAcc neurons during hippocampal ripples was more frequent for ripples happening in their preferred phase of respiration. However, in contrast to the study by Liu et al. (2017), ablating OSNs with methimazole did not affect ripple entrainment, suggesting that a corollary discharge rather than a peripheral feedback mechanism *via* the OSN-OB route might underlie ripple entrainment. Despite different mechanistic results, these studies suggest that ongoing respiration-driven oscillations contribute to the organization of ripple activity, and might thus provide a causal link to memory consolidation.

Modulation of Neuronal Assemblies

The building blocks of cortical computations are thought to be comprised of groups of coactive cells, called neuronal assemblies, rather than single neurons (Buzsáki, 2010; Papadimitriou et al., 2020; El-Gaby et al., 2021). Assembly neurons become active together and are presumed to efficiently impact downstream

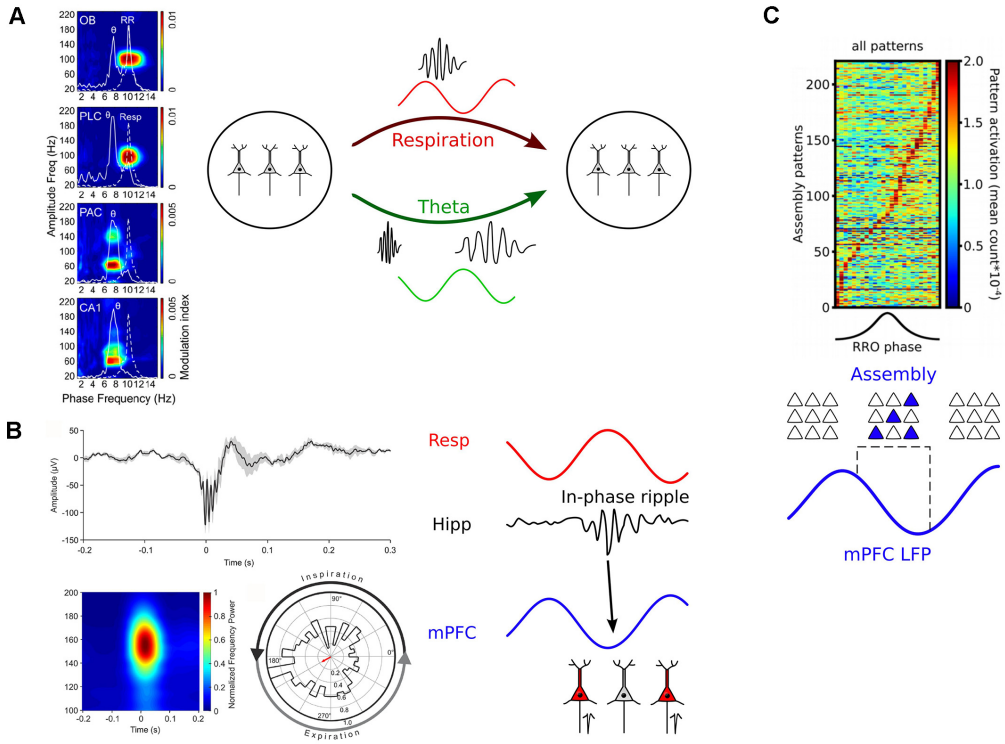

FIGURE 5 | Mechanisms of how breathing might impact cognition. **(A)** Left: RR entrains fast gamma activities across brain circuits. PLC, prelimbic cortex; PAC, parietal cortex. Reprinted from Zhong et al. (2017). Right: Respiration and theta oscillations provide timing signals for gamma oscillations of different frequencies (Biskamp et al., 2017; Zhong et al., 2017). **(B)** Left: Respiration paces ripples. Top: Example of a hippocampal ripple. Bottom: Average ripple power spectrum (left) and distribution of ripple events as a function of respiration phase. Reprinted from Liu et al. (2017) under CC BY 4.0. Right: RR-entrained ripples might enable efficient communication between hippocampal and neocortical circuits (Liu et al., 2017; Karalis and Sirota, 2018). **(C)** Top: Neuronal assemblies activate during the descending part of the prefrontal respiration-related oscillation (RRO). Reprinted from Folschweiller and Sauer (2021) under CC BY 4.0. Bottom: RR creates time windows for assembly activation and might thus orchestrate the joint activity of distributed assembly members or facilitate assembly stabilization by offline reactivation (Dejean et al., 2016; Folschweiller and Sauer, 2021).

readers due to their synchronized activation (Buzsáki, 2010). Given that respiration provides windows of preferred neuronal activity, it would be conceivable that respiration might directly regulate when neuronal assemblies activate. In recent years, it has become possible to reliably extract assembly activations from electrophysiological data using dimensionality reduction and strict statistical methods that allow the detection of transient and repeated neuronal coactivity (for review see Lopes-dos-Santos et al., 2013). In a pioneering study, Dejean et al. (2016) established a link between neuronal assembly activation and the expression of fear memory in mice. They showed that freezing responses of mice are accompanied by the emergence of assembly activations specifically in the ascending phase of ongoing 4 Hz oscillations. Although not directly demonstrated in that study, several laboratories have since shown that freezing-related 4 Hz activities are respiration-driven oscillations (Karalis and Sirota, 2018; Moberly et al., 2018; Bagur et al., 2021). Interestingly, optogenetic manipulation of fear-related assemblies in a 4 Hz phase-specific manner could bi-directionally modulate the amount of freezing, suggesting a causal role of assembly activity nested in respiration-driven prefrontal oscillations (Dejean et al., 2016). More recently, recordings from head-fixed mice presented evidence that the modulation of assembly patterns by RR might generalize to behavioral states other than fear (**Figure 5**C; Folschweiller and Sauer, 2021). In the absence of fearful stimuli, prefrontal assembly patterns are preferentially activated during the descending phase of respiration-driven oscillations. These data jointly show that respiration provides windows of opportunity for assembly activation, and that distinct phases of respiration might be linked with distinct cognitive/emotional content (e.g., freezing responses during the ascending phase vs. default or neutral state during the descending phase). On the mechanistic level, phase-specific pooling of assembly activity could support the brain-wide synchronization of distributed assembly members (Karalis et al., 2016), or facilitate spontaneous reactivation of assemblies as proposed by theoretical accounts to protect assemblies against degradation by synapse turnover (Fauth and van Rossum, 2019).

CONCLUSIONS AND OUTLOOK

There is a clear reciprocal relationship between emotions and respiration: while emotion and cognition modify the respiratory pattern to best fit the context-dependent bodily needs for oxygen,

RRs entrain brain circuits to support neuronal computation. RRs come about *via* sensorial afferences from the OB, which are paced by the airflow in the nasal cavity and target multiple brain regions along the rostro-caudal axis. While the exact pathway(s) from the OB to associative areas is still unclear, there is evidence of the involvement of interneurons in the broadcasting of this slow oscillation in the neocortex. The ubiquitous feature of the RR is highly conserved across species and it has been recorded widely across the brain in a large variety of emotional and arousal states. Finally, the modulation of faster brain oscillations and transient synchronization of neurons as assemblies shows that the RR plays a role at the core of neuronal processing.

While tremendous progress in the field of respiration-driven pacing of brain circuits has been made in recent years, we are still far from having a clear picture of the mechanisms by which respiration impacts cognitive functions. We propose the following key challenges to be addressed in future experiments to close that gap in our understanding:

(1) Tackling the translation problem:

It will be crucial to understand how respiration-synchronous activities are converted to local respiration-rhythmic oscillations in the neocortex. Inspiration might be drawn from well-studied oscillation species such as gamma activities, which rely on parvalbumin-positive interneurons (Sohal et al., 2009; for review see Hu et al., 2014). Recordings from identified interneuron types, preferably with access to subthreshold membrane oscillations *via* whole-cell recording or voltage-sensitive dye imaging might be a preferred experimental strategy to shed light on the contribution of different circuit components to the translation of respiration-driven signals. Furthermore, monitoring which inter-areal axonal projections show respiration-paced activities might help in guiding toward a more complete understanding of how respiration-driven patterns are distributed across the neocortex.

(2) Dissecting external feedback vs. corollary discharge:

We require more knowledge about the contribution of the OSN-OB pathway and the presumed direct efference copy from the brain stem to local effects of respiration. Reversible silencing of both pathways combined with unit recording during behavior might be the ideal way. However, while the OSN-OB pathway has been successfully manipulated using optogenetics (Bagur et al., 2021), the complex anatomy of the brain stem, the so far unclear route(s) of the presumed corollary discharge mechanism to the neocortex, and the vital function of many brain stem center render optogenetic silencing experiments during behavior difficult. An alternative approch could be to study the impact of external feedback vs. corollary discharge on local unit activity in species capable of natural mouth breathing (e.g., cats, Cavelli et al., 2020).

(3) Understanding respiration-dependent synchronization on mesoscopic scales:

Coherent respiration-synchronous oscillations among different brain regions have been described but have so far been limited to few regions and/or behavioral states (e.g., synchronous 4 Hz activity between mPFC and amygdala during fear memory; Karalis et al., 2016). It would be appreciable to reveal inter-regional synchronization between multiple brain areas (e.g., across the neocortex) and across behaviors (e.g., neutral, aversive, and appetitive states). Multi-region electrophysiological recording techniques (Khodagholy et al., 2017) or whole-hemisphere voltage-sensitive dye imaging could prove useful for such endeavors.

(4)Identifying universal functional principles.

Respiration-paced activities occur across species. However, respiration frequency differs by an order of magnitude between mice (∼2–5 Hz in rest) and humans (∼0.2–0.3 Hz in rest), while the frequencies of faster brain oscillations and action potential kinetics are largely preserved (Buzsáki et al., 2013). This raises the question to what extend the pacing of brain circuits by respiration might follow common principles, and which mechanisms might be species-specific.

AUTHOR CONTRIBUTIONS

SF and J-FS performed literature research and wrote the manuscript. All authors contribute to the article and approved the submitted version.

FUNDING

This work was supported by the German Science Foundation (Deutsche Forschungsgemeinschaft, grant SA 3609/1-1).

REFERENCES

Adrian, E. D. (1942). Olfactory reactions in the brain of the hedgehog. *J. Physiol.* 100, 459–473. doi: 10.1113/jphysiol.1942.sp003955

Arshamian, A., Iravani, B., Majid, A., and Lundström, J. N. (2018). Respiration modulates olfactory memory consolidation in humans. *J. Neurosci.* 38, 10286–10294. doi: 10.1523/JNEUROSCI.3360-17.2018

Bagur, S., Lefort, J. M., Lacroix, M. M., de Lavilléon, G., Herry, C., Chouvaeff, M., et al. (2021). Breathing-driven prefrontal oscillations regulate maintenance of conditioned-fear evoked freezing independently of initiation. *Nat. Commun.* 12:2605. doi: 10.1038/s41467-021-22798-6

Bergman, U., Ostergren, A., Gustafson, A.-L., and Brittebo, B. (2002). Differential effects of olfactory toxicants on olfactory regeneration. *Arch. Toxicol.* 76, 104–112. doi: 10.1007/s00204-002-0321-2

Biskamp, J., Bartos, M., and Sauer, J.-F. (2017). Organization of prefrontal network activity by respiration-related oscillations. *Sci. Rep.* 7:45508. doi: 10.1038/srep45508

Buck, L., and Axel, R. (1991). A novel multigene family may encode odorant receptors: a molecular basis for odor recognition. *Cell* 65, 175–187. doi: 10.1016/0092-8674(91)90418-x

Buzsáki, G. (2010). Neural syntax: cell assemblies, synapsembles and readers. *Neuron* 68, 362–385. doi: 10.1016/j.neuron.2010.09.023

Buzsáki, G. (2015). Hippocampal sharp wave-ripple: a cognitive biomarker for episodic memory and planning. *Hippocampus* 25, 1073–1188. doi: 10.1002/hipo.22488

Buzsáki, G., and Draguhn, A. (2004). Neuronal oscillations in cortical networks. *Science* 304, 1926–1929. doi: 10.1126/science.1099745

Buzsáki, G., Logothetis, N., and Singer, W. (2013). Scaling brain size, keeping timing: evolutionary preservation of brain rhythms. *Neurons* 80, 751–764. doi: 10.1016/j.neuron.2013.10.002

Canning, K. J., Wu, K., Peloquin, P., Kloosterman, F., and Leung, L. S. (2000). Physiology of the entorhinal and perirhinal projections to the hippocampus studied by current source density analysis. *Ann. N. Y. Acad. Sci.* 911, 55–72. doi: 10.1111/j.1749-6632.2000.tb06719.x

Carey, R. M., Verhagen, J. V., Wesson, D. W., Pírez, N., and Wachowiak, M. (2009). Temporal structure of receptor neuron input to the olfactory bulb imaged in behaving rats. *J. Neurophysiol.* 101, 1073–1088. doi: 10.1152/jn.90902.2008

Carmichael, S. T., Clugnet, M.-C., and Price, J. L. (1994). Central olfactory connections in the macaque monkey. *J. Comp. Neurol.* 346, 403–434. doi: 10.1002/cne.903460306

Cavelli, M., Castro-Zaballa, S., Gonzalez, J., Rojas-Líbano, D., Rubido, N., Velásquez, N., et al. (2020). Nasal respiration entrains neocortical long-range gamma coherence during wakefulness. *Eur. J. Neurosci.* 51, 1463–1477. doi: 10.1111/ejn.14560

Colgin, L. L. (2015). Theta-gamma coupling in the entorhinal-hippocampal system. *Curr. Opin. Neurobiol.* 31, 45–50. doi: 10.1016/j.conb.2014.08.001

Connelly, T., Yu, Y., Grosmaitre, X., Wang, J., Santarelli, L. C., Savigner, A., et al. (2015). G protein-coupled odorant receptors underlie mechanosensitivity in mammalian olfactory sensory neurons. *Proc. Natl. Acad. Sci. U S A* 112, 590–595. doi: 10.1073/pnas.1418515112

Connor, C. E., and Knierim, J. J. (2017). Integration of objects and space in perception and memory. *Nat. Neurosci.* 20, 1493–1503. doi: 10.1038/nn.4657

Croy, I., Negoias, S., Novakova, L., Landis, B. N., and Hummel, T. (2012). Learning about the functions of the olfactory system from people without a sense of smell. *PLoS One* 7:e33365. doi: 10.1371/journal.pone.0033365

Dejean, C., Courtin, J., Karalis, N., Chaudun, F., Wurtz, H., Bienvenu, T. C. M., et al. (2016). Prefrontal neuronal assemblies temporally control fear behaviour. *Nature* 535, 420–424. doi: 10.1038/nature18630

Diba, K., and Buzsáki, G. (2007). Forward and reverse hippocampal place-cell sequences during ripples. *Nat. Neurosci.* 10, 1241–1242. doi: 10.1038/nn1961

El-Gaby, M., Reeve, H. M., Lopes-Dos-Santos, V., Campo-Urriza, N., Perestenko, P. V., Morley, A., et al. (2021). An emergent neural coactivity code for dynamic memory. *Nat. Neurosci.* 24, 694–704. doi: 10.1038/s41593-021-00820-w

Fauth, M. J., and van Rossum, M. C. (2019). Self-organized reactivation maintains and reinforces memories despite synaptic turnover. *eLife* 8:e43717. doi: 10.7554/eLife.43717

Feldman, J. L., and Del Negro, C. A. (2006). Looking for inspiration: new perspectives on respiratory rhythm. *Nat. Rev. Neurosci.* 7, 232–241. doi: 10.1038/nrn1871

Fernández-Ruiz, A., Oliva, A., Soula, M., Rocha-Almeida, F., Nagy, G. A., Martin-Vazquez, G., et al. (2021). Gamma rhythm communication between entorhinal cortex and dentate gyrus neuronal assemblies. *Science* 372:eabf3119. doi: 10.1126/science.abf3119

Folschweiller, S., and Sauer, J.-F. (2021). Phase-specific pooling of sparse assembly activity by respiration-related brain oscillations. *biorXiv* [Preprint]. doi: 10.1101/2021.06.09.447658

Fontanini, A., and Bower, J. M. (2006). Slow-waves in the olfactory system: an olfactory perspective on cortical rhythms. *Trends Neurosci.* 29, 429–437. doi: 10.1016/j.tins.2006.06.013

Fontanini, A., Spano, P., and Bower, J. M. (2003). Ketamine-xylazine-induced slow (<1.5 Hz) oscillations in the rate piriform (olfactory) cortex are functionally correlated with respiration. *J. Neurosci.* 23, 7993–8001. doi: 10.1523/JNEUROSCI.23-22-07993.2003

Foster, D. J., and Wilson, M. A. (2006). Reverse replay of behavioural sequences in hippocampal place cells during the awake state. *Nature* 440, 680–683. doi: 10.1038/nature04587

Gabbott, P. L. A., Warner, T. A., Jays, P. R. L., Salway, P., and Busby, S. J. (2005). Prefrontal cortex in the rat: projections to subcortical autonomic, motor and limbic centers. *J. Comp. Neurol.* 492, 145–177. doi: 10.1002/cne.20738

Girardeau, G., Benchenane, K., Wiener, S. I., Buzsáki, G., and Zugaro, M. B. (2009). Selective suppression of hippocampal ripples impairs spatial memory. *Nat. Neurosci.* 12, 1222–1223. doi: 10.1038/nn.2384

Girin, B., Juventin, M., Garcia, S., Lefèvre, L., Amat, C., Fourcaud-Trocmé, N., et al. (2021). The deeo and slow breathing characterizing rest favors brain respiratory-drive. *Sci. Rep.* 11:7044. doi: 10.1038/s41598-021-86525-3

Grosmaitre, X., Santarelli, L. C., Tan, J., Luo, M., and Ma, M. (2007). Dual functions of mammalian olfactory sensory neurons as odor detectors and mechanical sensors. *Nat. Neurosci.* 10, 348–354. doi: 10.1038/nn1856

Hammer, M., Schwale, C., Brankačk, J., Draguhn, A., and Tort, A. B. L. (2021). Theta-gamma coupling during REM sleep depends on breathing rate. *Sleep* doi: 10.1093/sleep/zsab189. [Online ahead of print].

Herrero, J. L., Khuvis, S., Yeagle, E., Cerf, M., and Mehta, A. D. (2018). Breathing above the brain stem: volitional control and attentional modulation in humans. *J. Neurophysiol.* 119, 145–159. doi: 10.1152/jn.00551.2017

Hu, H., Gan, J., and Jonas, P. (2014). Interneurons. Fast-spiking, parvalbumin^{+} GABAergic interneurons: from cellular design to microcircuit function. *Science* 345:1255263. doi: 10.1126/science.1255263

Igarashi, K. M., Lu, L., Colgin, L. L., Moser, M.-B., and Moser, E. I. (2014). Coordination of entorhinal-hippocampal ensemble activity during associative learning. *Nature* 510, 143–147. doi: 10.1038/nature13162

Ikemoto, S. (2003). Involvement of the olfactory tubercle in cocaine reward: intracranial self-administration studies. *J. Neurosci.* 23, 9305–9311. doi: 10.1523/JNEUROSCI.23-28-09305.2003

Insausti, R., Marcos, P., Arroyo-Jiménez, M. M., Blaizot, X., and Martínez-Marcos, A. (2002). Comparative aspects of the olfactory portion of the entorhinal cortex and its projection to the hippocampus in rodents, nonhuman primates and the human brain. *Brain Res. Bull.* 57, 557–560. doi: 10.1016/s0361-9230(01)00684-0

Isosaka, T., Matsuo, T., Yamaguchi, T., Funabiki, K., Nakanishi, S., Kobayakawa, R., et al. (2015). Htr2a-expressing cells in the central amygdala control the hierarchy between innate and learned fear. *Cell* 163, 1153–1164. doi: 10.1016/j.cell.2015.10.047

Ito, J., Roy, S., Liu, Y., Cao, Y., Fletcher, M., Lu, L., et al. (2014). Whisker barrel cortex delta oscillations and gamma power in the awake mouse are linked to respiration. *Nat. Commun.* 5:3572. doi: 10.1038/ncomms4572

Jung, F., Yanovsky, Y., Brankačk, J., Tort, A. B., and Draguhn, A. (2019). Respiration competes with theta for modulating parietal cortex neurons. *bioRxiv* [Preprint]. doi: 10.1101/707331

Kamiloglu, R. G., Smeets, M. A. M., de Groot, J. H. B., and Semin, G. R. (2018). Fear odor facilitates the detection of fear expressions over other negative expressions. *Chem. Senses* 43, 419–426. doi: 10.1093/chemse/bjy029

Karalis, N., Dejean, C., Chaudun, F., Khoder, S., R Rozeske, R., Wurtz, H., et al. (2016). 4-Hz oscillations synchronize prefrontal-amygdala circuits during fear behavior. *Nat. Neurosci.* 19, 605–612. doi: 10.1038/nn.4251

Karalis, N., and Sirota, A. (2018). Breathing coordinates limbic network dynamics underlying memory consolidation. *bioRxiv* [Preprint]. doi: 10.1101/392530

Khodagholy, D., Gelinas, J. N., and Buzsáki, G. (2017). Learning-enhanced coupling between ripple oscillations in association cortices and hippocampus. *Science* 358, 369–372. doi: 10.1126/science.aan6203

Kleinfeld, D., Deschênes, M., Wang, F., and Moore, J. D. (2014). More than a rhythm of life: breathing as a binder of orofacial sensation. *Nat. Neurosci.* 17, 647–651. doi: 10.1038/nn.3693

Kluger, D. S., and Gross, J. (2020). Respiration modulates oscillatory neural network activity at rest. *bioRxiv* [Preprint]. doi:10.1101/2020.04.23.057216

Kőszeghy, Á., Lasztóczi, B., Forro, T., and Klausberger, T. (2018). Spike-timing of orbitofrontal neurons is synchronized with breathing. *Front. Cell. Neurosci.* 12:105. doi: 10.3389/fncel.2018.00105

Kunik, M. E., Roundy, K., Veazey, C., Souchek, J., Richardson, P., Wray, N. P., et al. (2005). Surprisingly high prevalence of anxiety and depression in chronic breathing disorders. *Chest* 127, 1205–1211. doi: 10.1378/chest.127.4.1205

Lane, G., Zhou, G., Noto, T., and Zelano, C. (2020). Assessment of direct knowledge of the human olfactory system. *Exp. Neurol.* 329:113304. doi: 10.1016/j.expneurol.2020.113304

Lee, A. K., and Wilson, M. A. (2002). Memory of sequential experience in the hippocampus during slow wave sleep. *Neuron* 36, 1183–1194. doi: 10.1016/s0896-6273(02)01096-6

Liu, Y., McAfee, S. S., and Heck, D. H. (2017). Hippocampal sharp-wave ripples in awake mice are entrained by respiration. *Sci. Rep.* 7:8950. doi: 10.1038/s41598-017-09511-8

Lockmann, A. L. V., Laplagne, D. A., Leão, R. N., and Tort, A. B. L. (2016). A respiration-coupled rhythm in the rat hippocampus independent of theta and slow oscillations. *J. Neurosci.* 36, 5338–5352. doi: 10.1523/JNEUROSCI.3452-15.2016

Lopes-dos-Santos, V., Ribeiro, S., and Tort, A. B. L. (2013). Detecting cell assemblies in large neuronal populations. *J. Neurosci. Methods* 220, 149–166. doi: 10.1016/j.jneumeth.2013.04.010

Macrides, F., and Chorover, S. L. (1972). Olfactory bulb units: activity correlated with inhalation cycles and odor quality. *Science* 175, 84–87. doi: 10.1126/science.175.4017.84

Masaoka, Y., and Homma, I. (2000). The source generator of respiratory-related anxiety potential in the human brain. *Neurosci. Lett.* 283, 21–24. doi: 10.1016/s0304-3940(00)00895-8

Mcdonald, A. J., Mascagni, F., and Guo, L. (1996). Projections of the medial and lateral prefrontal cortices to the amygdala: A Phaseolus vulgaris leucoagglutinin study in the rat. *Neuroscience* 71, 55–75. doi: 10.1016/0306-4522(95)00417-3

Moberly, A. H., Schreck, M., Bhattarai, J. P., Zweifel, L. S., Luo, W., and Ma, M. (2018). Olfactory inputs modulate respiration-related rhythmic activity in the prefrontal cortex and freezing behavior. *Nat. Commun.* 9:1528. doi: 10.1038/s41467-018-03988-1

Morris, J. S., Frith, C. D., Perrett, D. I., Rowland, D., Young, A. W., Calder, A. J., et al. (1996). A differential neural response in the human amygdala to fearful and happy facial expressions. *Nature* 383, 812–815. doi: 10.1038/383812a0

Nakamura, N. H., Fukunaga, M., and Oku, Y. (2018). Respiratory modulation of cognitive performance during the retrieval process. *PLoS One* 13:e0204021. doi: 10.1371/journal.pone.0204021

Nguyen Chi, V., Müller, C., Wolfenstetter, T., Yanovsky, Y., Draguhn, A., Tort, A. B. L., et al. (2016). Hippocampal respiration-driven rhythm distinct from theta oscillations in awake mice. *J. Neurosci.* 36, 162–177. doi: 10.1523/JNEUROSCI.2848-15.2016

Noonan, M. P., Kolling, N., Walton, M. E., and Rushworth, M. F. S. (2012). Re-evaluating the role of the orbitofrontal cortex in reward and reinforcement. *Eur. J. Neurosci.* 35, 997–1010. doi: 10.1111/j.1460-9568.2012.08023.x

O'Keefe, J. (1976). Place units in the hippocampus of the freely moving rat. *Exp. Neurol.* 51, 78–109. doi: 10.1016/0014-4886(76)90055-8

Papadimitriou, C. H., Vempala, S. S., Mitropolsky, D., Collins, M., and Maass, W. (2020). Brain computation by assemblies of neurons. *Proc. Natl. Acad. Sci. U S A* 117, 14464–14472. doi: 10.1073/pnas.2001893117

Philippot, P., Chapelle, G., and Blairy, S. (2002). Respiratory feedback in the generation of emotion. *Cogn. Emotion* 16, 605–627. doi: 10.1080/02699930143000392

Rojas-Líbano, D., Wimmer del Solar, J., Aguilar-Rivera, M., Montefusco-Siegmund, R., and Maldonado, P. E. (2018). Local cortical activity of distant brain areas can phase-lock to the olfactory bulb's respiratory rhythm in the freely behaving rat. *J. Neurophysiol.* 120, 960–972. doi: 10.1007/s11060-021-03834-3

Root, C. M., Denny, C. A., Hen, R., and Axel, R. (2014). The participation of cortical amygdala in innate, odour-driven behaviour. *Nature* 515, 269–273. doi: 10.1038/nature13897

Sierra-Mercado, D., Padilla-Coreano, N., and Quirk, G. J. (2011). Dissociable roles of prelimbic and infralimbic cortices, ventral hippocampus and basolateral amygdala in the expression and extinction of conditioned fear. *Neuropsychopharmacology* 36, 529–538. doi: 10.1038/npp.2010.184

Sirota, A., Montgomery, S., Fujisawa, S., Isomura, Y., Zugaro, M., and Buzsáki, G. (2008). Entrainment of neocortical neurons and gamma oscillations by the hippocampal theta rhythm. *Neuron* 60, 683–697. doi: 10.1016/j.neuron.2008.09.014

Sohal, V. S., Zhang, F., Yizhar, O., and Deisseroth, K. (2009). Parvalbumin neurons and gamma rhythms enhance cortical circuit performance. *Nature* 459, 698–702. doi: 10.1038/nature07991

Song, C., and Leonard, B. E. (2005). The olfactory bulbectomised rat as a model of depression. *Neurosci. Biobehav. Rev.* 29, 627–647. doi: 10.1016/j.neubiorev.2005.03.010

Sperry, R. W. (1950). Neural basis of the spontaneous optokinetic response produced by visual inversion. *J. Comp. Physiol. Psychol.* 43, 482–489. doi: 10.1037/h0055479

Tort, A. B. L., Hammer, M., Zhang, J., Brankačk, J., and Draguhn, A. (2021). Temporal relations between cortical network oscillations and breathing frequency during REM sleep. *J. Neurosci.* 41, 5229–5242. doi: 10.1523/JNEUROSCI.3067-20.2021

Tort, A. B. L., Komorowski, R. W., Manns, J. R., Kopell, N. J., and Eichenbaum, H. (2009). Theta-gamma coupling increases during the learning of item-context associations. *Proc. Natl. Acad. Sci. U.S.A.* 106, 20942–20947. doi: 10.1073/pnas.0911331106

Tort, A. B. L., Ponsel, S., Jessberger, J., Yanovsky, Y., Brankačk, J., and Draguhn, A. (2018). Parallel detection of theta and respiration-coupled oscillations throughout the mouse brain. *Sci. Rep.* 8:6432. doi: 10.1038/s41598-018-24629-z

Uhlhaas, P. J., and Singer, W. (2010). Abnormal neural oscillations and synchrony in schizophrenia. *Nat. Rev. Neurosci.* 11, 100–113. doi: 10.1038/nrn2774

von Holst, E., and Mittelstaedt, H. (1950). Das Reafferenzprinzip. *Naturwissenschaften* 37, 464–476. doi: 10.1007/BF00622503

Voorn, P., Vanderschuren, L. J. M. J., Groenewegen, H. J., Robbins, T. W., and Pennartz, C. M. A. (2004). Putting a spin on the dorsal-ventral divide of the striatum. *Trends Neurosci.* 27, 468–474. doi: 10.1016/j.tins.2004.06.006

Warden, M. R., Selimbeyoglu, A., Mirzabekov, J. J., Lo, M., Thompson, K. R., Kim, S.-Y., et al. (2012). A prefrontal cortex-brainstem neuronal projection that controls response to behavioural challenge. *Nature* 492, 428–432. doi: 10.1038/nature11617

Wesson, D. W., and Wilson, D. A. (2011). Sniffing out the contributions of the olfactory tubercle to the sense of smell: hedonics, sensory integration and more? *Neurosci. Biobehav. Rev.* 35, 655–668. doi: 10.1016/j.neubiorev.2010.08.004

Yackle, K., Schwarz, L. A., Kam, K., Sorokin, J. M., Huguenard, J. R., Feldman, J. L., et al. (2017). Breathing control center neurons that promote arousal in mice. *Science* 355, 1411–1415. doi: 10.1126/science.aai7984

Yamamoto, J., Suh, J., Takeuchi, D., and Tonegawa, S. (2014). Successful execution of working memory linked to synchronized high-frequency gamma oscillations. *Cell* 157, 845–857. doi: 10.1016/j.cell.2014.04.009

Yang, C. F., and Feldman, J. L. (2017). Efferent projections of excitatory and inhibitory preBötzinger Complex neurons. *J. Comp. Neurol.* 526, 1389–1402. doi: 10.1002/cne.24415

Yanovsky, Y., Ciatipis, M., Draguhn, A., Tort, A. B. L., and Brankačk, J. (2014). Slow oscillations in the mouse hippocampus entrained by nasal respiration. *J. Neurosci.* 34, 5949–5964. doi: 10.1523/JNEUROSCI.5287-13.2014

Zelano, C., Jiang, H., Zhou, G., Arora, N., Schuele, S., Rosenow, J., et al. (2016). Nasal respiration entrains human limbic oscillations and modulates cognitive function. *J. Neurosci.* 36, 12448–12467. doi: 10.1523/JNEUROSCI.2586-16.2016

Zhang, J. X., Harper, R. M., and Frysinger, R. C. (1986). Respiratory modulation of neuronal discharge in the central nucleus of the amygdala during sleep and waking states. *Exp. Neurol.* 91, 193–207. doi: 10.1016/0014-4886(86)90037-3

Zhong, W., Ciatipis, M., Wolfenstetter, T., Jessberger, J., Müller, C., Ponsel, S., et al. (2017). Selective entrainment of gamma subbands by different slow network oscillations. *Proc. Natl. Acad. Sci. U. S. A.* 114, 4519–4524. doi: 10.1073/pnas.1617249114

Conflict of Interest: The authors declare that the research was conducted in the absence of any commercial or financial relationships that could be construed as a potential conflict of interest.

Publisher's Note: All claims expressed in this article are solely those of the authors and do not necessarily represent those of their affiliated organizations, or those of the publisher, the editors and the reviewers. Any product that may be evaluated in this article, or claim that may be made by its manufacturer, is not guaranteed or endorsed by the publisher.

frontiers in Neural Circuits

ORIGINAL RESEARCH
published: 03 December 2021
doi: 10.3389/fncir.2021.758939

Enriched Environment Modulates Sharp Wave-Ripple (SPW-R) Activity in Hippocampal Slices

Lucie Landeck[1], *Martin E. Kaiser*[1], *Dimitri Hefter*[1,2], *Andreas Draguhn*[1] *and Martin Both*[1]*

[1]Institute of Physiology and Pathophysiology, Heidelberg University, Heidelberg, Germany, [2]RG Animal Models in Psychiatry, Department of Psychiatry and Psychotherapy, Central Institute of Mental Health, Medical Faculty Mannheim, University of Heidelberg, Heidelberg, Germany

Behavioral flexibility depends on neuronal plasticity which forms and adapts the central nervous system in an experience-dependent manner. Thus, plasticity depends on interactions between the organism and its environment. A key experimental paradigm for studying this concept is the exposure of rodents to an enriched environment (EE), followed by studying differences to control animals kept under standard conditions (SC). While multiple changes induced by EE have been found at the cellular-molecular and cognitive-behavioral levels, little is known about EE-dependent alterations at the intermediate level of network activity. We, therefore, studied spontaneous network activity in hippocampal slices from mice which had previously experienced EE for 10–15 days. Compared to control animals from standard conditions (SC) and mice with enhanced motor activity (MC) we found several differences in sharp wave-ripple complexes (SPW-R), a memory-related activity pattern. Sharp wave amplitude, unit firing during sharp waves, and the number of superimposed ripple cycles were increased in tissue from the EE group. On the other hand, spiking precision with respect to the ripple oscillations was reduced. Recordings from single pyramidal cells revealed a reduction in synaptic inhibition during SPW-R together with a reduced inhibition-excitation ratio. The number of inhibitory neurons, including parvalbumin-positive interneurons, was unchanged. Altered activation or efficacy of synaptic inhibition may thus underlie changes in memory-related network activity patterns which, in turn, may be important for the cognitive-behavioral effects of EE exposure.

Keywords: hippocampus, sharp waves, ripples, plasticity, network oscillations

OPEN ACCESS

Edited by:
Gabrielle Girardeau, INSERM U839 Institut du Fer à Moulin (IFM), France

Reviewed by:
Nikolaus Maier, Charité University Medicine Berlin, Germany
Rebecca Ann Piskorowski, INSERM U1266 Institut de Psychiatrie et Neurosciences de Paris, France

***Correspondence:**
Martin Both
mboth@physiologie.uni-heidelberg.de

Received: *15 August 2021*
Accepted: *15 November 2021*
Published: *03 December 2021*

Citation:
Landeck L, Kaiser ME, Hefter D, Draguhn A and Both M (2021) Enriched Environment Modulates Sharp Wave-Ripple (SPW-R) Activity in Hippocampal Slices. Front. Neural Circuits 15:758939. doi: 10.3389/fncir.2021.758939

INTRODUCTION

Complex nervous systems support experience-dependent learning, lending behavioral flexibility and individuality to animals. Such adaptive processes require lasting changes at the molecular, cellular, network, and system-wide levels. At the same time, much of the brain's structure and function is genetically determined, posing the question of gene-environment interactions (GEI) in the formation of individually adapted neuronal mechanisms. The mechanisms and extent of gene-environment interactions have become a major topic in basic and clinical neurosciences (Ohline and Abraham, 2019; Rogers et al., 2019).

Animal studies on GEI rely strongly on comparisons between groups of animals raised or kept in different environments. A key paradigm is the so-called "enriched environment" (EE) approach in which animals (mostly rodents) are kept in extended cages supplied with different objects, devices facilitating complex movements, and conspecifics. Following earlier, unsystematic studies, pioneering work performed by M.R. Rosenzweig and others in the 1960s revealed major structural, cellular, and neurochemical differences between the brains of rats living in EE as compared to standard conditions (SC; Bennett et al., 1964). These, and multiple subsequent studies revealed a plethora of changes induced by exposure to a more challenging environment than the standard laboratory conditions which, arguably, may be characterized as a paradigm for sensory, motor, and social deprivation (Consorti et al., 2019; Rogers et al., 2019). Most of these changes converge on mechanisms increasing the adaptive plasticity of the brain, in line with the positive effects of EE on behavioral flexibility and experience-dependent learning (Donato et al., 2013; Ball et al., 2019; Gelfo, 2019). Of note, the cognitive-behavioral effects of EE include improved spatial memory formation (Leggio et al., 2005; Bennett et al., 2006; Eckert et al., 2010), highlighting the importance of hippocampal and neocortical networks which are, indeed, strongly affected by EE.

At the molecular and cellular level, effects of EE include increased expression of neurotrophic factors like BDNF (Novkovic et al., 2015; von Bohlen und Halbach and von Bohlen und Halbach, 2018), increased efficacy of synaptic transmission and plasticity (Ohline and Abraham, 2019; Cooper and Frenguelli, 2021), alterations in perineuronal nets (Sale et al., 2007), increased adult neurogenesis (Kempermann, 2019) and others. At the network level, changes in the number and function of inhibitory interneurons lead to changes in excitation-inhibition ratio, favoring increased activity of cortical principal cells (Sale et al., 2007; Greifzu et al., 2014). Finally, recordings from freely behaving rats have shown selective changes in multi-cellular representations of spatial contexts including increased sparsity and increased propensity to the remapping of place cells (Bilkey et al., 2017). Together, exposure of rodents to enriched environments results in multiple alterations at different system levels which, together, increase behavioral flexibility and adaptation. Importantly, genuine effects of an enriched environment can be differentiated from the effects of increased motor activity which, by itself, also induces multiple changes in cells and networks (Rogers et al., 2019).

Recent years have revealed much insight into the network-level functions supporting spatial memory formation and consolidation in rodents. A central concept is that memory formation is supported by highly specific spatio-temporal activity patterns of selected neurons. These patterns form on top of state-dependent network oscillations providing a temporal scaffold for the ordered spiking of neuronal ensembles (O'Keefe and Recce, 1993; Wilson and McNaughton, 1994; Buzsaki and Draguhn, 2004). Despite impressive progress in this field, there is, however, little information about alterations in hippocampal network oscillations by exposure to EE. We hypothesized that experience of an enriched physical and social environment is likely to induce alterations at this level which forms a critical link between cellular-molecular and cognitive-behavioral processes. We focused on a particular pattern of network activity in the hippocampus called sharp wave-ripple complexes (SPW-R). These complexes form propagating waves of increased synaptic activity superimposed by high-frequency oscillations at around 200 Hz (Buzsaki et al., 1992). Pyramidal cells fire with high precision within this fast rhythm, enabling re-activation of previously formed neuronal ensembles (Wilson and McNaughton, 1994; Ylinen et al., 1995; Lee and Wilson, 2002). These activity patterns are then transferred to the neocortex and are believed to support the consolidation of previously acquired spatial information (Buzsaki, 2015; Khodagholy et al., 2017).

In order to test for potential effects of EE on memory-related network patterns in the hippocampus, we exposed mice to an enriched environment for 10–15 days and subsequently studied spontaneous network activity in hippocampal slices *in vitro*. We report several characteristic alterations in sharp wave-ripple complexes compared to both, mice kept in standard conditions and in conditions with increased motor activity. Thus, an enriched environment alters coordinated activity patterns in memory-related hippocampal networks.

MATERIALS AND METHODS

Animals

All experiments were performed with male C57/Bl6N mice (Charles River, Sulzfeld, Germany) in compliance with the Federation of European Laboratory Animal Science Association (FELASA) guidelines and were approved by the federal government of Baden-Württemberg (AZ G-30/17 and G-188/15). Mice were kept at 21–24°C and 40–60% relative humidity in Scantainers (Scanbur BK A/S, Denmark) with a 12-h light and dark cycle. Food and water were provided *ad libitum*.

Enriched Environment Paradigm

Eight-week-old mice were housed for 10–15 days under three different conditions: Enriched Environment (EE), Motor Control (MC), or Standard Conditions (SC). Animals under SC and MC conditions were housed in groups of three in a standard-sized cage, whereas mice under EE conditions were kept as a group of 12 in a large cage sized 120 cm × 45 cm × 26 cm. Cages for standard conditions measured 27 cm × 22 cm × 14 cm and cages for motor control 36 cm × 24 cm × 19 cm. The EE cage (**Figure 1A**) was equipped with different kinds of stimuli, such as toys made of different types of materials (plastic tunnels, coconut caves, wooden bridges, and suspension bridges, running wheels, sticks), and several kinds of bedding (gravel, sand, mulch, and standard bedding). In order to control for increased physical activity in the EE group, mice in the MC group were provided with a running wheel. Mice that were taken out of the cage for experiments were not replaced.

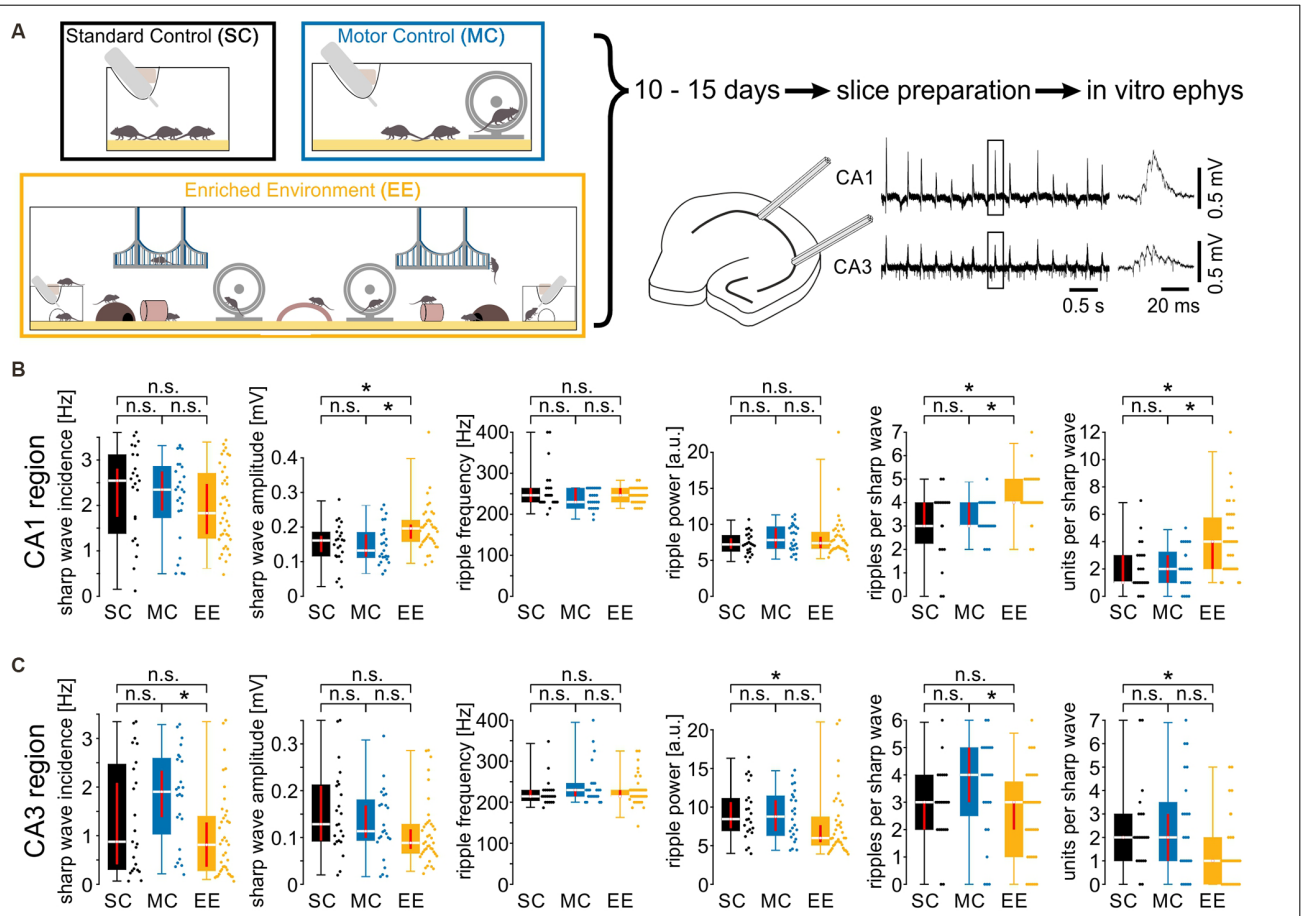

FIGURE 1 | Environmental enrichment increases amplitude, ripple cycles, and unit activity during sharp wave-ripple oscillations. **(A)** Mice were kept in one of three housing conditions for 10–15 days: standard conditions, motor control, or enriched environment (for details, see "Materials and Methods" section). Subsequently, hippocampal slices were prepared to record local field potentials and unit discharges during spontaneous sharp wave-ripple oscillations. **(B)** Sharp wave amplitudes, ripples per sharp wave and units per sharp wave were increased in the CA1 region of slices from EE animals. **(C)** Activity in the CA3 region did not show any consistent alterations. *N* = 23 slices from six mice for standard conditions, *N* = 25 slices from five mice for motor control, and *N* = 39 slices from eight mice for environmental enrichment. Asterisks denote *p*-values < 0.05 from *post-hoc* testing followed by a significant Kruskal-Wallis test. Red lines depict the confidence intervals of the median assessed by bootstrapping. n.s., not significant.

Preparation of Mouse Brain Slices

After the loss of the righting reflex under gradual CO_2 anesthesia, the mice were rapidly decapitated and the brain was removed and stored in cooled (1–4°C), carbogen (95% O_2/5% CO_2) gassed, artificial cerebrospinal fluid (ACSF), containing in mM: 124 NaCl, 1.8 $MgSO_4$, 1.6 $CaCl_2$, 10 glucose, 1.25 NaH_2PO_4, 26 $NaHCO_3$ (pH 7.4 at 37°C). The brain was then cut into 450 μm thick slices using a Leica VT1000S vibratome (Leica, Nussloch, Germany) and stored in a Haas-type interface recording chamber, where the slices were continuously perfused with oxygenated ACSF (1–2 ml/min) at 34 ± 1°C. Experiments were started after a recovery time of at least 3 h.

Extracellular Recordings

Field potentials and unit discharges were recorded by lowering tetrodes made of four twisted tungsten wires (California Fine Wire, 12.5 μm diameter) into the pyramidal layer of the CA1 and the CA3 hippocampal region. The tetrodes were connected to an EXT-T2 amplifier (npi electronics). Signals were amplified 200×, low-pass filtered at 8 kHz, high-pass filtered at 0.3 Hz, and digitized at 20 kHz for off-line analysis (1401 ADC interface and Spike-2 data acquisition program, Cambridge Electronic Design CED, Cambridge, UK).

Analysis was done by custom routines written in Matlab (The MathWorks). Sharp waves were detected from low-pass filtered raw data (50 Hz) as local maxima with amplitudes larger than 0.12 mV within a 30 ms time window. This value corresponds to 4 SDs of event-free baseline noise (Both et al., 2008) yielding stable and reliable detection of SPW-Rs (as confirmed by visual inspection of traces and detected events). In order to assess potential differences in sharp wave incidence or properties, we included also events without visible superimposed ripples (see data points with 0 ripples per sharp wave in **Figures 1B,C**). Sorting sharp waves of each recording by amplitude and selecting the 50% largest events for analysis resulted in a data set of sharp waves which all contained ripples. Analysis of these data revealed

qualitatively the same results, thus validating our unbiased approach.

Subsequently, SPW-R complexes were analyzed with continuous wavelet transform (complex Morlet wavelet, Both et al., 2008), starting 33 ms before and ending 67 ms after the peak of the detected sharp wave. From this wavelet spectrogram (50–300 Hz divided into 81 bins on a log scale), we extracted the leading ripple frequency and the peak power of the oscillation at frequencies >140 Hz. The number of ripple cycles of individual SPW-R were quantified from band-pass filtered raw data (140–250 Hz) and ripple troughs were detected as negative peaks exceeding three times the standard deviation of event-free baseline noise.

To detect extracellularly recorded action potentials, raw data were high-pass filtered at 500 Hz, and single events were extracted by setting a negative threshold at 4.5 SDs from background noise. Phase-coupling with respect to ripple oscillations was computed by assigning to each event a phase within one ripple cycle (see **Figure 3**). Ripple cycles were described as circular data of 360 degrees with ripple troughs set to zero degree. From these phases, the mean preferred firing angle and the precision were calculated. Precision is described by the length of the normalized mean vector (range 0–1). These parameters were determined for recordings with at least 33 SPW-R-associated action potentials which allowed for reliable calculation.

Whole-Cell Patch-Clamp Recordings

For voltage clamp, glass pipettes (5–7 MΩ) were filled with an internal solution containing (in mM): 136 Cs-gluconate, 4 CsCl, 10 HEPES, 4 Mg-ATP, 0.3 Mg-GTP, and 10 Na_2-phosphocreatine, adjusted to pH 7.3 with CsOH. For single cell staining and morphological analysis, cells were filled with biocytin (1–5%; Sigma-Aldrich #B4261). Blind patch-clamp recordings of pyramidal neurons in the hippocampal CA1 region were performed by lowering glass pipettes under continuous positive pressure into the cell layer until an increase in series resistance was observed. Subsequently, a seal was formed by applying light suction. After obtaining a gigaohm seal and breaking through the patch, the cell was clamped to −74 mV. Signals were recorded using a MultiClamp 700 B amplifier (Axon Instruments, Burlingame, CA) connected to a 1401 ADC interface (CED, Cambridge, UK) using Signal4 and Spike2 (v7) Software. To measure the conductance properties of the individual cells, we used the method described by Borg-Graham et al. (1998) and Haider et al. (2006). Under voltage clamp conditions, individual cells were held at five different membrane potentials (−84 mV, −64 mV, −54 mV, +16 mV) for 60 s separated by 10 s breaks at "resting" membrane potential (−74 mV) while simultaneously recording spontaneously occurring SPW-R oscillations. Ripples were then aligned by the peak of individual sharp waves, and input conductance $G_{in}(t)$ was calculated from the slope of the linear regression of the I-V relation between I(t) and $V_{holding}$ (see **Figure 4A**). The apparent reversal potential E_{rev} was computed from the intersection between the linear regression at 0 s, i.e., at rest, and at time t. The change in conductance was taken as $G_{syn}(t) = G_{in}(t) - G_{in}(0)$. Inhibitory and excitatory conductances were then computed as $G_{syn,i} = G_{syn} \cdot (E_{rev} - E_{AMPA})/(E_{GABA} - E_{AMPA})$. $G_{syn,e} = G_{syn} - G_{syn,i}$. E_{AMPA} was set to 0 mV and E_{GABA} to −75 mV.

Immunohistochemistry and Confocal Microscopy

Under deep anesthesia (Ketamin/Xylazin, 120 and 16 mg/kg), mice were perfused with polychlorinated biphenyl (PCB) and subsequently with 4% paraformaldehyde (PFA). The perfused brain was removed from the skull and stored at 4°C in a 4% PFA solution. After fixation, the brain was cut into 50 μm thick slices using a vibratome (Leica VT 1200S). For antigen retrieval, slices were stored in a citrate-buffered phosphate-buffered saline (PBS) solution with a pH of 6.0 and kept in a compartment dryer at 100°C for 25 min. The slices were rinsed three times in PBS for 10 min before they were pretreated with a blocking solution containing 5% normal goat serum (NGS) in PBS for 1 h. After rinsing the slices (three times for 10 min), the primary antibodies (mouse anti-GAD67; 1:500; MAB5406, Merck Millipore; rabbit anti-PV; 1:1,000; PV 27, Swant) were applied and the slices were incubated overnight. The slices were again rinsed (three times for 10 min) and incubated in a PBS solution containing the secondary antibodies (Alexa Fluor 488 anti-rabbit; 1:1,000; A-11008, Molecular Probes by ThermoFisher Scientific; Cy3 anti-mouse; 1:500; 115-165-003, Dianova) for 2 h at room temperature. Subsequently, after rinsing the slices (three times for 10 min), a DAPI staining (1:10,000; Carl Roth, Germany) was performed for 2 min at room temperature. The slices were washed once again for 15 min and then mounted onto glass slides in Mowiol (81381, Sigma-Aldrich). The confocal images were acquired using a Nikon A1R point scanning confocal microscope (Nikon Imaging Center (NIC), Heidelberg University) with a 20× (0.75 NA) objective in air or a 60× (1.4 NA) oil immersion objective. The images were taken with a resolution of 1024 × 1024 pixels in z-stacks with a step size of 1 μm. After the acquisition, the images were analyzed in ImageJ/Fiji (Wayne Rasband, NIH, open source).

Statistics

Data are represented as box plots in which medians are indicated by a line and the box limits denote the interquartile range (25%; 75%). Whiskers of box plots extend to the 2.5th and 97.5th percentile. Confidence intervals for the medians were estimated by means of bootstrapping, i.e., by computing the 2.5th and 97.5th percentile of the distribution of medians from 10,000 resamples. These confidence intervals are plotted as red vertical lines in the box plots. In the text, values are reported as medians and their confidence intervals. Statistical significance was calculated by the Kruskal-Wallis test for three groups, followed by a Dunn-Bonferroni *post hoc* test if testing reached significance or the Mann–Whitney U test for two groups. A p-value <0.05 was regarded as significant. To test for a potentially biased recording location of whole-cell patch clamp recordings we took the following approach: the location of seven out of 18 cells (5/11 MC cells and 2/7 EE cells) was histologically identified. Based on these data we computed the probability for a

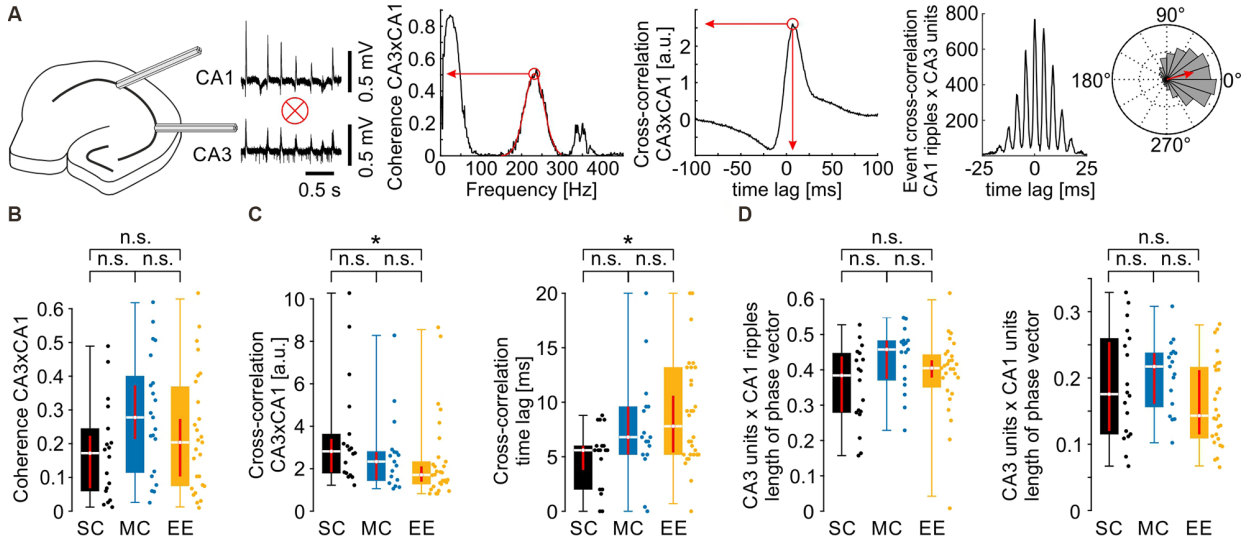

FIGURE 2 | Propagation of network activity from CA3 to CA1 is not affected by environmental enrichment. **(A)** Schematics of the quantification of different parameters. For the normalized mean phase vector see also **Figure 3A**. **(B)** Coherence between CA3 and CA1 in the ripple frequency band was not different between groups. **(C)** Waveform cross-correlation between CA3 and CA1 showed differences between SC and EE but not between MC and EE or SC and MC. **(D)** CA3 unit to CA1 ripple (left) and CA3 unit to CA1 unit (right) phase coupling was not different after environmental enrichment. *N* = 23 slices from six mice for standard conditions, *N* = 25 slices from five mice for motor control, and *N* = 39 slices from eight mice for environmental enrichment. Asterisks denote *p*-values <0.05 from *post-hoc* testing followed by a significant Kruskal-Wallis test. Red lines depict the confidence intervals of the median assessed by bootstrapping. n.s., not significant.

strong bias in the respective cell populations (i.e., 70% or more MC cells from one layer and 70% or more EE cells from the other layer). This was done by performing 100,000 simulations, assuming a 50% chance to record a cell from either layer. In a second approach, we substituted the 50% chance level by the observed percentages in histologically reconstituted cells (five superficial cells of seven in total). The probability of a strong bias was 1,028/100,000 cases (∼1%) for 50% probability and 136/100,000 cases (∼ 0.14%) for the 5/7 probability (see "Results" section).

RESULTS

Environmental Enrichment Increases Amplitude, Ripple Cycles, and Unit Activity During Sharp Wave-Ripple Oscillations in CA1 but Not CA3

Mice were kept in one of three conditions: standard conditions with no additional stimuli (SC), standard cages with an added running wheel ("motor control"; MC), and enriched environment including enhanced social interactions ('enriched environment'; EE) for 10–15 days (**Figure 1A** left panel). Subsequently, we recorded network-, multi unit- and cellular activity in acutely prepared hippocampal slices (see "Materials and Methods" section). Field potentials in CA1 and CA3, respectively, revealed spontaneous network events resembling sharp wave-ripple complexes (SPW-R, Maier et al., 2003, **Figure 1A** right panel). While there were no obvious changes in SPW-R waveforms, a quantitative analysis revealed several differences between the three conditions. In CA1, sharp wave amplitudes and the number of ripples per sharp wave were enhanced following an enriched environment (**Figure 1B**). Such differences were absent between animals with enhanced motor activity and standard conditions (SPW amplitudes [in mV, median and {confidence interval}]: SC: 0.16 {0.13, 0.17}; MC: 0.13 {0.11, 0.18}; EE: 0.20 {0.17, 0.21}; number of ripple cycles [per SPW]: SC: 3 {3, 4}; MC: 3 {3, 4}; EE: 4 {4, 4}; SC: *N* = 23 slices from six animals; MC: *N* = 25 slices from five animals; EE: *N* = 39 slices from eight animals). Sharp wave incidence, ripple frequency, and ripple power were not different between all three groups. Network patterns like sharp wave-ripple complexes provide a framework for the coordination of neuronal activity. We, therefore, extracted unit activity from the recordings and quantified the number of discharges per sharp wave. Following enriched environment conditions firing of units was clearly enhanced (**Figure 1B**, right panel; [per SPW]: SC: 1 {1, 3}; MC: 2 {1, 3}; EE: 4 {2, 4}). In contrast, recordings in CA3 did not reveal any consistent differences between enriched environment, motor control, and standard conditions (**Figure 1C**). Thus, the three different conditions revealed region-specific changes in coordinated network and unit activity during SPW-R.

Propagation of Network and Unit Activity Is Not Altered by Environmental Enrichment

SPW-R are propagated from CA3 to CA1 (Both et al., 2008). We therefore tested whether environmental enrichment has an effect on this coordinated activity (**Figure 2**). Coherence between CA3 and CA1 in the ripple frequency band was not different between the three housing conditions (**Figure 2B**, SC: 0.17 {0.06, 0.22}; MC: 0.28 {0.21, 0.37}; EE: 0.20 {0.10, 0.27}). Similarly, there

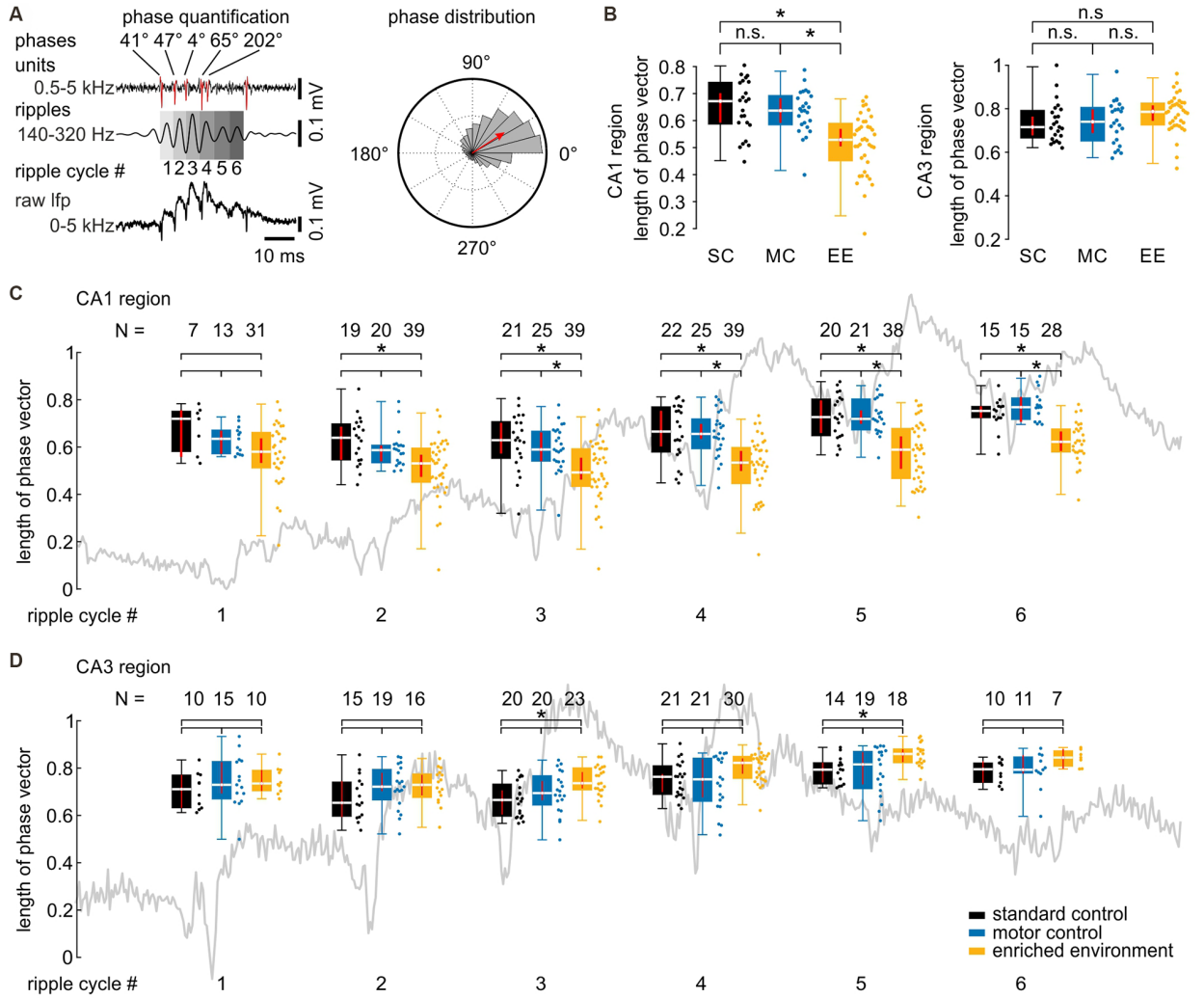

FIGURE 3 | Coupling precision between spikes and field ripples is decreased after environmental enrichment. **(A)** Schematics of firing precision quantification. Each ripple cycle was divided into 360° starting with the first detectable ripple trough of a sharp wave-ripple complex. Spike time was measured as the phase within the respective ripple cycle (left panel, upper values). Precision was then quantified by the length of the normalized mean vector (red arrow in the right panel). **(B)** Firing precision is reduced in CA1 but not CA3 as can be seen by the decreased length of the phase vector. *N* = 23 slices from six mice for SC, *N* = 25 slices from five mice for MC, and *N* = 39 slices from eight mice for EE. **(C)** EE-induced differences in firing precision develop over the time course of SPW-R. **(D)** The CA3 region shows no differences in firing precision between EE and the two control groups. The N values above the graphs show the number of slices included in the analysis of the respective ripple cycle (minimum of 33 spikes, see "Materials and Methods" section; length of normalized mean vector in CA1 [median and {confidence interval}]: ripple cycle #1: SC: 0.72 {0.56, 0.76}; MC: 0.64 {0.57, 0.67}; EE: 0.58 {0.53, 0.64}; ripple cycle #2: SC: 0.64 {0.55, 0.69}; MC: 0.59 {0.54, 0.61}; EE: 0.53 {0.47, 0.57}; ripple cycle #3: SC: 0.63 {0.57, 0.70}; MC: 0.59 {0.54, 0.66}; EE: 0.49 {0.46, 0.55}; ripple cycle #4: SC: 0.67 {0.59, 0.75}; MC: 0.66 {0.61, 0.70}; EE: 0.53 {0.50, 0.58}; ripple cycle #5: SC: 0.73 {0.66, 0.80}; MC: 0.72 {0.70, 0.76}; EE: 0.59 {0.51, 0.65}; ripple cycle #6: SC: 0.75 {0.72, 0.77}; MC: 0.77 {0.71, 0.81}; EE: 0.62 {0.58, 0.67}). Asterisks denote *p*-values <0.05 from *post-hoc* testing following a significant Kruskal-Wallis test. Red lines depict the confidence intervals of the median assessed by bootstrapping. n.s., not significant.

was no consistent change in cross-correlation between CA3 and CA1, despite small differences between standard control and environmental enrichment (**Figure 2C**, cross-correlation value: SC: 2.82 {1.83, 3.41}; MC: 2.34 {1.47, 2.79}; EE: 1.71 {1.39, 2.11}; cross-correlation time lag [ms]: SC: 5.6 {3.5, 6.0}; MC: 6.8 {5.2, 9.6}; EE: 7.8 {5.4, 10.6}). We next tested whether timing precision of units to the events propagating from CA3 to CA1was different between groups. Unit discharges in CA3 were correlated with the phase of the respective ripple cycle or unit discharges in CA1 as visualized in event cross-correlation histograms or circular plots (**Figure 2A** right, see also **Figure 3A**). To compensate for the delay during SPW-R propagation, time points of unit discharges and ripple troughs in CA1 were shifted by the time lag quantified by the cross-correlation of sharp waves between CA3 and CA1. Temporal firing precision was assessed by the normalized length of the summed phase vector. Neither CA3 unit to CA1 ripple coupling nor CA3 unit to CA1 unit coupling was altered by environmental enrichment (**Figure 2D**; CA3 unit × CA1 ripple

phase vector length: SC: 0.38 {0.28, 0.44}; MC: 0.46 {0.37, 0.48}; EE: 0.40 {0.38, 0.43}; CA3 unit × CA1 unit phase vector length: SC: 0.18 {0.12, 0.25}; MC: 0.22 {0.16, 0.24}; EE: 0.14 {0.11, 0.21}).

The Precision of Cell Firing Is Reduced Following Environmental Enrichment In CA1 but Not CA3

Temporal firing synchrony is not only propagated from CA3 to CA1 but is especially precisely synchronized within local networks in CA3 and CA1 (Ylinen et al., 1995; Both et al., 2008; Bahner et al., 2011). We, therefore, tested whether timing precision was different between groups, in addition to the increased unit firing rate in EE animals (**Figure 3**). Normalized length of the summed phase vector revealed a significant decrease in firing precision following enriched environment in CA1 but not in CA3 (**Figure 3B**; length of normalized mean vector in CA1 [median and {confidence interval}]: SC: 0.67 {0.59, 0.74}; MC: 0.64 {0.59, 0.68}; EE: 0.53 {0.50, 0.57}; CA3: SC: 0.72 {0.68, 0.76}; MC: 0.74 {0.69, 0.80}; EE: 0.79 {0.74, 0.82}; SC: $N = 23$ slices from six animals; MC: $N = 25$ slices from five animals; EE: $N = 39$ slices from eight animals). A more detailed analysis revealed that the loss in precision developed over time during each sharp wave: while there was no difference in spike precision on the initial ripple cycles, a pronounced reduction in the precision of neurons from the enriched environment group occurred during the second half of the sharp wave-ripple complex (**Figure 3C**). Again, CA3 did not show any alterations of unit precision on any ripple cycles (**Figure 3D**).

Inhibitory Input but Not Excitatory Input During Sharp Wave-Ripples Is Reduced Following Environmental Enrichment

Previous work has revealed that propagating SPW-R involves strong synaptic excitation of CA1 pyramidal cells followed by pronounced, rhythmic perisomatic inhibition at ripple frequency (Ellender et al., 2010; Maier et al., 2011; Gan et al., 2017; Geschwill et al., 2020). We, therefore, analyzed the contribution of inhibitory and excitatory synaptic input during SPW-R in animals from enriched environments compared to motor controls. Standard conditions were not included in this analysis due to the absence of any differences to MC in the field- and unit activity. Whole-cell patch clamp recordings from CA1 pyramidal cells were performed at different holding potentials, aligned with SPW-R, and analyzed for the relative contribution of excitatory and inhibitory synaptic inputs, respectively; Borg-Graham et al., 1998; Haider et al., 2006; **Figure 4A**). Cells were recorded 'blindly' by inserting the patch clamp electrode into the stratum pyramidale guided by a low-magnification stereo microscope that was not able to resolve single cells. Therefore, recordings likely include neurons from both, the deep and the superficial pyramidal cell layer. PV basket cells are highly active during SPW-R and exert stronger inhibition on deep layer pyramidal cells compared to superficial neurons (Lee et al., 2014; Valero et al., 2015). Therefore, we aimed to assess the position of the recorded cells to exclude a possible bias between the two groups. From the 11 cells recorded after MC treatment, we recovered five cells (one deep, four superficial) and from the seven cells recorded after EE we recovered two cells (one deep, one superficial, **Figure 4B**). We then calculated the probability that both samples were highly different, with at least 70% superficial cells in the MC group (i.e., 8 out of 11) and at least 70% deep cells in the EE group (i.e., five out of seven). This strongly biased distribution has a probability of 1.0% (see "Materials and Methods" section). Taking into account the observed bias towards superficial cells (five superficial vs. two deep cells), the probability lowers to 0.14%. This control largely excludes that the observed differences between cells from MC and EE conditions are due to different locations of neurons between the samples.

We then calculated the apparent reversal potential (E_{rev}) of mixed excitatory and inhibitory postsynaptic currents during SPW-R. E_{rev} of mice from the enriched environment group was significantly shifted towards more positive values on the ascending phase of the SPW-R as compared to the motor control group (**Figure 4C**). Consequently, peak conductance of inhibitory inputs was significantly reduced in slices from enriched environment while the apparent excitatory conductance change did not show any alterations (**Figure 4D**; inhibitory conductance change [nS, median and {confidence interval}]: MC: 4.4 {2.8, 6.5}; EE: 1.8 {1.3, 4.1}; excitatory conductance change: MC: 0.90 {0.52, 1.84}; EE: 0.85 {0.60, 1.08}; MC: $N = 11$ cells from four animals; EE: $N = 7$ cells from four animals). In consequence, the inhibition-excitation (I/E) ratio was reduced following environmental enrichment (MC: 4.4 {3.9, 5.8}; EE: 2.4 {2.0, 3.4}). Timing of excitatory and inhibitory conductance changes was not different between motor controls and enriched environment (**Figure 4B**; [in ms] MC: 3.3 {0.6, 4.6}; EE: 6.2 {0.4, 7.3}). To quantify the dynamics of inhibitory and excitatory conductance changes, we calculated the rise and decay times between 20% and 80% of the maximal conductance change. Similar to the peak timing, we did not observe any differences between the two groups (**Figure 4E**; excitation rise time [in ms] MC: 9.3 {8.1, 10.1}; EE: 7.8 {6.9, 8.9}; excitation decay time [in ms] MC: 12.4 {11.0, 13.2}; EE: 10.0 {8.4, 11.2}; inhibition rise time [in ms] MC: 7.8 {6.1, 9.6}; EE: 8.7 {5.7, 10.2}; inhibition decay time [in ms] MC: 13.1 {11.3, 18.9}; EE: 15.7 {15.2, 19.0}). Thus, inhibition during SPW-R is reduced after EE, in line with the increase in unit discharge rate.

Neither the Number of Inhibitory Cells nor the Number of PV$^+$ Inhibitory Cells Is Altered Following Environmental Enrichment

SPW-R go along with increased activity of inhibitory interneurons, particularly involving fast-spiking perisomatically inhibiting parvalbumin-expressing (PV$^+$) neurons (Klausberger and Somogyi, 2008). In order to control for potential differences in the number of these inhibitory interneurons, we stained slices from all experimental groups for parvalbumin and the global GABAergic marker GAD67 (glutamate decarboxylase 67; **Figure 5A**). However, none of the quantifications revealed any

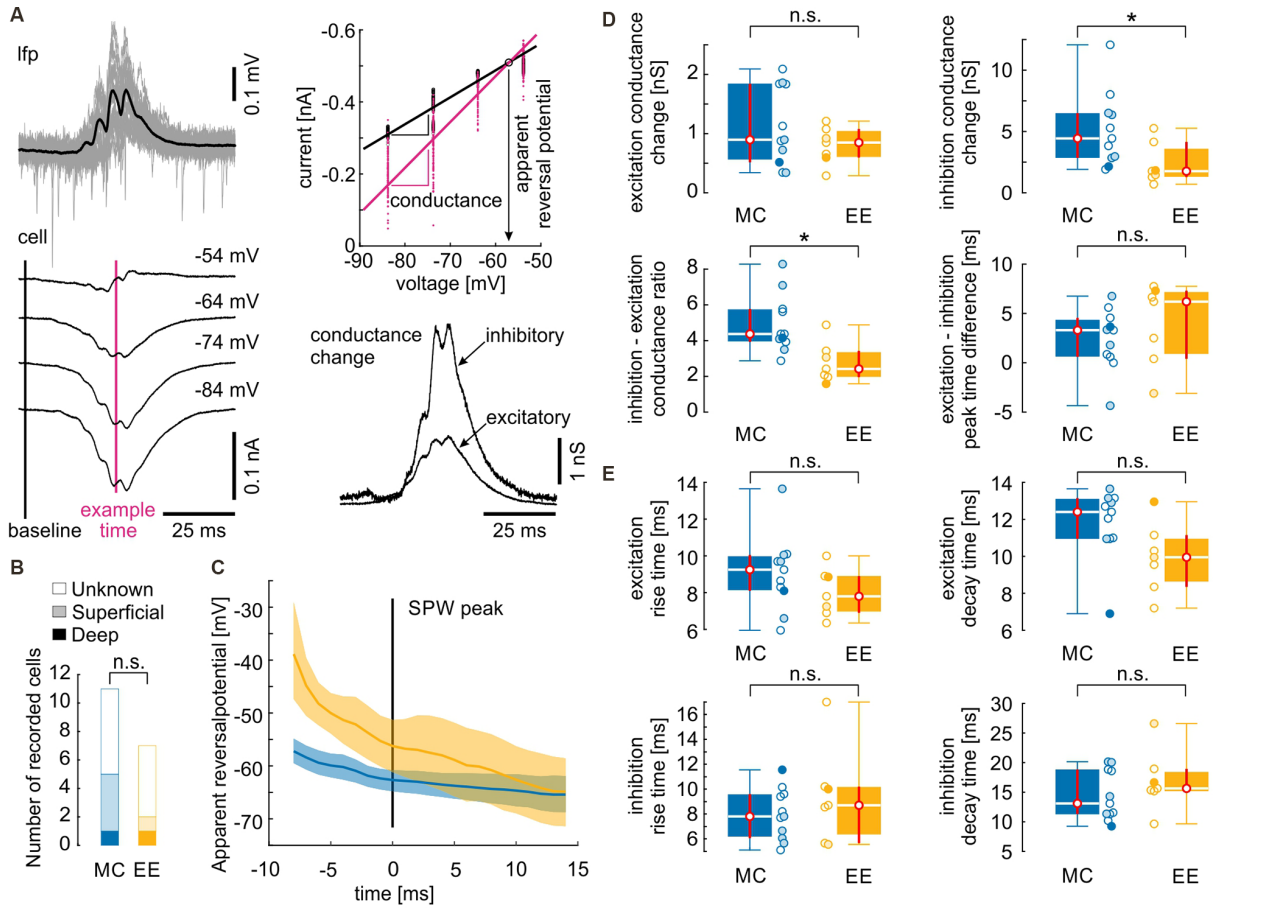

FIGURE 4 | Inhibitory inputs during sharp waves are reduced after environmental enrichment. **(A)** Illustration of conductance analysis (similar to Borg-Graham et al., 1998; Haider et al., 2006). SPW-R were aligned by their peak (upper left panel, black line is the mean SPW-R). Currents from different holding potentials (lower left panel; mean currents from one recording) yielded instantaneous membrane conductance by fitting their I–E relation (upper right panel): black line is the linear regression fitted to the individual values 30 ms before the SPW peak. The slope of the linear regression yields the input conductance of the cell. Every subsequent time point can be similarly fitted. As an example, the time point near the SPW peak is depicted in magenta. The intersection with the baseline regression yields the apparent reversal potential of the conductance change. This allows a separation of the conductance change into an inhibitory and an excitatory component which is depicted in the lower right panel (see also "Materials and Methods" section). **(B)** From the 18 recorded cells, only seven locations could be recovered. However, there is no evidence that the MC group mainly consisted of superficial cells while the EE group mainly consisted of deep cells or *vice versa*. **(C)** Time course of the apparent reversal potential. Lines depict the median values, the shaded areas depict the 95% confidence intervals assessed by bootstrapping. Apparent reversal potential is shifted towards more positive values in EE cells at the ascending phase of the SPW. **(D)** Excitatory conductance changes and timing between excitatory and inhibitory inputs do not differ between control and environmental enrichment. However, inhibitory conductance changes and inhibitory–excitatory conductance change ratio is decreased after environmental enrichment. **(E)** Dynamics of conductance changes quantified as the time between the 20% and the 80% value did not change after environmental enrichment. Open circles depict cells with unknown locations, lightly filled circles depict cells from the superficial layer and filled circles depict cells from the deep layer. $N = 11$ cells from four mice for motor control and $N = 7$ cells from four mice for environmental enrichment. Asterisks denote p-values < 0.05 computed by a Mann–Whitney U test. Red lines depict the confidence intervals of the median assessed by bootstrapping. n.s., not significant.

significant differences between the cell populations or the ratio between PV^+ and $GAD67^+$ (**Figure 5B**; number of $GAD67^+$ cells [per image, median and {confidence intervals}]: SC: 69.5 {51, 78}; MC: 68.5 {55, 84}; EE: 61 {56.5, 70.5}; number of PV^+ cells: SC: 19.5 {17.5, 25}; MC: 28 {20, 30.5}; EE: 22.5 {19.5, 28}; percentage of PV^+ cells: SC: 32.7 {28.3, 39.0}; MC: 37.4 {33.8, 40.1}; EE: 39.2 {33.3, 40.6}; SC: $N = 10$ slices from five animals; MC: $N = 12$ slices from six animals; EE: $N = 12$ slices from six animals). Thus, the different environmental conditions used in this study do not alter the number or percentage of PV^+ interneurons in the hippocampus.

DISCUSSION

Environmental enrichment has been a mainstream paradigm in neuroplasticity research for several decades (Bennett et al., 1964; Consorti et al., 2019). Although there is much knowledge about the effects of EE at the molecular, cellular, and behavioral levels, much less is known about changes at the network level. We, therefore, analyzed memory-related network activity in the mouse hippocampus following exposure to EE for 10–15 days. We report that environmental enrichment in adult mice leads to an increase in network activity during sharp wave-ripple

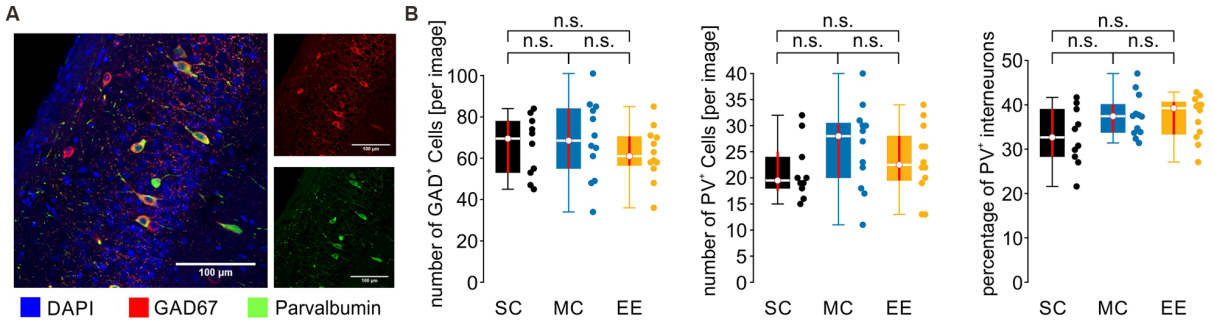

FIGURE 5 | The number and distribution of inhibitory and PV+ inhibitory cells are not different between control animals and environmental enrichment. **(A)** Example image from CA1. Cell nuclei are stained by DAPI in blue, inhibitory cells by GAD67 in red, and PV+ inhibitory cells in green. **(B)** Neither the number nor the percentage of inhibitory and PV+ inhibitory cells is changed by environmental enrichment. *N* = 10 slices from five mice for standard conditions, *N* = 12 slices from six mice for motor control, and *N* = 12 slices from six mice for environmental enrichment. Red lines depict the confidence intervals of the median assessed by bootstrapping. n.s., not significant.

complexes (SPW-R) in CA1. At the cellular level, these changes are accompanied by decreased inhibition during sharp waves and with less precise firing during ripple oscillations. Thus, EE induces specific alterations of a spatio-temporal pattern of network activity which is involved in memory consolidation and retrieval (Lee and Wilson, 2002; Buzsaki, 2015; Khodagholy et al., 2017).

EE has profound effects on memory processing, including the formation, consolidation, and retrieval of spatial and declarative memory (Bilkey et al., 2017; Ohline and Abraham, 2019; Smail et al., 2020). The mechanisms underlying this cognitive function have been intensely studied during the past decades, including experience-dependent tuning of single neurons (e.g., place cells) and complex multi-neuronal patterns which are formed on top of coherent network oscillations (Wilson and McNaughton, 1994; Lee and Wilson, 2002; Frank et al., 2006; Klausberger and Somogyi, 2008). These patterns may be the network-level correlate of memories. We focused on SPW-R (Buzsaki et al., 1992) which are involved in the consolidation of memories after the initial formation of place-encoding patterns in the hippocampus (Buzsaki, 2015; Khodagholy et al., 2017). SPW-R contains local network oscillations of particularly high frequency (∼200 Hz). Neurons in the rodent hippocampus fire action potentials with strong coupling to this fast rhythm, reaching firing precision in the ms range (Ylinen et al., 1995). Key features of SPW-R are present in spontaneous network activity in mouse hippocampal slices (Maier et al., 2003; Bahner et al., 2011), making them an ideal model system to test for subtle alterations in inhibition-excitation balance, event-related network activity, and firing precision.

We found several differences of SPW-R in CA1 between EE and the two control groups, MC and SC: (i) increased amplitude of sharp waves; (ii) increased firing of units during SPW-R; (iii) increased number of ripple cycles per sharp wave; (iv) decreased precision of firing with respect to individual ripple cycles; and (v) decreased inhibition-excitation ratio in CA1 pyramidal cells. While the mechanisms underlying SPW-R are not entirely clear, most of these changes can be coherently explained by reduced synaptic inhibition during the events. Converging evidence from different groups has shown that SPW-R is accompanied by strong activation of fast-spiking interneurons mediating potent perisomatic inhibition of pyramidal cells (Ylinen et al., 1995; Klausberger and Somogyi, 2008; Gan et al., 2017). The resulting inhibitory postsynaptic potentials generate a strong rhythmic signal at the population level which has been suggested to entrain pyramidal cells into the ripple cycles (Ylinen et al., 1995; Schlingloff et al., 2014; Gulyas and Freund, 2015). Experimental evidence and computer models suggest that electrical coupling between pyramidal cell axons (Draguhn et al., 1998; Schmitz et al., 2001; Traub et al., 2002, 2012) or supra-linear integration of excitatory inputs to pyramidal cell dendrites (Buzsaki et al., 1996; Memmesheimer, 2010; Jahnke et al., 2015) are important additional mechanisms contributing to spike-ripple coupling. While these models are not mutually exclusive, the crucial contribution of rhythmic inhibition to oscillating network patterns is undisputed.

As noted above, differences between EE and controls were most pronounced in CA1 while field potentials and unit discharges were not consistently changed in CA3. While the reasons underlying this discrepancy remain presently unknown, there are several relevant differences between both sub-networks: CA3 pyramidal neurons express extensive recurrent excitatory connections which are likely involved in the initiation of SPW-R (Miles and Wong, 1986; Buzsaki, 2015; Guzman et al., 2016); feedforward inhibition is strongly driven by inputs from mossy fibers in CA3 and by Schaffer collaterals and entorhinal cortex inputs in CA1 (Sun et al., 2017; Valero and de la Prida, 2018); in addition, the relative abundance of different interneuron subtypes differs between regions, including a lower incidence of VIP-positive interneurons in CA3 compared to CA1 (Botcher et al., 2014). The latter difference may be particularly important since VIP-positive interneurons inhibit parvalbumin-expressing interneurons which are strongly activated during SPW-R (Klausberger and Somogyi, 2008; Guet-McCreight et al., 2020). An enriched environment has been shown to decrease inhibition of hippocampal principal cells following changes

in VIP interneuron-mediated innervation of PV-expressing interneurons (Donato et al., 2013). Due to the larger fraction of VIP-expressing interneurons, this mechanism might be more pronounced in CA1 compared to CA3, providing a potential explanation for the selective increase in amplitude and unit firing during SPW-R in CA1.

In line with the potential decrease in activation of fast-spiking interneurons in CA1 we observed a reduction in inhibitory conductance change during SPW-R in CA1 pyramidal cells following EE exposure. This might explain the increased rate of unit discharges during SPW-R. A potential confound is the diversity of hippocampal principal cells which have recently been shown to differ with respect to localization, expression of calbindin, and efficacy of synaptic inhibition (Valero et al., 2015). We controlled for a possible bias with respect to superficial vs. deep layer cells and to exclude this possibility for the present data. As a consequence of reduced synaptic inhibition, net excitatory input to pyramidal cells may be prolonged, in line with the larger number of ripple cycles. The increase in sharp wave amplitude is less easily explained. We have previously shown that this extracellular voltage transient in the pyramidal layer is mostly generated by inhibitory synaptic currents, at least in brain slices (Schonberger et al., 2014). Other suggestions, however, include a contribution of return currents from dendritic excitatory inputs which, in turn, would again be compatible with enhanced pyramidal cell activity following reduced inhibition (Ylinen et al., 1995).

The precise mechanisms underlying the reduced inhibition during SPW-R remain presently elusive. We did not find any evidence for decreases in the total number of GABAergic cells or in the relative abundance of PV^+ interneurons. Thus, it is likely that functional changes at inhibitory synapses or reduced recruitment of fast-spiking interneurons underlie the present observation. Indeed, previous work shows that EE alters the recruitment of interneurons and, hence, activity-dependent inhibition (Sale et al., 2007; Baroncelli et al., 2010; Eckert et al., 2010; Fu et al., 2015). The underlying mechanisms may include a reduction in perineuronal nets around inhibitory synapses (Kwok et al., 2011; Cattaud et al., 2018). In any case, the net decrease in inhibition during SPW-R is in line with most changes observed at the level of field potentials and unit discharges. This mechanism may be useful for developing new therapeutic strategies to increase synaptic plasticity in clinical situations like amblyopia (Consorti et al., 2019) or intellectual disability (Fernandez and Garner, 2007; Begenisic et al., 2011).

Motor activity has profound effects on neuronal network activity and plasticity (Voss et al., 2013; Ohline and Abraham, 2019). An enriched environment is expected to trigger increased motor activity which, hence, may account partially for EE-induced changes (van Praag et al., 1999; Donato et al., 2013; Vivar et al., 2013). We, therefore, included a second control group in our study, where mice were offered a running wheel in their home cages. These mice showed no consistent alterations in all examined parameters at the field potential level compared to controls in standard housing conditions. It is, thus, likely that our present findings are specific for environmental enrichment, possibly including a larger spectrum of sensory inputs, social interactions, or other factors. We do not exclude that the motor activity itself induced changes at the cellular level which we did not examine for standard controls. Indeed, such changes have been shown in the motor cortex (Donato et al., 2013) but also in the hippocampus where increased motor activity promotes adult neurogenesis and learning (van Praag et al., 1999, 2005; Bolz et al., 2015). We focused, however, on memory-related network activity which was not altered by a mere increase in motor activity. At the network level, our present analysis was restricted to SPW-R which are mostly involved in memory consolidation. Previous work, however, has shown that gamma oscillations, which are involved in memory encoding, are also enhanced by EE (Shinohara et al., 2013). Together, the resulting changes of network activity may contribute to the specific cognitive effects of EE, especially those related to spatial or declarative memory processing (Donato et al., 2013; Ball et al., 2019; Gelfo, 2019). Revealing such EE-induced changes at the network level may instruct future attempts to increase neuronal plasticity or mnemonic functions in neuro-psychiatric disorders where EE has already been shown to exert beneficial effects (Nithianantharajah and Hannan, 2006; Rogers et al., 2019).

In summary, our results show specific changes of spatio-temporal activity patterns and neuronal excitability during SPW-R following a short (10–15 days) exposure to an enriched environment. These changes are in line with, and potentially mediated by, a decrease in synaptic inhibition of pyramidal cells during SPW-R.

DATA AVAILABILITY STATEMENT

The raw data supporting the conclusions of this article will be made available by the authors, without undue reservation.

ETHICS STATEMENT

The animal study was reviewed and approved by Regierungspräsidium Karlsruhe, 76247 Karlsruhe.

AUTHOR CONTRIBUTIONS

MB and AD conceived and designed the experiments. LL, MK, and DH performed experiments. LL, MK, DH, and MB analyzed the data. MB, AD, and LL wrote the original manuscript. All authors revised and edited the manuscript. All authors contributed to the article and approved the submitted version.

FUNDING

This work was supported by the Deutsche Forschungsgemeinschaft (SFB1134/A01, A03, and BO 3512/1-1).

ACKNOWLEDGMENTS

We thank Nadine Zuber, Katja Lankisch, and Tina Sackmann for excellent technical assistance.

REFERENCES

Bahner, F., Weiss, E. K., Birke, G., Maier, N., Schmitz, D., Rudolph, U., et al. (2011). Cellular correlate of assembly formation in oscillating hippocampal networks *in vitro*. *Proc. Natl. Acad. Sci. U S A* 108, E607–E616. doi: 10.1073/pnas.1103546108

Ball, N. J., Mercado, E., 3rd, and Orduna, I. (2019). Enriched environments as a potential treatment for developmental disorders: a critical assessment. *Front. Psychol.* 10:466. doi: 10.3389/fpsyg.2019.00466

Baroncelli, L., Sale, A., Viegi, A., Maya Vetencourt, J. F., De Pasquale, R., Baldini, S., et al. (2010). Experience-dependent reactivation of ocular dominance plasticity in the adult visual cortex. *Exp. Neurol.* 226, 100–109. doi: 10.1016/j.expneurol.2010.08.009

Begenisic, T., Spolidoro, M., Braschi, C., Baroncelli, L., Milanese, M., Pietra, G., et al. (2011). Environmental enrichment decreases GABAergic inhibition and improves cognitive abilities, synaptic plasticity and visual functions in a mouse model of Down syndrome. *Front. Cell. Neurosci.* 5:29. doi: 10.3389/fncel.2011.00029

Bennett, E. L., Diamond, M. C., Krech, D., and Rosenzweig, M. R. (1964). Chemical and anatomical plasticity brain. *Science* 146, 610–619. doi: 10.1126/science.146.3644.610

Bennett, J. C., McRae, P. A., Levy, L. J., and Frick, K. M. (2006). Long-term continuous, but not daily, environmental enrichment reduces spatial memory decline in aged male mice. *Neurobiol. Learn. Mem.* 85, 139–152. doi: 10.1016/j.nlm.2005.09.003

Bilkey, D. K., Cheyne, K. R., Eckert, M. J., Lu, X., Chowdhury, S., Worley, P. F., et al. (2017). Exposure to complex environments results in more sparse representations of space in the hippocampus. *Hippocampus* 27, 1178–1191. doi: 10.1002/hipo.22762

Bolz, L., Heigele, S., and Bischofberger, J. (2015). Running improves pattern separation during novel object recognition. *Brain Plast.* 1, 129–141. doi: 10.3233/BPL-150010

Borg-Graham, L. J., Monier, C., and Fregnac, Y. (1998). Visual input evokes transient and strong shunting inhibition in visual cortical neurons. *Nature* 393, 369–373. doi: 10.1038/30735

Botcher, N. A., Falck, J. E., Thomson, A. M., and Mercer, A. (2014). Distribution of interneurons in the CA2 region of the rat hippocampus. *Front. Neuroanat.* 8:104. doi: 10.3389/fnana.2014.00104

Both, M., Bahner, F., von Bohlen und Halbach, O., and Draguhn, A. (2008). Propagation of specific network patterns through the mouse hippocampus. *Hippocampus* 18, 899–908. doi: 10.1002/hipo.20446

Buzsaki, G. (2015). Hippocampal sharp wave-ripple: a cognitive biomarker for episodic memory and planning. *Hippocampus* 25, 1073–1188. doi: 10.1002/hipo.22488

Buzsaki, G., and Draguhn, A. (2004). Neuronal oscillations in cortical networks. *Science* 304, 1926–1929. doi: 10.1126/science.1099745

Buzsaki, G., Horvath, Z., Urioste, R., Hetke, J., and Wise, K. (1992). High-frequency network oscillation in the hippocampus. *Science* 256, 1025–1027. doi: 10.1126/science.1589772

Buzsaki, G., Penttonen, M., Nadasdy, Z., and Bragin, A. (1996). Pattern and inhibition-dependent invasion of pyramidal cell dendrites by fast spikes in the hippocampus *in vivo*. *Proc. Natl. Acad. Sci. U S A* 93, 9921–9925. doi: 10.1073/pnas.93.18.9921

Cattaud, V., Bezzina, C., Rey, C. C., Lejards, C., Dahan, L., and Verret, L. (2018). Early disruption of parvalbumin expression and perineuronal nets in the hippocampus of the Tg2576 mouse model of Alzheimer's disease can be rescued by enriched environment. *Neurobiol. Aging* 72, 147–158. doi: 10.1016/j.neurobiolaging.2018.08.024

Consorti, A., Sansevero, G., Torelli, C., Berardi, N., and Sale, A. (2019). From basic visual science to neurodevelopmental disorders: the voyage of environmental enrichment-like stimulation. *Neural Plast.* 2019:5653180. doi: 10.1155/2019/5653180

Cooper, D. D., and Frenguelli, B. G. (2021). The influence of sensory experience on the glutamatergic synapse. *Neuropharmacology* 193:108620. doi: 10.1016/j.neuropharm.2021.108620

Donato, F., Rompani, S. B., and Caroni, P. (2013). Parvalbumin-expressing basket-cell network plasticity induced by experience regulates adult learning. *Nature* 504, 272–276. doi: 10.1038/nature12866

Draguhn, A., Traub, R. D., Schmitz, D., and Jefferys, J. G. (1998). Electrical coupling underlies high-frequency oscillations in the hippocampus *in vitro*. *Nature* 394, 189–192. doi: 10.1038/28184

Eckert, M. J., Bilkey, D. K., and Abraham, W. C. (2010). Altered plasticity in hippocampal CA1, but not dentate gyrus, following long-term environmental enrichment. *J. Neurophysiol.* 103, 3320–3329. doi: 10.1152/jn.01037.2009

Ellender, T. J., Nissen, W., Colgin, L. L., Mann, E. O., and Paulsen, O. (2010). Priming of hippocampal population bursts by individual perisomatic-targeting interneurons. *J. Neurosci.* 30, 5979–5991. doi: 10.1523/JNEUROSCI.3962-09.2010

Fernandez, F., and Garner, C. C. (2007). Over-inhibition: a model for developmental intellectual disability. *Trends Neurosci.* 30, 497–503. doi: 10.1016/j.tins.2007.07.005

Frank, L. M., Brown, E. N., and Stanley, G. B. (2006). Hippocampal and cortical place cell plasticity: implications for episodic memory. *Hippocampus* 16, 775–784. doi: 10.1002/hipo.20200

Fu, Y., Kaneko, M., Tang, Y., Alvarez-Buylla, A., and Stryker, M. P. (2015). A cortical disinhibitory circuit for enhancing adult plasticity. *eLife* 4:e05558. doi: 10.7554/eLife.05558

Gan, J., Weng, S. M., Pernia-Andrade, A. J., Csicsvari, J., and Jonas, P. (2017). Phase-locked inhibition, but not excitation, underlies hippocampal ripple oscillations in awake mice *in vivo*. *Neuron* 93, 308–314. doi: 10.1016/j.neuron.2016.12.018

Gelfo, F. (2019). Does experience enhance cognitive flexibility? an overview of the evidence provided by the environmental enrichment studies. *Front. Behav. Neurosci.* 13:150. doi: 10.3389/fnbeh.2019.00150

Geschwill, P., Kaiser, M. E., Grube, P., Lehmann, N., Thome, C., Draguhn, A., et al. (2020). Synchronicity of excitatory inputs drives hippocampal networks to distinct oscillatory patterns. *Hippocampus* 30, 1044–1057. doi: 10.1002/hipo.23214

Greifzu, F., Pielecka-Fortuna, J., Kalogeraki, E., Krempler, K., Favaro, P. D., Schluter, O. M., et al. (2014). Environmental enrichment extends ocular dominance plasticity into adulthood and protects from stroke-induced impairments of plasticity. *Proc. Natl. Acad. Sci. U S A* 111, 1150–1155. doi: 10.1073/pnas.1313385111

Guet-McCreight, A., Skinner, F. K., and Topolnik, L. (2020). Common principles in functional organization of VIP/calretinin cell-driven disinhibitory circuits across cortical areas. *Front. Neural Circuits* 14:32. doi: 10.3389/fncir.2020.00032

Gulyas, A. I., and Freund, T. T. (2015). Generation of physiological and pathological high frequency oscillations: the role of perisomatic inhibition in sharp-wave ripple and interictal spike generation. *Curr. Opin. Neurobiol.* 31, 26–32. doi: 10.1016/j.conb.2014.07.020

Guzman, S. J., Schlogl, A., Frotscher, M., and Jonas, P. (2016). Synaptic mechanisms of pattern completion in the hippocampal CA3 network. *Science* 353, 1117–1123. doi: 10.1126/science.aaf1836

Haider, B., Duque, A., Hasenstaub, A. R., and McCormick, D. A. (2006). Neocortical network activity *in vivo* is generated through a dynamic balance of excitation and inhibition. *J. Neurosci.* 26, 4535–4545. doi: 10.1523/JNEUROSCI.5297-05.2006

Jahnke, S., Timme, M., and Memmesheimer, R. M. (2015). A unified dynamic model for learning, replay and sharp-wave/ripples. *J. Neurosci.* 35, 16236–16258. doi: 10.1523/JNEUROSCI.3977-14.2015

Kempermann, G. (2019). Environmental enrichment, new neurons and the neurobiology of individuality. *Nat. Rev. Neurosci.* 20, 235–245. doi: 10.1038/s41583-019-0120-x

Khodagholy, D., Gelinas, J. N., and Buzsaki, G. (2017). Learning-enhanced coupling between ripple oscillations in association cortices and hippocampus. *Science* 358, 369–372. doi: 10.1126/science.aan6203

Klausberger, T., and Somogyi, P. (2008). Neuronal diversity and temporal dynamics: the unity of hippocampal circuit operations. *Science* 321, 53–57. doi: 10.1126/science.1149381

Kwok, J. C., Dick, G., Wang, D., and Fawcett, J. W. (2011). Extracellular matrix and perineuronal nets in CNS repair. *Dev. Neurobiol.* 71, 1073–1089. doi: 10.1002/dneu.20974

Lee, S. H., Marchionni, I., Bezaire, M., Varga, C., Danielson, N., Lovett-Barron, M., et al. (2014). Parvalbumin-positive basket cells differentiate among hippocampal pyramidal cells. *Neuron* 82, 1129–1144. doi: 10.1016/j.neuron.2014.03.034

Lee, A. K., and Wilson, M. A. (2002). Memory of sequential experience in the hippocampus during slow wave sleep. *Neuron* 36, 1183–1194. doi: 10.1016/s0896-6273(02)01096-6

Leggio, M. G., Mandolesi, L., Federico, F., Spirito, F., Ricci, B., Gelfo, F., et al. (2005). Environmental enrichment promotes improved spatial abilities and enhanced dendritic growth in the rat. *Behav. Brain Res.* 163, 78–90. doi: 10.1016/j.bbr.2005.04.009

Maier, N., Nimmrich, V., and Draguhn, A. (2003). Cellular and network mechanisms underlying spontaneous sharp wave-ripple complexes in mouse hippocampal slices. *J. Physiol.* 550, 873–887. doi: 10.1113/jphysiol.2003.044602

Maier, N., Tejero-Cantero, A., Dorrn, A. L., Winterer, J., Beed, P. S., Morris, G., et al. (2011). Coherent phasic excitation during hippocampal ripples. *Neuron* 72, 137–152. doi: 10.1016/j.neuron.2011.08.016

Memmesheimer, R. M. (2010). Quantitative prediction of intermittent high-frequency oscillations in neural networks with supralinear dendritic interactions. *Proc. Natl. Acad. Sci. U S A* 107, 11092–11097. doi: 10.1073/pnas.0909615107

Miles, R., and Wong, R. K. (1986). Excitatory synaptic interactions between CA3 neurones in the guinea-pig hippocampus. *J. Physiol.* 373, 397–418. doi: 10.1113/jphysiol.1986.sp016055

Nithianantharajah, J., and Hannan, A. J. (2006). Enriched environments, experience-dependent plasticity and disorders of the nervous system. *Nat. Rev. Neurosci.* 7, 697–709. doi: 10.1038/nrn1970

Novkovic, T., Mittmann, T., and Manahan-Vaughan, D. (2015). BDNF contributes to the facilitation of hippocampal synaptic plasticity and learning enabled by environmental enrichment. *Hippocampus* 25, 1–15. doi: 10.1002/hipo.22342

Ohline, S. M., and Abraham, W. C. (2019). Environmental enrichment effects on synaptic and cellular physiology of hippocampal neurons. *Neuropharmacology* 145, 3–12. doi: 10.1016/j.neuropharm.2018.04.007

O'Keefe, J., and Recce, M. L. (1993). Phase relationship between hippocampal place units and the EEG theta rhythm. *Hippocampus* 3, 317–330. doi: 10.1002/hipo.450030307

Rogers, J., Renoir, T., and Hannan, A. J. (2019). Gene-environment interactions informing therapeutic approaches to cognitive and affective disorders. *Neuropharmacology* 145, 37–48. doi: 10.1016/j.neuropharm.2017.12.038

Sale, A., Maya Vetencourt, J. F., Medini, P., Cenni, M. C., Baroncelli, L., De Pasquale, R., et al. (2007). Environmental enrichment in adulthood promotes amblyopia recovery through a reduction of intracortical inhibition. *Nat. Neurosci.* 10, 679–681. doi: 10.1038/nn1899

Schlingloff, D., Kali, S., Freund, T. F., Hajos, N., and Gulyas, A. I. (2014). Mechanisms of sharp wave initiation and ripple generation. *J. Neurosci.* 34, 11385–11398. doi: 10.1523/JNEUROSCI.0867-14.2014

Schmitz, D., Schuchmann, S., Fisahn, A., Draguhn, A., Buhl, E. H., Petrasch-Parwez, E., et al. (2001). Axo-axonal coupling. a novel mechanism for ultrafast neuronal communication. *Neuron* 31, 831–840. doi: 10.1016/s0896-6273(01)00410-x

Schonberger, J., Draguhn, A., and Both, M. (2014). Lamina-specific contribution of glutamatergic and GABAergic potentials to hippocampal sharp wave-ripple complexes. *Front. Neural Circuits* 8:103. doi: 10.3389/fncir.2014.00103

Shinohara, Y., Hosoya, A., and Hirase, H. (2013). Experience enhances gamma oscillations and interhemispheric asymmetry in the hippocampus. *Nat. Commun.* 4:1652. doi: 10.1038/ncomms2658

Smail, M. A., Smith, B. L., Nawreen, N., and Herman, J. P. (2020). Differential impact of stress and environmental enrichment on corticolimbic circuits. *Pharmacol. Biochem. Behav.* 197:172993. doi: 10.1016/j.pbb.2020.172993

Sun, Q., Sotayo, A., Cazzulino, A. S., Snyder, A. M., Denny, C. A., and Siegelbaum, S. A. (2017). Proximodistal heterogeneity of hippocampal CA3 pyramidal neuron intrinsic properties, connectivity and reactivation during memory recall. *Neuron* 95, 656–672.e3. doi: 10.1016/j.neuron.2017.07.012

Traub, R. D., Draguhn, A., Whittington, M. A., Baldeweg, T., Bibbig, A., Buhl, E. H., et al. (2002). Axonal gap junctions between principal neurons: a novel source of network oscillations and perhaps epileptogenesis. *Rev. Neurosci.* 13, 1–30. doi: 10.1515/revneuro.2002.13.1.1

Traub, R. D., Schmitz, D., Maier, N., Whittington, M. A., and Draguhn, A. (2012). Axonal properties determine somatic firing in a model of *in vitro* CA1 hippocampal sharp wave/ripples and persistent gamma oscillations. *Eur. J. Neurosci.* 36, 2650–2660. doi: 10.1111/j.1460-9568.2012.08184.x

Valero, M., Cid, E., Averkin, R. G., Aguilar, J., Sanchez-Aguilera, A., Viney, T. J., et al. (2015). Determinants of different deep and superficial CA1 pyramidal cell dynamics during sharp-wave ripples. *Nat. Neurosci.* 18, 1281–1290. doi: 10.1038/nn.4074

Valero, M., and de la Prida, L. M. (2018). The hippocampus in depth: a sublayer-specific perspective of entorhinal-hippocampal function. *Curr. Opin. Neurobiol.* 52, 107–114. doi: 10.1016/j.conb.2018.04.013

van Praag, H., Kempermann, G., and Gage, F. H. (1999). Running increases cell proliferation and neurogenesis in the adult mouse dentate gyrus. *Nat. Neurosci.* 2, 266–270. doi: 10.1038/6368

van Praag, H., Shubert, T., Zhao, C., and Gage, F. H. (2005). Exercise enhances learning and hippocampal neurogenesis in aged mice. *J. Neurosci.* 25, 8680–8685. doi: 10.1523/JNEUROSCI.1731-05.2005

Vivar, C., Potter, M. C., and van Praag, H. (2013). All about running: synaptic plasticity, growth factors and adult hippocampal neurogenesis. *Curr. Top. Behav. Neurosci.* 15, 189–210. doi: 10.1007/7854_2012_220

von Bohlen und Halbach, O., and von Bohlen und Halbach, V. (2018). BDNF effects on dendritic spine morphology and hippocampal function. *Cell Tissue Res.* 373, 729–741. doi: 10.1007/s00441-017-2782-x

Voss, M. W., Vivar, C., Kramer, A. F., and van Praag, H. (2013). Bridging animal and human models of exercise-induced brain plasticity. *Trends Cogn. Sci.* 17, 525–544. doi: 10.1016/j.tics.2013.08.001

Wilson, M. A., and McNaughton, B. L. (1994). Reactivation of hippocampal ensemble memories during sleep. *Science* 265, 676–679. doi: 10.1126/science.8036517

Ylinen, A., Bragin, A., Nadasdy, Z., Jando, G., Szabo, I., Sik, A., et al. (1995). Sharp wave-associated high-frequency oscillation (200 Hz) in the intact hippocampus: network and intracellular mechanisms. *J. Neurosci.* 15, 30–46. doi: 10.1523/JNEUROSCI.15-01-00030.1995

Conflict of Interest: The authors declare that the research was conducted in the absence of any commercial or financial relationships that could be construed as a potential conflict of interest.

Publisher's Note: All claims expressed in this article are solely those of the authors and do not necessarily represent those of their affiliated organizations, or those of the publisher, the editors and the reviewers. Any product that may be evaluated in this article, or claim that may be made by its manufacturer, is not guaranteed or endorsed by the publisher.

frontiers in Neural Circuits

REVIEW
published: 08 December 2021
doi: 10.3389/fncir.2021.784085

Temporally Targeted Interactions With Pathologic Oscillations as Therapeutical Targets in Epilepsy and Beyond

Tamás Földi[1,2,3,4], *Magor L. Lőrincz*[1,2,5,6] *and Antal Berényi*[1,2,3,7]*

[1] MTA-SZTE "Momentum" Oscillatory Neuronal Networks Research Group, Department of Physiology, University of Szeged, Szeged, Hungary, [2] Neurocybernetics Excellence Center, University of Szeged, Szeged, Hungary, [3] HCEMM-USZ Magnetotherapeutics Research Group, University of Szeged, Szeged, Hungary, [4] Child and Adolescent Psychiatry, Department of the Child Health Center, University of Szeged, Szeged, Hungary, [5] Department of Physiology, Anatomy and Neuroscience, Faculty of Sciences University of Szeged, Szeged, Hungary, [6] Neuroscience Division, Cardiff University, Cardiff, United Kingdom, [7] Neuroscience Institute, New York University, New York, NY, United States

Self-organized neuronal oscillations rely on precisely orchestrated ensemble activity in reverberating neuronal networks. Chronic, non-malignant disorders of the brain are often coupled to pathological neuronal activity patterns. In addition to the characteristic behavioral symptoms, these disturbances are giving rise to both transient and persistent changes of various brain rhythms. Increasing evidence support the causal role of these "oscillopathies" in the phenotypic emergence of the disease symptoms, identifying neuronal network oscillations as potential therapeutic targets. While the kinetics of pharmacological therapy is not suitable to compensate the disease related fine-scale disturbances of network oscillations, external biophysical modalities (e.g., electrical stimulation) can alter spike timing in a temporally precise manner. These perturbations can warp rhythmic oscillatory patterns via resonance or entrainment. Properly timed phasic stimuli can even switch between the stable states of networks acting as multistable oscillators, substantially changing the emergent oscillatory patterns. Novel transcranial electric stimulation (TES) approaches offer more reliable neuronal control by allowing higher intensities with tolerable side-effect profiles. This precise temporal steerability combined with the non- or minimally invasive nature of these novel TES interventions make them promising therapeutic candidates for functional disorders of the brain. Here we review the key experimental findings and theoretical background concerning various pathological aspects of neuronal network activity leading to the generation of epileptic seizures. The conceptual and practical state of the art of temporally targeted brain stimulation is discussed focusing on the prevention and early termination of epileptic seizures.

Keywords: oscillation, oscillopathy, brain stimulation, closed-loop, epilepsy

OPEN ACCESS

Edited by:
Sanja Mikulovic,
Leibniz Institute for Neurobiology (LG), Germany

Reviewed by:
Romain Goutagny,
UMR 7364 Laboratoire de Neurosciences Cognitives et Adaptatives (LNCA), France
Gürsel Caliskan,
Otto von Guericke University Magdeburg, Germany

***Correspondence:**
Antal Berényi
drberenyi@gmail.com

Received: *27 September 2021*
Accepted: *10 November 2021*
Published: *08 December 2021*

Citation:
Földi T, Lőrincz ML and Berényi A (2021) Temporally Targeted Interactions With Pathologic Oscillations as Therapeutical Targets in Epilepsy and Beyond. Front. Neural Circuits 15:784085. doi: 10.3389/fncir.2021.784085

INTRODUCTION: PHYSIOLOGICAL AND PATHOLOGICAL BRAIN OSCILLATIONS

Neuronal oscillations are rhythmic neuronal activities that synchronize different operations within and across neuronal networks (Buzsáki, 2009). The broadband neural signals recorded as the potential fluctuations of the extracellular electrical field can be analyzed to extract signals of various frequency bands. On one hand, the low frequency local field potentials (LFPs), representing the summed transmembrane currents from numerous neurons and on the other hand fast transients (lasting less than a millisecond) represent action potentials (APs) (Buzsáki et al., 2012). Action potentials and LFPs present in raw recording traces can be decomposed by Fourier transformation into various frequency bands on a spectrogram with LFPs and action potentials inhabiting distinct frequency bands (in general < 250 Hz for physiological LFPs, and > 250 Hz for single-unit action potentials). These can be discriminated by applying analog or digital filtering to preferentially pass signals in lower or higher frequency bands, respectively (Hong and Lieber, 2019). The primary origin of neuronal oscillations is the periodical synchronization of synaptic potentials influenced by the periodical fluctuation of excitability in clusters of neurons. The rhythmicity hail from network structures comprising a variety of distinct cell types and population activities (Buzsáki and Watson, 2012). In addition to synaptic activity extracellular field potentials can influence the neuronal membrane potential via ephaptic coupling resulting in altered neuronal firing (Anastassiou et al., 2011). Hence, oscillations and neuronal activities in the brain are cohesive and self-arranged. Oscillations offer an effective potential mechanism for integrating the activity of single neurons toward microcircuits and extensive functional neuronal networks facilitating interregional communication and information processing (Engel et al., 2001; Buzsáki and Draguhn, 2004). Oscillations indicate applicable network conditions, impact neuronal population operations in the network; and constitute the dynamics of macroscopic neuronal networks intimately linked to the behavioral phenotypes on several levels of biological systems (Leuchter et al., 2015). Therefore, the concurrence of altered pathological oscillations and abnormal behavioral phenotypes in neurological and psychiatric diseases is unsurprising; these disorders can be regarded as "Oscillopathies" (Mathalon and Sohal, 2015). Pathologic oscillations represent multiple interactions and a causal relationship with abnormal brain states and functions, respectively. Thus, the pathological oscillations constitute a potential target for therapeutic intervention by applying the recently developed time-and space-targeted brain stimulation technologies (Berényi et al., 2012; Vöröslakos et al., 2018), an approach termed "Oscillotherapeutics" (Takeuchi and Berényi, 2020).

EPILEPSY

Epilepsy is a typical oscillopathy, where the altered neuronal activity results in altered oscillations leading to impaired brain functions. Epilepsy is a common neurological disease characterized by a chronic susceptibility to develop recurring epileptic seizures (Fisher et al., 2014). An epileptic seizure is a temporal behavioral alteration that can mediate objective, noticeable (e.g., muscular contractions) or subjective, covert manifestations (e.g., loss of consciousness). These alterations are presumably generated by hypersynchronous neural activities in various brain networks. Electroencephalography (EEG) is a non-invasive method which, measures the electrical activity of large, synchronously firing populations of neurons with electrodes placed on the scalp. The synchronized neural activity is evident in EEG or intracerebral LFP records during seizures (termed ictal periods) and will lead to specific behavioral manifestations, such as tonic and clonic convulsions among others. Effective pharmacotherapy and neurosurgical intervention in epileptic patients can systematically decrease the occurrence rate of electrographic and behavioral seizures (Glauser et al., 2006). In addition, time-targeted intervention of the abnormal neural oscillations characterizing preictal or ictal states can curtail their behavioral manifestation (Morrell, 2011) indicating a causal association between pathological oscillations and the symptoms of epilepsy.

CLINICAL SIGNIFICANCE

The Role of the Hippocampus in Temporal Lobe Epilepsy

Temporal lobe epilepsy (TLE) is frequently pharmaco-resistant and its uncontrolled generalized seizures increase the risk of sudden unexpected death in epilepsy (Bone et al., 2012; Massey et al., 2014). Surgical resection of the seizure focus is irreversible, massively invasive and can frequently lead to cognitive disorders (Hamberger and Drake, 2006). Furthermore, its implementation in patients with ambiguous or multifocal bilateral TLE is not feasible (Berg et al., 2003; Holmes et al., 2003). Multiple studies have shown altered functional networks in TLE, including those explicitly involving the seizure focus in the hippocampus (Bettus et al., 2010; Englot et al., 2016). Functional network alterations have been reported to relate to neurocognitive disability and surgical treatment outcome (Holmes et al., 2014; Morgan et al., 2017, 2020b). On the other hand, it is well known that physiological hippocampal function requires a complex and particular spatiotemporal activation system (Cooper and Ritchey, 2019). Even in the case of high frequency oscillations the phase coherence of these signals fluctuates on the order of seconds. A recent study showed that increases in the variance

Abbreviations: AP, action potential; AR, autoregressive; AUC, area under the curve; CRG, Cognitive Rhythm Generator; DBS, deep brain stimulation; DLPFC, dorsolateral prefrontal cortex; ECG, electrocardiogram; EEG, electroencephalogram; ETP, educated temporal prediction; EPSC, excitatory postsynaptic current; FC, functional connectivity; FFT, Fast Fourier transform; ISP, intersectional-short pulse; LFP, local field potential; HD-tDCS, high definition transcranial direct current stimulation; HD-tACS, high definition transcranial alternating current stimulation; MDD, major depressive disorder; MRI, magnetic resonance imaging; PFC, prefrontal cortex; ROC, receiver operating characteristic; SED, spontaneous epileptiform discharge; STN, subthalamic nucleus; tACS, transcranial alternating current stimulation; tDCS, transcranial direct current stimulation; TES, transcranial electrical stimulation; TI, temporal interference; TLE, temporal lobe epilepsy; TMS, transcranial magnetic stimulation.

of signal fluctuations occurring at the hippocampal seizure focus in patients with TLE might contribute to disruptions in physiological functional connectivity (FC) network dynamics that contribute to decreases in static hippocampal FC on fMRI scans (Morgan et al., 2020a).

We have previously shown that closed-loop electrical stimulation of the medial septum can quickly terminate intrahippocampal seizures while also suppressing their secondary generalization in a rat kindling model (Takeuchi et al., 2021). Still, as was the case for DBS, further translational research is required to employ the transcranial techniques.

Absence Epilepsy

TES has already been proven to successfully reduce the duration of spike-and-wave discharges (the electrographic hallmarks of human absence epilepsy) in a rodent model of generalized epilepsy (Berényi et al., 2012). Its efficient clinical application will rely on closed-loop feedback stimulation of the target circuits, as their modulation can interfere with the emerging pathological pattern (Berényi et al., 2012; Kozák and Berényi, 2017). In addition, closed-loop seizure suppression using TES can remain effective for long periods (i.e., months) (Kozák and Berényi, 2017).

Other Neuropsychiatric Disorders

Many neurological and psychiatric disorders are related to clinically discernible, altered brain dynamics. These pathological oscillations may be a target for therapeutic intervention for the disorders using time-and space-targeted brain stimulation technologies.

Major depressive disorder (MDD) is a common and chronic psychiatric disorder characterized by excessive feelings of sadness and low mood (American Psychiatric Association, 2013). The most relevant oscillopathic features of MDD are: increased alpha-band (8–13 Hz) activity in the temporo-parietal area, elevated frontal theta-band (4–7 Hz) activity, alpha frontal asymmetry (left hemispheric hypoactivity and right hemispheric hyperactivity expressed as theta, alpha and beta band activities) and decreased gamma band activity in the neocortex (Baskaran et al., 2012; Eidelman-Rothman et al., 2016; Fitzgerald and Watson, 2018). These features relate to MDD symptoms and predict the efficiency of pharmacological treatment and electroconvulsive therapy. In addition, a causal relationship between oscillopathies and symptoms of (major) depression may exist. Indeed, restoration of the frontal alpha symmetry using anodal tDCS on the dorsolateral prefrontal cortex (DLPFC) (Loo et al., 2012) and neurofeedback improved the symptoms of depression (Mennella et al., 2017). These pathological oscillations can be targeted using pharmacological and electrical stimulation methods in combination with cognitive (behavioral) methods to alleviate depression symptoms (Leuchter et al., 2015).

Posttraumatic stress disorder (PTSD) is a widespread neuropsychiatric disorder with a high burden of disease. Primary symptoms include anxiety, cognitive impairments, mood changes and consistent avoidance of trauma-related stimuli (American Psychiatric Association, 2013). The panic, fear, and sympathetic response to the trigger stimulus results from altered activity in the amygdala (Cisler et al., 2015). Deficiency of fear extinction is also a salient feature of PTSD. Closed-loop intervention can rely on real-time correlates of neural network activation and various symptoms. In PTSD patients hyperactivity characterizes resting magnetoencephalography (MEG) recordings of the amygdala, the hippocampus, and the insular cortex (Huang et al., 2014). Altered activity also characterizes EEG recordings of PSTD patients i.e., intrinsic sensory hyperactivity in the visual cortex (suppressed alpha power) and decreased alpha power-mediated inhibition to the frontal cortex (Clancy et al., 2017). Closed-loop stimulation of the amygdala can reduce dysregulated amygdala responses (Stidd et al., 2013; Koek et al., 2016).

NETWORK MODELS OF PATHOLOGICAL PATTERNS AND WHAT CAN WE CONCLUDE FROM THEM

Cellular Activity Underlying Seizures and Epilepsy

Generally, epilepsy is thought to root in neuronal hyperexcitability (Fisher et al., 2005). Several underlying mechanisms have been proposed based mainly on the results obtained from animal models, including impaired inhibition (Bekenstein and Lothman, 1993) or a change in excitatory neurons' intrinsic conductances, leading to an overall increase of network output and synchrony (Avoli et al., 2005). Monitoring the activity of single neurons in the human brain can reveal important aspects of brain function. However, it is more challenging to identify the role of individual neurons in epilepsy primarily because of the sparseness of seizures and the technical limitations of long-term single-unit recordings. There are far more studies concerning the interictal neuronal activity in human epilepsy, which revealed significant differences between affected and non-affected areas, including differences in firing rates, bursting and synchrony (Staba et al., 2002; Gast et al., 2016). The few successful attempts in which the ictal activity of single neocortical or hippocampal neurons was recorded revealed surprising results. Synchronous firing of neighboring neurons was rarely seen except at the onset of ictal events (Wyler et al., 1982). Seizures can provide intense and synchronous, yet sparse and heterogeneous activation (Bower et al., 2012). Besides this surprising heterogeneity, a general lack of hypersynchrony suggests that specific interactions among subsets of neurons initiate seizures (Truccolo et al., 2014; Lambrecq et al., 2017). On the other hand, seizure termination is characterized by a relatively homogeneous suppression of firing (Truccolo et al., 2014).

SEIZURE ACTIVITY AND COUPLED OSCILLATIONS

A recent study showed that in the intact isolated mouse hippocampus, a paroxysmal activity can spread through the hippocampus following seizure onset, both from a focal stimulation locus or if low magnesium was applied locally

to either longitudinal ends of the preparation (Derchansky et al., 2006). Bursts of activity within a seizure can become bidirectional, with frequency specific propagation patterns. In the low magnesium model, independent bidirectional activity was observed on both sides when the isolated intact hippocampus was severed along the septotemporal axis. These activities are in agreement with the function of coupled neuronal network oscillatory systems. Local coherence and ictal activity transfer was assessed in the recordings from intra-hippocampal depth electrodes implanted in epileptic patients being evaluated for possible resective surgery (Duckrow and Spencer, 1992). It was found that although ictal neural rhythmicity involves a temporal interaction between brain regions, the maintenance of this interaction is not essential for persistent seizure activity. These findings are in line with the idea of seizures being the manifestation of a multistate network of oscillatory systems showing various degrees of coupling and uncoupling.

"Coupled Oscillators" Model of Hyperexcitable Neuroglial Networks

Epilepsy is a dynamic disorder showing characteristics of neural networks with the incidence of at least two states, known as interictal and ictal activities (Lopes da Silva et al., 2003). The brain can be considered as a system of coupled oscillatory (multistate) units, and epilepsy a pathological expression of this system. The advantage of using a coupled oscillator approximation to model epilepsy is its ability to effectively model intermittent phenomena in epileptic brain networks (Zalay and Bardakjian, 2009). An attractor state is a transiently self-sustaining state (Meindertsma and Steenbeek, 2012). Unlike the multistate bistable attractor technique, intermittence corresponds to ictal events integral in the interictal attractor (or state) and doesn't require system noise for state transition (in these models, the critical mechanism for transitions to and from epileptic seizures is the existence of multiple attractors). A model that exploits this approach has been used to analyze different pathways leading to hyperexcitability and recommended a critical role for astrocytes and microglia in generating spontaneous epileptiform discharges (SEDs) (Farah et al., 2019). This model was built on the concept of coupled Cognitive Rhythm Generators (CRGs). The CRG is a mesoscopic mathematical modeling frame, used to model different physiological phenomena, such as directional selectivity, phase preference and phase precession (Zalay and Bardakjian, 2009). In addition, a network of four coupled CRGs has been used to model hippocampal neurons and generate SEDs (Zalay et al., 2010). This oscillator approximation might be a clock with a universal rhythm or a labile clock, where the oscillator is only active when the input is higher than a set threshold. The model included 16 CRGs organized into four subgroups with excitatory pyramidal cells, inhibitory interneurons, microglia and astrocytes. Pyramidal cell CRGs exhibited constant rhythmicity with intrinsic frequencies in the theta range (McNaughton et al., 1983), similar to results obtained from experimental recordings (Bezaire et al., 2016). Bursting activity of interneurons was characterized by labile clock behavior in the ripple HFO frequency range (80–250 Hz) (Sik et al., 1995), as is seen in experimental seizure-like events (Zalay et al., 2010). Microglial CRGs were modeled as a clock ring device with slow oscillations (0.2–0.5 Hz) (Wake et al., 2009). Lastly, the activity of astrocytes was characterized by labile clock behavior spanning the 1–4 Hz frequency range (Amzica and Steriade, 2000).

Astrocytes can regulate the excitability of adjacent neuronal synapses (Perea et al., 2009) and astrocytic dysfunction is related to several neurological disorders including epilepsy (Seifert et al., 2010). Earlier modeling studies highlighted the importance of glial function in K^+ homeostasis in hyperexcitability, suggesting glial function can act as a biomarker for epilepsy (Grigorovsky and Bardakjian, 2018). The increase in neuron-astrocyte coupling provoked a higher occurrence of SEDs, coherent with studies indicating that the release of specific gliotransmitters by astrocytes can predispose neuronal circuits to seizures. In contrast, the magnitude of neuron-microglia coupling was negatively correlated to hyperexcitability, with less SEDs of shorter duration appearing as the microglia-neuron coupling increased (Fellin et al., 2004; Carmignoto and Haydon, 2012). These latter modeling approaches are also consistent with experimental results showing that microglia can preferentially connect to hyperactive neurons, reduce their EPSC rate and down-regulating their activity (Li et al., 2012; Ji et al., 2013). Manipulating certain microglial functions is also related to the occurrence of seizures (Derecki et al., 2012; Eyo et al., 2014).

MULTISTATE AND BISTABLE NETWORK MODELS

Seizure Dynamics: Initiation, Development, and Termination

Epilepsy is a network malfunction described by bistable or multistable oscillatory states (e.g., interictal and ictal states) and their dynamic alternations. To investigate whether this multistate bistable approach can capture seizure dynamics, a divided system of bistable neural units built on an analytic, non-linear complex model was used (Izhikevich, 2001; Kalitzin et al., 2011). Depending on various parameters, this model is able to represent steady-state dynamics, limit cycle dynamics, or both. Ad absurdum, the model could be mentioned as a bistable unit. Based on the primary conditions, the bistable unit can either be in its steady-state point or a limit cycle (appearing as the total synchronization or seizure). Linking several units permits the design of a system consisting of multiple states (Koppert et al., 2014). Notably, such a system can engross a diversity of alternative oscillatory excited states, while state transitions occur solely as a consequence of external disturbances. A computational model (Bauer et al., 2017) has indicated that the addition of a global expression to the dynamics of the multistate system prevents hypersynchronous activity and discloses multiple phenomena described by the model. For example, when fitting state duration distributions to an exponential distribution, the distribution of times spent in one state will follow a particular case of the gamma distribution with less than one shape parameter. Thus, external

stochastic perturbations cause transitions from one state to another. A distributed model built from complex bistable units can practically simulate the seizure onset, maintenance and termination processes (Bauer et al., 2017).

Multistate Models—State Holding Close to the Transition Point

The bistable model formulates a valid hypothesis to assess the proximity to ictal transition even at the level of single neurons. When the system is disturbed, the closer it comes to the region splitting the normal steady-state from the oscillatory limit cycle (the model seizure), the longer is the time for responses or the time needed to return to the baseline state (Petkov et al., 2018). This result is caused by the fact that the separatrix (i.e., the boundary separating two modes of behavior in a differential equation) is diverse under an unstable asymptotic state acting as a limit cycle. Thus, the forces necessary to shift the system out of it are minute in the local network. This feature was used to develop a biomarker that can be combined with transcranial electrical stimulation (TES) or transcranial magnetic stimulation (TMS) for diagnostic and therapeutic prognosis protocols.

PHASE DETECTION, PHASE PREDICTION AND TIME AND SPACE TARGETING

Phase Detection and Prediction Algorithms

The phase of brain oscillations is an essential feature of neural processing (Thut et al., 2012; Maris et al., 2016). Therefore, it can act as an index of brain excitability, temporally guiding the delivery of brain stimulation. Several different algorithms have been developed to detect and predict the phase of various EEG oscillations for TES and TMS based closed-loop stimulation, as follows.

Fast Fourier Transform Prediction

The crucial feature of this algorithm is to use the frequency domain of the EEG signal for forwarding prediction (Mansouri et al., 2017). One specific implementation uses Laplacian montage with a central electrode of interest and eight surrounding electrodes as the brain signal for the region of interest (Shirinpour et al., 2020). The signal's phase in the dominant frequency is estimated from the angular factor of the complex Fast Fourier Transform (FFT) signal. A sine wave of the dominant oscillation with a given frequency and phase is calculated in the earlier steps and used for forwarding prediction.

Auto Regressive Prediction

In this approach, the signal is predicted in the time domain (Chen et al., 2013; Zrenner et al., 2018) in the following steps. First, the Laplacian of the electrodes corresponding to the region of interest is calculated. Next, the signal is zero-phase band-pass filtered in the frequency band of interest using an finite impulse response (FIR) filter [the FIR filter is a non-recursive filter in that the output from the filter is calculated by using the current and previous inputs (Mokhatab and Poe, 2012)] and the edges of the signal are curtailed to remove edge artifacts due to filtering. The residual signal is used to calculate the coefficients for the autoregressive model [i.e., the Yule-Walker method (Walker, 1931; Yule, 2012)]. The signal is heuristically forward predicted depending upon the parameters of the Auto Regressive (AR) coefficients. The instantaneous phase of the predicted signal is calculated using the Hilbert transformation.

Educated Temporal Prediction

This method integrates a short training step for the algorithm before the real-time application aiming to learn the individual statistical characteristics of the oscillation of interest. It uses a robust and straightforward method to extract inter-peak intervals and their central moment (Shirinpour et al., 2020). Presuming that brain oscillations are quasi-stable over the brief measurement epochs; one can determine the characteristic interval period between subsequent signal peaks (relating to 360° in signal phase). To predict the time-point at which the next target phase, i.e., the peak, will arise, one can add the average measured period between signal peaks to the time of the last peak recorded in order to predict the next peak.

Time-and Space-Targeting

Pathological oscillations can be modulated using open- or closed-loop approaches depending on how the stimulation is performed in the temporal domain. Analyzing various parameters of the outputs of the neuronal networks can be utilized to optimize the effect of stimulation. The feedback input allows the modulation to be time-targeted using on-demand stimulation (Berényi et al., 2012; Takeuchi and Berényi, 2020).

Closed-Loop Interventions

Closed-loop techniques for oscillotherapeutics are brain stimulation protocols based on intrinsic biosignal feedback [e.g., EEG, electrocardiogram (ECG), LFP]. The feedback input enables on-demand targeted intervention in the temporal domain preventing over-stimulation and undesired out-of-phase interferences. Closed-loop intervention can lower the side effects of relatively intensive stimulation; in contrast, chronic stimulation using a non-responsive, open-loop method can become involuntarily excessive. Indeed, inadequate stimulation can develop adverse effects by disturbing physiological activity in the brain. Remarkably, patients advised to turn on deep brain stimulation (DBS) in an on-demand manner for essential tremor show improved long term effects compared to open-loop continuous stimulation (Kronenbuerger et al., 2006).

The closed-loop method can be implemented in various ways according to the characteristics and impact of the intrinsic biosignal (**Figure 1**). The first possible configuration is "closed-loop responsive" stimulation, whereby predefined stimulus pulses are delivered only when stimulation is required (on-demand). In this setup, biosignals are continuously monitored for the automated launch of a preset stimulation pattern. The second closed-loop configuration for brain stimulation is the "closed-loop adaptive" stimulation, where various parameters of the input

biosignal gate output variables for stimulation. For example, the power of beta oscillations recorded in the subthalamic nucleus (STN) specifies the intensity of DBS in the STN for Parkinson's disease patients (Bouthour et al., 2019). The third, most advanced implementation of closed-loop stimulation is "phase-targeting" stimulation. Conceptually, phase-targeting electrical stimulation is highly effective in suppressing pathological oscillations. In the restoration of reduced physiological oscillations, counter-phase stimulation suppresses pathological oscillations and in-phase stimulation recovers decreased physiological oscillations (**Figure 1**). Practically, appropriately timed phase-targeting stimulus delivery has been demonstrated to be essential for the closed-loop intervention by suppressing ongoing pathological oscillations in epilepsy that effectively shortens the duration of absence seizures in rats (Berényi et al., 2012), and can remain effective for months when used in a closed-loop manner (Kozák and Berényi, 2017). We also showed that accurate stimulus timing controlled by internal seizure dynamics is critical for the termination of epileptic seizures when applying closed-loop stimulation to the medial septum (Takeuchi et al., 2021).

Focused Transcranial Electrical Stimulation Technologies

Transcranial electrical stimulation is a non-invasive brain stimulation protocol: as stimulation electrodes are located outside the skull, it is a low-risk and reversible adjunctive therapy. The focality of TES is poorer than DBS because of its transcranial nature. On the other hand, its diffuse modulation over the cortex may be considered as an advantage for intervention with generalized pathological oscillations hijacking wide cortical areas, as in the case of absence seizures (Berényi et al., 2012; Kozák and Berényi, 2017).

High-Definition Transcranial Direct Current Stimulation

Transcranial direct current stimulation (tDCS) is utilized to induce plastic changes by introducing sub-threshold membrane potential alterations in neurons of the cerebral cortex. Classical tDCS applies two large electrodes generating subthreshold depolarization of cortical neurons under the anodal electrode and hyperpolarization under the cathodal electrode, respectively. To increase the focality of tDCS, reducing the size of the large stimulus electrode placed over the target area, increasing the size of the return electrode, or changing the location of the return electrode (for example, over the arms, neck, shoulders, or knees) can be considered. An electrode configuration with improved stimulation focality has been developed based on modeling electrical field strength, termed high-definition tDCS (HD-tDCS) (Nitsche et al., 2015). Considering that the spacing between the HD-tDCS electrodes is relatively small, shunting is enhanced relative to the more conventional electrode configurations. Hence, current density has to be relatively high to generate electric fields comparable to those generated by large electrode pads with larger spacing. Studies have revealed that HD-tDCS treatment can alleviate epilepsy and pain perception (Castillo-Saavedra et al., 2016; Meiron et al., 2019).

High-Definition Transcranial Alternating Current Stimulation

Transcranial alternating current stimulation (tACS) is a stimulation technique that non-invasively modulates cortical activity and excitability. tACS is supposed to affect neuronal membrane potentials by oscillatory electrical stimulation using a well-defined stimulation frequency (Nitsche et al., 2015). As HD-tDCS, tACS focality can also be drastically increased by applying one stimulating electrode on the target area surrounded by multiple anti-phase returning electrodes (named as HD-tACS). Numerous cortical regions can be individually stimulated with well-defined oscillatory stimulus waveforms. This technique has been used to synchronize and desynchronize the activity of the human medial frontal cortex and the lateral PFC in the theta (∼6 Hz) frequency band resulting in the effective modulation of executive functions (Reinhart, 2017).

Temporal Interference Stimulation

Temporal interference (TI) stimulation is a novel TES method that promises to empower DBS without affecting superficial, off-target structures (Grossman et al., 2017). TI stimulation exploits the temporal interference among two electrical fields with alternating vectorial directions using similar, but slightly different frequencies in the kHz frequency band (i.e., 2 and 2.1 kHz). During TI stimulation one delivers the brain multiple electric fields at frequencies too high to recruit neural firing, but which differ by a frequency amenable to recruit neural activity. Effective electrical stimulation of neurons is suggested to occur across a local area where the interference among the multiple fields generates an emergent electric field envelope modulated at the difference frequency (i.e., 0.1 kHz) without excessive side effects. Spatial targeting of TI is confirmed in computational models, slice experiments and in anesthetized rodents (Grossman et al., 2017; Esmaeilpour et al., 2021), spatial resolution depends on the number and alignment of electrodes over the scalp. The possible off-target effects of high-frequency electrical fields over large brain areas could present an issue as strong kHz-frequency electrical fields can block the spreading of compound action potentials in peripheral nerves (Kilgore and Bhadra, 2014). The long-term effects of kHz stimulation of TI are yet unknown. The temporal resolution of TI simulation is limited, as the generation of kHz electrical fields in short ramp-up times induces rapid, spatially unfocused activation of neurons, while slow ramp-up does not (Grossman et al., 2017). Due to this limitation, precisely timed closed-loop TI (i.e., phase-targeting stimulation) is not achievable. Accordingly, TI stimulation appears to be preferable to applications for inducing plasticity in subcortical brain regions (Chaieb et al., 2011).

Intersectional Short Pulse Stimulation

We have previously developed a novel TES approach (Intersectional-Short Pulse (ISP) stimulation) which allows to programmatically steer the effect of TES in the intracranial space and allows considerably higher electrical currents to be used, while preserving the high temporal precision of the stimulation (Vöröslakos et al., 2018). ISP applies a repeated sequence of brief, amplitude modulated electrical pulses through

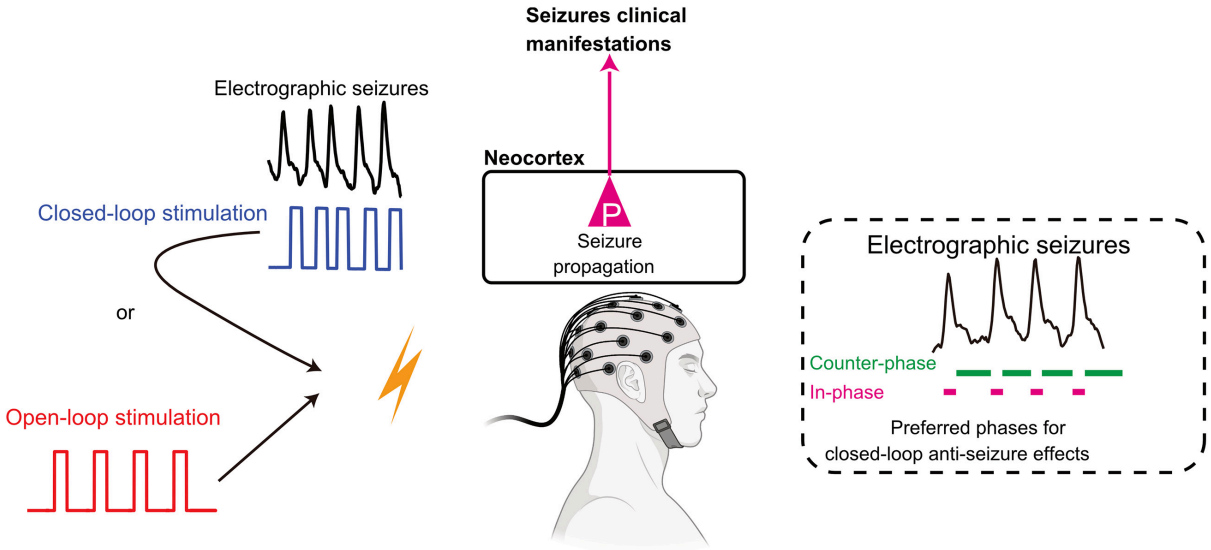

FIGURE 1 | Open-loop and closed-loop interventions in epileptic seizures. Open-loop intervention delivers preset stimulation naive to the ongoing rhythmicity of brain activity., while closed-loop intervention governs stimulation pattern by the real-time processing of network oscillations. Counter-phase stimulation cancels intrinsic oscillations by destructive interference. In contrast, in-phase stimulation can enhance or restore decreased oscillations by constructive interference. See details in the main text. Adapted from Huang et al. (2019) and Takeuchi et al. (2021)

multiple independent electrode pairs. The ISP method exploits the temporal integration of the subthreshold changes induced by the multiple consecutive electrical gradients due to the capacitive properties of the neuronal membranes. Accordingly, due to this neuronal "blurring" ISP stimulation can transcranially mimic the neuronal readout that would be caused by a strong (>1 mV/mm), continuous electrical field in a target brain region to directly induce or inhibit action potentials without generating excessive current densities on the scalp (i.e., causing less peripheral effects). Using ISP, the activity of hippocampal neurons can be modulated in a hemisphere-specific way (Vöröslakos et al., 2018). In addition, the 1 Hz ISP stimulation can modulate the amplitude of alpha-band oscillations in EEG recordings of healthy volunteers in a hemisphere-and phase-specific manner (Vöröslakos et al., 2018).

The advantages of ISP compared to other electrical stimulation techniques are several. It has better spatial steerability and can be implemented with a phase-targeted closed-loop configuration with millisecond precision. Currents as much as 16 mA can be applied (one order of magnitude larger than conventional TES), but the current density on each electrode stays similar to those used by traditional TES. Identical effects (i.e., excitation or inhibition) can be simultaneously achieved on both hemispheres by appropriate electrode alignment in contrast to conventional TES, which generates opposing anodal-cathodal effects over the two hemispheres. The direction of electrical fields along the axo-dendritic axis of neurons determines whether the electrical fields activate or inhibit the target neurons (Chan and Nicholson, 1986; Liu et al., 2018). Furthermore, several distinct stimulus waveforms can be employed in an interwoven fashion, yet independently. This stimulation technique is expected to allow non-invasive on-demand closed-loop control with space-and time-targeted brain stimulation for the treatment of various neuropsychiatric disorders.

The Matter of Stimulus Intensity/Effect Size to Reach Reliable Control on Oscillatory Network Patterns

TES applied at ± 1 mA peak intensity induces < 0.5 V/m electric fields in the human brain (Opitz et al., 2016; Huang et al., 2017; Chhatbar et al., 2018). This is enough to induce 0.1–0.2 mV alterations in the membrane potential of neurons within the stimulated area. As these alterations are markedly lower than the ∼20 mV depolarization necessary to push a neuron from its resting potential to spike threshold *in vitro*, TES is unable to obtain prompt, highly reproducible changes in spiking activity. In contrast, the mild electrical fields generated may be more efficient when applied to distract or reinforce ongoing rhythms rather than introducing novel activity patterns. Targeting the stimulation to the optimal phase of endogenous rhythms in a closed-loop implementation may be the most effective solution (Berényi et al., 2012). However, responsive implementations require in depth characterization of the altered network with simultaneous monitoring and adjustment of the relevant rhythms (Krook-Magnuson et al., 2015). This might be achieved by using mild electric fields, but other applications may require higher field intensities for improved efficacy. For example, immediate control of spiking activity (e.g., to terminate a seizure) might require field strengths larger than 5 V/m (Kozák and Berényi, 2017).

Taking into account the intrinsic circuit structures of a given brain area is an essential factor for the effective control of oscillatory networks as stimulation of structural hubs effectively

modulates the ongoing oscillatory activity with high spatial propagation. The applied stimulation frequency needs to match the frequency range of activity of various elements of the targeted neuronal circuit. Supposing the targeted brain region has divergent projections to multiple brain regions, oscillatory activity applied to the target region can extend to various destination brain regions. TES of the prefrontal cortex (PFC) for the treatment of depression readily utilizes this concept because the PFC has widespread synaptic connections to limbic areas (Loo et al., 2012; Ferenczi et al., 2016). The interference of a "congestion" relay station in the brain effectively intervenes in disseminating massive oscillatory activity like epileptic seizures (Takeuchi et al., 2021). In this respect, the entorhinal cortex and the subiculum are chokepoint-like structures broadcasting the activity from the hippocampus to the neocortex. Stimulation on these structures can effectively suppress the secondary generalization of seizures originating in the hippocampus (Lu et al., 2016; Wang et al., 2017). On the other hand, the STN and the thalamus are chokepoints in post-stroke epilepsy and absence epilepsy (Paz and Huguenard, 2015).

FUTURE DIRECTIONS

Seizure Detection and Prediction

The real-time prediction of seizures is more challenging than detecting seizures because of atypical feature changes and smaller signal-to-noise ratios. However, the prediction would be more beneficial than detection as it enables prevention.

Attempts to develop reliable seizure prediction algorithms have an extensive history, dating back to the 1970s (Viglione and Walsh, 1975) with minimal data sets looking only at pre-seizure (preictal) events minutes to seconds before seizures. Massively evolving over the past 50 years, current methods use mathematical tools to analyze continuous days of multiscale EEG recordings (Lehnertz and Litt, 2005). One of the most salient features of seizures is their unpredictability. From a more comprehensive view, seizure prediction research has also transformed how we understand epilepsy and the basic mechanisms underlying seizure generation. Seizures were formerly considered isolated and abrupt events, but we now consider them processes that develop over space and time in epileptic networks (Burns et al., 2014). Therefore, what started as predicting seizures for clinical applications has evolved into a field committed to understanding seizure generation.

Seizure Prediction Algorithms

Seizure prediction algorithms typically follow the same route/logic: biosignals are recorded and pre-processed, prediction features and/or pre-ictal biomarkers are then extracted. The decision system processes the temporal stream of feature prediction values and detects changes that indicate an upcoming seizure. To reach a decision, thresholds can be set for various features, or machine learning classifiers can be used to make decisions based on multiple features. The decision system then involves the advisory system, which warns the patient if a seizure is likely to occur soon. Constantly acquired biosignals, most frequently EEG or intracranial EEG, are analyzed with advanced time series analysis methods to identify predictive features. A pre-ictal biomarker is a predictive feature derived from physiological signals (for example the EEG) that becomes apparent during a defined period before a seizure but not at other times. Such a feature might or might not be visually evident, reflects underlying signals' alterations and predicts seizures within an explicit range of values. Features are commonly used instead of the raw signals because they simplify the essential changes of the signals. A pre-ictal feature can be considered clinically beneficial as a warning system if it can be detected early enough and can minimize the time under false warning. Features evaluated for their predictive value, particularly those of EEG signals, range from simple to complex and rely on univariate, bivariate or multivariate linear, or non-linear analysis. The effectiveness of individual features for seizure prediction can be evaluated individually, but combinations of features are often delivered as inputs to machine learning algorithms, acting as pattern recognition systems. These algorithms allow the estimation of the seizure prediction properties of features in combination (Freestone et al., 2015; Brinkmann et al., 2016; Gadhoumi et al., 2016). In turn, these temporal features are utilized in decision algorithms to trigger the delivery of pharmacological or non-pharmacological control of seizures in a closed-loop system. Algorithms need additional development based on neurophysiology, multimodal imaging, seizure mechanisms, control theory and computational modeling (Kuhlmann et al., 2015). Numerous guidelines and approaches are used to develop seizure prediction algorithms (Mormann et al., 2007). These methods require receiver operating characteristic (ROC) curves that measure the true positive rate against the false-positive rate during pre-ictal or inter-ictal periods. Overall algorithm performance can be quantified and ranked by the area under the curve (AUC) for true positive vs. false-positive rates.

Biomarkers of epilepsy incorporate interictal epileptiform discharges and bursts, interictal spikes and high-frequency oscillations, which are nowadays used in diagnosis, surgical planning and treatment bearing obvious clinical significance (Matsumoto and Marsan, 1964; Schulze-Bonhage, 2016). The hope for seizure prediction was high in the early twenty first century following the development of a plethora of seizure prediction algorithms. Still, the result of stringent testing on the reliability of seizure prediction indicates no evidence of above-chance prediction (Mormann et al., 2007). No predictive feature or pre-ictal characteristic that is generic among people with epilepsy and that can predict the precise time of an individual's subsequent seizure has been yet identified (Kuhlmann et al., 2010, 2018; Gadhoumi et al., 2015; Karoly et al., 2017; Kiral-Kornek et al., 2018; Truong et al., 2018). Thus, it is important to decide whether promising seizure predictors forecast seizures rather than detect random fluctuations in EEG signals unrelated to seizures. This principle challenge in seizure prediction requires a standardized stringent mathematical calculation of predictive performance (Mormann et al., 2007) because seizure events are sparse and interictal periods generally long. A first step for such analysis is to compare the performance of a prediction algorithm with that of a random predictor (Schelter et al., 2006; Snyder et al.,

2008) that generates predictions at random times at the same rate as that of the algorithm. Where appropriate, a random predictor can be adapted to account for a subject's diurnal variability in seizure distribution or features (Karoly et al., 2017). More evolved methods utilize Monte Carlo simulations to generate predictor substitutes, such as randomizing seizure times to generate false seizure times (Andrzejak et al., 2003, 2009; Kreuz et al., 2004). The performance of the prediction algorithm is then mathematically compared with the efficacy of these predictor substitutes. Comparing the performance of a prediction algorithm with a random predictor is algorithmically the most effective form of mathematical calculation. Substitute-based methods have higher temporal complexity but improve confidence in concluding whether an algorithm performs better than chance and can report the non-random occurrence of seizures. The importance of rigorous mathematical testing of seizure prediction algorithms is crucial for understanding the significance of the results of seizure prediction.

PRECISE LOCALIZATION AND TARGETING OF A SEIZURE FOCUS IN THE BRAIN

Increasing the number of pairs of stimulating electrodes is essential for improving the spatial resolution of ISP stimulation (this is also the case for TI stimulation). A dedicated EEG cap with multiple recording and stimulating electrodes is needed for transcranial closed-loop intervention with ISP stimulation. Subscalp or intracranial implantation of the stimulus electrodes will boost the efficiency and focality at the expense of a more invasive intervention. The placement of stimulating electrodes must be adapted for each patient's requirements, especially in the case of focal seizures. The target brain region should be determined by a combination of high-density EEG, functional tomography and long-term video monitoring of seizures. Structural brain imaging [i.e., magnetic resonance imaging (MRI)] is also required for planning the ISP stimulation targets. A recent study described a multi-electrode model for electrical stimulation (Huang et al., 2019). Mathematical investigations (solving linear programming problems) showed a patient-specific MRI-based model to determine the electrode positions and current intensities that optimize the induced electric fields in either intensity or focality at the target location. In addition, the achievable focality is limited by the safety constraint on maximum currents (Dmochowski et al., 2011). Although electrical artifacts of ISP stimulation are smaller than those of conventional TES, feedforward removal of gross artifacts from applied currents is required (Vöröslakos et al., 2018; Kohli and Casson, 2019). Optimizing stimulation parameters (duration, intensity, etc.) is crucial for optimal performance. Empirical optimization presently used by clinicians is a labor and time-consuming process. Machine learning algorithms could be utilized instead for optimizing closed-loop ISP stimulation (timing and parameters) for the control of epileptic seizures.

CLOSED-LOOP IMPLEMENTATIONS

The first studies using early seizure-detection algorithms in combination with responsive brain stimulation have yielded positive results (Kossoff et al., 2004; Fountas et al., 2005; Osorio et al., 2005). For any responsive brain-stimulation configuration, a key issue is the placement of both afferent and efferent electrodes, that is, electrodes for detecting a pre-seizure state and stimulation electrodes, respectively. The location and number of electrodes used may be essential for the early detection of an impending seizure followed by locally applied, spatially constrained stimulation, in a way that the patient does not wittingly perceive the intervention.

The ultimate aim in designing a reliable seizure-prediction algorithm can be seen in a device capable of warning of an impending seizure and preventing it from happening. An ideal intervention system would control the development of an episode before the onset of the clinical symptoms. Its tolerance toward false alarms leading to unnecessary interventions would depend on the magnitude of side effects. The principal feasibility of different seizure-intervention strategies such as local application of short-acting drugs (Stein et al., 2000), electrical stimulation techniques (Berényi et al., 2012), local cooling (Hill et al., 2000), or biofeedback operant conditioning (Sterman, 2000) has been described in the literature. Presently, much research is directed toward designing a closed-loop intervention system using deep brain or transcranial stimulation (Morrell, 2006; Kozák and Berényi, 2017; Takeuchi et al., 2021). Such an EEG-based closed-loop stimulation system could be based either on prediction algorithms or algorithms for early seizure detection. Nowadays, prediction algorithms are limited in performance to verify clinical trials with closed-loop stimulation using the techniques described above. For early seizure-detection algorithms, the challenge is whether an intervention after the onset of an electrographic seizure can prevent its full clinical manifestation or whether the brain has already passed the "point of no return." Detection algorithms should be optimized to be implemented into a micro processing unit. Extensive parallelization will be necessary to enable real-time computation in a small device with a limited clock rate without substantial delays. Phase-locked stimulation is essential for efficient intervention with pathological oscillations. New algorithms for instantaneous phase calculation will be valuable if implemented in the closed-loop system for efficient intervention in pathological oscillations (Mansouri et al., 2017). Even if appropriate offline modeling methods are time demanding, the online detection of specific oscillatory patterns based on the constituted model can be achievable as it does not demand calculations as intense as the modeling process itself. A reduction in the dimensionality and complexity of the model may be required for online intervention.

AUTHOR CONTRIBUTIONS

TF and AB developed the idea. TF prepared the figure. TF and ML wrote the original draft. TF, ML, and AB discussed and

commented on the manuscript. All authors contributed to the article and approved the submitted version.

FUNDING

This work was supported by the Momentum program II of the Hungarian Academy of Sciences, EFOP-3.6.1-16-2016-00008, EFOP 3.6.6-VEKOP-16-2017-00009, and KKP133871/KKP20 grants of the National Research, Development and Innovation Office, Hungary, the 20391-3/2018/FEKUSTRAT of the Ministry of Human Capacities, Hungary, and the EU Horizon 2020 Research and Innovation Program (No. 739593—HCEMM), Hungarian Scientific Research Fund (Grants NN125601 and FK123831 to ML), the Hungarian Brain Research Program (grant KTIA_NAP_13-2-2014-0014 to ML). UNKP-20-5 New National Excellence Program of the Ministry for Innovation and Technology from the source of the National Research, Development and Innovation Fund to ML. ML was a grantee of the János Bolyai Fellowship.

REFERENCES

American Psychiatric Association (2013). *Diagnostic and Statistical Manual of Mental Disorders*, 5th Edn. Arlington, VA: American Psychiatric Association.

Amzica, F., and Steriade, M. (2000). Neuronal and glial membrane potentials during sleep and paroxysmal oscillations in the neocortex. *J.Neurosci.* 20, 6648–6665. doi: 10.1523/jneurosci.20-17-06648.2000

Anastassiou, C. A., Perin, R., Markram, H., and Koch, C. (2011). Ephaptic coupling of cortical neurons. *Nat. Neurosci.* 14, 217–224. doi: 10.1038/nn.2727

Andrzejak, R. G., Chicharro, D., Elger, C. E., and Mormann, F. (2009). Seizure prediction: any better than chance? *Clin. Neurophysiol.* 120, 1465–1478. doi: 10.1016/j.clinph.2009.05.019

Andrzejak, R. G., Mormann, F., Kreuz, T., Rieke, C., Kraskov, A., Elger, C. E., et al. (2003). Testing the null hypothesis of the nonexistence of a preseizure state. *Phy. Rev. E* 67:4. doi: 10.1103/PhysRevE.67.010901

Avoli, M., Louvel, J., Pumain, R., and Köhling, R. (2005). Cellular and molecular mechanisms of epilepsy in the human brain. *Prog. Neurobiol.* 77, 166–200. doi: 10.1016/j.pneurobio.2005.09.006

Baskaran, A., Milev, R., and McIntyre, R. S. (2012). The neurobiology of the EEG biomarker as a predictor of treatment response in depression. *Neuropharmacology* 63, 507–513. doi: 10.1016/j.neuropharm.2012.04.021

Bauer, P. R., Thijs, R. D., Lamberts, R. J., Velis, D. N., Visser, G. H., Tolner, E. A., et al. (2017). Dynamics of convulsive seizure termination and postictal generalized EEG suppression. *Brain* 140, 655–668. doi: 10.1093/brain/aww322

Bekenstein, J. W., and Lothman, E. W. (1993). Dormancy of inhibitory interneurons in a model of temporal lobe epilepsy. *Science* 259, 97–100. doi: 10.1126/science.8093417

Berényi, A., Belluscio, M., Mao, D., and Buzsáki, G. (2012). Closed-loop control of epilepsy by transcranial electrical stimulation. *Science* 337, 735–737. doi: 10.1126/science.1223154

Berg, A. T., Vickrey, B. G., Langfitt, J. T., Sperling, M. R., Walczak, T. S., Shinnar, S., et al. (2003). The multicenter study of epilepsy surgery: recruitment and selection for surgery. *Epilepsia* 44, 1425–1433. doi: 10.1046/j.1528-1157.2003.24203.x

Bettus, G., Bartolomei, F., Confort-Gouny, S., Guedj, E., Chauvel, P., Cozzone, P. J., et al. (2010). Role of resting state functional connectivity MRI in presurgical investigation of mesial temporal lobe epilepsy. *J. Neurol. Neurosurg. Psychiatry* 81, 1147–1154. doi: 10.1136/jnnp.2009.191460

Bezaire, M. J., Raikov, I., Burk, K., Vyas, D., and Soltesz, I. (2016). Interneuronal mechanisms of hippocampal theta oscillations in a full-scale model of the rodent CA1 circuit. *Elife* 5:e18566. doi: 10.7554/eLife.18566

Bone, B., Fogarasi, A., Schulz, R., Gyimesi, C., Kalmar, Z., Kovacs, N., et al. (2012). Secondarily generalized seizures in temporal lobe epilepsy. *Epilepsia* 53, 817–824. doi: 10.1111/j.1528-1167.2012.03435.x

Bouthour, W., Mégevand, P., Donoghue, J., Lüscher, C., Birbaumer, N., and Krack, P. (2019).). Biomarkers for closed-loop deep brain stimulation in Parkinson disease and beyond. *Nat. Rev. Neurol.* 15, 343–352. doi: 10.1038/s41582-019-0166-4

Bower, M. R., Stead, M., Meyer, F. B., Marsh, W. R., and Worrell, G. A. (2012). Spatiotemporal neuronal correlates of seizure generation in focal epilepsy. *Epilepsia* 53, 807–816. doi: 10.1111/j.1528-1167.2012.03417.x

Brinkmann, B. H., Wagenaar, J., Abbot, D., Adkins, P., Bosshard, S. C., Chen, M., et al. (2016). Crowdsourcing reproducible seizure forecasting in human and canine epilepsy. *Brain* 139, 1713–1722. doi: 10.1093/brain/aww045

Burns, S. P., Santaniello, S., Yaffe, R. B., Jouny, C. C., Crone, N. E., Bergey, G. K., et al. (2014). Network dynamics of the brain and influence of the epileptic seizure onset zone. *Proc. Natl. Acad. Sci. U.S.A.* 111, E5321–E5330. doi: 10.1073/pnas.1401752111

Buzsáki, G. (2009). *Rhythms of the Brain*. Oxford: Oxford University Press.

Buzsáki, G., Anastassiou, C. A., and Koch, C. (2012). The origin of extracellular fields and currents-EEG, ECoG, LFP and spikes. *Nat. Rev. Neurosci.* 13, 407–420. doi: 10.1038/nrn3241

Buzsáki, G., and Draguhn, A. (2004). Neuronal olscillations in cortical networks. *Science* 304, 1926–1929. doi: 10.1126/science.1099745

Buzsáki, G., and Watson, B. O. (2012). Brain rhythms and neural syntax: implications for efficient coding of cognitive content and neuropsychiatric disease. *Dialogues Clin. Neurosci.* 14, 345–367. doi: 10.31887/dcns.2012.14.4/gbuzsaki

Carmignoto, G., and Haydon, P. G. (2012). Astrocyte calcium signaling and epilepsy. *Glia* 60, 1227–1233. doi: 10.1002/glia.22318

Castillo-Saavedra, L., Gebodh, N., Bikson, M., Diaz-Cruz, C., Brandao, R., Coutinho, L., et al. (2016). Clinically effective treatment of fibromyalgia pain with high-definition transcranial direct current stimulation: phase II open-label dose optimization. *J. Pain* 17, 14–26. doi: 10.1016/j.jpain.2015.09.009

Chaieb, L., Antal, A., and Paulus, W. (2011). Transcranial alternating current stimulation in the low kHz range increases motor cortex excitability. *Restor. Neurol. Neurosci.* 29, 167–175. doi: 10.3233/RNN-2011-0589

Chan, C. Y., and Nicholson, C. (1986). Modulation by applied electric fields of Purkinje and stellate cell activity in the isolated turtle cerebellum. *J. Physiol.* 371, 89–114. doi: 10.1113/jphysiol.1986.sp015963

Chen, L. L., Madhavan, R., Rapoport, B. I., and Anderson, W. S. (2013). Real-time brain oscillation detection and phase-locked stimulation using autoregressive spectral estimation and time-series forward prediction. *IEEE Trans. Biomed. Eng.* 60, 753–762. doi: 10.1109/TBME.2011.2109715

Chhatbar, P. Y., Kautz, S. A., Takacs, I., Rowland, N. C., Revuelta, G. J., George, M. S., et al. (2018). Evidence of transcranial direct current stimulation-generated electric fields at subthalamic level in human brain in vivo. *Brain Stimul.* 11, 727–733. doi: 10.1016/j.brs.2018.03.006

Cisler, J. M., Sigel, B. A., Kramer, T. L., Smitherman, S., Vanderzee, K., Pemberton, J., et al. (2015). Amygdala response predicts trajectory of symptom reduction during trauma-focused cognitive-behavioral therapy among adolescent girls with PTSD. *J. Psychiatr. Res.* 71, 33–40. doi: 10.1016/j.jpsychires.2015.09.011

Clancy, K., Ding, M., Bernat, E., Schmidt, N. B., and Li, W. (2017). Restless "rest": Intrinsic sensory hyperactivity and disinhibition in post-traumatic stress disorder. *Brain* 140, 2041–2050. doi: 10.1093/brain/awx116

Cooper, R. A., and Ritchey, M. (2019). Cortico-hippocampal network connections support the multidimensional quality of episodic memory. *Elife* 8:e45591. doi: 10.7554/eLife.45591

Derchansky, M., Rokni, D., Rick, J. T., Wennberg, R., Bardakjian, B. L., Zhang, L., et al. (2006). Bidirectional multisite seizure propagation in the intact isolated hippocampus: the multifocality of the seizure "focus.". *Neurobiol. Dis.* 23, 312–328. doi: 10.1016/j.nbd.2006.03.014

Derecki, N. C., Cronk, J. C., Lu, Z., Xu, E., Abbott, S. B. G., Guyenet, P. G., et al. (2012). Wild-type microglia arrest pathology in a mouse model of Rett syndrome. *Nature* 484, 105–109. doi: 10.1038/nature10907

Dmochowski, J. P., Datta, A., Bikson, M., Su, Y., and Parra, L. C. (2011). Optimized multi-electrode stimulation increases focality and intensity at target. *J. Neural Eng.* 8:046011. doi: 10.1088/1741-2560/8/4/046011

Duckrow, R. B., and Spencer, S. S. (1992). Regional coherence and the transfer of ictal activity during seizure onset in the medial temporal lobe. *Electroencephalogr. Clin. Neurophysiol.* 82, 415–422. doi: 10.1016/0013-4694(92)90046-K

Eidelman-Rothman, M., Levy, J., and Feldman, R. (2016). Alpha oscillations and their impairment in affective and post-traumatic stress disorders. *Neurosci. Biobehav. Rev.* 68, 794–815. doi: 10.1016/j.neubiorev.2016.07.005

Engel, A. K., Fries, P., and Singer, W. (2001). Dynamic predictions: oscillations and synchrony in top–down processing. *Nat. Rev. Neurosci.* 2, 704–716. doi: 10.1038/35094565

Englot, D. J., Konrad, P. E., and Morgan, V. L. (2016). Regional and global connectivity disturbances in focal epilepsy, related neurocognitive sequelae, and potential mechanistic underpinnings. *Epilepsia* 57, 1546–1557. doi: 10.1111/epi.13510

Esmaeilpour, Z., Kronberg, G., Reato, D., Parra, L. C., and Bikson, M. (2021). Temporal interference stimulation targets deep brain regions by modulating neural oscillations. *Brain Stimul.* 14, 55–65. doi: 10.1016/j.brs.2020.11.007

Eyo, U. B., Peng, J., Swiatkowski, P., Mukherjee, A., Bispo, A., and Wu, L. J. (2014). Neuronal hyperactivity recruits microglial processes via neuronal NMDA receptors and microglial P2Y12 receptors after status epilepticus. *J. Neurosci.* 34, 10528–10540. doi: 10.1523/JNEUROSCI.0416-14.2014

Farah, F. H., Grigorovsky, V., and Bardakjian, B. L. (2019). Coupled oscillators model of hyperexcitable neuroglial networks. *Int. J.Neural Syst.* 29:1850041. doi: 10.1142/S0129065718500417

Fellin, T., Pascual, O., Gobbo, S., Pozzan, T., Haydon, P. G., and Carmignoto, G. (2004). Neuronal synchrony mediated by astrocytic glutamate through activation of extrasynaptic NMDA receptors. *Neuron* 43, 729–743. doi: 10.1016/j.neuron.2004.08.011

Ferenczi, E. A., Zalocusky, K. A., Liston, C., Grosenick, L., Warden, M. R., Amatya, D., et al. (2016). Prefrontal cortical regulation of brainwide circuit dynamics and reward-related behavior. *Science* 351:6268. doi: 10.1126/science.aac9698

Fisher, R. S., Acevedo, C., Arzimanoglou, A., Bogacz, A., Cross, J. H., Elger, C. E., et al. (2014). ILAE official report: a practical clinical definition of epilepsy. *Epilepsia* 55, 475–482. doi: 10.1111/epi.12550

Fisher, R. S., Van Emde Boas, W., Blume, W., Elger, C., Genton, P., Lee, P., et al. (2005). Epileptic seizures and epilepsy: definitions proposed by the International League Against Epilepsy (ILAE) and the International Bureau for Epilepsy (IBE). *Epilepsia* 46, 470–472. doi: 10.1111/j.0013-9580.2005.66104.x

Fitzgerald, P. J., and Watson, B. O. (2018). Gamma oscillations as a biomarker for major depression: an emerging topic. *Transl. Psychiatry* 8:177. doi: 10.1038/s41398-018-0239-y

Fountas, K. N., Smith, J. R., Murro, A. M., Politsky, J., Park, Y. D., and Jenkins, P. D. (2005). Implantation of a closed-loop stimulation in the management of medically refractory focal epilepsy: a technical note. *Stereotact. Funct. Neurosurg.* 83, 153–158. doi: 10.1159/000088656

Freestone, D. R., Karoly, P. J., Peterson, A. D. H., Kuhlmann, L., Lai, A., Goodarzy, F., et al. (2015). Seizure prediction: science fiction or soon to become reality? *Curr. Neurol. Neurosci. Rep.* 15:73. doi: 10.1007/s11910-015-0596-3

Gadhoumi, K., Gotman, J., and Lina, J. M. (2015). Scale invariance properties of intracerebral eeg improve seizure prediction in mesial temporal lobe epilepsy. *PLoS One* 10:e0121182. doi: 10.1371/journal.pone.0121182

Gadhoumi, K., Lina, J. M., Mormann, F., and Gotman, J. (2016). Seizure prediction for therapeutic devices: a review. *J. Neurosci. Methods* 260, 270–282. doi: 10.1016/j.jneumeth.2015.06.010

Gast, H., Niediek, J., Schindler, K., Boström, J., Coenen, V. A., Beck, H., et al. (2016). Burst firing of single neurons in the human medial temporal lobe changes before epileptic seizures. *Clin. Neurophysiol.* 127, 3329–3334. doi: 10.1016/j.clinph.2016.08.010

Glauser, T., Ben-Menachem, E., Bourgeois, B., Cnaan, A., Chadwick, D., Guerreiro, C., et al. (2006). ILAE treatment guidelines: evidence-based analysis of antiepileptic drug efficacy and effectiveness as initial monotherapy for epileptic seizures and syndromes. *Epilepsia* 47, 1094–1120. doi: 10.1111/j.1528-1167.2006.00585.x

Grigorovsky, V., and Bardakjian, B. L. (2018). Neuro-Glial network model of postictal generalized EEG suppression (PGES). *Annu. Int. Conf. IEEE Eng. Med. Biol. Soc.* 2018, 2044–2047. doi: 10.1109/EMBC.2018.8512661

Grossman, N., Bono, D., Dedic, N., Kodandaramaiah, S. B., Rudenko, A., Suk, H. J., et al. (2017). Noninvasive deep brain stimulation via temporally interfering electric fields. *Cell* 169, 1029–1041.e16. doi: 10.1016/j.cell.2017.05.024

Hamberger, M. J., and Drake, E. B. (2006). Cognitive functioning following epilepsy surgery. *Curr. Neurol. Neurosci. Rep.* 6, 319–326. doi: 10.1007/s11910-006-0025-8

Hill, M. W., Wong, M., Amarakone, A., and Rothman, S. M. (2000). Rapid cooling aborts seizure-like activity in rodent hippocampal-entorhinal slices. *Epilepsia* 41, 1241–1248. doi: 10.1111/j.1528-1157.2000.tb04601.x

Holmes, M., Folley, B. S., Sonmezturk, H. H., Gore, J. C., Kang, H., Abou-Khalil, B., et al. (2014). Resting state functional connectivity of the hippocampus associated with neurocognitive function in left temporal lobe epilepsy. *Hum. Brain Mapp.* 35, 735–744. doi: 10.1002/hbm.22210

Holmes, M. D., Miles, A. N., Dodrill, C. B., Ojemann, G. A., and Wilensky, A. J. (2003). Identifying potential surgical candidates in patients with evidence of bitemporal epilepsy. *Epilepsia* 44, 1075–1079. doi: 10.1046/j.1528-1157.2003.58302.x

Hong, G., and Lieber, C. M. (2019). Novel electrode technologies for neural recordings. *Nat. Rev. Neurosci.* 20, 330–345. doi: 10.1038/s41583-019-0140-6

Huang, M. X., Yurgil, K. A., Robb, A., Angeles, A., Diwakar, M., Risbrough, V. B., et al. (2014). Voxel-wise resting-state MEG source magnitude imaging study reveals neurocircuitry abnormality in active-duty service members and veterans with PTSD. *Neuroimage* 5, 408–419. doi: 10.1016/j.nicl.2014.08.004

Huang, Y., Datta, A., Bikson, M., and Parra, L. C. (2019). Realistic volumetric-approach to simulate transcranial electric stimulation - ROAST–a fully automated open-source pipeline. *J. Neural. Eng.* 16:056006. doi: 10.1088/1741-2552/ab208d

Huang, Y., Liu, A. A., Lafon, B., Friedman, D., Dayan, M., Wang, X., et al. (2017). Measurements and models of electric fields in the in vivo human brain during transcranial electric stimulation. *Elife* 6:e18834. doi: 10.7554/eLife.18834

Izhikevich, E. M. (2001). Synchronization of elliptic bursters. *SIAM Rev.* 43, 315–344. doi: 10.1137/S0036144500382064

Ji, K., Akgul, G., Wollmuth, L. P., and Tsirka, S. E. (2013). Microglia actively regulate the number of functional synapses. *PLoS One* 8:e56293. doi: 10.1371/journal.pone.0056293

Kalitzin, S., Koppert, M., Petkov, G., Velis, D., and da Silva, F. L. (2011). Computational model prospective on the observation of proictal states in epileptic neuronal systems. *Epilepsy Behav.* 22(Suppl. 1), S102–S109. doi: 10.1016/j.yebeh.2011.08.017

Karoly, P. J., Ung, H., Grayden, D. B., Kuhlmann, L., Leyde, K., Cook, M. J., et al. (2017). The circadian profile of epilepsy improves seizure forecasting. *Brain* 140, 2169–2182. doi: 10.1093/brain/awx173

Kilgore, K. L., and Bhadra, N. (2014). Reversible nerve conduction block using kilohertz frequency alternating current. *Neuromodulation* 17, 242–255. doi: 10.1111/ner.12100

Kiral-Kornek, I., Roy, S., Nurse, E., Mashford, B., Karoly, P., Carroll, T., et al. (2018). Epileptic seizure prediction using big data and deep learning: toward a mobile system. *EBioMedicine* 27, 103–111. doi: 10.1016/j.ebiom.2017.11.032

Koek, R. J., Schwartz, H. N., Scully, S., Langevin, J. P., Spangler, S., Korotinsky, A., et al. (2016). Treatment-refractory posttraumatic stress disorder (TRPTSD): a review and framework for the future. *Prog. Neuropsychopharmacol. Biol. Psychiatry* 70, 170–218. doi: 10.1016/j.pnpbp.2016.01.015

Kohli, S., and Casson, A. J. (2019). Removal of gross artifacts of transcranial alternating current stimulation in simultaneous EEG monitoring. *Sensors* 19:190. doi: 10.3390/s19010190

Koppert, M., Kalitzin, S., Velis, D., Lopes Da Silva, F., and Viergever, M. A. (2014). Dynamics of collective multi-stability in models of multi-unit neuronal systems. *Int. J. Neural. Syst.* 24:1430004. doi: 10.1142/S0129065714300046

Kossoff, E. H., Ritzl, E. K., Politsky, J. M., Murro, A. M., Smith, J. R., Duckrow, R. B., et al. (2004). Effect of an external responsive neurostimulator on seizures and electrographic discharges during subdural electrode monitoring. *Epilepsia* 45, 1560–1567. doi: 10.1111/j.0013-9580.2004.26104.x

Kozák, G., and Berényi, A. (2017). Sustained efficacy of closed loop electrical stimulation for long-term treatment of absence epilepsy in rats. *Sci. Rep.* 7:6300. doi: 10.1038/s41598-017-06684-0

Kreuz, T., Andrzejak, R. G., Mormann, F., Kraskov, A., Stögbauer, H., Elger, C. E., et al. (2004). Measure profile surrogates: a method to validate the performance of epileptic seizure prediction algorithms. *Phys. Rev. E* 69:9. doi: 10.1103/PhysRevE.69.061915

Kronenbuerger, M., Fromm, C., Block, F., Coenen, V. A., Rohde, I., Rohde, V., et al. (2006). On-demand deep brain stimulation for essential tremor: a report on four cases. *Mov. Disord.* 21, 401–405. doi: 10.1002/mds.20714

Krook-Magnuson, E., Gelinas, J. N., Soltesz, I., and Buzsáki, G. (2015). Neuroelectronics and biooptics: closed-loop technologies in neurological disorders. *JAMA Neurol.* 72, 823–829. doi: 10.1001/jamaneurol.2015.0608

Kuhlmann, L., Freestone, D., Lai, A., Burkitt, A. N., Fuller, K., Grayden, D. B., et al. (2010). Patient-specific bivariate-synchrony-based seizure prediction for short prediction horizons. *Epilepsy Res.* 91, 214–231. doi: 10.1016/j.eplepsyres.2010.07.014

Kuhlmann, L., Grayden, D. B., Wendling, F., and Schiff, S. J. (2015). Role of multiple-scale modeling of epilepsy in seizure forecasting. *J. Clin. Neurophysiol.* 32, 220–226. doi: 10.1097/WNP.0000000000000149

Kuhlmann, L., Karoly, P., Freestone, D. R., Brinkmann, B. H., Temko, A., Barachant, A., et al. (2018). Epilepsyecosystem.org: crowd-sourcing reproducible seizure prediction with long-term human intracranial EEG. *Brain* 141, 2619–2630. doi: 10.1093/brain/awy210

Lambrecq, V., Lehongre, K., Adam, C., Frazzini, V., Mathon, B., Clemenceau, S., et al. (2017). Single-unit activities during the transition to seizures in deep mesial structures. *Ann. Neurol.* 82, 1022–1028. doi: 10.1002/ana.25111

Lehnertz, K., and Litt, B. (2005). The first international collaborative workshop on seizure prediction: summary and data description. *Clin. Neurophysiol.* 116, 493–505. doi: 10.1016/j.clinph.2004.08.020

Leuchter, A. F., Hunter, A. M., Krantz, D. E., and Cook, I. A. (2015). Rhythms and blues: modulation of oscillatory synchrony and the mechanism of action of antidepressant treatments. *Ann. N. Y. Acad. Sci.* 1344, 78–91. doi: 10.1111/nyas.12742

Li, Y., Du, X. F., Liu, C. S., Wen, Z. L., and Du, J. L. (2012). Reciprocal regulation between resting microglial dynamics and neuronal activity in vivo. *Dev. Cell* 23, 1189–1202. doi: 10.1016/j.devcel.2012.10.027

Liu, A., Vöröslakos, M., Kronberg, G., Henin, S., Krause, M. R., Huang, Y., et al. (2018). Immediate neurophysiological effects of transcranial electrical stimulation. *Nat. Commun.* 9:5092. doi: 10.1038/s41467-018-07233-7

Loo, C. K., Alonzo, A., Martin, D., Mitchell, P. B., Galvez, V., and Sachdev, P. (2012). Transcranial direct current stimulation for depression: 3-Week, randomised, sham-controlled trial. *Br. J. Psychiatry* 200, 52–59. doi: 10.1192/bjp.bp.111.097634

Lopes da Silva, F., Blanes, W., Kalitzin, S. N., Parra, J., Suffczynski, P., and Velis, D. N. (2003). Epilepsies as dynamical diseases of brain systems: basic models of the transition between normal and epileptic activity. *Epilepsia* 44(Suppl. 12), 72–83. doi: 10.1111/j.0013-9580.2003.12005.x

Lu, Y., Zhong, C., Wang, L., Wei, P., He, W., Huang, K., et al. (2016). Optogenetic dissection of ictal propagation in the hippocampal-entorhinal cortex structures. *Nat. Commun.* 7:10962. doi: 10.1038/ncomms10962

Mansouri, F., Dunlop, K., Giacobbe, P., Downar, J., and Zariffa, J. (2017). A fast EEG forecasting algorithm for phase-locked transcranial electrical stimulation of the human brain. *Front. Neurosci.* 11:401. doi: 10.3389/fnins.2017.00401

Maris, E., Fries, P., and van Ede, F. (2016). Diverse phase relations among neuronal rhythms and their potential function. *Trends Neurosci.* 39, 86–99. doi: 10.1016/j.tins.2015.12.004

Massey, C. A., Sowers, L. P., Dlouhy, B. J., and Richerson, G. B. (2014). Mechanisms of sudden unexpected death in epilepsy: the pathway to prevention. *Nat. Rev. Neurol.* 10, 271–282. doi: 10.1038/nrneurol.2014.64

Mathalon, D. H., and Sohal, V. S. (2015). Neural oscillations and synchrony in brain dysfunction and neuropsychiatric disorders it's about time. *JAMA Psychiatry* 72, 840–844. doi: 10.1001/jamapsychiatry.2015.0483

Matsumoto, H., and Marsan, C. A. (1964). Cortical cellular phenomena in experimental epilepsy: ictal manifestations. *Exp. Neurol.* 9, 305–326. doi: 10.1016/0014-4886(64)90026-3

McNaughton, B. L., Barnes, C. A., and O'Keefe, J. (1983). The contributions of position, direction, and velocity to single unit activity in the hippocampus of freely-moving rats. *Exp. Brain Res.* 52, 41–49. doi: 10.1007/BF00237147

Meindertsma, H., and Steenbeek, H. (2012). Application of skill theory to compare scientific reasoning of young children in different tasks. *Neth. J. Psychol.* 67, 9–19.

Meiron, O., Gale, R., Namestnic, J., Bennet-Back, O., Gebodh, N., Esmaeilpour, Z., et al. (2019). Antiepileptic effects of a novel noninvasive neuromodulation treatment in a subject with early-onset epileptic encephalopathy: case report with 20 sessions of HDTDCS intervention. *Front. Neurosci.* 13:547. doi: 10.3389/fnins.2019.00547

Mennella, R., Patron, E., and Palomba, D. (2017). Frontal alpha asymmetry neurofeedback for the reduction of negative affect and anxiety. *Behav. Res. Ther.* 92, 32–40. doi: 10.1016/j.brat.2017.02.002

Mokhatab, S., and Poe, W. A. (eds) (2012). "Process modeling in the natural gas processing industry," in *Handbook of Natural Gas Transmission and Processing*, (Waltham, MA: Gulf Professional Publishing), 511–541. doi: 10.1016/b978-0-12-386914-2.00015-7

Morgan, V. L., Chang, C., Englot, D. J., and Rogers, B. P. (2020a). Temporal lobe epilepsy alters spatio-temporal dynamics of the hippocampal functional network. *Neuroimage Clin.* 26:102254. doi: 10.1016/j.nicl.2020.102254

Morgan, V. L., Rogers, B. P., Anderson, A. W., Landman, B. A., and Englot, D. J. (2020b). Divergent network properties that predict early surgical failure versus late recurrence in temporal lobe epilepsy. *J. Neurosurg.* 132, 1324–1333. doi: 10.3171/2019.1.JNS182875

Morgan, V. L., Englot, D. J., Rogers, B. P., Landman, B. A., Cakir, A., Abou-Khalil, B. W., et al. (2017). Magnetic resonance imaging connectivity for the prediction of seizure outcome in temporal lobe epilepsy. *Epilepsia* 58, 1251–1260. doi: 10.1111/epi.13762

Mormann, F., Andrzejak, R. G., Elger, C. E., and Lehnertz, K. (2007). Seizure prediction: the long and winding road. *Brain* 130, 314–333. doi: 10.1093/brain/awl241

Morrell, M. (2006). Brain stimulation for epilepsy: can scheduled or responsive neurostimulation stop seizures? *Curr. Opin. Neurol.* 19, 164–168. doi: 10.1097/01.wco.0000218233.60217.84

Morrell, M. J. (2011). Responsive cortical stimulation for the treatment of medically intractable partial epilepsy. *Neurology* 77, 1295–1304. doi: 10.1212/WNL.0b013e3182302056

Nitsche, M. A., Polania, R., and Kuo, M. F. (2015). "Transcranial direct current stimulation: modulation of brain pathways and potential clinical applications," in *Brain Stimulation: Methodologies and Interventions*, ed. I. M. Reti (Hoboken, NJ: John Wiley & Sons, Inc.), 233–254. doi: 10.1002/9781118568323.ch13

Opitz, A., Falchier, A., Yan, C. G., Yeagle, E. M., Linn, G. S., Megevand, P., et al. (2016). Spatiotemporal structure of intracranial electric fields induced by transcranial electric stimulation in humans and nonhuman primates. *Sci. Rep.* 6:31236. doi: 10.1038/srep31236

Osorio, I., Frei, M. G., Sunderam, S., Giftakis, J., Bhavaraju, N. C., Schaffner, S. F., et al. (2005). Automated seizure abatement in humans using electrical stimulation. *Ann. Neurol.* 57, 258–268. doi: 10.1002/ana.20377

Paz, J. T., and Huguenard, J. R. (2015). Microcircuits and their interactions in epilepsy: is the focus out of focus? *Nat. Neurosci.* 18, 351–359. doi: 10.1038/nn.3950

Perea, G., Navarrete, M., and Araque, A. (2009). Tripartite synapses: astrocytes process and control synaptic information. *Trends Neurosci.* 32, 421–431. doi: 10.1016/j.tins.2009.05.001

Petkov, G., Kalitzin, S., Demuru, M., Widman, G., Suffczynski, P., and Lopes Da Silva, F. (2018). Computational model exploration of stimulation based paradigm for detection of epileptic systems. *Front. Artif. Intell. Appl.* 310:324–335. doi: 10.3233/978-1-61499-929-4-324

Reinhart, R. M. G. (2017). Disruption and rescue of interareal theta phase coupling and adaptive behavior. *Proc. Natl. Acad Sci. U.S.A.* 114, 11542–11547. doi: 10.1073/pnas.1710257114

Schelter, B., Winterhalder, M., Maiwald, T., Brandt, A., Schad, A., Schulze-Bonhage, A., et al. (2006). Testing statistical significance of multivariate time series analysis techniques for epileptic seizure prediction. *Chaos* 16:013108. doi: 10.1063/1.2137623

Schulze-Bonhage, A. (2016). "An introduction to epileptiform activities and seizure patterns obtained by scalp and invasive eeg recordings," in *Epilepsy: The Intersection of Neurosciences, Biology, Mathematics, Engineering, and Physics* (Hoboken, NJ: CRC Press), 51–64. doi: 10.1201/b10866-9

Seifert, G., Carmignoto, G., and Steinhäuser, C. (2010). Astrocyte dysfunction in epilepsy. *Brain Res. Rev.* 63, 212–221. doi: 10.1016/j.brainresrev.2009.10.004

Shirinpour, S., Alekseichuk, I., Mantell, K., and Opitz, A. (2020). Experimental evaluation of methods for real-time EEG phase-specific transcranial magnetic stimulation. *J. Neural Eng.* 17, 1–13. doi: 10.1088/1741-2552/ab9dba

Sik, A., Penttonen, M., Ylinen, A., and Buzsáki, G. (1995). Hippocampal CA1 interneurons: an in vivo intracellular labeling study. *J. Neurosci.* 15, 6651–6665. doi: 10.1523/jneurosci.15-10-06651.1995

Snyder, D. E., Echauz, J., Grimes, D. B., and Litt, B. (2008). The statistics of a practical seizure warning system. *J. Neural Eng.* 5, 392–401. doi: 10.1088/1741-2560/5/4/004

Staba, R. J., Wilson, C. L., Bragin, A., Fried, I., and Engel, J. (2002). Sleep states differentiate single neuron activity recorded from human epileptic hippocampus, entorhinal cortex, and subiculum. *J. Neurosci.* 22, 5694–5704. doi: 10.1523/jneurosci.22-13-05694.2002

Stein, A. G., Eder, H. G., Blum, D. E., Drachev, A., and Fisher, R. S. (2000). An automated drug delivery system for focal epilepsy. *Epilepsy Res.* 39, 103–114. doi: 10.1016/S0920-1211(99)00107-2

Sterman, M. B. (2000). Basic concepts and clinical findings in the treatment of seizure disorders with EEG operant conditioning. *Clin. EEG Neurosci.* 31, 45–55. doi: 10.1177/155005940003100111

Stidd, D. A., Vogelsang, K., Krahl, S. E., Langevin, J. P., and Fellous, J. M. (2013). Amygdala deep brain stimulation is superior to paroxetine treatment in a rat model of posttraumatic stress disorder. *Brain Stimul.* 6, 837–844. doi: 10.1016/j.brs.2013.05.008

Takeuchi, Y., and Berényi, A. (2020). Oscillotherapeutics-time-targeted interventions in epilepsy and beyond. *Neurosci. Res.* 152, 87–107. doi: 10.1016/j.neures.2020.01.002

Takeuchi, Y., Harangozó, M., Pedraza, L., Földi, T., Kozák, G., Li, Q., et al. (2021). Closed-loop stimulation of the medial septum terminates epileptic seizures. *Brain* 144, 885–908. doi: 10.1093/brain/awaa450

Thut, G., Miniussi, C., and Gross, J. (2012). The functional importance of rhythmic activity in the brain. *Curr. Biol.* 22, R658–R663. doi: 10.1016/j.cub.2012.06.061

Truccolo, W., Ahmed, O. J., Harrison, M. T., Eskandar, E. N., Rees Cosgrove, G., Madsen, J. R., et al. (2014). Neuronal ensemble synchrony during human focal seizures. *J. Neurosci.* 34, 9927–9944. doi: 10.1523/JNEUROSCI.4567-13.2014

Truong, N. D., Nguyen, A. D., Kuhlmann, L., Bonyadi, M. R., Yang, J., Ippolito, S., et al. (2018). Convolutional neural networks for seizure prediction using intracranial and scalp electroencephalogram. *Neural Netw.* 105, 104–111. doi: 10.1016/j.neunet.2018.04.018

Viglione, S. S., and Walsh, G. O. (1975). Proceedings: epileptic seizure prediction. *Electroencephalogr. Clin. Neurophysiol.* 39, 435–436.

Vöröslakos, M., Takeuchi, Y., Brinyiczki, K., Zombori, T., Oliva, A., Fernández-Ruiz, A., et al. (2018). Direct effects of transcranial electric stimulation on brain circuits in rats and humans. *Nat. Commun.* 9:483. doi: 10.1038/s41467-018-02928-3

Wake, H., Moorhouse, A. J., Jinno, S., Kohsaka, S., and Nabekura, J. (2009). Resting microglia directly monitor the functional state of synapses in vivo and determine the fate of ischemic terminals. *J. Neurosci.* 29, 3974–3980. doi: 10.1523/JNEUROSCI.4363-08.2009

Walker, G. (1931). On periodicity in series of related terms. *Mon. Weather Rev.* 59, 277–278.

Wang, Y., Xu, C., Xu, Z., Ji, C., Liang, J., Wang, Y., et al. (2017). Depolarized GABAergic signaling in subicular microcircuits mediates generalized seizure in temporal lobe epilepsy. *Neuron* 95, 92–105.e5. doi: 10.1016/j.neuron.2017.06.004

Wyler, A. R., Ojemann, G. A., and Ward, A. A. (1982). Neurons in human epileptic cortex: correlation between unit and EEG activity. *Ann. Neurol.* 11, 301–308. doi: 10.1002/ana.410110311

Yule, G. U. (2012). On a method of investigating periodicities in disturbed series, with special reference to wolfer's sunspot numbers. *Philos. Trans. R. Soc. Lond. A* 226, 267–273. doi: 10.1017/cbo9781139170116.013

Zalay, O. C., and Bardakjian, B. L. (2009). Theta phase precession and phase selectivity: a cognitive device description of neural coding. *J. Neural Eng.* 6:036002. doi: 10.1088/1741-2560/6/3/036002

Zalay, O. C., Serletis, D., Carlen, P. L., and Bardakjian, B. L. (2010). System characterization of neuronal excitability in the hippocampus and its relevance to observed dynamics of spontaneous seizure-like transitions. *J. Neural Eng.* 7:036002. doi: 10.1088/1741-2560/7/3/036002

Zrenner, C., Desideri, D., Belardinelli, P., and Ziemann, U. (2018). Real-time EEG-defined excitability states determine efficacy of TMS-induced plasticity in human motor cortex. *Brain Stimul.* 11, 374–389. doi: 10.1016/j.brs.2017.11.016

Conflict of Interest: AB was the owner of Amplipex Llc. and a shareholder of Neunos Ltd., Szeged, Hungary, manufacturers of signal-multiplexed neuronal amplifiers and neurostimulator devices.

The remaining authors declare that the research was conducted in the absence of any commercial or financial relationships that could be construed as a potential conflict of interest.

Publisher's Note: All claims expressed in this article are solely those of the authors and do not necessarily represent those of their affiliated organizations, or those of the publisher, the editors and the reviewers. Any product that may be evaluated in this article, or claim that may be made by its manufacturer, is not guaranteed or endorsed by the publisher.

frontiers in Neural Circuits

ORIGINAL RESEARCH
published: 17 December 2021
doi: 10.3389/fncir.2021.784034

Activity and Coupling to Hippocampal Oscillations of Median Raphe GABAergic Cells in Awake Mice

Marta Jelitai[1†], Albert M. Barth[1†], Ferenc Komlósi[1‡], Tamás F. Freund[2] and Viktor Varga[1*]*

[1] Subcortical Modulation Research Group, Institute of Experimental Medicine, Budapest, Hungary, [2] Laboratory of Cerebral Cortex Research, Institute of Experimental Medicine, Budapest, Hungary

Ascending serotonergic/glutamatergic projection from the median raphe region (MRR) to the hippocampal formation regulates both encoding and consolidation of memory and the oscillations associated with them. The firing of various types of MRR neurons exhibits rhythmic modulation coupled to hippocampal oscillatory activity. A possible intermediary between rhythm-generating forebrain regions and entrained ascending modulation may be the GABAergic circuit in the MRR, known to be targeted by a diverse array of top-down inputs. However, the activity of inhibitory MRR neurons in an awake animal is still largely unexplored. In this study, we utilized whole cell patch-clamp, single cell, and multichannel extracellular recordings of GABAergic and non-GABAergic MRR neurons in awake, head-fixed mice. First, we have demonstrated that glutamatergic and serotonergic neurons receive both transient, phasic, and sustained tonic inhibition. Then, we observed substantial heterogeneity of GABAergic firing patterns but a marked modulation of activity by brain states and fine timescale coupling of spiking to theta and ripple oscillations. We also uncovered a correlation between the preferred theta phase and the direction of activity change during ripples, suggesting the segregation of inhibitory neurons into functional groups. Finally, we could detect complementary alteration of non-GABAergic neurons' ripple-coupled activity. Our findings support the assumption that the local inhibitory circuit in the MRR may synchronize ascending serotonergic/glutamatergic modulation with hippocampal activity on a subsecond timescale.

Keywords: GABA, median raphe, *in vivo* awake patch-clamp, theta oscillation, hippocampal ripple

OPEN ACCESS

Edited by:
Sanja Mikulovic, Leibniz Institute for Neurobiology (LG), Germany

Reviewed by:
Mihaly Hajos, Yale University, United States
Claudia Boehm, Janelia Research Campus, United States

***Correspondence:**
Marta Jelitai
jelitai.marta@koki.hu
Viktor Varga
varga.viktor@koki.hu

[†]These authors share first authorship

[‡]Present address:
Ferenc Komlósi, Faculty of Medicine, Heart and Vascular Centre, Semmelweis University, Budapest, Hungary

Received: *27 September 2021*
Accepted: *10 November 2021*
Published: *17 December 2021*

Citation:
Jelitai M, Barth AM, Komlósi F, Freund TF and Varga V (2021) Activity and Coupling to Hippocampal Oscillations of Median Raphe GABAergic Cells in Awake Mice. Front. Neural Circuits 15:784034. doi: 10.3389/fncir.2021.784034

INTRODUCTION

"Timing is everything" is declared by one of the most famous quotes. Brain oscillations are expressive examples underscoring the validity of this claim. The synchronous activity of neurons is indispensable for communication within and across neural networks and for the plastic changes of their connections (Buzsáki and Draguhn, 2004; Paulsen and Sejnowski, 2006). Brain states coupled with disjunct stages of information processing, i.e., acquisition and consolidation are characterized by different oscillations. During exploration, when unfamiliar stimuli are encountered, the highly

regular theta oscillation dominates brain circuits engaged in encoding the novel information (Vanderwolf, 1969). The same circuits switch to a distinct mode of operation, whereas the newly acquired information is being consolidated, marked by large amplitude waves cooccurring with high frequency transients termed sharp wave ripples (Buzsáki et al., 1992). The hippocampus and connected regions form the core of the information storing circuit and subcortical modulators are key regulators of its operational state. Serotonergic/glutamatergic pathways from the median raphe nucleus, one of the major nuclei of the ascending serotonergic system, have profound effects on hippocampal activity and hippocampus-dependent behaviors (Nitz and McNaughton, 1999; Varga et al., 2009; Wang et al., 2015; Szőnyi et al., 2019). The majority of raphe neurons' activity fluctuates in concert with alternating brain states (Jacobs and Azmitia, 1992; Sakai and Crochet, 2001). However, in recent years, a considerable proportion of both serotonergic and non-serotonergic neurons were shown to exhibit rhythmic discharge synchronized to the hippocampal theta rhythm, and some of these cells' firing probability changed during ripples (Prisco et al., 2002; Kocsis et al., 2006). A key, yet unanswered question, is how an oscillatory activity is imposed on modulatory neurons. In many regions, the orchestration of neuronal activity during the emergence of oscillations relies on rhythmic inhibition (Wang, 2010). In the midbrain raphe complex, besides forming a feedback circuit excited by locally released serotonin (Boothman and Sharp, 2005), GABAergic neurons collect forebrain inputs and convert them to a fluctuating inhibitory tone (Varga et al., 2003). Here, we aim to characterize the state-dependent activity and coupling to the major hippocampal oscillations of MRR GABAergic cells, whereby the inhibitory network of the median raphe may be capable of coupling ascending serotonergic/glutamatergic modulation to the hippocampal rhythmic patterns.

MATERIALS AND METHODS

Animal Care and Housing

Male 8–12-week old, vGAT-iRES-Cre (Jackson Laboratory, JAX:016962) and vGAT-IRES-Cre/Gt(ROSA)26Sor_CAG/ZsGreen1 mice were used in this study. Gt(ROSA)26Sor_CAG/ZsGreen1 mouse strain originates from Jackson Laboratory, JAX:007906. Mice, two to three animals per cage, were housed on a reversed 12-h light/dark cycle. Food and water were available *ad libitum*. All experiments were approved by the Animal Care and Use Committee of the Institute of Experimental Medicine and the Committee for Scientific Ethics of Animal Research of the National Food Chain Safety Office under the project number PE/EA/200-2/2020 and were performed according to the 2010/63/EU Directive of the EC Council. All efforts were made to minimize pain and suffering and to reduce the number of animals used.

Surgical Procedures

Virus injections were performed under general anesthesia by intraperitoneal injection of ketamine–xylazine mixture (dose by body weight, 100 and 10 mg/kg, respectively), and analgesic (Buprenorphine 0.1 μg/g, s.c.) was applied at the beginning of surgery. MRR region was targeted *via* a burr hole (AP, –4.1 mm, ML, 0.0 mm) perpendicular to the skull surface using a standard stereotaxic frame (David Kopf Instruments, Tujunga, CA, United States). AAV-EF1a-DIO-hChR2(H134R)-eYFP (UNC Vector Core, Chapel Hill, NC, United States) or AAV-CAG-FLEX-ArchT-GFP (UNC Vector Core, Chapel Hill, NC, United States) was injected at a depth of 4.6–4.5 mm from the skull surface through a pulled glass micropipette using Nanoject II precision microinjector pump (Drummond, Broomall, PA, United States). After injection, mice were allowed to recover for at least 2 weeks to ensure sufficient expression of the virus.

Surgeries for whole cell patch-clamp recordings were done under isoflurane anesthesia (0.5–1.5%), and analgesic (Buprenorphine 0.1 μg/g, s.c.) was applied at the beginning of surgery. A small lightweight headplate was attached to the skull using Optibond adhesive (Kerr, Brea, CA, United States) and Paladur dental acrylic (Kulzer, Hanau, Germany). During whole cell recordings, mice were head-restrained with a downward tilted head position (pitch angle: 20°). For optogenetic experiments, an optic fiber (100 μm core diameter, Thorlabs GmbH, Newton, NJ, United States) was implanted above MRR (AP, –5.4 mm, ML, 0.9 mm at 18° ML angle) and fixed with dental acrylic. On the day of recording, at least 2 days after headplate surgeries, craniotomies were drilled above MRR (AP, –5.6 mm, ML, –0.7 mm, patch electrode ML at 10° angle) and dorsal hippocampus (AP, –3.2 mm, ML, –2.2 mm, LFP electrode AP, 20° ML at 10° angle). The craniotomies were covered with fast sealant (Body Double, Smooth-On, Easton, PA, United States), and recording was performed at least 1 h after surgery to allow recovering from anesthesia.

Headplate surgeries for multichannel recordings were done under isoflurane anesthesia (0.5–1.5%), and analgesic (Buprenorphine 0.1 μg/g, s.c.) was applied at the beginning of surgery. A small lightweight headplate was attached to the skull using Optibond adhesive (Kerr, Brea, CA, United States) and Paladur dental acrylic (Kulzer, Hanau, Germany). During multichannel recordings, mice were head-restrained with a downward tilted head position (pitch angle: 20°). Two cranial windows (1.5 × 1.5 mm) were drilled above the left hippocampus (AP, –2.5 mm; ML, 2.5 mm) and MRR (AP, –6.1 mm; ML, 0.0 mm, MRR probe ML at 4° angle) under stereotaxic guidance. For the optic fiber and ground electrode a hole was drilled above MRR (AP, –6.1 mm; ML, 0.0 mm) and cerebellum (AP, –5.6 mm; ML, 2.0 mm) respectively. The craniotomies and drill holes were covered with fast sealant (Body Double, Smooth-On, Easton, PA, United States). After surgery, the mice were continuously monitored until recovered, and then they were returned to their home cages for at least 48 h before starting habituation to the head restraint.

Whole Cell Patch-Clamp Recordings

Mice were habituated to the head restraint and experimental setup for 1–2 days before each recording session. Head restrained mice were free to run, walk, or sit on the treadmill equipped with a 2-m-long belt. Current-clamp recordings

were performed from MRR, 4,200–4,800 μm from the pial surface using a Multiclamp 700B amplifier (Molecular Devices, CA, United States). The data were digitized using CED Micro 1401 laboratory interface (Cambridge Electronic Design Limited, Cambridge, United Kingdom) and recorded using Spike 2 acquisition software. No bias current was applied during recordings and series resistances ranged between 20 and 60 MΩ. Once we got a stabilized recording, optical stimulations (light source: 447 nm diode or 593 nm DPSS laser, Roithner Lasertechnik GmbH, Austria, Ikecool, Corporation, United States, respectively, the latter no longer operational) were applied following 1–2 min of the control period. Both whole cell patch-clamp and cell-attached recordings were stabile during quiet wakefulness but we abruptly lost the cells at the onset of movement. For the analysis, we selected periods with stabile membrane potential; thus, the usual recording length was 150–250 s (median 181 s, interquartile range 99.5–301 s) with the shortest period of 30 s (**Supplementary Table 1**). For anesthetized experiments urethane (0.007 mL/g of 20%) was ip. administered at the beginning of the recording. *In vivo* external solution contained (in mM) 150 NaCl, 2.5 KCl, 10 HEPES, 1.5 $CaCl_2$, and 1 $MgCl_2$ (pH 7.3). Patch pipettes (5–8 MΩ) were filled with (in mM) 125 K-gluconate, 7 KCl, 10 HEPES, 10 sodium phosphocreatine, 0.1 EGTA, 2 MgATP, 2 Na_2ATP, 0.5 Na_2GTP (pH 7.2, 280–295 mOsm), and 2 mg/mL biocytin was added before recording. At the end of the recording, mice were transcardially perfused with 4% paraformaldehyde (PFA) and the brain was removed for *post-hoc* immunohistochemistry.

Multichannel Electrophysiological Recordings

Mice were habituated to head restraint and experimental setup for 1–2 days. Head-restrained mice were free to run, walk, or sit on air supported free-floating 20 cm diameter polystyrene ball. On the day of recording Buzsaki64 or Poly5 silicon probes (Neuronexus, Ann-Arbor, MI, United States) were lowered through the cranial window to the left dorsal hippocampus and MRR under isoflurane anesthesia (0.75–1.5%). The optical fiber was inserted in the MRR at 4.1 mm depth from the skull surface. Probes and optical fiber were coated with a lipophilic fluorescent dye, DiI (Thermo Fisher Scientific, Waltham, MA, United States), for later histological verification of the location. A ground electrode was placed above the cerebellum. Mice were allowed to recover from anesthesia for ∼1 h before recording.

The probe in the hippocampus was advanced using a micromanipulator (David Kopf Instruments, Tujunga, CA, United States) until the pyramidal layer was detected by increased unit activity and the occurrence of ripple events. In the MRR, unit activity was monitored from 4.2 to 5.2 mm depth, and the final position was determined based on the appearance of units ceasing their firing upon 2 s long laser stimulation (593 nm, Ikecool Corporation, United States). Once we found optically silenced units, the recording was commenced after an approximately 1 h waiting period for letting the tissue settle around the probe. Electrophysiological recordings were performed by a signal multiplexing head-stage (RHD 128, Intan Technologies, LA, United States) and an OpenEphys data acquisition board[1]. Signals were acquired at 20 k sample/s (Open Ephys 0.4.4.1). Mouse locomotor activity was monitored with an optical computer mouse positioned close to the polystyrene ball at the equator. Speed was calculated by a custom written macro in Igor Pro. At the end of the recording, mice were transcardially perfused with 4% PFA and the brain was removed for *post-hoc* immunohistochemistry.

Neuronal spikes were detected and automatically sorted by a template-matching algorithm using the Spyking Circus software (Yger et al., 2018), followed by manual curation of the clusters using the Phy software (Rossant et al., 2016) to obtain well-isolated single units. Spike sorting quality was assessed with a refractory period violation, and visual inspection of auto- and crosscorrelations; poor quality clusters were discarded.

Cell Identification

The location of the recorded cell was confirmed by biocytin labeling. We analyzed only those recordings in which the recording electrode, visible by the non-specifically labeled biocytin track, was inside the MRR region. Out of 108 recorded cells, we obtained 27 whole cell recordings. Of these, 13 were unequivocally identified as GABAergic or non-GABAergic. If we had been not able to find the biocytin labeled cell or there were more, equally labeled cells, we classified the registered neurons as non-identified (NI). The neurotransmitter phenotype of the recovered biocytin-labeled cells was determined by the colocalization of ZsGreen1 (selectively expressed by GABAergic neurons in the ZsGreen reporter mice, see above) or alternatively, by *post hoc* immunohistochemistry.

Optotagging was also used for cell identification. In AAV-EF1a-DIO-hChR2(H134R)-eYFP-injected vGAT-ires-Cre mice, if light stimulation (447 nm) had evoked depolarization and spiking, or hyperpolarization and spike suppression, the cell was identified as GABAergic or non-GABAergic, respectively. If the delivery of 593 nm light in AAV-CAG-FLEX-ArchT-GFP-injected vGAT-ires-Cre mice silenced the cell or evoked marked depolarization, the neuron was classified as GABAergic or non-GABAergic, respectively.

Immunohistochemistry

For the reconstruction of neuronal morphology and probe locations, coronal or parasagittal sections (60 μm) were cut using a vibratome (Leica Microsystems, Wetzlar, Germany). Sections were first incubated in blocking solution for 2 h (10% normal goat serum (NGS), 0.5% Triton X-100 in 0.1 M phosphate-buffered saline (PBS), and then incubated overnight in streptavidin AlexaFluor-488 or Cy3 (1:1,000, Jackson Immuno Research) to reveal the identity of the biocytin-filled neuron. To amplify the signal of the virally delivered fluorescent reporter protein, coexpressed with ChR2 or ArchT, sections from transduced brains were incubated in chicken anti-Green Fluorescent Protein (GFP, 1:2,000, Life Technologies) primary and anti-chicken AlexaFluor-488 secondary antibodies (1.1,000, Thermo Fisher Scientific). 5-HT and vGlut3 content were investigated by

[1] open-ephys.org

incubating the sections in guinea pig anti-vGlut3 (1:1,000, Frontier Institute, Nittobo Medical Co.) and rabbit anti-5HT (Immunostar) primary and anti-guinea pig AlexaFluor-647 or AlexaFluor-405 and anti-rabbit AlexaFluor-647 or 405 (1:1,000, Thermo Fisher Scientific or Jackson Immuno Research). All antibodies were diluted in carrier solution (0.1 M PBS, 1% NGS, 0.2% Triton-X100) and incubated overnight at room temperature. Fluorescence signals (DiI, streptavidin Alexa, or fluorescent reporter protein of ChR2, ArchT, and vGAT) were inspected using an Axioplan 2 microscope (Carl Zeiss, Oberkochen, Germany). To investigate the neurochemical content (vGlut3, 5-HT, vGAT) of biocytin-labeled cells, *z* stack images were acquired using a Nikon C2 confocal microscope (x40 objective, Nikon, Europe).

Data Analysis

All *in vivo* data were analyzed in Igor Pro 8 (Wavemetrics, Lake Oswego, OR, United States). Action potentials from whole cell recording voltage traces were detected automatically using an amplitude threshold algorithm (TaroTools, custom written macro in Igor Pro)[2] and were manually verified. The membrane potential spike threshold was computed as the second derivative of the voltage trace. Average membrane potential was calculated after clipping spikes above the threshold voltage. To calculate theta phase coupling, recording channels with maximal ripple amplitude, corresponding to the pyramidal layer, were selected. LFPs were filtered in the theta range (4–12 Hz). The phase of the theta oscillation was calculated by computing the Hilbert transform. Each single unit spike had been assigned to its coincident phase value and then the phase distribution was computed. Theta-coupling was assessed by performing Rayleigh's test for circular uniformity ($p > 0.05$). For computing theta rhythmicity index, autocorrelograms of every single unit were calculated, and theta rhythmicity index was defined as the ratio of the local minimum and maximum in a time window between 80 and 200 ms. To investigate the correlation between firing frequency and speed, the latter was normalized by its maximum in every animal and then divided into 25 bins. The firing rate of the neuron in each speed bin was then plotted and the resulting point cloud was fitted by linear regression. To analyze ripple coupling, hippocampal recording channels with maximal ripple amplitude were selected and then downsampled to 1 kHz. The LFPs were band-pass filtered in the 120–250 Hz range and the Hilbert transform was computed. Ripples were detected as events exceeding 3 SD of the signal with a minimal duration of 20 ms. The *z*-scored ripple peak triggered perievent histograms (PETH) were created for every single unit. Fast ripple-coupled units were defined if the *z*-scored PETH exceeded 2 SD in either the positive or negative direction for at least 20 ms in a 300 ms window around ripple peak. Slow reduction of ripple-coupled firing suppression was defined as a > 2 SD decrease of the *z*-scored PETH values for at least 500 ms in a 5-s-long window preceding the ripple peak. The onset and offset of ripple-coupled activity were defined as the 1 SD crossings. For the stimulus-triggered wavelet, the LFP was subjected to continuous wavelet transformation, utilizing a Morlet mother wavelet.

In whole cell experiments in each session shuffled PETHs were generated by selecting random timepoints matching the number of ripples in that session repeated 100 times. The ripple-triggered PETHs were plotted with the corresponding 95% confidence bounds of the shuffled data. If bin values exceeded the 95% confidence bounds for at least 20 ms, it was defined as a significant deviation.

All statistical analyses were performed with standard Igor Pro 8 functions. For comparisons, Student's *t*-test or Mann–Whitney and Wilcoxon test were used. The value $p < 0.05$ was considered significant. All values indicate mean ± SD unless stated otherwise.

RESULTS

Heterogeneous GABAergic Population in Median Raphe Region

To uncover the physiological characteristics and state-dependent activity of GABAergic and non-GABAergic neurons in the median raphe nucleus and surrounding paramedian raphe [together termed median raphe region (MRR)], we performed whole cell patch-clamp or cell-attached recordings from MRR with the simultaneous registration of local field potentials (LFP) in the hippocampal CA1 region in head-fixed behaving mice (**Figure 1A**). LFP was recorded from the pyramidal layer of dorsal CA1, identified based on the occurrence of ripple waves during immobility. The location of the recorded cell was confirmed by biocytin labeling. We analyzed only those sessions in which the recording electrode (visible by the biocytin-labeled track) was inside the MRR (**Figure 1B**).

We obtained 27 whole cell recordings and 81 cell attached recordings ($N = 62$ mice) from the MRR in single cell recording experiments. There was no difference in the firing frequency (median 4.72 Hz, interquartile range 2.59–8.71 Hz vs. median 7.45 Hz, interquartile range 3.21–14.09 Hz, Wilcoxon signed-rank test) nor in the coefficient of variation of inter-spike intervals (CV_{ISI}, median 1.06, interquartile range 0.79–1.35 vs. median 1.13, interquartile range 0.80–1.66, Wilcoxon signed-rank test) between whole cell and cell attached recordings.

For the identification of GABAergic cells, we have used a double transgenic mouse line, generated by crossing ZsGreen1 fluorescent reporter mice with vesicular GABA transporter (vGAT)-Cre mice, in which GABAergic cells expressed the ZsGreen fluorescent protein. Non-GABAergic neurons were labeled *post hoc* for vesicular glutamate transporter 3 (vGlut3) and serotonin (5HT). The unequivocal neurochemical classification was possible in 25 out of 108 recorded MRR cells: 12 cells were GABAergic whereas 13 cells were proved to be non-GABAergic (NG). In the remaining 83 cells, the neurotransmitter phenotype could not be determined (non-identified cells, NI). Firing frequency varied widely in each group, from 0.33 to 13.9 Hz in GABAergic cells ($n = 12$, median 5.78 Hz), 0.35–34.18 Hz in non-GABAergic neurons ($n = 13$, median 5.54 Hz), and between 0.18 and 38.16 Hz in

[2] sites.google.com/site/tarotoolsregister

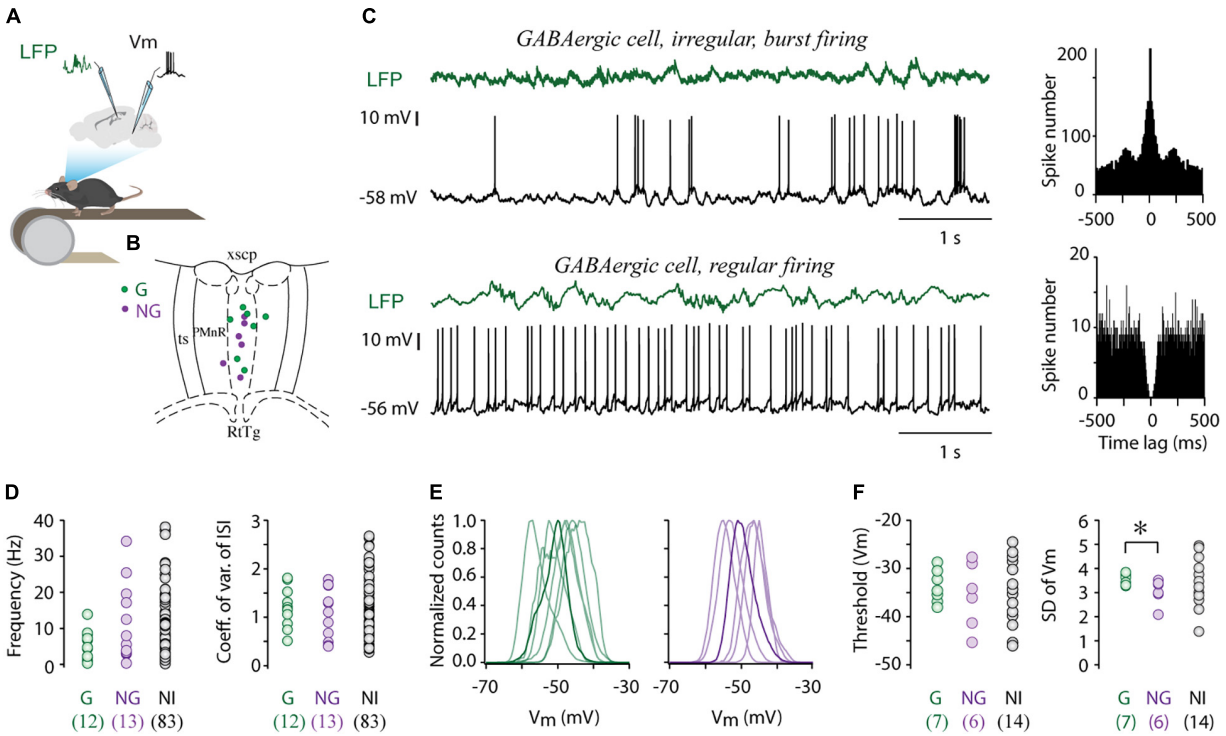

FIGURE 1 | Electrophysiological properties of MRR GABAergic cells. **(A)** Schematic showing the recording configuration. Whole cell recordings were collected from the MRR, simultaneously with local field potentials (LFP) from the dorsal hippocampal CA1 region in head-fixed behaving mice. **(B)** Colored dots (G: GABAergic, NG: non-GABAergic) mark the position of whole cell recorded and neurochemically identified neurons overlaid onto representative coronal diagrams of MRR (median raphe and paramedian raphe region). RtTg, reticulotegmental nucleus of the pons; PMnR, paramedian raphe nucleus; ts, tectospinal tract; xscp, decussation of the superior cerebellar peduncle. **(C)** Representative examples of whole cell current-clamp recordings and associated LFP (green) of an irregular (top trace) and regular (lower trace) GABAergic cell. Associated autocorrelograms are on the right sides. **(D)** Average firing rates and coefficient of variations of inter-spike intervals of GABAergic cells (G, $n = 12$), identified non-GABAergic (NG, $n = 13$) cells and non-identified cells (NI, $n = 83$). Open circles represent individual MRR neurons. **(E)** Normalized membrane potential (Vm) distribution of seven GABAergic (left) and six non-GABAergic (right) cells, thick lines highlight a single typical Vm distribution. **(F)** Average action potential threshold and standard deviation of membrane potential (SD of Vm) of GABAergic cells (G, $n = 7$), identified non-GABAergic (NG, $n = 6$) cells and non-identified cells (NI, $n = 14$). Circles represent individual MRR neurons. $^*p < 0.05$, two-tailed t-test.

case of NI neurons ($n = 83$, median 7.41 Hz, **Figure 1D** but see **Supplementary Table 1**). Accordingly, both GABAergic and non-GABAergic cells displayed a broad range of ISIs without significant difference in their distribution (median 145.95 ms, interquartile range 118.12–457.87 ms vs. median 179.70 ms, interquartile range 58.33–315.30 ms, Wilcoxon signed-rank test). The firing pattern regularity of GABAergic neurons formed a continuum from regular to irregular reflected in the broad distribution of CV_{ISI} (median 1.18, range 0.51–1.81. **Figures 1C,D**). The majority of these cells typically displayed irregular firing patterns with intermittent bursting (**Figure 1C**), sharply distinct from the characteristic clock-like, tonic, serotonergic firing pattern (Aghajanian et al., 1978; Prisco et al., 2002; Kocsis et al., 2006). The resting membrane potential of GABAergic cells varied between –44.02 and –55.46 mV ($n = 7$, –49.50 ± 4.03 mV) and they displayed unimodal subthreshold Vm distribution, centered around –50 mV (**Figure 1E**). The membrane potential distribution of GABAergic and non-GABAergic cells ($n = 6$, –48.70 ± 4.03 mV, two-tailed t-test) was not statistically different. Action potential threshold of GABAergic cells (–33.77 ± 3.42) was also in the same range as that of non-GABAergic neurons (–35.6 ± 6.88, **Figure 1F**). However, large subthreshold Vm fluctuations characterized the former population thus, the standard deviation (SD) of Vm of GABAergic and non-GABAergic cells was significantly different (3.56 ± 0.22 vs. 3.04 ± 0.52, two-tailed t-test, $^*p < 0.05$, **Figure 1F**).

Tonic Inhibition of Non-GABAergic Projection Neurons by Local GABAergic Cells

To directly investigate the effect of local GABAergic cells on the spike output of non-GABAergic putative projection neurons (Jacobs and Azmitia, 1992; Hioki et al., 2009; Jackson et al., 2009; Varga et al., 2009; Szőnyi et al., 2014, 2019), we combined cell type-selective optogenetic manipulation of the former with whole-cell patch clamp recordings from MRR neurons. In several cases, we abruptly lost the cells at the middle of the stimulation because of movement, therefore some of the experiments ($n = 6/6$ at ChR2 and $n = 3/11$ at ArchT) were carried out under urethane anesthesia. Channelrhodopsin 2 (ChR2) was

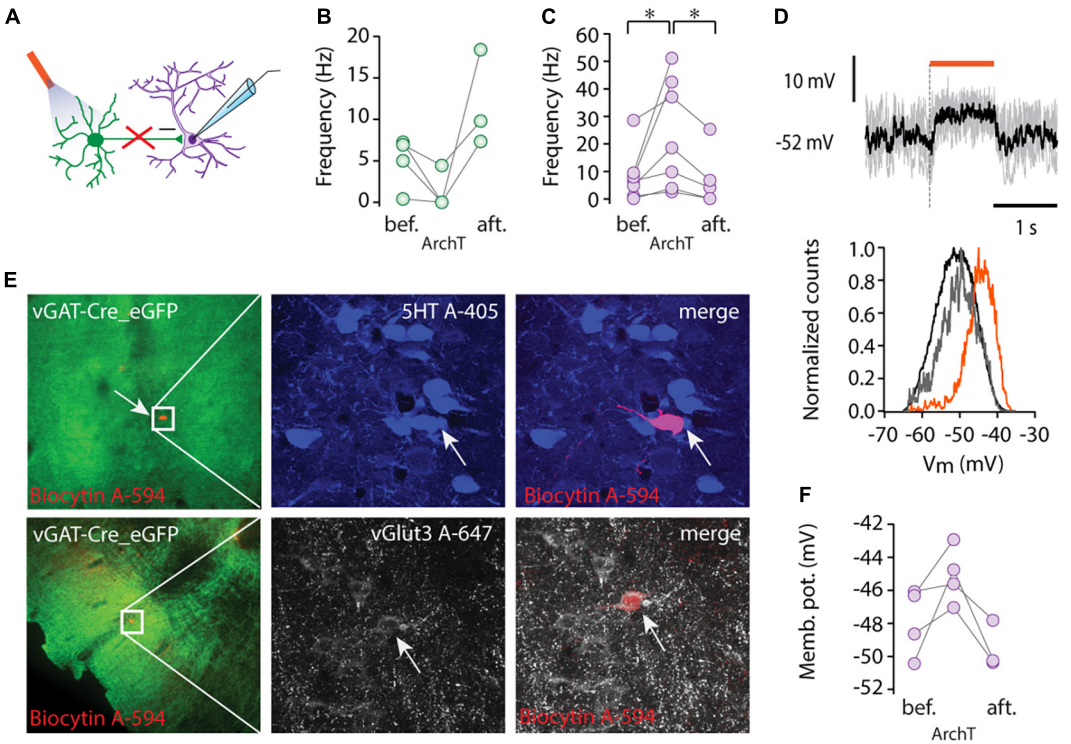

FIGURE 2 | Tonic inhibition by local GABAergic neurons. **(A)** Schematic showing recording configuration during optogenetic stimulation of GABAergic cells (ArchT, 593 nm). **(B)** Average firing rate of GABAergic cells (n = 4) before (bef.), during light stimulation (ArchT), and after light stimulation (aft.). **(C)** Average firing rate of non-GABAergic cells (n = 7) before (bef.), during light stimulation (ArchT), and after light stimulation (aft.), $^*p < 0.05$, Wilcoxon signed-rank test. **(D)** Membrane potential of a representative non-GABAergic cell (upper panel) during light stimulation (orange bar, 1s pulse of 593 nm light stimulation), five consecutive traces are overlaid (gray) and the black trace shows the average Vm. Representative normalized Vm distribution (lower panel) before light stimulation (black), during light stimulation (orange) and after light stimulation (gray). **(E)** Lower (left column) and higher magnification immunofluorescent images (middle, right columns) of representative recorded cells labelled by biocytin (red) from virus injected vGAT-Cre mice (ArchT-eGFP, green). One cell was serotonin positive (5HT, blue, top row) and the other one was immunoreactive for vGlut3 (white, lower row). **(F)** Average membrane potential of four non-GABAergic cells before (bef.), during light stimulation (ArchT) and after light stimulation (aft.).

targeted to MRR cells using the vGAT-Cre transgenic mouse line and viral gene transfer (AAV vector). One millisecond-long optogenetic single pulse stimulation did not evoke a detectable effect in the membrane potential but lengthening the pulse to 3 or 10 ms resulted in marked depolarization or spiking in GABAergic cells (n = 3) and phasic hyperpolarization (–3.36 and –5.39 mV, respectively) in non-GABAergic cells (n = 3) (**Supplementary Figure 1**).

ArchaerhodopsinT [ArchT, Han et al. (2011)] was utilized for suppressing neuronal activity (**Figure 2A**). To assess the efficiency of ArchT, we recorded from GABAergic neurons and found that illumination (5 s pulse, 593 nm) caused marked hyperpolarization (delta Vm: –10.9 ± 12.32 mV, n = 3) and silencing of three out of four tested cells (n = 4, **Figure 2B**).

Inactivation of the GABAergic circuit in the MRR revealed a marked tonic inhibition of non-GABAergic projection neurons. ArchT mediated suppression (1–2 s pulses) of GABA-mediated inhibition caused depolarization and a rightward shift in Vm distributions in the neighboring, non-GABAergic cells (**Figure 2D**). The membrane potential depolarization (from –47.87 ± 2.07 mV to –45.08 ± 1.72 mV, n = 4, **Figure 2F**) was only observed during light stimulation and returned to baseline after stimulus cessation (onset and offset latencies were 30.72 ± 3.17 ms and 38.64 ± 14.98 ms, respectively). Depolarization during the suppression of local inhibition was paralleled by a marked increase in non-GABAergic cells' firing rates (n = 7, from 0.88 to 3.66 Hz, median, $^*p < 0.05$, Wilcoxon signed-rank test, **Figure 2C**). After the termination of light delivery, a small rebound hyperpolarization (–3.36 ± 2.39 mV) was observed in the majority of recorded non-GABAergic units (n = 3/4).

Among the intracellularly recorded neurons (n = 4), we found one 5HT positive/vGlut3 negative cell, one vGlut3 positive neuron (**Figure 2E**), and a putative vGlut2 positive cell, which was negative for both 5HT and vGlut3. These results confirm that each major type of non-GABAergic projection neuron in the MRR is under a tonic inhibitory control by local GABAergic cells.

State Dependent Firing of Median Raphe Region GABAergic Cells

State-dependence is a hallmark of neuronal activity in the median raphe, possibly shaped by the MRR GABAergic circuit.

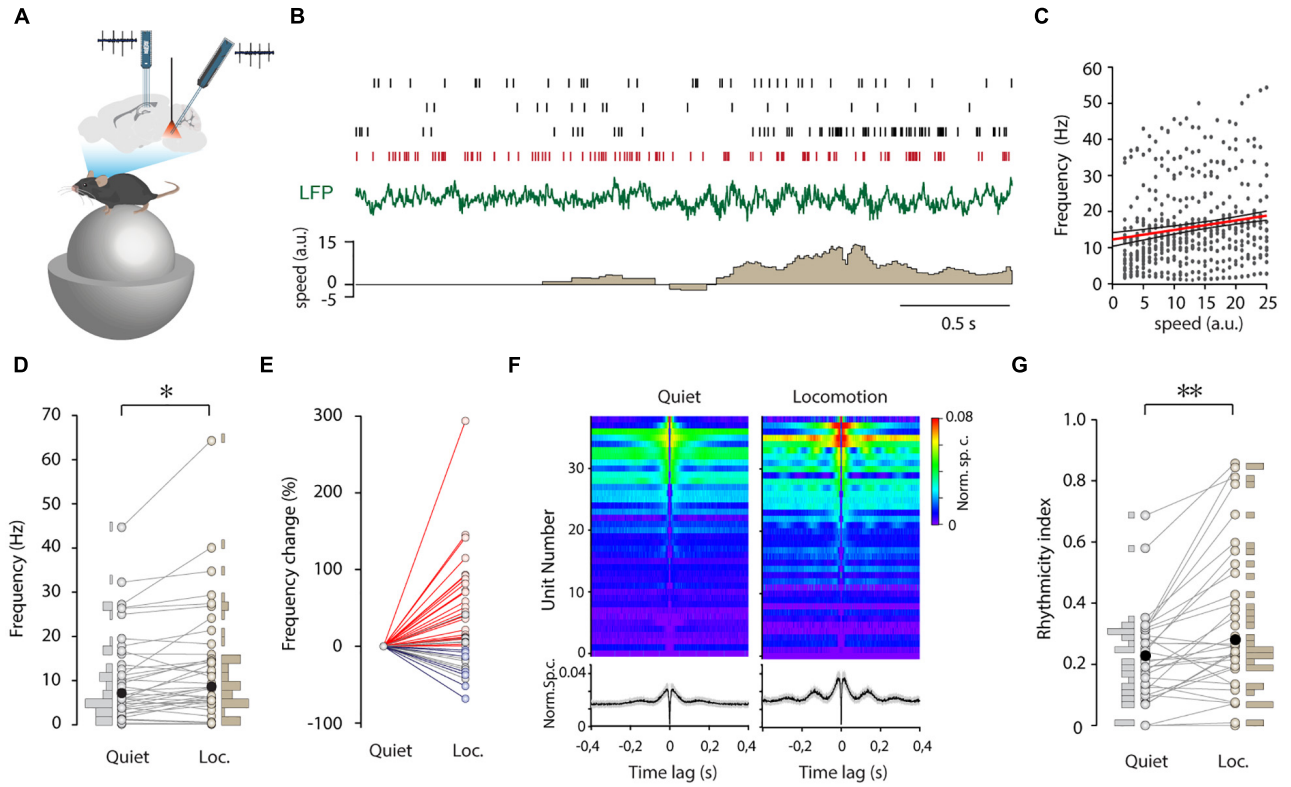

FIGURE 3 | State-dependent firing of MRR GABAergic cells. **(A)** Schematic showing the recording configuration. Dual silicon probe recordings were collected from the median raphe region (MRR) and CA1 of the dorsal hippocampus in head-fixed, behaving mice. The optic fiber was placed above the MRR. **(B)** Representative traces with four concurrently registered GABAergic cells from one session. Spike raster plots (top), LFP (middle, green), and speed (lower, brown) during a non-theta to a theta state transition. Note the emergence of theta oscillation with movement (a.u., arbitrary units). Spikes of a typical theta rhythmic GABAergic cell are colored red. **(C)** Frequency of positively correlated GABAergic cells (21/39) as a function of normalized speed. The red line marks the linear fit with a 95% confidence interval (black lines). **(D)** Average firing rate of GABAergic cells (n = 39) and its distribution during quiet wakefulness (Quiet) and locomotion (Loc.) Black filled circles represent the median. *$p < 0.05$, Wilcoxon signed-rank test. **(E)** Change in firing rate during quiet wakefulness (Quiet) and locomotion (Loc.) normalized to a quiet state. Colored circles represent GABAergic cells that displayed an increase (red lines and markers), decrease (blue lines and markers), or no significant (gray) change in firing rate. For testing significance Wilcoxon-Mann-Whitney test, $p < 0.05$ was used. **(F)** Autocorrelograms of GABAergic units (n = 39) during quiet wakefulness (left) and locomotion (right). Autocorrelograms were ordered by average values between 3 and 20 ms during locomotion. Lower panels display the average autocorrelograms (black line and gray shadow: mean ± s.e.). **(G)** Paired plot of rhythmicity of GABAergic cells (n = 39) and its distribution during quiet wakefulness (Quiet) and locomotion (Loc.) Black symbols represent median. **$p < 0.01$, Wilcoxon signed-rank test.

Hence, we compared the firing of MRR GABAergic cells during non-theta and theta states. Due to microwobbling amplified by the proximity of the basilar artery and the central aquaeduct to the MRR, whole cell recording was possible only during immobility (n = 27 of 108 neurons). Nevertheless, short theta segments could be isolated in 15 cells (n = 15/27), and the membrane potential of GABAergic cells was found to be unchanged while transient theta epochs emerged compared to the non-theta state (**Supplementary Figure 2A**). To study state-dependence in a larger population of GABAergic neurons, we deployed multichannel recording combined with inhibitory optical tagging (**Figure 3A**). ArchT was targeted to MRR GABAergic cells by viral gene transfer in vGAT-Cre mice. MRR and hippocampal activity were simultaneously sampled by silicone probes in head-fixed, awake animals running or sitting on air-supported free-floating (20 cm diameter) polystyrene balls. Delivery of 2-s long laser pulses enabled the tagging of even low activity cells (**Supplementary Figure 2B**). We could identify 39 GABAergic units from five animals. Their firing frequency varied in a wide range from 0.06 to 24.29 Hz (median 5.08 Hz) and did not differ significantly from the frequency of GABAergic neurons recorded by the whole cell patch-clamp (**Supplementary Figure 2C**). The appearance of theta was accompanied by the change of firing activity in the majority of GABAergic neurons (**Figure 3B**). During locomotion, the firing frequency increased, decreased, or remained unaffected in n = 23/39, 7/39, and 9/39 cells, respectively (**Figures 3D,E**). The direction of firing rate modulation did not depend on the magnitude of firing rate during quiet wakefulness (r = –0.114, p = 0.487), but GABAergic cells varied in their sensitivity to movement. That is, 21/39 GABAergic cells displayed a firing rate increase that was positively correlated with speed (**Figure 3C**), 16/39 cells showed no correlation, whereas 2/39 cells were inversely correlated. Besides the level of activity, we also explored how the firing pattern regularity of these neurons is affected by state transitions. Various patterns ranging from regular to

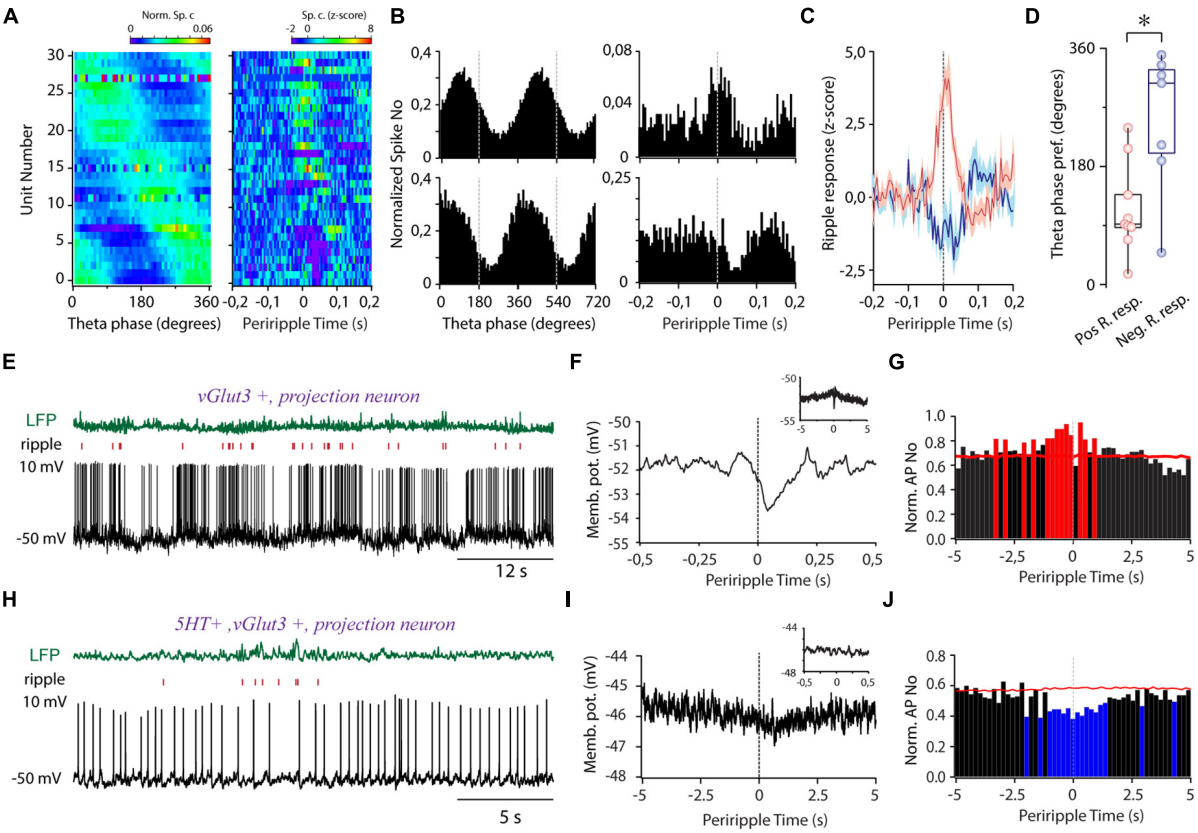

FIGURE 4 | Theta and sharp wave ripple-coupled firing in the MRR. **(A)** Preferred theta phase ordered phase histograms (left panel) (n = 31) and the corresponding peripple firing histograms of theta coupled GABAergic cells. **(B)** Two representative examples demonstrating theta- (left panels) and ripple- (right panels) coupled firing of GABAergic cells (bin size 5 ms). **(C)** Averaged peripple firing histograms of GABAergic cells with fast transient elevation (red, n = 8) and fast transient suppression (blue, n = 7) during ripples. **(D)** Theta phase preference of cells with positive transient (Pos. R resp., pink, n = 8) and negative transient (Neg. R. resp., blue, n = 7) during ripple waves. Circles represent individual GABAergic cells, boxes denote the medians and interquartile ranges. For testing significance, Wheeler-Watson and Whatson-Williams tests, $^*p < 0.05$ were used. **(E)** LFP (green, top), ripple raster plot (red, middle), and voltage trace (lower panel) from a non-GABAergic ripple-coupled cell. **(F)** The membrane potential of the cell **(E)** as a function of peripple time. Inset: Ripple peak aligned membrane potential at second-long timescale. **(G)** Normalized peripple firing histogram (bin size = 200 ms) of the cell **(E)**. The red color denotes the significant increase in the firing rate. **(H)** LFP (green, top), raster plot (red, middle), and voltage trace (lower panel) from a non-GABAergic ripple suppressed cell. **(I)** The membrane potential of the cell **(H)** as a function of peripple time on a slow timescale. Inset: ripple peak aligned membrane potential on a subsecond timescale. **(J)** Ripple peak aligned averaged normalized firing histogram (bin size = 200 ms) of the cell **(H)**. The blue color denotes a significant decrease in the firing rate.

irregular were observed spreading along a continuum reflected in the broad distribution of CV_{ISI} (**Supplementary Figure 2C**). Non-theta to theta state transition at the onset of movement altered the firing pattern, resulting in augmented rhythmicity and the occasional clustering of spiking (**Figures 3B,F**). In addition, there was no correlation between the rhythmicity during quiet wakefulness and the magnitude of the rhythmicity change (r = –0.223, p = 0.237), albeit the more rhythmic the cells were, the larger increase of frequency was detected during locomotion (r = 0.505, p = 0.004). Interestingly, there was an abrupt increase of theta power in the hippocampus with accompanying suppression of subtheta bands parallel with the light stimulation when the majority of MRR GABAergic cells were presumably silenced (**Supplementary Figure 3**). Importantly, the elevation of theta frequency preceded the onset of movement.

Hippocampal Theta and Sharp Wave Ripple-Coupled Firing of Median Raphe Region GABAergic Neurons

Next, we aimed to unravel the temporal relationship of the activity of MRR GABAergic cells to hippocampal theta. The majority of GABAergic cells showed theta phase-coupled firing (n = 31/39, Rayleigh test for uniformity, $p < 0.05$, mean resultant length 0.27 ± 0.02) covering the whole theta cycle as a population (**Figure 4A**). A subgroup of theta preferring MRR GABAergic neurons (n = 16/31, **Figures 4A,B**) exhibited ripple correlated-activity (absolute z-score values higher than 2 for at least 20 ms in a 300-ms window around ripple peak). Ripple activated cells covered mostly the ascending phase of theta, whereas cells with fast transient suppression of activity during ripples concentrated near the trough (**Figure 4D**). Transient activation (n = 9/31)

lasted about 52 ms on average (51.67 ± 17.5 ms) centered around ripple peaks. On average, rapid suppressions (n = 7/31, 46.43 ± 22.3 ms) tended to start later compared with activation relative to ripple peaks (23.89 ± 11.11 vs. 10.71 ± 24.57 ms before ripple peaks (**Figure 4C**), but the difference did not reach significance. Ripple-associated transient increase of activity was also observed in two cells (n = 2/8) with no theta preference (n = 8/39) (**Supplementary Figure 4A**). Ripple-coupled fast transient membrane potential changes could not be observed in the identified whole cell recorded GABAergic cells (n = 0/7).

The Ripple-Correlated Output of Median Raphe Region

We aimed to explore if alteration of local inhibition during ripples is mirrored by a complementary change in the ripple-coupled firing of the MRR's non-GABAergic output neurons. To this end, we investigated the ripple-correlated firing of these neurons recorded in whole cell mode.

One glutamatergic cell (5HT-, vGlut3+) showed fast transient suppression of spiking (**Figure 4E**) after ripple peak paralleled by a marked membrane potential hyperpolarization, reaching its maximum postpeak (**Figure 4F**). In the background of the rapid hyperpolarizing transient, we could also detect a slow depolarization on multiple second-long timescales, resulting in a significant elevation of activity around ripples (**Figure 4G**). In a serotonergic/glutamatergic cell (5HT+, vGlut3+), we observed slow gradual hyperpolarization and simultaneous decrease of activity concurrently with ripples (**Figures 4H–J**), but without any detectable ripple-locked fast transient. The diverging timescales and opposite direction of activity change suggest that different mechanisms govern the ripple-associated activity of MRR neurons.

The observed second-long ripple-correlated activity change prompted us to investigate the ripple-associated activity at a longer timescale in the identified GABAergic group. One whole cell recorded GABAergic cell showed slow hyperpolarization, and 9 out of 39 GABAergic neurons suppressed their activity for 1.50 ± 1.19 s around ripples (**Supplementary Figure 4B**). Strikingly, the majority of these neurons (n = 6/9) exhibited fast transient ripple-coincident activation embedded in longer-lasting suppression thus, exhibiting contrasting activity change simultaneously on different timescales. We did not detect multiple second-long elevations of activity among GABAergic cells around ripples.

DISCUSSION

GABAergic neurons form the largest subgroup in the median raphe nucleus and surrounding paramedian raphe (MRR). However, we know surprisingly little about this component of the raphe circuit. Here, by employing extracellular single or multichannel recording and whole cell patch-clamp in awake mice, we uncovered significant firing pattern heterogeneity, state-dependent activity, and tight coupling to hippocampal oscillations of MRR GABAergic cells. Utilizing whole cell patch clamp in awake animals let us observe the characteristics of inhibition in the most intact preparation.

Early *in vivo* pharmacological studies demonstrated the tonic control of serotonergic neurons in the MRR by GABAergic transmission (Forchetti and Meek, 1981). Later, slice experiments corroborated and extended these findings by characterizing GABAA-receptor mediated synaptic currents (IPSC) in serotonergic neurons of the midbrain raphe nuclei (Lemos et al., 2006). Comparison of IPSCs in serotonergic neurons of the MRR vs. the DRN exposed higher inhibitory activity in the former. These findings were further strengthened by the immunocytochemical and pharmacological detection of alpha3 subunit-containing GABAA receptors in serotonergic cells (Rodríguez-Pallares et al., 2001; Judge et al., 2006). A surprising report showed a higher than 90% colocalization of serotonin and GABAB-receptors in both the dorsal and median raphe nuclei, thus hinting about the tight regulation of the serotonergic output by both fast and long-acting GABAergic inhibition (Varga et al., 2002). In accordance with these preceding studies, we observed a powerful phasic inhibition of serotonergic and vesicular glutamate transporter type 3-expressing glutamatergic neurons in response to brief stimulation of GABAergic cells. Additionally, suppression of the inhibitory circuit uncovered the tonic inhibition of non-GABAergic units.

A series of *in vivo* pathway stimulation studies and recently, retrograde viral tracing in the dorsal raphe demonstrated that the GABAergic circuit is targeted by a large variety of raphe afferents (Wang and Aghajanian, 1977; Varga et al., 2001, 2003; Weissbourd et al., 2014) and may thus be in a key position to convert inputs to a complex, yet uncharacterized inhibitory pattern. For example, stimulation of the medial prefrontal cortex and the lateral habenula, two major raphe-projecting forebrain areas, evokes GABAA-mediated suppression of activity in the majority of putative serotonergic neurons (Wang and Aghajanian, 1977; Varga et al., 2001, 2003; Weissbourd et al., 2014). Besides distant projections, GABAergic neurons are influenced by locally released serotonin *via* 5-HT2A/C receptors, whereby they are key constituents of a local feedback circuit (Boothman and Sharp, 2005). The diversity of inputs is reflected by the irregularity of their firing as reported in a preceding study that utilized juxtacellular recording and labeling of dorsal raphe neurons in anesthetized rats (Allers and Sharp, 2003). We could show that irregular firing pattern was underlined by complex membrane potential dynamics reflected in its high variability in the undrugged animal.

Vigilance states are principal correlates of neuronal activity in many subcortical regions, including the median raphe (Lee and Dan, 2012). Furthermore, serotonergic cells, in concert with other subcortical modulators, were proposed to be major regulators of the sleep-wake cycle (Jacobs and Azmitia, 1992). Thus, sleep-wake stage-coupled discharge of serotonergic neurons is at least partly controlled by their interplay with other modulators. Here, we found that the activity of most MRR GABAergic neurons reliably followed behavioral activation, i.e., transition from immobile state to running. Since serotonergic neurons excite the local GABAergic circuit *via* 5-HT2A/C receptors, elevated serotonergic activity can turn up GABAergic inhibition

as well. In turn, the latter can serve as a break synergistically with the autoinhibition of serotonergic neurons. Besides fluctuation on long time scales, we observed the coupling of GABAergic spiking to both of the disjunct hippocampal oscillatory patterns: theta rhythm and sharp wave ripples. An unexpected discovery revealed the serotonergic identity of previously described theta-coupled rhythmic raphe neurons (Kocsis et al., 2006). This finding went against the widely accepted view of regular, metronome-like firing pattern, as a defining characteristic of serotonergic cells (Aghajanian et al., 1978). Phase-locked activity, albeit weaker, was also observed in glutamatergic cells of the MRR (Domonkos et al., 2016). A key question concerned the source of this rhythm. Theta-modulated GABAergic neurons described in our study may be prime candidates for conveying theta drive from forebrain rhythm-generating networks, most notably the medial septum, to the serotonergic and glutamatergic neurons of the MRR. Timing neuromodulation with theta timescale precision would dramatically increase its computational capacity, thus, activity in memory and executive circuits can be tailored to moment-to-moment changes of a challenging behavioral situation. The range of preferred theta phases covering the entire cycle would raise the intriguing possibility of functional subgroups of GABAergic cells dividing neuromodulation in the temporal domain. This scenario would be analogous to the hippocampus where activity in principal cell compartments is temporally segmented by the various interneuron subtypes linked to different phase ranges of theta (Klausberger and Somogyi, 2008). Besides theta, MRR GABAergic cells also exhibited ripple-correlated activity. The role of hippocampal ripples in memory consolidation is supported by many elegant studies (Girardeau et al., 2009; Nakashiba et al., 2009; Fernández-Ruiz et al., 2019). The antagonism of cholinergic and serotonergic modulation and ripple genesis is also well-established (Vandecasteele et al., 2014; Wang et al., 2015; Zhang et al., 2021). As in the case of theta-coupling of serotonergic and glutamatergic MRR neurons, the question arises about mechanisms that suppress the activity of these modulatory cells during ripple genesis. In a recent study, selective activation of GABAergic MRR neurons failed to change the rate of ripple occurrence, but following the stimulation transient suppression of ripples ensued possibly due to the rebound activation of GABA-targeted serotonergic/glutamatergic neurons (Wang et al., 2015). In our experiments, about a two-third majority of GABAergic MRR cells were activated during ripples. The increase of their activity started before the ripple peak and returned to baseline around the end of ripples. This tight coupling to the ripple window is orders of magnitude faster than the slow disfacilitation of MRR cell activity reported in the aforementioned study and suggests that the rapid rise of inhibition may switch off its target modulators and opens a narrow window of opportunity for communication between the hippocampus and its connected cortical partners (e.g., Sanda et al., 2020). This assumption was supported by the rapid hyperpolarization during ripples of an intracellularly recorded glutamatergic neuron. As theta coupling, this mode of operation is radically different from the slow modulation, traditionally associated with the serotonergic and other subcortical modulators. Notably, the firing of the remaining one-third of GABAergic MRR neurons was dampened, but on a comparably short timescale as activation. Here, the yet unanswered question can be posed whether this subgroup of ripple-suppressed inhibitory cells may influence a different target population of non-GABAergic neurons than the facilitated cells. The complementary ripple coincident change of firing of activated and inhibited GABAergic neurons also points to mutual inhibition among these cells. Strikingly, activity during ripples was correlated with theta phase preference. This observation strengthens the possibility that multiple functional groups exist in the MRR's inhibitory circuit capable of temporally segmenting neuromodulation depending not just on brain states, but also on momentary changes of activity patterns in target regions. Correlated theta- and ripple-coupling also indicate a common source capable of linking MRR GABAergic activity, and *via* inhibition, a large part of ascending modulation from the MRR to these oscillatory patterns. One such source can be the medial septum known to project to brainstem modulatory centers, including the median raphe nucleus. Importantly, short timescale ripple-coupling was embedded in multiple second-long alterations of spiking. The presence and direction of rapid change of activity were not correlated with long timescale modulation. Thus, the two phenomena may be controlled by diverging mechanisms. In summary, our results provide correlative evidence for the role of the GABAergic circuit of the MRR in enabling the rapid segmentation of modulation on a subsecond timescale. This raises the possibility of entirely novel, yet unknown forms of modulation acting on high temporospatial resolution.

DATA AVAILABILITY STATEMENT

The raw data supporting the conclusions of this article will be made available by the authors, without undue reservation.

ETHICS STATEMENT

The animal study was reviewed and approved by the Animal Care and Use Committee of the Institute of Experimental Medicine and the Committee for Scientific Ethics of Animal Research of the National Food Chain Safety Office of Hungary.

AUTHOR CONTRIBUTIONS

MJ, AB, and VV designed the experiments. MJ and FK carried out experiments. MJ and AB performed the analysis. MJ and VV wrote the original manuscript. AB and VV acquired the funding. All authors contributed to the discussion and interpretation of the results.

FUNDING

This work was funded by the National Research, Development and Innovation Office, Hungary FK129019 grant to AB and

K132735 grant to VV. AB was supported by the New National Excellence Program of the Ministry for Innovation and Technology (ÚNKP_19-4) and the Bolyai János Research Fellowship of the Hungarian Academy of Sciences.

ACKNOWLEDGMENTS

We thank Emőke Szépné Simon for essential technical assistance and thank the former and present members of the Subcortical Modulation Research Group, Andor Domonkos, Kathrin Petrik, and Flóra M. Vásárhelyi-Nagy for their assistance with the present work. We thank Scidraw.io for providing the availability of the drawings doi.org/10.5281/zenodo.3925913 and doi.org/10.5281/zenodo.3925905. Confocal microscopy was performed in the Nikon Microscopy Centre at the Institute of Experimental Medicine, Nikon Austria GmbH, and Auro-Science Consulting Ltd.

SUPPLEMENTARY MATERIAL

The Supplementary Material for this article can be found online at: https://www.frontiersin.org/articles/10.3389/fncir.2021.784034/full#supplementary-material

REFERENCES

Aghajanian, G. K., Wang, R. Y., and Baraban, J. (1978). Serotonergic and non-serotonergic neurons of the dorsal raphe: reciprocal changes in firing induced by peripheral nerve stimulation. *Brain Res.* 153, 169–175. doi: 10.1016/0006-89937891140-x

Allers, K. A., and Sharp, T. (2003). Neurochemical and anatomical identification of fast- and slow-firing neurones in the rat dorsal raphe nucleus using juxtacellular labelling methods in vivo. *Neuroscience* 122, 193–204.

Boothman, L. J., and Sharp, T. (2005). A role for midbrain raphe γ aminobutyric acid neurons in 5-hydroxytryptamine feedback control. *Neuroreport* 16, 891–896. doi: 10.1097/00001756-200506210-200506214

Buzsáki, G., and Draguhn, A. (2004). Neuronal oscillations in cortical networks. *Science (New York, N.Y.)* 304, 1926–1929. doi: 10.1126/science.1099745

Buzsáki, G., Horváth, Z., Urioste, R., Hetke, J., and Wise, K. (1992). High-frequency network oscillation in the hippocampus. *Science* 256, 1025–1027. doi: 10.1126/science.1589772

Domonkos, A., Ledri, L. N., Laszlovszky, T., Cserép, C., Borhegyi, Z., Papp, E., et al. (2016). Divergent in vivo activity of non-serotonergic and serotonergic VGluT3-neurones in the median raphe region. *J. Physiol.* 594, 3775–3790. doi: 10.1113/jp272036

Fernández-Ruiz, A., Oliva, A., de Oliveira, E. F., Rocha-Almeida, F., Tingley, D., and Buzsáki, G. (2019). Long-duration hippocampal sharp wave ripples improve memory. *Science* 364, 1082–1086. doi: 10.1126/science.aax0758

Forchetti, C. M., and Meek, J. L. (1981). Evidence for a tonic GABAergic control of serotonin neurons in the median raphe nucleus. *Brain Res.* 206, 208–212.

Girardeau, G., Benchenane, K., Wiener, S. I., Buzsáki, G., and Zugaro, M. B. (2009). Selective suppression of hippocampal ripples impairs spatial memory. *Nat. Neurosci.* 12, 1222–1223. doi: 10.1038/nn.2384

Han, X., Chow, B. Y., Zhou, H., Klapoetke, N. C., Chuong, A., Rajimehr, R., et al. (2011). A high-light sensitivity optical neural silencer: development and application to optogenetic control of non-human primate cortex. *Front. Syst. Neurosci.* 5:18. doi: 10.3389/fnsys.2011.00018

Hioki, H., Nakamura, H., Ma, Y.-F., Konno, M., Hayakawa, T., Nakamura, K. C., et al. (2009). Vesicular glutamate transporter 3-expressing nonserotonergic projection neurons constitute a subregion in the rat midbrain raphe nuclei. *J. Comp. Neurol.* 518, 668–686. doi: 10.1002/cne.22237

Jackson, J., Bland, B. H., and Antle, M. C. (2009). Nonserotonergic projection neurons in the midbrain raphe nuclei contain the vesicular glutamate transporter VGLUT3. *Synapse* 63, 31–41. doi: 10.1002/syn20581

Jacobs, B. L., and Azmitia, E. C. (1992). Structure and function of the brain serotonin system. *Physiol. Rev.* 72, 165–229. doi: 10.1152/physrev.1992.72.1.165

Judge, S. J., Young, R. L., and Gartside, S. E. (2006). GABAA receptor modulation of 5-HT neuronal firing in the median raphe nucleus: implications for the action of anxiolytics. *Eur. Neuropsychopharm.* 16, 612–619. doi: 10.1016/j.euroneuro.2006.01.010

Klausberger, T., and Somogyi, P. (2008). Neuronal diversity and temporal dynamics: the unity of hippocampal circuit operations. *Science (New York, N.Y.)* 321, 53–57. doi: 10.1126/science.1149381

Kocsis, B., Varga, V., Dahan, L., and Sík, A. (2006). Serotonergic neuron diversity: identification of raphe neurons with discharges time-locked to the hippocampal theta rhythm. *Proc. Natl. Acad. Sci. U. S. A.* 103, 1059–1064. doi: 10.1073/pnas.0508360103

Lee, S.-H., and Dan, Y. (2012). Neuromodulation of Brain States. *Neuron* 76, 209–222. doi: 10.1016/j.neuron.2012.09.012

Lemos, J. C., Pan, Y., Ma, X., Lamy, C., Akanwa, A. C., and Beck, S. G. (2006). Selective 5-HT1B receptor inhibition of glutamatergic and GABAergic synaptic activity in the rat dorsal and median raphe. *Eur. J. Neurosci.* 24, 3415–3430. doi: 10.1111/j.1460-9568.2006.05222.x

Nakashiba, T., Buhl, D. L., McHugh, T. J., and Tonegawa, S. (2009). Hippocampal CA3 output is crucial for ripple-associated reactivation and consolidation of memory. *Neuron* 62, 781–787. doi: 10.1016/j.neuron.2009.05.013

Nitz, D. A., and McNaughton, B. L. (1999). Hippocampal EEG and unit activity responses to modulation of serotonergic median raphe neurons in the freely behaving rat. *Learn. Mem. Cold Spring Harb. N. Y.* 6, 153–167.

Paulsen, O., and Sejnowski, T. J. (2006). From invertebrate olfaction to human cognition: emerging computational functions of synchronized oscillatory activity. *J. Neurosci.* 26, 1661–1662. doi: 10.1523/jneurosci.3737-05a.2006

Prisco, G. V. D., Albo, Z., Vertes, R. P., and Kocsis, B. (2002). Discharge properties of neurons of the median raphe nucleus during hippocampal theta rhythm in the rat. *Exp. Brain Res.* 145, 383–394. doi: 10.1007/s00221-002-1123-1128

Rodríguez-Pallares, J., Caruncho, H. J., López-Real, A., Wójcik, S., Guerra, M. J., and Labandeira-García, J. L. (2001). Rat brain cholinergic, dopaminergic, noradrenergic and serotonergic neurons express GABAA receptors derived from the alpha3 subunit. *Receptor Channel* 7, 471–478.

Rossant, C., Kadir, S. N., Goodman, D. F. M., Schulman, J., Hunter, M. L. D., Saleem, A. B., et al. (2016). Spike sorting for large, dense electrode arrays. *Nat. Neurosci.* 19, 634–641. doi: 10.1038/nn.4268

Sakai, K., and Crochet, S. (2001). Differentiation of presumed serotonergic dorsal raphe neurons in relation to behavior and wake-sleep states. *Neuroscience* 104, 1141–1155. doi: 10.1016/s0306-45220100103-108

Sanda, P., Malerba, P., Jiang, X., Krishnan, G. P., Gonzalez-Martinez, J., Halgren, E., et al. (2020). Bidirectional interaction of hippocampal ripples and cortical slow waves leads to coordinated spiking activity during NREM sle ep. *Cereb. Cortex* 31, 324–340. doi: 10.1093/cercor/bhaa228

Szőnyi, A., Mayer, M. I., Cserép, C., Takács, V. T., Watanabe, M., Freund, T. F., et al. (2014). The ascending median raphe projections are mainly glutamatergic in the mouse forebrain. *Brain Structure Funct.* 221, 1–17. doi: 10.1007/s00429-014-0935-931

Szőnyi, A., Zichó, K., Barth, A. M., Gönczi, R. T., Schlingloff, D., Török, B., et al. (2019). Median raphe controls acquisition of negative experience in the mouse. *Science (New York, N.Y.)* 366:eaay8746. doi: 10.1126/science.aay8746

Vandecasteele, M., Varga, V., Berényi, A., Papp, E., Barthó, P., Venance, L., et al. (2014). Optogenetic activation of septal cholinergic neurons suppresses sharp wave ripples and enhances theta oscillations in the hippocampus. *Proc. Natl. Acad. Sci. U. S. A.* 111, 13535–13540. doi: 10.1073/pnas.1411233111

Vanderwolf, C. H. (1969). Hippocampal electrical activity and voluntary movement in the rat. *Electroen Clin. Neuro* 26, 407–418. doi: 10.1016/0013-46946990092-90093

Varga, V., Kocsis, B., and Sharp, T. (2003). Electrophysiological evidence for convergence of inputs from the medial prefrontal cortex and lateral habenula on single neurons in the dorsal raphe nucleus. *Eur. J. Neurosci.* 17, 280–286.

Varga, V., Losonczy, A., Zemelman, B. V., Borhegyi, Z., Nyiri, G., Domonkos, A., et al. (2009). Fast synaptic subcortical control of hippocampal circuits. *Science* 326, 449–453. doi: 10.1126/science.1178307

Varga, V., Sik, A., Freund, T. F., and Kocsis, B. (2002). GABA(B) receptors in the median raphe nucleus: distribution and role in the serotonergic control of hippocampal activity. *Neuroscience* 109, 119–132.

Varga, V., Székely, A. D., Csillag, A., Sharp, T., and Hajós, M. (2001). Evidence for a role of GABA interneurones in the cortical modulation of midbrain 5-hydroxytryptamine neurones. *Neuroscience* 106, 783–792.

Wang, D. V., Yau, H.-J., Broker, C. J., Tsou, J.-H., Bonci, A., and Ikemoto, S. (2015). Mesopontine median raphe regulates hippocampal ripple oscillation and memory consolidation. *Nat. Neurosci.* 18, 728–735. doi: 10.1038/nn.3998

Wang, R. Y., and Aghajanian, G. K. (1977). Physiological evidence for habenula as major link between forebrain and midbrain raphe. *Science* 197, 89–91.

Wang, X.-J. (2010). Neurophysiological and computational principles of cortical rhythms in cognition. *Physiol. Rev.* 90, 1195–1268. doi: 10.1152/physrev.00035.2008

Weissbourd, B., Ren, J., DeLoach, K. E., Guenthner, C. J., Miyamichi, K., and Luo, L. (2014). Presynaptic partners of dorsal raphe serotonergic and GABAergic neurons. *Neuron* 83, 645–662. doi: 10.1016/j.neuron.2014.06.024

Yger, P., Spampinato, G. L., Esposito, E., Lefebvre, B., Deny, S., Gardella, C., et al. (2018). A spike sorting toolbox for up to thousands of electrodes validated with ground truth recordings in vitro and in vivo. *eLife* 7:e34518. doi: 10.7554/elife.34518

Zhang, Y., Cao, L., Varga, V., Jing, M., Karadas, M., Li, Y., et al. (2021). Cholinergic suppression of hippocampal sharp-wave ripples impairs working memory. *Proc. Natl. Acad. Sci. U. S. A.* 118:e2016432118. doi: 10.1073/pnas.2016432118

Conflict of Interest: The authors declare that the research was conducted in the absence of any commercial or financial relationships that could be construed as a potential conflict of interest.

Publisher's Note: All claims expressed in this article are solely those of the authors and do not necessarily represent those of their affiliated organizations, or those of the publisher, the editors and the reviewers. Any product that may be evaluated in this article, or claim that may be made by its manufacturer, is not guaranteed or endorsed by the publisher.

frontiers in Neural Circuits

ORIGINAL RESEARCH
published: 26 January 2022
doi: 10.3389/fncir.2021.778022

Regulation of Hippocampal Gamma Oscillations by Modulation of Intrinsic Neuronal Excitability

*Alexander Klemz, Florian Wildner, Ecem Tütüncü and Zoltan Gerevich**

Institute of Neurophysiology, Charité—Universitätsmedizin, Berlin, Germany

Ion channels activated around the subthreshold membrane potential determine the likelihood of neuronal firing in response to synaptic inputs, a process described as intrinsic neuronal excitability. Long-term plasticity of chemical synaptic transmission is traditionally considered the main cellular mechanism of information storage in the brain; however, voltage- and calcium-activated channels modulating the inputs or outputs of neurons are also subjects of plastic changes and play a major role in learning and memory formation. Gamma oscillations are associated with numerous higher cognitive functions such as learning and memory, but our knowledge of their dependence on intrinsic plasticity is by far limited. Here we investigated the roles of potassium and calcium channels activated at near subthreshold membrane potentials in cholinergically induced persistent gamma oscillations measured in the CA3 area of rat hippocampal slices. Among potassium channels, which are responsible for the afterhyperpolarization in CA3 pyramidal cells, we found that blockers of SK ($K_{Ca}2$) and $K_V7.2/7.3$ (KCNQ2/3), but not the BK ($K_{Ca}1.1$) and IK ($K_{Ca}3.1$) channels, increased the power of gamma oscillations. On the contrary, activators of these channels had an attenuating effect without affecting the frequency. Pharmacological blockade of the low voltage-activated T-type calcium channels ($Ca_V3.1$–3.3) reduced gamma power and increased the oscillation peak frequency. Enhancement of these channels also inhibited the peak power without altering the frequency of the oscillations. The presented data suggest that voltage- and calcium-activated ion channels involved in intrinsic excitability strongly regulate the power of hippocampal gamma oscillations. Targeting these channels could represent a valuable pharmacological strategy against cognitive impairment.

Keywords: SK channel, BK channel, IK channel, KCNQ2, KCNQ3, Cav3, Cav3.2, Cav3.3

OPEN ACCESS

Edited by:
Gürsel Caliskan,
Otto von Guericke University Magdeburg, Germany

Reviewed by:
Oliver Kann,
Heidelberg University, Germany
Motoharu Yoshida,
Leibniz Institute for Neurobiology (LG), Germany

****Correspondence:***
Zoltan Gerevich
zoltan.gerevich@charite.de

Received: *16 September 2021*
Accepted: *21 December 2021*
Published: *26 January 2022*

Citation:
Klemz A, Wildner F, Tütüncü E and Gerevich Z (2022) Regulation of Hippocampal Gamma Oscillations by Modulation of Intrinsic Neuronal Excitability. Front. Neural Circuits 15:778022. doi: 10.3389/fncir.2021.778022

INTRODUCTION

The intrinsic excitability of a neuron describes the probability of action potential firing in response to synaptic inputs (Dunn and Kaczorowski, 2019). The magnitude of excitability is plastic and under ongoing modulation by voltage- and calcium-activated ion channels located directly at the input or output side of neurons, a phenomenon called intrinsic

plasticity (Kourrich et al., 2015; Debanne et al., 2019). Alongside its better-known counterpart synaptic plasticity, intrinsic plasticity is thought to play a major role in information processing, learning, and memory (Lisman et al., 2018). Reduction in baseline intrinsic excitability or disturbance in intrinsic plasticity has been linked to cognitive deficits in both normal aging and neuropsychiatric disorders such as Alzheimer's disease (Kaczorowski and Disterhoft, 2009; Eslamizade et al., 2015).

Several subthreshold voltage and calcium-activated channels are expressed in hippocampal neurons, open below the threshold of action potentials at around −55 mV and are thus able to modulate intrinsic excitability in hippocampal networks. Potassium channels activated by increases in the intracellular calcium concentration (K_{Ca}) have been shown to effectively modulate the firing patterns of neurons (King et al., 2015). Among them, the firstly described big-conductance K_{Ca} channel (BK, Slo1, or $K_{Ca}1.1$) is the only one that is also activated by voltage (Almássy and Nánási, 2019). It is expressed in the brain and contributes mainly to the repolarization phase of action potentials and the fast component of afterhyperpolarization (AHP; Contet et al., 2016). Three subtypes of the small conductance K_{Ca} channels (SK1-3 or $K_{Ca}2.1$-3) and one intermediate-conductance K_{Ca} (IK or $K_{Ca}3.1$) are known (Adelman et al., 2012). They are all voltage-independent, gated directly by submicromolar concentrations of intracellular Ca^{2+}, and rapidly modulate the intrinsic excitability of neurons mainly by generating the slower components of the AHP (Bond et al., 2005; Pedarzani and Stocker, 2008). Blockade of $K_{Ca}2$ channels with apamine has been shown to improve hippocampus-dependent learning in rodents (Deschaux et al., 1997; Stackman et al., 2002).

The voltage-activated Kv7 channels (KCNQ) also open at near resting membrane potential. Their slow gating kinetics, missing inactivation, and location at input and output sites of neurons make them ideal for controlling the intrinsic excitability and the output of neurons (Greene and Hoshi, 2017). The current through the Kv7.2/3 subtypes (KCNQ2/3) was originally described as the M-current because the channel is coupled to the muscarinic M1 and M3 receptors and activation of these Gq coupled receptors suppresses the current increasing neuronal excitability (Brown and Adams, 1980). Other Gq coupled receptors are also able to block KCNQ2/3 channels and depolarize the resting membrane potential, lower the threshold of action potentials and increase predominantly the slow component of the AHP (Shapiro, 2000; Delmas and Brown, 2005). Blockade of the KCNQ2/3 channels by ligands such as linopirdine or XE991 has been shown to have pro-cognitive/memory-enhancing effects in both animal models and humans (Chorvat et al., 1998; Gribkoff, 2003; Baculis et al., 2020).

T-type calcium channels (Cav3.1-3) are the only voltage-gated Ca^{2+} channels that are activated below the threshold (Weiss and Zamponi, 2019). They are expressed on both the dendrites and axon initial segments and are able to impact the intrinsic excitability of neurons efficiently. Loss-of-function mutations of T-type channels have been linked to autism spectrum disorder (Splawski et al., 2006), and schizophrenia (Andrade et al., 2016), and activation of the channel was shown to enhance long-term potentiation in cortical slices (Moriguchi et al., 2012) and memory-related behavior (Gangarossa et al., 2014; Yabuki et al., 2017; Fukunaga et al., 2019; Degawa et al., 2021; Yuan et al., 2021).

Gamma oscillations are rhythmic fluctuations of neuronal activity at frequencies from 30 to 90 Hz generated by a circuit containing feedback inhibitory inputs predominantly from parvalbumin-positive fast-spiking inhibitory interneurons providing perisomatic inhibition onto pyramidal cells (Bartos et al., 2001; Buzsáki and Wang, 2012). They are thought to play a key role in higher cognitive functions by supplying the background of information processing within and between brain areas (Womelsdorf and Fries, 2006) and their disturbances have been observed in a wide range of neuropsychiatric diseases with cognitive symptoms (Mably and Colgin, 2018), such as schizophrenia (Kwon et al., 1999; Hunt et al., 2017; Lemercier et al., 2017), autism (Grice et al., 2001; Casanova et al., 2020; Kayarian et al., 2020) and Alzheimer's disease (Ribary et al., 1991; Arroyo-García et al., 2021). The gamma oscillation generating circuit is connected by excitatory and inhibitory synapses; however, the firing and therefore synaptic output of the cells depend on the intrinsic excitability of the neurons involved in the circuit. While the synaptic components of the circuits and their modulation of gamma oscillations have been widely investigated in the last decades, the role of intrinsic plasticity remained much less examined. The goal of the present work was to explore which subthreshold activated ion channels, involved in intrinsic plasticity, are able to modulate cholinergically induced gamma oscillations in the hippocampus. Hyperpolarization-activated cyclic nucleotide-gated (HCN) channels were excluded from the study because their effect on gamma oscillations was intensively investigated in previous works (Fisahn et al., 2002, 2004; Boehlen et al., 2009; Pietersen et al., 2009; Neymotin et al., 2013).

METHODS AND MATERIALS

Animals and Slice Preparation

All animal procedures were conducted in accordance with the guidelines of the European Communities Council and the institutional guidelines approved by the Berlin Animal Ethics Committee (Landesamt für Gesundheit und Soziales Berlin, T0330/12). All studies involving animals are reported in accordance with the ARRIVE guidelines (du Sert et al., 2020).

For local field potential (LFP) recordings, Wistar rats of both sexes at an age of 5–9 weeks were anesthetized with isoflurane and then decapitated as described earlier (Schulz et al., 2012a; Lemercier et al., 2015). Their brains were quickly removed from the skull and submerged in ice-cold carbogenated (95% O_2, 5% CO_2) sucrose-based solution with an osmolality of ∼330 mOsm/kg of the following composition (in mM): NaCl, 80; $NaHCO_3$, 25; NaH_2PO_4, 1.25; KCl, 2.5; glucose, 25; sucrose, 85; $CaCl_2$, 0.5; MgCl, 3. Hippocampal slices were prepared by cutting the brain into 400 μm thick horizontal slices at an angle of 13° in fronto-occipital direction with a DTK-1000 vibratome (DSK, Dosaka, Japan) and immediately transferred to an

interface-type recording chamber perfused with carbogenated, warm (32–34°C) artificial cerebrospinal fluid (ACSF; flow rate of 1.6–1.7 ml/min; osmolality of ∼300 mOsm/kg) containing (in mM): NaCl, 129; NaH_2PO_4, 1.25; $NaHCO_3$, 21; glucose, 10; $MgSO_4$, 1.8; $CaCl_2$, 1.6; KCl, 3. Slices were left for recovery for at least 1 h before the beginning of recordings.

For patch clamp experiments, acute brain slices were obtained from 20- to 26-day-old male Wistar rats. Horizontal hippocampal slices (300 μm thick) were cut using a vibratome (Leica VT 1200, Leica Biosystems, Wetzlar, Germany). After preparation, slices were stored at 34°C in submerged condition for at least 30 min for recovery and kept at room temperature afterwards. The same sucrose-based solution as described above was used for slicing and storage.

Extracellular Recordings and Analysis

Measurement electrodes were put into glass pipettes filled with ACSF and then placed in the stratum pyramidale in CA3b of the hippocampus. LFPs were low-pass filtered at 1 kHz and digitized by a CED 1401 interface (Cambridge Electronic Design, Cambridge, UK) at 5 kHz (Klemz et al., 2021). Gamma oscillations were induced by bath application of acetylcholine (ACh, 10 μM) and the acetylcholine esterase inhibitor physostigmine (Phys; 2 μM; Schulz et al., 2012b). After stabilization of gamma oscillations, drugs were administered 100 min after induction for 60 min. Since induced gamma oscillations are not stable during long application times, time-matched control experiments without drug applications were carried out simultaneously with slices from the same animals.

Analysis of extracellular recordings was carried out by calculating power spectra every 2 min with a 120 s window throughout the whole recording (Meier et al., 2020). Peak power and peak frequency of the oscillations were extracted using a custom-made script for the Spike2 software (Cambridge Electronic Design, Cambridge, UK). Network activity was considered a gamma oscillation when the power spectrum had a peak between 30 and 80 Hz and the Q factor (peak frequency/half bandwidth) of the oscillation was supercritical (>0.5; Lemercier et al., 2017). Peak power and peak frequency were normalized to a 10-min window after 90 min of induction where oscillations were already stabilized. This period corresponds to the time immediately before drug application (90–100 min) or the time-matched period in control experiments. Normalized peak power and peak frequency of a 10-min window 60 min after drug application (150–160 min) were compared to time-matched control of the same time window. Data are presented as mean ± SEM. Statistical comparison was made using Student's *t*-test or ANOVA with a *post-hoc* test. The baseline activity for XE991 experiments was analyzed by creating power spectra of 10 min before the induction and after 160 min of bath application of XE991 and calculating the mean power (integral power divided by the number of bins) between 10 and 50 Hz. Since the power of LFP signals is log-normally distributed, mean power data are presented as geometric mean and statistically analyzed by Student's *t*-test of the logarithms. The significance level was set at $p < 0.05$.

Patch Clamp Recordings and Analysis

After the recovery period, slices were individually transferred to a submerged type recording chamber and continuously perfused at a flow rate of ∼5 ml/min with carbogenated ACSF containing (in mM): NaCl, 95; TEA-Cl, 25; $NaHCO_3$, 25; NaH_2PO_4, 1.25; KCl, 2.5; $CaCl_2$, 2; $MgCl_2$, 1; Glucose, 25 (osmolality 310 ± 5 mOsm/kg) at room temperature (22–24°C). For detection of calcium currents, tetrodotoxin (0.5 μM), picrotoxin (100 μM), 6-cyano-7-nitroquinoxaline-2,3-dione (CNQX, 10 μM), and D-(−)-2-amino-5-phosphonopentanoic acid (D-APV, 50 μM) were added to the external solution to block voltage-gated sodium channels, $GABA_A$ receptors, AMPA receptors, and NMDA receptors, respectively. Whole-cell patch clamp recordings were performed on CA1 pyramidal cells in voltage clamp mode. CA1 pyramidal cells were used for these experiments as a model, since they are less active spontaneously and express T-type channels similar to CA3 pyramidal cells (McKay et al., 2006). The developmental expression of the channels in the hippocampus peaks at around P21 and then declines at P60 (Aguado et al., 2016), enabling the investigation of younger animals in the patch clamp recordings. CA1 neurons were identified visually using infrared differential interference contrast microscopy of a Zeiss Axioskop (Carl Zeiss AG, Oberkochen, Germany). Patch electrodes were pulled from borosilicate glass capillaries (1.5 mm outer/0.86 mm inner diameter; Science Products, Hofheim, Germany) and had a resistance of 3–6 MΩ when filled with internal solution containing (in mM): CsCl, 115; TEA-Cl, 20; HEPES, 10; EGTA, 10; $MgCl_2$, 2; Na_2-ATP, 2; Na_2-GTP, 0.5; Na_2-phosphocreatin, 5; pH adjusted to 7.2 using CsOH, osmolality ∼300 mOsm/kg. Recordings were obtained using an EPC9 amplifier (HEKA, Heidelberg, Germany). Signals were low-pass filtered at 2.9 kHz using the amplifier's built-in 4-pole low-pass Bessel filter and digitized at 10 kHz. Series resistance was not corrected but monitored by application of a brief voltage step of −10 mV and recordings were discarded if they changed by more than 30%. Whole-cell capacitance was compensated during these recordings using the amplifier's automatic capacitance transient cancellation circuitry. Liquid junction potential was not corrected. PatchMaster and FitMaster software (HEKA, Heidelberg, Germany) were used for acquisition and analysis, respectively. To evoke voltage-gated calcium currents, cells were held at a membrane potential of −80 mV, and steps to depolarized voltages were applied. To separate low voltage-activated from high voltage-activated calcium currents, a two-step protocol with depolarizing voltage steps from −80 to −40 and subsequently from −40 to −10 mV was applied. Data were leak corrected by a P/4-protocol as described earlier (Chad and Eckert, 1986; Büsselberg et al., 1992). Values are given as mean ± SEM. If not stated differently, the significance of differences before and after drug application was assessed using paired Student's *t*-test. The differences were considered significant when $p < 0.05$.

Drugs

Physostigmine (Phys), NS309, NS6180, UCL1684, NS19504, Penitrem A, XE991, ICA110381, SAK3, and NNC55-0396,

CNQX, D-APV, and TTX were obtained from Tocris Bioscience (Bristol, UK). Acetylcholine (ACh) was purchased from Sigma-Aldrich (Taufkirchen, Germany), TTA-P2 from Alomone Labs (Jerusalem, Israel), picrotoxin from Abcam (Cambridge, UK). Drugs were dissolved in water or DMSO and further diluted with ACSF to achieve the respective drug concentrations. Final DMSO concentration was held below 0.02% or DMSO control experiments were carried out. We did not investigate the effect of DMSO on gamma oscillation power systematically; however, it is known that DMSO reduces neuronal excitability (Tamagnini et al., 2014), which can explain the lower normalized DMSO control values. In patch clamp experiments, the final DMSO concentration was 0.2%.

RESULTS

Activation of $K_{Ca}2$ Channels Inhibits and Blockade Increases Gamma Oscillations

We first investigated whether pharmacological manipulation of K_{Ca} channels can modulate gamma oscillations. Gamma oscillations were induced by bath application of acetylcholine (10 μM) and the acetylcholine esterase inhibitor physostigmine (2 μM) in the CA3 region of rat hippocampal slices. Peak power and frequency stabilized after about 80 min, enabling time-controlled pharmacological testing between slices. We applied activators and blockers of the different K_{Ca}-subtypes after 100 min of induction. The less selective activator of $K_{Ca}2$ and $K_{Ca}3.1$, NS309 (3 μM; 0.848 ± 0.078, n = 6), significantly decreased normalized gamma power compared to control (1.315 ± 0.077, n = 13; p = 0.0421; **Figures 1A,C,E**) suggesting that K_{Ca} channels are involved in hippocampal gamma oscillations. The peak frequency of the oscillations stayed unaffected (control: 0.992 ± 0.009; NS309: 1.014 ± 0.011; p = 0.664; **Figures 1A,F**). We then used more selective drugs to investigate the role of different K_{Ca} subtypes in more detail. NS6180 (1 μM), an antagonist of $K_{Ca}3.1$ channels, had no significant effect on either peak gamma power (control: 1.315 ± 0.077, n = 13; NS6180: 1.293 ± 0.237, n = 7, p = 0.990; **Figure 1E**) nor frequency (control: 0.992 ± 0.009; NS6180: 1.007 ± 0.025; p = 0.760; **Figure 1F**). In contrast, the $K_{Ca}2$ channel antagonist UCL1684 (0.1 μM) significantly increased peak gamma power (1.181 ± 0.100, n = 12; DMSO control: 0.966 ± 0.072, n = 8; p = 0.032; **Figures 1B,D,E**) without altering the frequency of the oscillations (1.030 ± 0.015; DMSO control: 1.014 ± 0.026; p = 0.858; **Figures 1B,F**), suggesting that $K_{Ca}2$ and not $K_{Ca}3.1$ channels are involved in the maintenance of cholinergic gamma oscillations. Finally, to complete our investigation of K_{Ca} we applied the $K_{Ca}1.1$ activator NS19504 (10 μM) and the $K_{Ca}1.1$ blocker Penitrem A (0.2 μM). Both ligands left gamma oscillations unaffected (power: DMSO control: 0.966 ± 0.072, n = 8; NS19504: 1.181 ± 0.100, n = 14, p = 0.565; Penitrem A: 1.117 ± 0.121, n = 10, p = 0.814; **Figure 1E**; frequency: DMSO control: 1.014 ± 0.026; NS19504: 1.020 ± 0.008, p = 0.988; Penitrem A: 0.992 ± 0.023, p = 0.767; **Figure 1F**). In conclusion, these results indicate that only $K_{Ca}2$ channels exert an influence over cholinergically induced gamma oscillations in the rat hippocampus. $K_{Ca}2$ activation decreases while blockade increases gamma oscillation power.

KCNQ2/3 Channel Activation Inhibits and Blockade Increases Gamma Oscillations

KCNQ2/3 (Kv7.2/3) channels are widely distributed in the hippocampus (Klinger et al., 2011) where they contribute to the control of neuronal excitability (Greene and Hoshi, 2017; Carver and Shapiro, 2019). Application of the KCNQ2/3 blocker XE991 (10 μM) strongly increased the peak power of fully developed oscillations (control: 1.315 ± 0.077, n = 13; XE991: 2.581 ± 0.658, n = 9; p = 0.009; **Figures 2A,C,D**) while the frequency did not change (control: 0.992 ± 0.009; XE991: 0.990 ± 0.030; p > 0.999; **Figures 2A,E**). ICA110381, a positive allosteric modulator of KCNQ2/3, applied at 30 μM harshly inhibited gamma oscillations and completely abolished them in six out of eight slices (0.039 ± 0.012; control: 1.315 ± 0.077, n = 13; p < 0.001; **Figures 2B–D**), which made the evaluation of the peak frequency unreliable (0.678 ± 0.0384; control: 0.992 ± 0.009; **Figures 2B,E**). Lower concentrations (10 and 1 μM) concentration-dependently decreased gamma power (control: 1.315 ± 0.077, n = 13; 10 μM: 0.121 ± 0.0481, n = 8, p = 0.019; 1 μM: 0.704 ± 0.156, n = 8, p > 0.381; **Figures 2C,D**) while the frequency was unchanged (control: 0.992 ± 0.009; 10 μM: 0.886 ± 0.063, p = 0.073; 1 μM: 0.995 ± 0.004, p > 0.999; **Figure 2E**). Since these results indicate that cholinergically induced gamma oscillations are highly dependent on KCNQ2/3 channels, we next tried to induce neuronal oscillations with XE991 (10 μM) in CA3. Bath application of the KCNQ2/3 blocker for up to 160 min neither induced gamma oscillations nor increased the baseline activity in the low gamma frequency range (baseline integral power: geometric mean: 0.064 μV^2; XE991: geometric mean: 0.058 μV^2, n = 7, p = 0.825; p = 0.825; **Figure 2F**) demonstrating that blockade of KCNQ2/3 channels alone is not sufficient to evoke synchronized oscillatory activity.

T-Type Calcium Channels Are Involved in Hippocampal Gamma Oscillations

Next we investigated the role of T-type calcium channels for cholinergic gamma oscillations in hippocampal slices. We applied $NiCl_2$, a blocker of T-type calcium channels, at a concentration of 0.5 mM which strongly reduced gamma power and in 8 out of 11 slices completely abolished it (0.138 ± 0.070; control: 1.401 ± 0.107, n = 13; p < 0.001; **Figures 3A,B,D**). The frequency decreased, however, the complete abolishment of oscillations in the majority of slices made the evaluation of peak frequency uncertain (0.845 ± 0.044; control: 0.946 ± 0.034; p = 0.088; **Figures 3A,C**). Therefore, we tested a lower concentration of 0.1 mM $NiCl_2$ and found a significant inhibition of gamma power (0.824 ± 0.149, n = 7; control: 1.401 ± 0.107, n = 13; p = 0.002; **Figures 3B,D**) with no significant alterations in oscillation frequency (1.002 ± 0.021; control: 0.946 ± 0.034; p = 0.406; **Figure 3C**).

Next, we asked whether the applied concentration of 0.5 mM $NiCl_2$ was selective for the T-type channels or other voltage-activated calcium channels were also blocked.

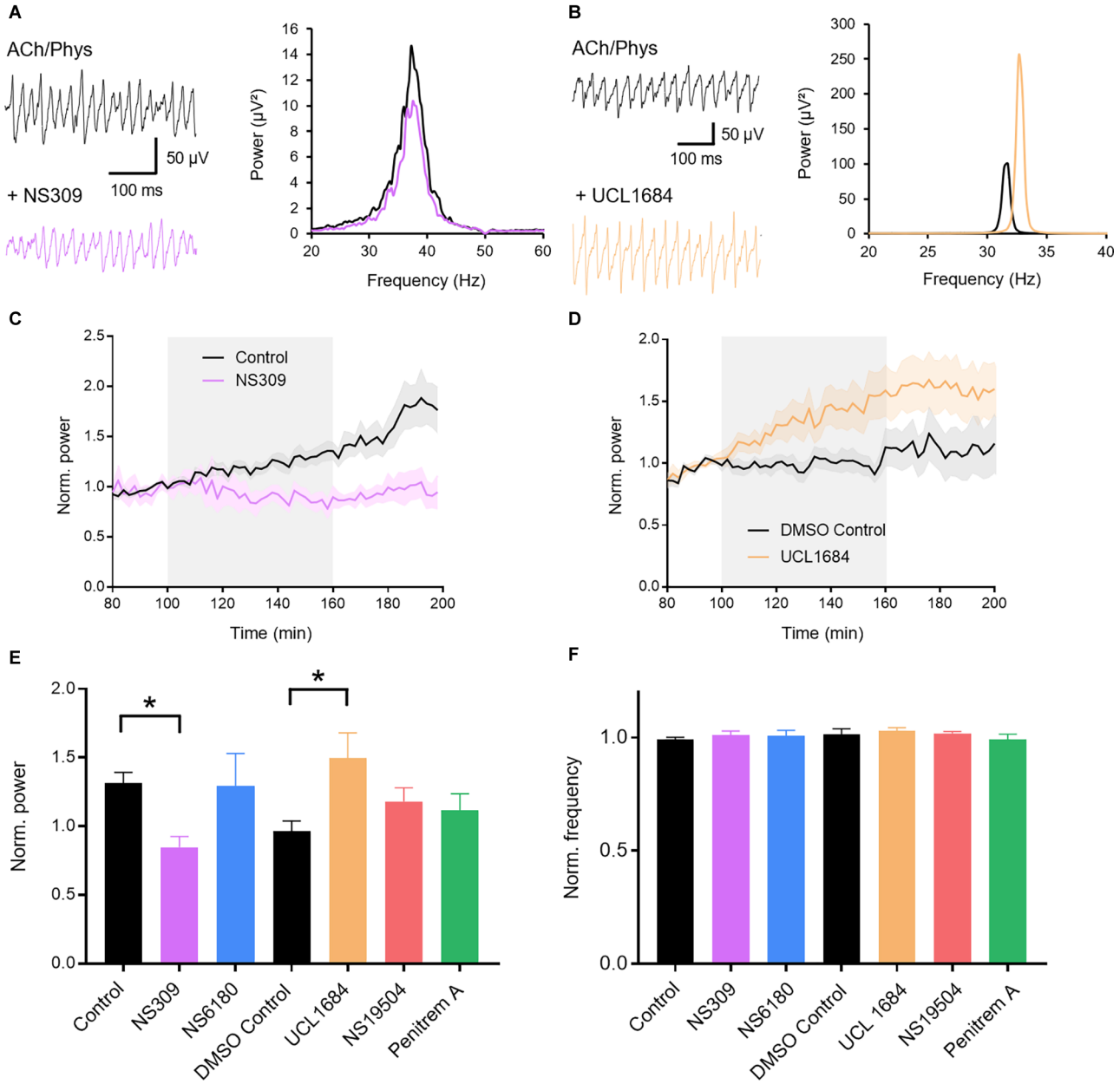

FIGURE 1 | Role of calcium-activated potassium channels (K_{Ca}) in hippocampal gamma oscillations. **(A)** Original traces (left) and power spectra (right) of cholinergic gamma oscillations before (black) and after (purple) bath application of the $K_{Ca}2$ and $K_{Ca}3.1$ activator NS309 (3 µM). **(B)** Original traces (left) and power spectra (right) of cholinergic gamma oscillations before (black) and after (orange) bath application of the $K_{Ca}2$ antagonist UCL1684 (0.1 µM). **(C)** Normalized gamma power before, during and after the application of NS309 (3 µM, gray area) in comparison to control. **(D)** Normalized gamma power over time around the application of UCL 1684 (0.1 µM, gray area) in comparison to control. **(E)** Effect of K_{Ca} activators and blockers on the normalized peak power of hippocampal gamma oscillations compared to time matched and solvent controls. Control: $n = 13$ slices, $N = 9$ animals; NS309 (3 µM): $n = 6$, $N = 3$, $p = 0.042$; NS6180 (1 µM): $n = 7$, $N = 3$, $p = 0.990$; DMSO control: $n = 8$, $N = 8$; UCL1684 (0.1 µM): $n = 12$, $N = 6$, $p = 0.032$; NS19504 (10 µM): $n = 14$, $N = 6$, $p = 0.565$; Penitrem A (0.2 µM): $n = 10$, $N = 5$, $p = 0.814$. See selectivity in "Results" section. **(F)** Effect of K_{Ca} activators and blockers on the normalized peak frequency of hippocampal gamma oscillations compared to time matched and solvent controls. NS309 (3 µM): $p = 0.664$; NS6180 (1 µM): $p = 0.760$; UCL1684 (0.1 µM): $p = 0.858$, NS19504 (10 µM): $p = 0.988$; Penitrem A (0.2 µM): $p = 0.767$. Recording temperature was between 32 and 34°C. Traces were lowpass filtered at 200 Hz and bandstop filtered at 50 Hz. Bars show mean ± SEM. *$p < 0.05$. ACh, acetylcholine; Phys, physostigmine.

Therefore, we evoked low voltage-activated calcium currents in CA1 pyramidal cells by voltage steps from −80 to −40 mV (**Figure 3E**) which correspond to the currents *via* T-type channels (**Figure 3E**). $NiCl_2$ (0.5 mM) significantly reduced these currents (910.9 ± 75.9 pA to 162.2 ± 17.89 pA, $p < 0.001$) without affecting the high voltage-activated currents evoked by a subsequent voltage step from −40 to −10 mV (682.3 ± 74.69 pA to 652.7 ± 76.52 pA, $p = 0.331$; **Figures 3E–H**). These

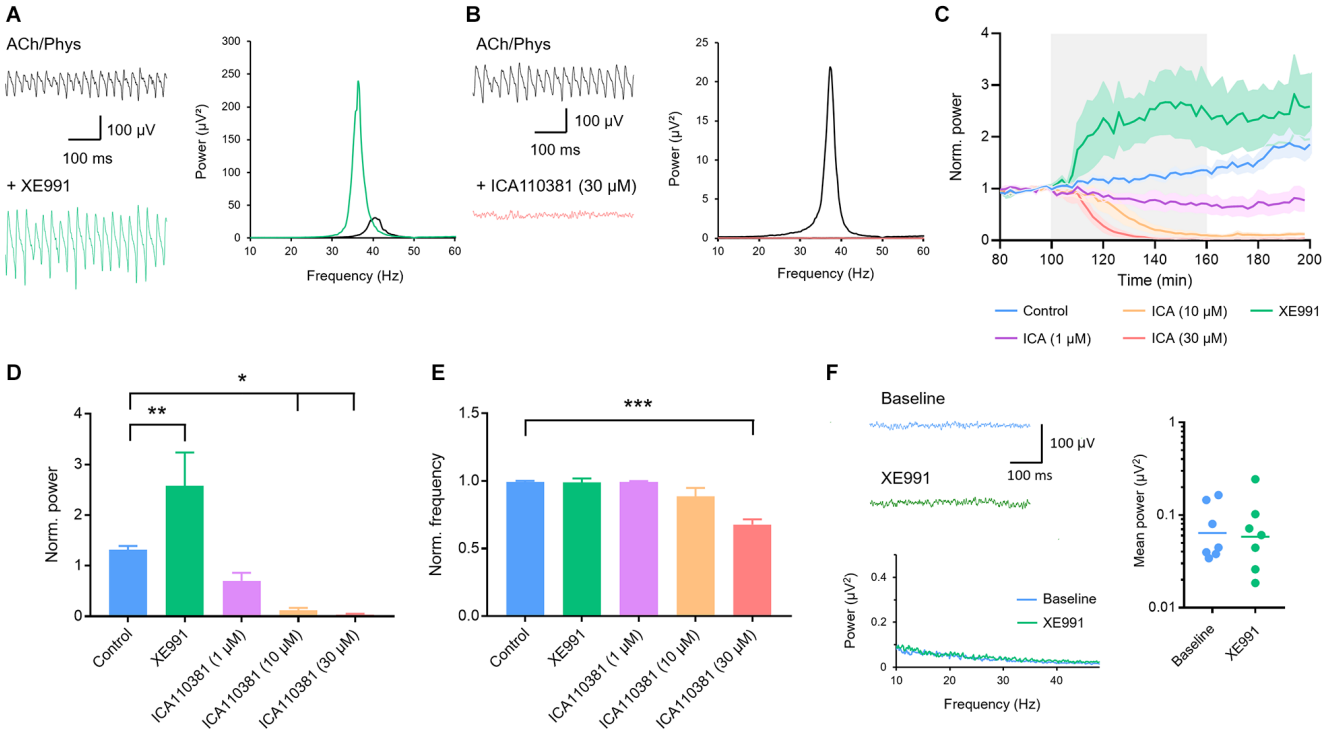

FIGURE 2 | Involvement of voltage-gated Kv7.2/3 (KCNQ2/3) channels in the modulation of hippocampal gamma oscillations. **(A)** Original traces (left) and power spectra (right) of cholinergically induced gamma oscillations before (black) and after (green) bath application of the KCNQ2/3 blocker XE991 (10 µM). **(B)** Original traces (left) and power spectra (right) of cholinergically induced gamma oscillations before (black) and after (red) bath application of the KCNQ2/3 positive allosteric modulator ICA110381 (30 µM). **(C)** Normalized gamma power before, during and after the application of XE991 (10 µM, green) and increasing concentrations of ICA110381 (1 µM; purple; 10 µM; orange; 30 µM red) compared to control (blue). The application of the drugs is highlighted in gray. **(D)** Effect of XE991 and ICA110381 on the normalized peak power of hippocampal gamma oscillations compared to control. Control (blue): $n = 13$ slices, $N = 9$ animals; XE991 (green): $n = 9$, $N = 4$, $p = 0.009$; ICA110381 1 µM: (purple): $n = 8$, $N = 5$, $p = 0.381$; 10 µM (orange): $n = 8$, $N = 4$, $p = 0.019$; 30 µM (red): $n = 8$, $N = 4$, $p = 0.011$. **(E)** Effect of XE991 and ICA110381 on the normalized peak frequency of hippocampal gamma oscillations compared to control. XE991 (green): $p > 0.999$; ICA110381 1 µM (purple): $p > 0.999$; 10 µM (orange): $p = 0.073$; 30 µM (red): $p < 0.001$. **(F)** Left, top: original traces of local field potentials (LFPs) before and after the application of XE991. Left, bottom: power spectra of LFPs before and after XE991 application. Right: scatter plot comparing the mean absolute power between 10 and 50 Hz before (baseline; blue) and after application of XE991 (green, $n = 7$, $p = 0.825$, bars show geometric mean). Recording temperature was between 34 and 36°C. Traces were lowpass filtered at 200 Hz and bandstop-filtered at 50 Hz. Bars show mean ± SEM. $^*p < 0.05$, $^{**}p < 0.01$, $^{***}p < 0.001$. ACh, acetylcholine; Phys, physostigmine.

results confirm that $NiCl_2$ at the applied concentration that inhibited gamma oscillations selectively blocked T-type calcium channels.

Further utilization of selective T-type channel ligands confirmed our findings with $NiCl_2$. The selective T-type blockers TTA-P2 (1 µM) and NNC55-0396 (100 µM) both significantly reduced gamma power (control: 1.401 ± 0.107, $n = 13$; TTA-P2: 0.895 ± 0.123, $n = 14$; $p = 0.005$; **Figures 4A,C,D**; NNC55-0396: 0.645 ± 0.096, $n = 6$, $p = 0.001$; **Figures 4C,D**) and increased oscillation frequency (control: 0.946 ± 0.034; TTA-P2: 1.049 ± 0.013, $p = 0.042$; NNC55-0396: 1.156 ± 0.072, $p = 0.001$; **Figure 4E**). The T-type activator SAK3 (0.1 µM) also significantly decreased gamma power (0.733 ± 0.057, $n = 10$, DMSO control: 0.966 ± 0.072, $n = 8$; $p = 0.020$; **Figures 4B,D**) with no effect on oscillation frequency (1.043 ± 0.014; DMSO control: 1.014 ± 0.026; $p = 0.306$; **Figures 4B,E**). In conclusion, these results suggest that subthreshold activated T-Type calcium channels regulate cholinergic gamma oscillations.

DISCUSSION

The present study was carried out to investigate which subthreshold activated channels are able to modulate gamma oscillations in the hippocampal CA3 area. These channels open by membrane voltage change below or around the threshold of action potentials or by an increase of intracellular calcium concentration and are important regulators of intrinsic neuronal excitability. Our results show for the first time that among these subthreshold channels, $K_{Ca}2$, Kv7.2/3, as well as T-type calcium channels can modulate the power and, in some cases, also the peak frequency of hippocampal gamma oscillations and herewith changes in neuronal networks. Since changes in gamma oscillation power may provide a disease biomarker to investigate novel therapies against cognitive impairment in diseases (Honda et al., 2020; Meier et al., 2020), the present data suggest that $K_{Ca}2$, KCNQ2/3, and T-type calcium channel modulators might be promising targets in these states.

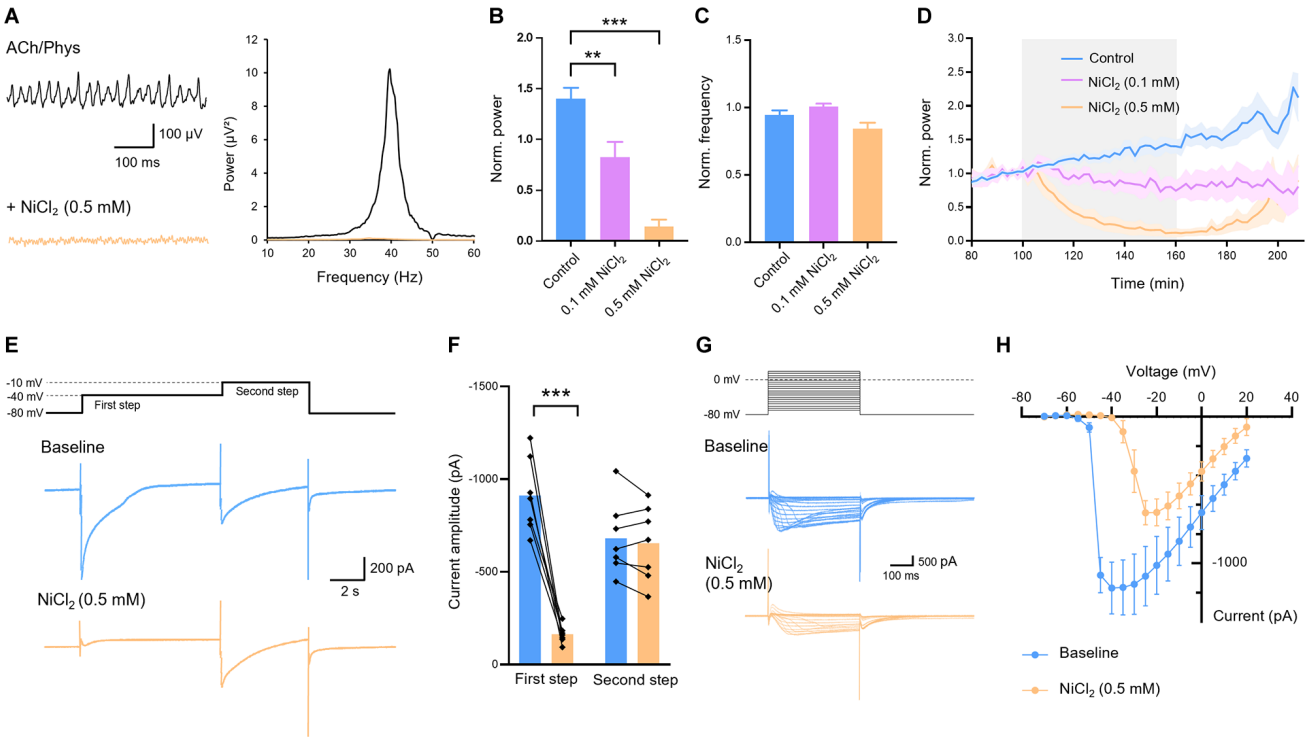

FIGURE 3 | Effect of T-Type calcium channel blocker nickel chloride ($NiCl_2$) on cholinergic gamma oscillations in the rat hippocampus. **(A)** Original traces (left) and power spectrum (right) of hippocampal gamma oscillations before (black) and after (orange) application of $NiCl_2$ (0.5 mM). Local field potential traces were lowpass filtered at 200 Hz and bandstop filtered at 50 Hz. **(B)** Normalized power of cholinergically induced gamma oscillations after bath application of $NiCl_2$ compared to control. Control (blue): $n = 13$ slices, $N = 9$ animals; $NiCl_2$ 0.1 mM (purple): $n = 7$, $N = 3$, $p = 0.002$; 0.5 mM (orange): $n = 11$, $N = 4$, $p < 0.001$. **(C)** Normalized frequency after application of $NiCl_2$ compared to control. $NiCl_2$0.1 mM (purple): $p = 0.406$; 0.5 mM (orange): $p = 0.088$. **(D)** Normalized power before, during and after bath application (gray) of different concentrations of $NiCl_2$ (0.1 mM, purple; 0.5 mM orange) compared to control (blue). **(E)** Low voltage- and high voltage-activated calcium currents recorded by a first depolarizing step from −80 to −40 mV and a second step from −40 to −10 mV, respectively, of the same cell before (blue) and after (orange) bath application of $NiCl_2$ (0.5 mM). **(F)** Amplitudes of low and high voltage-activated calcium currents evoked by the first and second step, respectively, before and after application of $NiCl_2$ (0.5 mM). First step: $p < 0.001$. Second step: $p = 0.331$; $n = 7$, $N = 4$, paired t-test. **(G)** Step protocol (above) and original traces of calcium currents (below) with voltage steps from −70 mV to +20 mV and holding potential of −80 mV before (blue) and after (orange) bath application of $NiCl_2$ (0.5 mM). **(H)** Amplitudes of calcium currents evoked by depolarizing steps as described in **(G)**. For LFP experiments recording temperature was between 34 and 36°C. Patch-clamp experiments were carried out at room temperature (22–24°C). Data shown as mean ± SEM. $^{**}p < 0.01$, $^{***}p < 0.001$. ACh, acetylcholine; Phys, physostigmine.

Since the postulate of Donald Hebb (Hebb, 1949) and the later discovery of long-term potentiation of synaptic transmission (Bliss and Lømo, 1973), activity-dependent changes in the strength of synapses were primarily thought to mediate memory storage in the brain. Therefore, investigation of synapses and the modulation of synaptic strength have dominated neuroscience research in the last decades. Accumulating evidence suggests, however, that synaptic plasticity is not the only neuronal change leading to the storage of information but global cellular properties such as intrinsic excitability of neurons and its plastic changes also play an important role in learning and memory (Disterhoft et al., 1986; Lisman et al., 2018). The plasticity of intrinsic excitability is like synaptic plasticity bi-directional and displays cell and input specificity (Debanne et al., 2019). It is mediated by ion channels located in dendrites, soma, and axon of the neuron able to modulate postsynaptic potentials, resting membrane potential, and action potential threshold, respectively.

The ion channels involved in these processes are heterogenous and predominantly activated by subthreshold voltage changes or increases in intracellular calcium concentration. Here, we investigated ion channels that are classically involved in intrinsic excitability in the CA3 area of the hippocampus. Increasing the intrinsic excitability by opening T-type channels or blocking potassium channels might increase the gamma power by reducing accommodation, enabling neurons to fire on more waves of an oscillation and promoting action potentials after perisomatic IPSPs (Traub et al., 2004). The power of *in vitro* gamma oscillations was shown to correlate well with *in vivo* gamma amplitudes and with cognitive functions of the test animals (Lu et al., 2011). K_{Ca} channels open by an increase of intracellular calcium concentration and effectively control the firing of neurons by pulling the membrane potential to the reversal potential of potassium (Pedarzani and Stocker, 2008; Adelman et al., 2012; Contet et al., 2016). The present study shows that selective blockade of $K_{Ca}2$ channels effectively increases the power of CA3 gamma oscillations evoked by cholinergic stimulation without noteworthy changes in the peak frequency. Since none of the selective activators and blockers

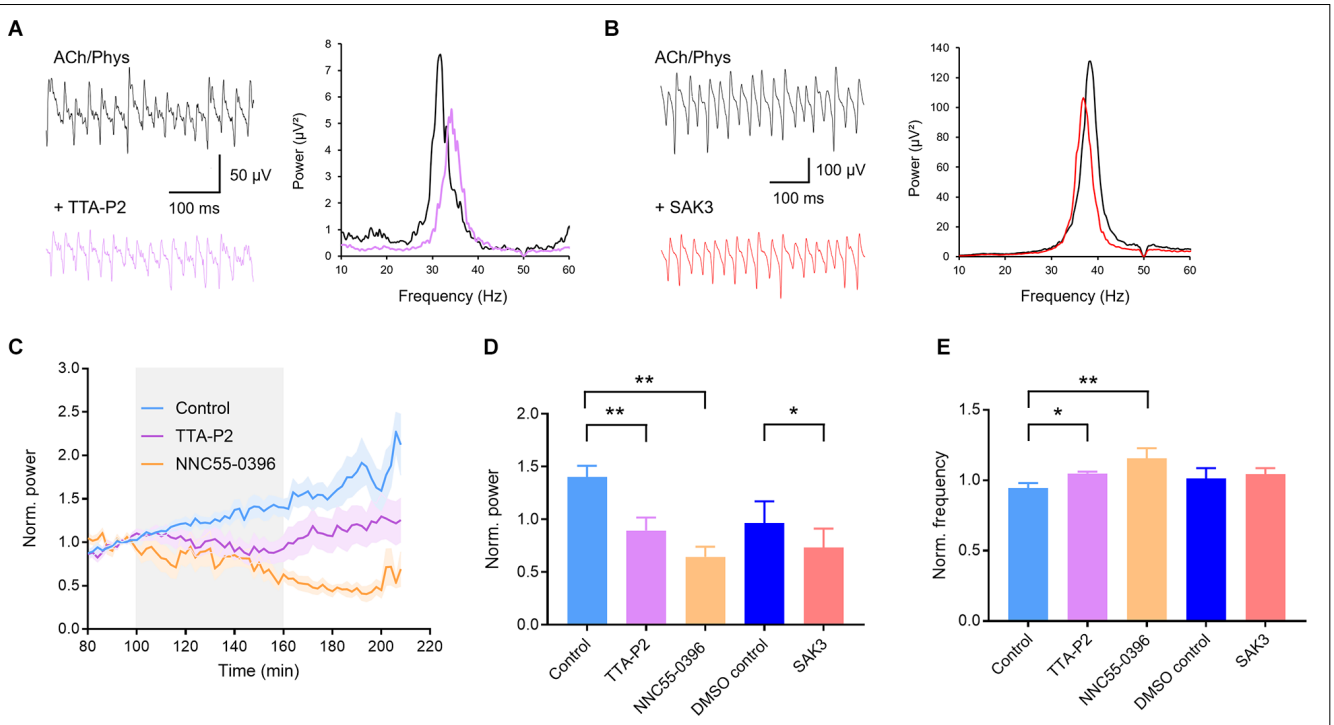

FIGURE 4 | Selective ligands of T-type calcium channels inhibit cholinergic gamma oscillations in rat hippocampal slices. **(A)** Original traces (left) and power spectra (right) of cholinergic gamma oscillations before (black) and after (purple) application of the selective T-type calcium channel blocker TTA-P2 (1 µM). **(B)** Original traces (left) and power spectra (right) of cholinergic gamma oscillations before (black) and after (red) application of the selective T-type calcium channel enhancer SAK3 (0.1 µM). **(C)** Normalized power before, during and after bath application (gray) of the selective T-type blocker TTA-P2 (1 µM, purple) and NNC55-0396 (100 µM, orange) compared to control (blue). **(D)** Effect of the T-type calcium channel blockers TTA-P2 and NNC55-0396 as well as the enhancer SAK3 on the power of hippocampal gamma oscillations compared to time matched and solvent control. Control (light blue): $n = 13$ slices, $N = 9$ animals; TTA-P2 (1 µM, purple): $n = 14$, $N = 6$, $p = 0.005$, NNC55-0396 (100 µM, orange): $n = 6$, $N = 2$, $p = 0.001$; DMSO control (dark blue): $n = 8$, $N = 7$; SAK3 (0.1 µM, red): $n = 10$, $N = 6$, $p = 0.020$. **(E)** Effect of the T-type calcium channel blockers TTA-P2 and NNC55-0396 as well as the enhancer SAK3 on the peak frequency of hippocampal gamma oscillations compared to time matched and solvent control. TTA-P2 (1 µM, purple): $p = 0.042$; NNC55-0396 (100 µM, orange): $p = 0.001$; SAK3 (0.1 µM, red): $p = 0.306$. Recording temperature was between 34 and 36°C. Traces were lowpass filtered at 200 Hz and bandstop filtered at 50 Hz. Bars show mean ± SEM. $^*p < 0.05$, $^{**}p < 0.01$. ACh, acetylcholine; Phys, physostigmine.

of $K_{Ca}1.1$ and $K_{Ca}3.1$ channels affected gamma network activity it can be concluded that among all K_{Ca} channels only the $K_{Ca}2$ channels had a gamma modulatory effect. $K_{Ca}2$ channels are expressed on CA3 pyramidal cells (Sailer et al., 2002) and are besides KCNQ2/3 channels the only K_{Ca} channel subtype that is involved in AHPs of medium duration (mAHP) in these neurons (Storm, 1989; Sailer et al., 2002). Although $K_{Ca}3.1$ channel proteins were found in the hippocampus (Turner et al., 2015), transcriptome and electrophysiological data suggest that they are not expressed in hippocampal cells and are not involved in the AHPs of pyramidal cells (Zeisel et al., 2015; Wang et al., 2016). The expression of $K_{Ca}1.1$ channels in the hippocampus is ambiguous. While the channel was not found on somata and dendrites of pyramidal cells (Hu et al., 2001; Misonou et al., 2006; Sailer et al., 2006) it was shown to be involved in the repolarization of APs (Hu et al., 2001). Although the channel was found presynaptically on pyramidal cells (Misonou et al., 2006) and is suggested to decrease neurotransmitter release (Contet et al., 2016), axon terminal APs were not affected by channel blockers (Hu et al., 2001). Fast-spiking interneurons, involved in gamma oscillations, do not express $K_{Ca}1.1$ channels (Erisir et al., 1999; Casale et al., 2015). Additionally, they are the only type of K_{Ca} channels which need membrane depolarization for opening and they have a lower Ca^{2+} activation affinity compared to $K_{Ca}2$ and $K_{Ca}3.1$ channels (Contet et al., 2016). Thus, for their opening $K_{Ca}1.1$ channels need a coincident membrane depolarization and a relatively strong intracellular Ca^{2+} influx very close (ca. 10–50 nm; Contet et al., 2016) to the channels, a condition, which might not be given during gamma oscillations. Additionally, whether they inhibit or excite network activity (and decrease or increase neurotransmitter release) depends on the specific β subunits of the channel which have different kinetics and thus determine whether the channel speeds up the repolarization phase of the AP (β2; increasing the firing rate) or take part in the AHP (β4: decreasing firing; Contet et al., 2016). Taken together, $K_{Ca}1.1$ channels seem to take part in the stabilization of network activity by getting activated by cumulated higher intracellular Ca^{2+} concentrations, which might explain their role in pathological processes in the brain such as epilepsy (Zhu et al., 2018). Our data, however, suggest that they don't play a role in physiological network activity such as gamma oscillations.

Blockers of $K_{Ca}2$ channels were shown to improve learning (Deschaux et al., 1997; Deschaux and Bizot, 2005; Kushwah

et al., 2018), especially hippocampus-dependent spatial memory (Ikonen and Riekkinen, 1999; Stackman et al., 2002) and contextual fear memory (Vick IV et al., 2010). In contrast, overexpression of the $K_{Ca}2.2$ channel severely impaired hippocampal-dependent spatial learning and memory (Hammond et al., 2006). Our results underscore these behavioral studies and suggest that $K_{Ca}2$ channels might influence learning and memory by their role in gamma oscillations.

The voltage-dependent Kv7.2/3 (KCNQ2/3) potassium channels open already close to the resting membrane potential and determine herewith effectively the excitability and output of neurons (Greene and Hoshi, 2017). They are expressed in hippocampal pyramidal cells, generate mAHP (Storm, 1989), and are inhibited by activation of muscarinic M1 and M3 receptors (Brown and Adams, 1980). Therefore, Kv7.2/3 channels might be involved in gamma oscillations evoked by cholinergic stimulation. Our results indicate that blockade of the channels by XE991 effectively increases cholinergically induced gamma oscillations while the activator ICA110381 concentration-dependently attenuates them, suggesting that the inhibition of the M-type current is involved in the generation or maintenance of cholinergic gamma oscillations. However, although XE991 was able to further potentiate fully developed gamma oscillations it was not able to evoke synchronized activity when applied alone and we did not measure a significant increase of neuronal activity in the low gamma frequency range. This finding indicates that although the blockade of KCNQ2/3 channels is involved in the maintenance of cholinergically induced gamma oscillations, other muscarinic or nicotinic mechanisms must also be involved such as inhibition of $K_{Ca}2$ channels (Buchanan et al., 2010) or activating a non-selective, presumably TRPC-based cation conductance (Yan et al., 2009). KCNQ channels seem not to affect the frequency since a decrease of the peak frequency was only observed when gamma oscillations were strongly or completely inhibited. Similar to our findings, KCNQ2/3 channel activators abolished or inhibited also kainate- or histamine-induced gamma oscillations (Boehlen et al., 2009, 2013; Andersson et al., 2017) indicating that KCNQ2/3 channels are not only involved in cholinergically evoked oscillations. Interestingly, XE991 was found to reduce the power of kainate-induced oscillations probably by loss of the periodicity of the increased firing of pyramidal cells (Boehlen et al., 2009; Leão et al., 2009) suggesting that the effect of the KCNQ2/3 blockers might depend on other channels affecting intrinsic excitability. In behavioral studies, inhibition of the M-current was shown to enhance learning and memory (Fontán-Lozano et al., 2011) and its suppression to be critical for memory consolidation (Kosenko et al., 2020), although the involvement of the KCNQ2/3 channels in memory is controversially discussed (Peters et al., 2005; Cavaliere et al., 2013; Li et al., 2014). Our results show that blockade of the M-current increases the power of hippocampal gamma oscillations induced by acetylcholine and suggest that this network mechanism might underlie the cognitive enhancing effects of KCNQ2/3 channel inhibitors.

The present study is to our knowledge the first that investigated the involvement of T-type calcium channels in gamma oscillations. T-type channels are low-voltage-activated channels that open near the foot of an action potential and play an important role in the generation of the afterdepolarizing potential and burst firing in CA3 pyramidal neurons, resulting in increased excitability of the cells (Xu and Clancy, 2008). Thus, the opening of these channels during cholinergic stimulation could be involved in the generation or maintenance of gamma oscillations. However, an enhanced calcium influx through an exogenous opening of T-type calcium channels, as seen after the application of SAK3, might activate K_{Ca} channels terminating the excitability of cells (Xu and Clancy, 2008) within the gamma circuit and decrease the power. Our results also show that a blockade of T-type channels increases the peak frequency of oscillations. The frequency of gamma oscillations can be modulated (increased) by the following mechanisms (Bartos et al., 2002; Jadi and Sejnowski, 2014): (a) shorter perisomatic inhibitory synaptic inputs; (b) reduced conduction delay in the gamma circuit; (c) decreased total inhibition on neurons of the circuit; and (d) reduced spacing between neurons (smaller network). Hippocampal interneurons express T-type channels more prominently compared to the cortex (McKay et al., 2006; Vinet and Sík, 2006; Aguado et al., 2016). Additionally, the downstream effect of T-type channels within individual cells might depend on the cellular and sub-cellular expression and activation state of K_{Ca} channels. Considering this, we can speculate that a blockade of T-type channels might affect interneurons stronger than pyramidal cells generating a decreased global inhibition of neurons within the network and an increase of the frequency.

Initially, low-voltage-activated T-type calcium channels were implicated in the synchronization of the thalamocortical circuit during sleep, absence seizures, and in peripheral and central pain transmission (Cheong and Shin, 2013). Later results, however, lead to the assumption that the channels might also be involved in higher cognitive functions, and both blockers and positive modulators were demonstrated to have pro-cognitive effects. Z944, an antagonist of the T-type channels, not only decreased seizure severity in a genetic rat model of absence epilepsy (Tringham et al., 2012) but also reversed learning and memory impairments (Marks et al., 2016, 2020). Similarly, the T-type channel enhancer SAK3 prevented cognitive impairment in different disease states and models such as hypothyroidism, ischemia, and AD models (Yabuki et al., 2017; Husain et al., 2018; Yuan et al., 2021) and showed beneficial effects in an animal model of intellectual disability syndrome (Dhanalakshmi et al., 2021). In addition, further studies suggest that enhancing these channels might have a pro-cognitive potential. Age-related downregulation of the channel mediated amyloid beta production (Rice et al., 2014) and SAK3 inhibited this in amyloid precursor protein transgenic animals (Xu et al., 2018). Moreover, T-type channel ($Ca_v3.2$) lacking mice were shown to have impaired memory (Gangarossa et al., 2014). Our results demonstrating that T-type channels participate in gamma oscillations are in agreement with these studies and suggest that modulation of gamma oscillations might represent at least one working mechanism of how pharmacological manipulation of T-type channels alters higher cognitive tasks. However, since both the used blockers and enhancers inhibited hippocampal

gamma oscillations, our data cannot help to answer the question whether a blockade or an opening of the channel is the preferential therapeutic strategy. Further studies are needed to assess the role of T-Type channels in synchronized network activity.

In conclusion, the present study investigated for the first time the role of K_{Ca} and T-type calcium channels in cholinergically evoked gamma oscillations. The presented data demonstrate that $K_{Ca}2$ and T-type calcium channels are strongly involved in the modulation of gamma network activity and represent, besides KCNQ2/3 channels, effective pharmacological or genetic targets to increase the power of hippocampal gamma oscillations. Since gamma oscillations are associated with learning and memory, their rare positive modulators represent potential agents to treat cognitive impairment in different disease states.

DATA AVAILABILITY STATEMENT

The raw data supporting the conclusions of this article will be made available by the authors on request, without undue reservation.

ETHICS STATEMENT

The animal study was reviewed and approved by Landesamt für Gesundheit und Soziales (LAGeSo) Berlin, Turmstraße 21, 10559 Berlin, Germany.

AUTHOR CONTRIBUTIONS

AK and ET performed the LFP experiments and analyzed the results. FW conducted the patch clamp recordings and analyzed the data. ZG designed the experiments, analyzed and interpreted the data. AK, FW, and ZG drafted the manuscript. All authors contributed to the article and approved the submitted version.

ACKNOWLEDGMENTS

We thank Richard Kovács, Jörg R. P. Geiger, and Michael D. Hadler for their critical comments on the study and/or the manuscript.

REFERENCES

Adelman, J. P., Maylie, J., and Sah, P. (2012). Small-conductance Ca 2+-activated K + channels: form and function. *Annu. Rev. Physiol.* 74, 245–269. doi: 10.1146/annurev-physiol-020911-153336

Aguado, C., García-Madrona, S., Gil-Minguez, M., and Luján, R. (2016). Ontogenic changes and differential localization of T-type Ca2+ channel subunits Cav3.1 and Cav3.2 in mouse hippocampus and cerebellum. *Front. Neuroanat.* 10:83. doi: 10.3389/fnana.2016.00083

Almássy, J., and Nánási, P. P. (2019). Brief structural insight into the allosteric gating mechanism of BK (Slo1) channel. *Can. J. Physiol. Pharmacol.* 97, 498–502. doi: 10.1139/cjpp-2018-0516

Andersson, R., Galter, D., Papadia, D., and Fisahn, A. (2017). Histamine induces KCNQ channel-dependent gamma oscillations in rat hippocampus *via* activation of the H1 receptor. *Neuropharmacology* 118, 13–25. doi: 10.1016/j.neuropharm.2017.03.003

Andrade, A., Hope, J., Allen, A., Yorgan, V., Lipscombe, D., and Pan, J. Q. (2016). A rare schizophrenia risk variant of CACNA1I disrupts CaV3.3 channel activity. *Sci. Rep.* 6:34233. doi: 10.1038/srep34233

Arroyo-García, L. E., Isla, A. G., Andrade-Talavera, Y., Balleza-Tapia, H., Loera-Valencia, R., Alvarez-Jimenez, L., et al. (2021). Impaired spike-gamma coupling of area CA3 fast-spiking interneurons as the earliest functional impairment in the AppNL-G-F mouse model of Alzheimer's disease. *Mol. Psychiatry* 1–11. doi: 10.1038/s41380-021-01257-0. [Online ahead of print].

Baculis, B. C., Zhang, J., and Chung, H. J. (2020). The role of Kv7 channels in neural plasticity and behavior. *Front. Physiol.* 11:568667. doi: 10.3389/fphys.2020.568667

Bartos, M., Vida, I., Frotscher, M., Geiger, J. R. P., and Jonas, P. (2001). Rapid signaling at inhibitory synapses in a dentate gyrus interneuron network. *J. Neurosci.* 21, 2687–2698. doi: 10.1523/JNEUROSCI.21-08-02687.2001

Bartos, M., Vida, I., Frotscher, M., Meyer, A., Monyer, H., Geiger, J. R. P., et al. (2002). Fast synaptic inhibition promotes synchronized gamma oscillations in hippocampal interneuron networks. *Proc. Natl. Acad. Sci. U S A* 99, 13222–13227. doi: 10.1073/pnas.192233099

Bliss, T. V. P., and Lømo, T. (1973). Long-lasting potentiation of synaptic transmission in the dentate area of the anaesthetized rabbit following stimulation of the perforant path. *J. Physiol.* 232, 331–356. doi: 10.1113/jphysiol.1973.sp010273

Boehlen, A., Kunert, A., and Heinemann, U. (2009). Effects of XE991, retigabine, losigamone and ZD7288 on kainate-induced theta-like and gamma network oscillations in the rat hippocampus *in vitro*. *Brain Res.* 1295, 44–58. doi: 10.1016/j.brainres.2009.08.031

Boehlen, A., Schwake, M., Dost, R., Kunert, A., Fidzinski, P., Heinemann, U., et al. (2013). The new KCNQ2 activator 4-Chlor-N-(6-chlor-pyridin-3-yl)-benzamid displays anticonvulsant potential. *Br. J. Pharmacol.* 168, 1182–1200. doi: 10.1111/bph.12065

Bond, C. T., Maylie, J., and Adelman, J. P. (2005). SK channels in excitability, pacemaking and synaptic integration. *Curr. Opin. Neurobiol.* 15, 305–311. doi: 10.1016/j.conb.2005.05.001

Brown, D. A., and Adams, P. R. (1980). Muscarinic suppression of a novel voltage-sensitive K+ current in a vertebrate neurone. *Nature* 283, 673–676. doi: 10.1038/283673a0

Buchanan, K. A., Petrovic, M. M., Chamberlain, S. E. L., Marrion, N. V., and Mellor, J. R. (2010). Facilitation of long-term potentiation by muscarinic M(1) receptors is mediated by inhibition of SK channels. *Neuron* 68, 948–963. doi: 10.1016/j.neuron.2010.11.018

Büsselberg, D., Michael, D., Evans, M. L., Carpenter, D. O., and Haas, H. L. (1992). Zinc (Zn2+) blocks voltage gated calcium channels in cultured rat dorsal root ganglion cells. *Brain Res.* 593, 77–81. doi: 10.1016/0006-8993(92)91266-h

Buzsáki, G., and Wang, X.-J. (2012). Mechanisms of gamma oscillations. *Annu. Rev. Neurosci.* 35, 203–225. doi: 10.1146/annurev-neuro-062111-150444

Carver, C. M., and Shapiro, M. S. (2019). Gq-coupled muscarinic receptor enhancement of KCNQ2/3 channels and activation of TRPC channels in multimodal control of excitability in dentate gyrus granule cells. *J. Neurosci.* 39, 1566–1587. doi: 10.1523/JNEUROSCI.1781-18.2018

Casale, A. E., Foust, A. J., Bal, T., and McCormick, D. A. (2015). Cortical interneuron subtypes vary in their axonal action potential properties. *J. Neurosci.* 35, 15555–15567. doi: 10.1523/JNEUROSCI.1467-13.2015

Casanova, M. F., Shaban, M., Ghazal, M., El-Baz, A. S., Casanova, E. L., Opris, I., et al. (2020). Effects of transcranial magnetic stimulation therapy on evoked and induced gamma oscillations in children with autism spectrum disorder. *Brain Sci.* 10:423. doi: 10.3390/brainsci10070423

Cavaliere, S., Malik, B. R., and Hodge, J. J. L. (2013). KCNQ channels regulate age-related memory impairment. *PLoS One* 8:62445. doi: 10.1371/journal.pone.0062445

Chad, J. E., and Eckert, R. (1986). An enzymatic mechanism for calcium current inactivation in dialysed Helix neurones. *J. Physiol.* 378, 31–51. doi: 10.1113/jphysiol.1986.sp016206

Cheong, E., and Shin, H. S. (2013). T-type Ca2+ channels in normal and abnormal brain functions. *Physiol. Rev.* 93, 961–992. doi: 10.1152/physrev.00010.2012

Chorvat, R. J., Zaczek, R., and Brown, B. S. (1998). Ion channel modulators that enhance acetylcholine release: potential therapies for Alzheimer's disease. *Expert Opin. Invest. Drugs* 7, 499–518. doi: 10.1517/13543784.7.4.499

Contet, C., Goulding, S. P., Kuljis, D. A., and Barth, A. L. (2016). BK Channels in the Central Nervous System. *Int. Rev. Neurobiol.* 128, 281–342. doi: 10.1016/bs.irn.2016.04.001

Debanne, D., Inglebert, Y., and Russier, M. (2019). Plasticity of intrinsic neuronal excitability. *Curr. Opin. Neurobiol.* 54, 73–82. doi: 10.1016/j.conb.2018.09.001

Degawa, T., Kawahata, I., Izumi, H., Shinoda, Y., and Fukunaga, K. (2021). T-type Ca2+ channel enhancer SAK3 administration improves the BPSD-like behaviors in AppNL−G-F/NL−G-F knock-in mice. *J. Pharmacol. Sci.* 146, 1–9. doi: 10.1016/j.jphs.2021.02.006

Delmas, P., and Brown, D. A. (2005). Pathways modulating neural KCNQ/M (Kv7) potassium channels. *Nat. Rev. Neurosci.* 6, 850–862. doi: 10.1038/nrn1785

Deschaux, O., and Bizot, J. C. (2005). Apamin produces selective improvements of learning in rats. *Neurosci. Lett.* 386, 5–8. doi: 10.1016/j.neulet.2005.05.050

Deschaux, O., Bizot, J. C., and Goyffon, M. (1997). Apamin improves learning in an object recognition task in rats. *Neurosci. Lett.* 222, 159–162. doi: 10.1016/s0304-3940(97)13367-5

Dhanalakshmi, C., Janakiraman, U., Moutal, A., Fukunaga, K., Khanna, R., and Nelson, M. A. (2021). Evaluation of the effects of the T-type calcium channel enhancer SAK3 in a rat model of TAF1 deficiency. *Neurobiol. Dis.* 149:105224. doi: 10.1016/j.nbd.2020.105224

Disterhoft, J. F., Coulter, D. A., and Alkon, D. L. (1986). Conditioning-specific membrane changes of rabbit hippocampal neurons measured *in vitro*. *Proc. Natl. Acad. Sci. U S A* 83, 2733–2737. doi: 10.1073/pnas.83.8.2733

du Sert, N. P., Ahluwalia, A., Alam, S., Avey, M. T., Baker, M., Browne, W. J., et al. (2020). Reporting animal research: explanation and elaboration for the arrive guidelines 2.0. *PLoS Biol.* 18:e3000411. doi: 10.1371/journal.pbio.3000411

Dunn, A. R., and Kaczorowski, C. C. (2019). Regulation of intrinsic excitability: roles for learning and memory, aging and Alzheimer's disease and genetic diversity. *Neurobiol. Learn. Mem.* 164:107069. doi: 10.1016/j.nlm.2019.107069

Erisir, A., Lau, D., Rudy, B., and Leonard, C. S. (1999). Function of specific K(+) channels in sustained high-frequency firing of fast-spiking neocortical interneurons. *J. Neurophysiol.* 82, 2476–2489. doi: 10.1152/jn.1999.82.5.2476

Eslamizade, M. J., Saffarzadeh, F., Mousavi, S. M. M., Meftahi, G. H., Hosseinmardi, N., Mehdizadeh, M., et al. (2015). Alterations in ca1 pyramidal neuronal intrinsic excitability mediated by iH channel currents in a rat model of amyloid beta pathology. *Neuroscience* 305, 279–292. doi: 10.1016/j.neuroscience.2015.07.087

Fisahn, A., Contractor, A., Traub, R. D., Buhl, E. H., Heinemann, S. F., and McBain, C. J. (2004). Distinct roles for the kainate receptor subunits GluR5 and GluR6 in kainate-induced hippocampal gamma oscillations. *J. Neurosci.* 24, 9658–9668. doi: 10.1523/JNEUROSCI.2973-04.2004

Fisahn, A., Yamada, M., Duttaroy, A., Gan, J. W., Deng, C. X., McBain, C. J., et al. (2002). Muscarinic induction of hippocampal gamma oscillations requires coupling of the M1 receptor to two mixed cation currents. *Neuron* 33, 615–624. doi: 10.1016/s0896-6273(02)00587-1

Fontán-Lozano, Á., Suárez-Pereira, I., Delgado-García, J. M., and Carrión, Á. M. (2011). The M-current inhibitor XE991 decreases the stimulation threshold for long-term synaptic plasticity in healthy mice and in models of cognitive disease. *Hippocampus* 21, 22–32. doi: 10.1002/hipo.20717

Fukunaga, K., Izumi, H., Yabuki, Y., Shinoda, Y., Shioda, N., and Han, F. (2019). Alzheimer's disease therapeutic candidate SAK3 is an enhancer of T-type calcium channels. *J. Pharmacol. Sci.* 139, 51–58. doi: 10.1016/j.jphs.2018.11.014

Gangarossa, G., Laffray, S., Bourinet, E., and Valjent, E. (2014). T-type calcium channel Cav3.2 deficient mice show elevated anxiety, impaired memory and reduced sensitivity to psychostimulants. *Front. Behav. Neurosci.* 8:92. doi: 10.3389/fnbeh.2014.00092

Greene, D. L., and Hoshi, N. (2017). Modulation of Kv7 channels and excitability in the brain. *Cell. Mol. Life Sci.* 74, 495–508. doi: 10.1007/s00018-016-2359-y

Gribkoff, V. K. (2003). The therapeutic potential of neuronal KCNQ channel modulators. *Expert Opin. Ther. Targets* 7, 737–748. doi: 10.1517/14728222.7.6.737

Grice, S. J., Spratling, M. W., Karmiloff-Smith, A., Halit, H., Csibra, G., de Haan, M., et al. (2001). Disordered visual processing and oscillatory brain activity in autism and Williams syndrome. *Neuroreport* 12, 2697–2700. doi: 10.1097/00001756-200108280-00021

Hammond, R. S., Bond, C. T., Strassmaier, T., Ngo-Anh, T. J., Adelman, J. P., Maylie, J., et al. (2006). Small-conductance Ca2+-activated K+ channel type 2 (SK2) modulates hippocampal learning, memory and synaptic plasticity. *J. Neurosci.* 26, 1844–1853. doi: 10.1523/JNEUROSCI.4106-05.2006

Hebb, D. (1949). *The Organization of Behavior: A Neuropsychological Theory*. New York: Wiley & Sons.

Honda, S., Matsumoto, M., Tajinda, K., and Mihara, T. (2020). Enhancing clinical trials through synergistic gamma power analysis. *Front. Psychiatry* 11:537. doi: 10.3389/fpsyt.2020.00537

Hu, H., Shao, L. R., Chavoshy, S., Gu, N., Trieb, M., Behrens, R., et al. (2001). Presynaptic Ca2+-activated K+ channels in glutamatergic hippocampal terminals and their role in spike repolarization and regulation of transmitter release. *J. Neurosci.* 21, 9585–9597. doi: 10.1523/JNEUROSCI.21-24-09585.2001

Hunt, M. J., Kopell, N. J., Traub, R. D., and Whittington, M. A. (2017). Aberrant network activity in schizophrenia. *Trends Neurosci.* 40, 371–382. doi: 10.1016/j.tins.2017.04.003

Husain, N., Yabuki, Y., Shinoda, Y., and Fukunaga, K. (2018). Acute treatment with T-Type calcium channel enhancer SAK3 reduces cognitive impairments caused by methimazole-induced hypothyroidism *via* activation of cholinergic signaling. *Pharmacology* 101, 309–321. doi: 10.1159/000488083

Ikonen, S., and Riekkinen, P., Jr. (1999). Effects of apamin on memory processing of hippocampal-lesioned mice. *Eur. J. Pharmacol.* 382, 151–156. doi: 10.1016/s0014-2999(99)00616-0

Jadi, M. P., and Sejnowski, T. J. (2014). Regulating cortical oscillations in an inhibition-stabilized network. *Proc. IEEE.* 102, 830–842. doi: 10.1109/JPROC.2014.2313113

Kaczorowski, C. C., and Disterhoft, J. F. (2009). Memory deficits are associated with impaired ability to modulate neuronal excitability in middle-aged mice. *Learn. Mem.* 16, 362–366. doi: 10.1101/lm.1365609

Kayarian, F. B., Jannati, A., Rotenberg, A., and Santarnecchi, E. (2020). Targeting gamma-related pathophysiology in autism spectrum disorder using transcranial electrical stimulation: opportunities and challenges. *Autism Res.* 13, 1051–1071. doi: 10.1002/aur.2312

King, B., Rizwan, A. P., Asmara, H., Heath, N. C., Engbers, J. D. T., Dykstra, S., et al. (2015). IKCa channels are a critical determinant of the slow AHP in CA1 pyramidal neurons. *Cell Rep.* 11, 175–182. doi: 10.1016/j.celrep.2015.03.026

Klemz, A., Kreis, P., Eickholt, B. J., and Gerevich, Z. (2021). The actin binding protein drebrin helps to protect against the development of seizure-like events in the entorhinal cortex. *Sci. Rep.* 11:8662. doi: 10.1038/s41598-021-87967-5

Klinger, F., Gould, G., Boehm, S., and Shapiro, M. S. (2011). Distribution of M-channel subunits KCNQ2 and KCNQ3 in rat hippocampus. *Neuroimage* 58, 761–769. doi: 10.1016/j.neuroimage.2011.07.003

Kosenko, A., Moftakhar, S., Wood, M. A., and Hoshi, N. (2020). *In vivo* attenuation of m-current suppression impairs consolidation of object recognition memory. *J. Neurosci.* 40, 5847–5856. doi: 10.1523/JNEUROSCI.0348-20.2020

Kourrich, S., Calu, D. J., and Bonci, A. (2015). Intrinsic plasticity: an emerging player in addiction. *Nat. Rev. Neurosci.* 16, 173–184. doi: 10.1038/nrn3877

Kushwah, N., Jain, V., Dheer, A., Kumar, R., Prasad, D., and Khan, N. (2018). Hypobaric hypoxia-induced learning and memory impairment: elucidating the role of small conductance Ca^{2+}-activated K^{+} channels. *Neuroscience* 388, 418–429. doi: 10.1016/j.neuroscience.2018.07.026

Kwon, J. S., O'Donnell, B. F., Wallenstein, G. V., Greene, R. W., Hirayasu, Y., Nestor, P. G., et al. (1999). Gamma frequency-range abnormalities to auditory stimulation in schizophrenia. *Arch. Gen. Psychiatry* 56, 1001–1005. doi: 10.1001/archpsyc.56.11.1001

Leão, R. N., Hui, M. T., and Fisahn, A. (2009). Kv7/KCNQ channels control action potential phasing of pyramidal neurons during hippocampal gamma oscillations *in vitro*. *J. Neurosci.* 29, 13353–13364. doi: 10.1523/JNEUROSCI.1463-09.2009

Lemercier, C. E., Holman, C., and Gerevich, Z. (2017). Aberrant alpha and gamma oscillations *ex vivo* after single application of the NMDA receptor antagonist MK-801. *Schizophr. Res.* 188, 118–124. doi: 10.1016/j.schres.2017.01.017

Lemercier, C. E., Schulz, S. B., Heidmann, K. E., Kovács, R., and Gerevich, Z. (2015). Dopamine D3 receptors inhibit hippocampal gamma oscillations by disturbing CA3 pyramidal cell firing synchrony. *Front. Pharmacol.* 6:297. doi: 10.3389/fphar.2015.00297

Li, C., Huang, P., Lu, Q., Zhou, M., Guo, L., and Xu, X. (2014). KCNQ/Kv7 channel activator flupirtine protects against acute stress-induced impairments of spatial memory retrieval and hippocampal LTP in rats. *Neuroscience* 280, 19–30. doi: 10.1016/j.neuroscience.2014.09.009

Lisman, J., Cooper, K., Sehgal, M., and Silva, A. J. (2018). Memory formation depends on both synapse-specific modifications of synaptic strength and cell-specific increases in excitability. *Nat. Neurosci.* 21, 309–314. doi: 10.1038/s41593-018-0076-6

Lu, C. B., Jefferys, J. G. R., Toescu, E. C., and Vreugdenhil, M. (2011). *in vitro* hippocampal gamma oscillation power as an index of *in vivo* CA3 gamma oscillation strength and spatial reference memory. *Neurobiol. Learn. Mem.* 95, 221–230. doi: 10.1016/j.nlm.2010.11.008

Mably, A. J., and Colgin, L. L. (2018). Gamma oscillations in cognitive disorders. *Curr. Opin. Neurobiol.* 52, 182–187. doi: 10.1016/j.conb.2018.07.009

Marks, W. N., Cain, S. M., Snutch, T. P., and Howland, J. G. (2016). The T-type calcium channel antagonist Z944 rescues impairments in crossmodal and visual recognition memory in genetic absence epilepsy rats from strasbourg. *Neurobiol. Dis.* 94, 106–115. doi: 10.1016/j.nbd.2016.06.001

Marks, W. N., Zabder, N. K., Snutch, T. P., and Howland, J. G. (2020). T-type calcium channels regulate the acquisition and recall of conditioned fear in male, Wistar rats. *Behav. Brain Res.* 393:112747. doi: 10.1016/j.bbr.2020.112747

McKay, B. E., McRory, J. E., Molineux, M. L., Hamid, J., Snutch, T. P., Zamponi, G. W., et al. (2006). CaV3 T-type calcium channel isoforms differentially distribute to somatic and dendritic compartments in rat central neurons. *Eur. J. Neurosci.* 24, 2581–2594. doi: 10.1111/j.1460-9568.2006.05136.x

Meier, M. A., Lemercier, C. E., Kulisch, C., Kiss, B., Lendvai, B., Adham, N., et al. (2020). The novel antipsychotic cariprazine stabilizes gamma oscillations in rat hippocampal slices. *Br. J. Pharmacol.* 177, 1622–1634. doi: 10.1111/bph.14923

Misonou, H., Menegola, M., Buchwalder, L., Park, E. W., Meredith, A., Rhodes, K. J., et al. (2006). Immunolocalization of the Ca2+-activated K+ channel slo1 in axons and nerve terminals of mammalian brain and cultured neurons. *J. Comp. Neurol.* 496, 289–302. doi: 10.1002/cne.20931

Moriguchi, S., Shioda, N., Yamamoto, Y., Tagashira, H., and Fukunaga, K. (2012). The T-type voltage-gated calcium channel as a molecular target of the novel cognitive enhancer ST101: enhancement of long-term potentiation and CaMKII autophosphorylation in rat cortical slices. *J. Neurochem.* 121, 44–53. doi: 10.1111/j.1471-4159.2012.07667.x

Neymotin, S. A., Hilscher, M. M., Moulin, T. C., Skolnick, Y., Lazarewicz, M. T., and Lytton, W. W. (2013). Ih tunes theta/gamma oscillations and cross-frequency coupling in an in silico CA3 model. *PLoS One* 8:e76285. doi: 10.1371/journal.pone.0076285

Pedarzani, P., and Stocker, M. (2008). Molecular and cellular basis of small- and intermediate-conductance, calcium-activated potassium channel function in the brain. *Cell. Mol. Life Sci.* 65, 3196–3217. doi: 10.1007/s00018-008-8216-x

Peters, H. C., Hu, H., Pongs, O., Storm, J. F., and Isbrandt, D. (2005). Conditional transgenic suppression of M channels in mouse brain reveals functions in neuronal excitability, resonance and behavior. *Nat. Neurosci.* 8, 51–60. doi: 10.1038/nn1375

Pietersen, A. N., Lancaster, D. M., Patel, N., Hamilton, J. B., and Vreugdenhil, M. (2009). Modulation of gamma oscillations by endogenous adenosine through A1 and A2A receptors in the mouse hippocampus. *Neuropharmacology* 56, 481–492. doi: 10.1016/j.neuropharm.2008.10.001

Ribary, U., Ioannides, A. A., Singh, K. D., Hasson, R., Bolton, J. P. R., Lado, F., et al. (1991). Magnetic field tomography of coherent thalamocortical 40-Hz oscillations in humans. *Proc. Natl. Acad. Sci. U S A* 88, 11037–11041. doi: 10.1073/pnas.88.24.11037

Rice, R. A., Berchtold, N. C., Cotman, C. W., and Green, K. N. (2014). Age-related downregulation of the CaV3.1 T-type calcium channel as a mediator of amyloid beta production. *Neurobiol. Aging* 35, 1002–1011. doi: 10.1016/j.neurobiolaging.2013.10.090

Sailer, C. A., Hu, H., Kaufmann, W. A., Trieb, M., Schwarzer, C., Storm, J. F., et al. (2002). Regional differences in distribution and functional expression of small-conductance Ca2+-activated K+ channels in rat brain. *J. Neurosci.* 22, 9698–9707. doi: 10.1523/JNEUROSCI.22-22-09698.2002

Sailer, C. A., Kaufmann, W. A., Kogler, M., Chen, L., Sausbier, U., Ottersen, O. P., et al. (2006). Immunolocalization of BK channels in hippocampal pyramidal neurons. *Eur. J. Neurosci.* 24, 442–454. doi: 10.1111/j.1460-9568.2006.04936.x

Schulz, S. B., Heidmann, K. E., Mike, A., Klaft, Z.-J., Heinemann, U., and Gerevich, Z. (2012a). First and second generation antipsychotics influence hippocampal gamma oscillations by interactions with 5-HT 3 and D 3 receptors. *Br. J. Pharmacol.* 167, 1480–1491. doi: 10.1111/j.1476-5381.2012.02107.x

Schulz, S. B., Klaft, Z. J., Rösler, A. R., Heinemann, U., and Gerevich, Z. (2012b). Purinergic P2X, P2Y and adenosine receptors differentially modulate hippocampal gamma oscillations. *Neuropharmacology* 62, 914–924. doi: 10.1016/j.neuropharm.2011.09.024

Shapiro, H. M. (2000). Membrane potential estimation by flow cytometry. *Methods* 21, 271–279. doi: 10.1006/meth.2000.1007

Splawski, I., Yoo, D. S., Stotz, S. C., Cherry, A., Clapham, D. E., and Keating, M. T. (2006). CACNA1H mutations in autism spectrum disorders. *J. Biol. Chem.* 281, 22085–22091. doi: 10.1074/jbc.M603316200

Stackman, R. W., Hammond, R. S., Linardatos, E., Gerlach, A., Maylie, J., Adelman, J. P., et al. (2002). Small conductance Ca2+-activated K+ channels modulate synaptic plasticity and memory encoding. *J. Neurosci.* 22, 10163–10171. doi: 10.1523/JNEUROSCI.22-23-10163.2002

Storm, J. F. (1989). An after-hyperpolarization of medium duration in rat hippocampal pyramidal cells. *J. Physiol.* 409, 171–190. doi: 10.1113/jphysiol.1989.sp017491

Tamagnini, F., Scullion, S., Brown, J. T., and Randall, A. D. (2014). Low concentrations of the solvent dimethyl sulphoxide alter intrinsic excitability properties of cortical and hippocampal pyramidal cells. *PLoS One* 9:e92557. doi: 10.1371/journal.pone.0092557

Traub, R. D., Bibbig, A., LeBeau, F. E. N., Buhl, E. H., and Whittington, M. A. (2004). Cellular mechanisms of neuronal population oscillations in the hippocampus *in vitro*. *Annu. Rev. Neurosci.* 27, 247–278. doi: 10.1146/annurev.neuro.27.070203.144303

Tringham, E., Powell, K. L., Cain, S. M., Kuplast, K., Mezeyova, J., Weerapura, M., et al. (2012). T-type calcium channel blockers that attenuate thalamic burst firing and suppress absence seizures. *Sci. Transl. Med.* 4:121ra19. doi: 10.1126/scitranslmed.3003120

Turner, R. W., Kruskic, M., Teves, M., Scheidl-Yee, T., Hameed, S., and Zamponi, G. W. (2015). Neuronal expression of the intermediate conductance calcium-activated potassium channel KCa3.1 in the mammalian central nervous system. *Pflugers Arch.* 467, 311–328. doi: 10.1007/s00424-014-1523-1

Vick IV, K. A., Guidi, M., and Stackman, R. W., Jr. (2010). *in vivo* pharmacological manipulation of small conductance Ca2+-activated K+ channels influences motor behavior, object memory and fear conditioning. *Neuropharmacology* 58, 650–659. doi: 10.1016/j.neuropharm.2009.11.008

Vinet, J., and Sík, A. (2006). Expression pattern of voltage-dependent calcium channel subunits in hippocampal inhibitory neurons in mice. *Neuroscience* 143, 189–212. doi: 10.1016/j.neuroscience.2006.07.019

Wang, Y., Roth, Z., and Pastakova, E. (2016). Synchronized excitability in a network enables generation of internal neuronal sequences. *eLife* 5:e20697. doi: 10.7554/eLife.20697

Weiss, N., and Zamponi, G. W. (2019). T-type calcium channels: from molecule to therapeutic opportunities. *Int. J. Biochem. Cell Biol.* 108, 34–39. doi: 10.1016/j.biocel.2019.01.008

Womelsdorf, T., and Fries, P. (2006). Neuronal coherence during selective attentional processing and sensory-motor integration. *J. Physiol. Paris* 100, 182–193. doi: 10.1016/j.jphysparis.2007.01.005

Xu, J., and Clancy, C. E. (2008). Ionic mechanisms of endogenous bursting in CA3 hippocampal pyramidal neurons: a model study. *PLoS One* 3:e2056. doi: 10.1371/journal.pone.0002056

Xu, J., Yabuki, Y., Yu, M., and Fukunaga, K. (2018). T-type calcium channel enhancer SAK3 produces anti-depressant-like effects by promoting adult hippocampal neurogenesis in olfactory bulbectomized mice. *J. Pharmacol. Sci.* 137, 333–341. doi: 10.1016/j.jphs.2018.07.006

Yabuki, Y., Matsuo, K., Izumi, H., Haga, H., Yoshida, T., Wakamori, M., et al. (2017). Pharmacological properties of SAK3, a novel T-type voltage-gated Ca2+ channel enhancer. *Neuropharmacology* 117, 1–13. doi: 10.1016/j.neuropharm.2017.01.011

Yan, H.-D., Villalobos, C., and Andrade, R. (2009). TRPC channels mediate a muscarinic receptor-induced afterdepolarization in cerebral cortex. *J. Neurosci.* 29, 10038–10046. doi: 10.1523/JNEUROSCI.1042-09.2009

Yuan, D., Cheng, A., Kawahata, I., Izumi, H., Xu, J., and Fukunaga, K. (2021). Single administration of the T-type calcium channel enhancer SAK3 reduces oxidative stress and improves cognition in olfactory bulbectomized mice. *Int. J. Mol. Sci.* 22:741. doi: 10.3390/ijms22020741

Zeisel, A., Munoz-Manchado, A. B., Codeluppi, S., Lönnerberg, P., Manno, G. L., Juréus, A., et al. (2015). Brain structure. Cell types in the mouse cortex and hippocampus revealed by single-cell RNA-seq. *Science* 347, 1138–1142. doi: 10.1126/science.aaa1934

Zhu, Y., Zhang, S., Feng, Y., Xiao, Q., Cheng, J., and Tao, J. (2018). The yin and yang of BK channels in epilepsy. *CNS Neurol. Disord. Drug Targets* 17, 272–279. doi: 10.2174/1871527317666180213142403

Conflict of Interest: The authors declare that the research was conducted in the absence of any commercial or financial relationships that could be construed as a potential conflict of interest.

frontiers in Behavioral Neuroscience

MINI REVIEW
published: 01 February 2022
doi: 10.3389/fnbeh.2022.811278

How Many Gammas? Redefining Hippocampal Theta-Gamma Dynamic During Spatial Learning

*Matthieu Aguilera[1], Vincent Douchamps[1], Demian Battaglia[2,3] and Romain Goutagny[1]**

[1] Laboratoire de Neurosciences Cognitives et Adaptatives (LNCA), Faculté de Psychologie, Université de Strasbourg, Strasbourg, France, [2] Institut de Neurosciences des Systèmes, CNRS, Aix-Marseille Université, Marseille, France, [3] University of Strasbourg Institute for Advanced Study (USIAS), Strasbourg, France

The hippocampal formation is one of the brain systems in which the functional roles of coordinated oscillations in information representation and communication are better studied. Within this circuit, neuronal oscillations are conceived as a mechanism to precisely coordinate upstream and downstream neuronal ensembles, underlying dynamic exchange of information. Within a global reference framework provided by theta (θ) oscillations, different gamma-frequency (γ) carriers would temporally segregate information originating from different sources, thereby allowing networks to disambiguate convergent inputs. Two γ sub-bands were thus defined according to their frequency (slow γ, 30–80 Hz; medium γ, 60–120 Hz) and differential power distribution across CA1 dendritic layers. According to this prevalent model, layer-specific γ oscillations in CA1 would reliably identify the temporal dynamics of afferent inputs and may therefore aid in identifying specific memory processes (encoding for medium γ vs. retrieval for slow γ). However, this influential view, derived from time-averages of either specific γ sub-bands or different projection methods, might not capture the complexity of CA1 θ-γ interactions. Recent studies investigating γ oscillations at the θ cycle timescale have revealed a more dynamic and diverse landscape of θ-γ motifs, with many θ cycles containing multiple γ bouts of various frequencies. To properly capture the hippocampal oscillatory complexity, we have argued in this review that we should consider the entirety of the data and its multidimensional complexity. This will call for a revision of the actual model and will require the use of new tools allowing the description of individual γ bouts in their full complexity.

Keywords: hippocampus, oscillations, spatial cognition, navigation, complexity, spatial learning

OPEN ACCESS

Edited by:
Gabrielle Girardeau, INSERM U839 Institut du Fer à Moulin (IFM), France

Reviewed by:
Antonio Fernández-Ruiz, New York University, United States

***Correspondence:**
Romain Goutagny
goutagny@unistra.fr

Specialty section:
This article was submitted to Learning and Memory, a section of the journal Frontiers in Behavioral Neuroscience

Received: *08 November 2021*
Accepted: *03 January 2022*
Published: *01 February 2022*

Citation:
Aguilera M, Douchamps V, Battaglia D and Goutagny R (2022) How Many Gammas? Redefining Hippocampal Theta-Gamma Dynamic During Spatial Learning. Front. Behav. Neurosci. 16:811278. doi: 10.3389/fnbeh.2022.811278

INTRODUCTION

The ability to represent the surrounding space is crucial for most evolved animals and is at the core of the ability to navigate in the environment, looking out for food, shelter, or other behaviorally relevant locations. For an organism to effectively navigate, it should possess the cognitive representations of critical regions in their environment (e.g., nest locations and food locations), to recall these regions when the need arises, and the means to exploit relations between such regions and their immediate position. In other words, the navigating agent constantly needs to

compare current sensory inputs (i.e., encoding of current information) with stored memories (i.e., retrieval of past information). These two seemingly opposed processes (encoding vs. retrieval) are thought to be mediated by two segregated areas of the medial temporal lobe: the hippocampal CA3 region and the entorhinal cortex (EC). Hippocampal CA3, through its massive recurrent network, would support retrieval of past memories (Rolls, 2018), whereas the EC (and more precisely its medial part; MEC) would support encoding of current sensory information (Brun et al., 2002, 2008; Fyhn et al., 2004; Hafting et al., 2005). These two regions in turn project to hippocampal region CA1, which is thought to act as a comparator to determine if ongoing sensory inputs represent new information that needs to be stored (Hasselmo et al., 2002). How does CA1 integrate these different inputs while minimizing interference? Current hypotheses suggest a critical role for brain oscillations in the selective routing of information (Fries, 2009). During spatial navigation, the hippocampus mainly exhibits theta (θ) and gamma (γ) oscillations. It is now accepted that hippocampal γ oscillations can be segregated into slow and medium (or fast, depending on the authors) γ rhythms, each originating from different brain regions and subserving different cognitive functions (Colgin et al., 2009; Schomburg et al., 2014). More recently, studies refining the time scale of analysis have shown that this model might be too simplistic, with a greater variability than initially expected. By putting in perspective these different studies, we have argued in this review that tackling this variability is needed to fully characterize the hippocampal θ-γ dynamic.

THE γ SUB-BANDS MODEL: A SUITABLE FRAMEWORK TO UNDERSTAND HIPPOCAMPAL COMPUTATION

Excellent reviews on the cellular mechanisms responsible for hippocampal θ (Buzsáki, 2002) and γ oscillations (Buzśaki and Wang, 2012) have already been published and fell outside the scope of the present review (see also Wang, 2010, for a comprehensive survey of the modeling literature).

Neuronal oscillations are conceived as a mechanism to precisely coordinate upstream and downstream neuronal ensembles, underlying the dynamic exchange of information (Fries, 2009). In the medial temporal lobe, it is proposed that, within a global reference framework provided by θ oscillations, different γ-frequency carriers would temporally segregate information originating from different sources, thereby allowing a target "reader" area to disambiguate convergent inputs (Buzsáki, 2010). As such, hippocampal CA1 γ oscillations, although initially described as forming a single wide frequency band (40–100 Hz; Bragin et al., 1995), were later dissociated into two sub-bands according to their frequency (i.e., slow γ, 25–55 Hz; fast γ, 65–140 Hz), and their phase of appearance related to pyramidal layer θ oscillations (i.e., early phase of the descending part for slow γ and trough for fast γ; Colgin et al., 2009). The fact that bursts of slow γ were associated with increased coherence between CA3 and CA1, whereas fast γ was associated with increased coherence between the MEC and CA1, prompted the authors to suggest that these two independent γ rhythms would selectively "route information" in the hippocampal entorhinal network (Colgin et al., 2009). Building on this framework and on the proposed specific role of CA3 and the MEC in memory processes, the same authors further proposed that these two γ rhythms in CA1 might subserve different cognitive operations, i.e., slow γ would be important for memory retrieval, whereas fast γ would support memory encoding (Colgin and Moser, 2010). While appealing in its simplicity, this model nevertheless carries some caveats. First, while the phase separation of inputs relative to θ oscillation would indeed allow for a separation of the information (Fries, 2009), the reported phase of fast γ does not fit with the "separate phases of encoding and retrieval (SPEAR)" model proposed by Hasselmo et al. (2002). Second, by using single-site recording in the CA1 pyramidal layer, Colgin et al. (2009) were not able to isolate the source of the slow- and fast-γ oscillations. Indeed, one should expect slow γ to be prominent in the CA1 *stratum radiatum* (str.rad), the input of CA3 through the Schaffer collaterals, and fast γ in the CA1 *stratum lacunosum-moleculare* (str.lm), the inputs of the MEC layer 3 through the temporo-ammonic pathway. Finally, while slow and fast γ differentially modulate place cells sequences according to the purported role of each γ rhythm (prospective vs. retrospective coding; Bieri et al., 2014), the authors never actually performed navigation task requiring allocentric memory [open field in Colgin et al. (2009) and linear track in Bieri et al. (2014)].

To fill these gaps, Schomburg et al. (2014) performed high-density multisite recording covering most layers of CA1 to CA3 and dentate gyrus (DG) regions along the transverse axis of the hippocampus in rats navigating in a linear track, a T maze, or an open field. Using a powerful source separation technique and focusing on the hippocampal CA1 area (independent component analysis; Fernández-Ruiz and Herreras, 2013), they were able to identify three γ independent components (ICs). The first component with a strong current sink was localized in the str.rad (termed rad IC), exhibiting slow-γ oscillations (30–80 Hz), phase-locked to the descending phase of CA1 pyramidal θ. The second γ component with a strong current sink was localized to the str.lm (termed lm IC), exhibiting mid-γ oscillations (60–120 Hz), phase-locked to the peak of CA1 pyramidal θ. Finally, the third component with a current source was localized in the CA1 pyramidal layer (termed CA1 pyr IC), exhibiting fast γ (>140 Hz), phase-locked to the through of CA1 pyramidal θ. Based on the location of the current sink/sources and single-unit recordings (in CA1, CA3, and the MEC), the authors proposed that slow γ would represent a communication channel between CA3 and CA1, whereas mid-γ would aid communication between the MEC and CA1. Importantly, there is a clear difference in the θ phase between the mid-γ reported by Schomburg et al. (2014) and the corresponding fast γ reported by Colgin et al. (2009), which can be due in part to the lack of source localization in the study by Colgin et al. Nevertheless, the relative phase of slow and medium γ in the Schomburg et al. (2014) study is coherent with the SPEAR model (Hasselmo et al., 2002). Do these different γ components subserve different cognitive operations? To answer this question, Schomburg and

colleagues characterized the dynamics of the γ components during different phases of a T-maze task. They showed that the θ-γ coupling strength of the rad IC selectively increased in the center arm of the maze, a place where memory recall is expected (i.e., in order to guide subsequent behavior). Recently, Fernández-Ruiz et al. (2021) extended this concept to the DG. Using the same decomposition method, they characterized three independent components, namely, a slow-γ IC (30–50 Hz) in the outer molecular layer of the DG, a mid-γ IC (60–80 Hz) in the inner molecular layer of the DG, and a fast-γ IC (100–150 Hz) in the middle molecular layer of the DG, coming from lateral EC associational and/or commissural, and MEC inputs, respectively. During spatial learning, fast-γ oscillations synchronize the MEC and DG, while during object learning, slow-γ oscillations synchronize the LEC and DG. To assess causality, the authors performed γ-frequency optogenetic perturbation of MEC and LEC. This led to reduced DG layer-specific fast- and slow-γ sub-bands and to learning impairments in a spatial and object learning task, respectively.

Altogether, these seminal studies set the stage for what we decided to call the "sub-bands model." The premise of this model is that if there are different rhythms generated by different brain regions, they must subserve different cognitive operations. However, a problem with influential models is that they tend to inform research in the field, biasing the interpretation of results and narrowing the spectrum of hypotheses that could be considered, e.g., to explain disruptions of function in pathology. For example, a decrease in hippocampal slow-γ power observed in several rodent models of Alzheimer's disease (Gillespie et al., 2016; Iaccarino et al., 2016; Mably et al., 2017) was linked to retrieval impairment (Mably and Colgin, 2018; Etter et al., 2019) in accordance to the purported role of those oscillations in memory retrieval.

A SUITABLE MODEL, BUT SURELY TOO RESTRICTIVE

As stated in the "Introduction" section, a navigating agent constantly needs to compare current sensory inputs (i.e., encoding of current information) with stored memories (i.e., retrieval of past information). To gain a better temporal resolution, one can study γ dynamic at the θ time-scale level (Dvorak et al., 2018; Lopes-dos-Santos et al., 2018; Zhang et al., 2019), a proposed unit of computation (Lisman, 2005; Lisman and Buzsáki, 2008). By using various methods of γ detection in a θ cycle by cycle manner (γ detector reported by Dvorak et al., 2018, Ensemble Empirical Mode Decomposition of a γ signal reported by Lopes-dos-Santos et al., 2018 and unsupervised clustering reported by Zhang et al., 2019), these studies showed a more complex landscape than initially proposed (with an increasing number of θ-γ motifs, with up to 5 prototypic motifs reported by Lopes-dos-Santos et al., 2018; **Figure 1**). Overall, all the studies agreed on the presence of at least three different γ oscillations, similar to the definition put forward by Schomburg et al. (2014) (**Figure 1**). Collectively, they support the concept that different γ frequencies subserve different cognitive operations by channeling information in specific pathways (refer to Zhou et al., 2019, for a critical view on the existence of a "real" slow-γ oscillation in the hippocampal network). At the first sight, they seem to consolidate the current γ sub-bands model. However, they also all report high diversity of coupling patterns across θ cycles, with most of the cycle containing multiple γ events. In other words, each θ cycle can simultaneously contain slow- and medium-γ events (**Figure 1**). This diversity was always mentioned, but surprisingly not properly studied, as they all acknowledge restricting analyses to either the highest amplitude γ events (Dvorak et al., 2018) or the one fitting the best canonical clustered results (Lopes-dos-Santos et al., 2018; Zhang et al., 2019). As such, they analyzed only a part of the available landscape of θ-γ motif (36% of all θ cycles reported by Lopes-dos-Santos et al., 2018). What does that imply in terms of local computation? It was indeed assumed that each θ cycle would subserve a specific function based on the associated dominant γ oscillation: in CA1, θ cycles with slow γ would be "retrieval cycles," whereas cycles with mid-γ would be "encoding cycles" (Colgin et al., 2009; Bieri et al., 2014; Schomburg et al., 2014). The fact that θ cycles mostly contain multiple, low-amplitude, different γ events complexifies this hypothesis (Bagur and Benchenane, 2018). What is the role of a θ cycle with concomitant, same-amplitude slow and medium γ? Can one θ cycle promote different cognitive operations? As an example of possible complexity, Lopes-dos-Santos and colleagues have shown that each θ-nested spectral component (tSC, equivalent of a specific θ-γ motif) represents a distinct spiking dynamic of distinguishable cell ensembles (Lopes-dos-Santos et al., 2018). Since each θ cycle does not present a single tSC but a weighted combination of multiple tSC, what will be the output of such θ cycles (e.g., multiple assemblies co-firing and sequential ordering of different assemblies).

Most, if not all, of the aforementioned studies have focused on the interaction between multiple γ and single θ oscillations (CA1 pyramidal θ). However, it was recently shown that θ oscillations themselves in the dorsal hippocampus are not a unitary process. Using ICA decomposition, López-Madrona et al. (2020) identified three independent θ ICs contributed by different synaptic pathways, namely, the first in the str.rad, the second in the str.lm, and the third in the mid-molecular layer of the DG. Thus, as there are multiple γ, there may also be multiple θ, opening the way to a potential combinatorial explosion of the number of possible θ-γ configurations.

As a concluding, near tautological, remark, we would like to stress that any method for the unsupervised extraction of classes of oscillatory events will end up finding them. The exact number of identified patterns will depend on the specificities of the experimental dataset and algorithm used but will always nevertheless remain a discrete integer number as the applied methods are designed to do so. In front of the inflation of the number of possibly relevant θ-γ patterns exhibited by the recent literature, and the diversity of γ sub-bands definition across aforementioned studies (see Zhou et al., 2019), it may be legitimate to wonder whether the paradigm of looking for discrete classes of events is well-grounded. From a complex dynamics perspective, a neural circuit with recurrent excitatory and inhibitory interconnections

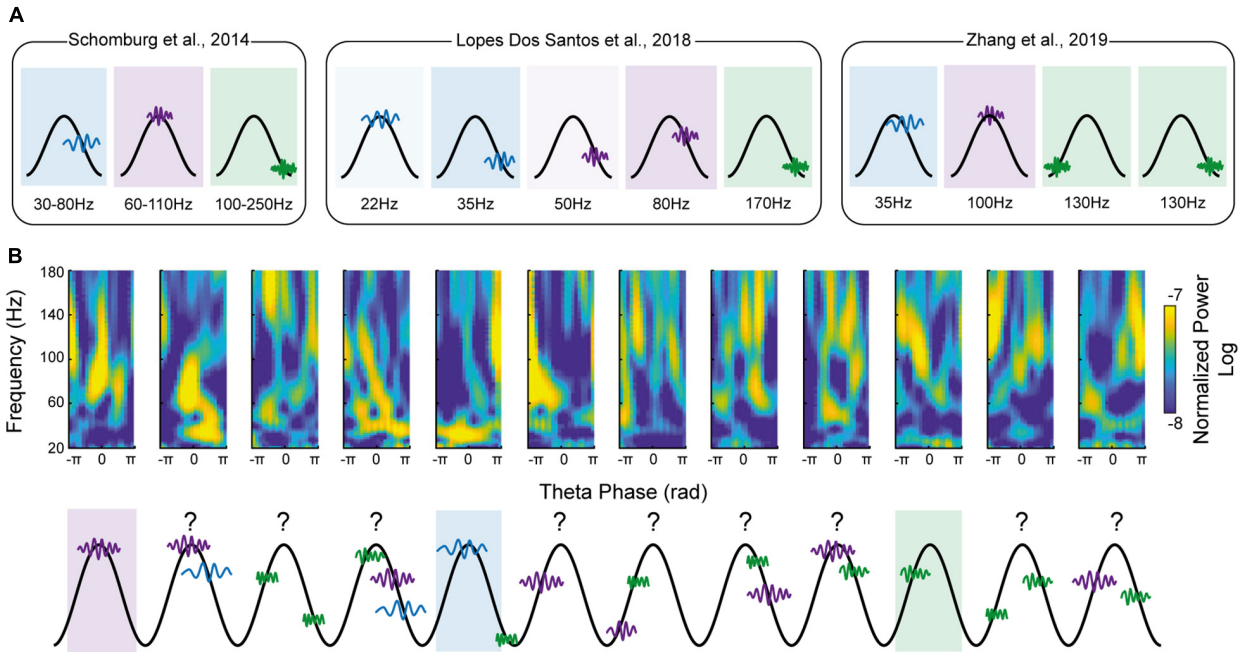

FIGURE 1 | Decomposing theta-gamma oscillations in discrete motifs do not capture the full gamma diversity. **(A)** Schematic representations of the main theta-gamma motifs found in the literature. Gamma frequency is color-coded (blue corresponding to slow-gamma, purple to mid-gamma and green to fast-gamma). Note the inflation of the different motifs since the initial proposal by Colgin et al. (2009) (from 2 in Colgin et al., 2009 to 5 in Lopes-dos-Santos et al., 2018). **(B)** Top: Raw example of theta-gamma motifs found in hippocampal CA1 pyramidal layer (reproduced from Figure 1B of Zhang et al., 2019 https://doi.org/10.7554/eLife.44320.002). Bottom: Schematic representation of the above theta-gamma motifs. Note that only few theta cycles present a prototypic motif as described in **(A)**. In fact, most of the theta cycles can be described as a weighted combination of the different prototypic motifs.

is supposed to give rise to oscillations that are not well-behaved and tuned metronomes but can fluctuate in frequency as a function of noisy background inputs (Brunel and Wang, 2003; Brunel and Hansel, 2006). Such stochastic-like oscillations, despite their highly transient and irregular nature, can still be fit for functions as selective information routing, thanks to emergent self-organization mechanisms (Palmigiano et al., 2017). It may thus be that the diversity of θ-γ oscillatory patterns displayed by neural recordings is not the manifestation of the coexistence of multiple, discrete generation mechanisms or sources, but instead the unique, diverse output of a common underlying circuit dynamics, non-linear and complex in nature.

It is noted that a similar debate has also occurred in the literature concerning the diversity of cortical interneurons, that may exist as a large number of discrete types with different functions (Markram et al., 2004; Burkhalter, 2008) and form an interneuron continuum (Parra et al., 1998) or a structured continuum with smooth tendencies (Battaglia et al., 2013).

CONCLUSION AND PERSPECTIVES: IS θ-γ LANDSCAPE RANDOM OR COMPLEX?

In this review, we have argued that the current model of hippocampal θ-γ oscillations might not capture the complexity of CA1 θ-γ interactions despite the evident appeal of its simplicity and the functional link to memory processes. Indeed, rather than containing a given γ event, most of the θ cycles contain multiple, low-amplitude, γ bouts. Furthermore, many of the observed γ frequencies do not fit well into a classification involving only a few discrete γ types. Should these low-amplitude events be dismissed as noise? To properly describe hippocampal oscillatory complexity, we believe the entirety of the data should be taken into consideration (without assuming that the strongest γ events are the only ones carrying information). This will require the use of new tools that do not assume *a priori* that certain classes of γ rhythms exist but instead enable the description of individual γ bouts in their full complexity. Individual oscillatory events may have wildly fluctuating frequency, amplitude, and phase with respect to ongoing θ. However, these fluctuations could still be correlated to behavior and memory processing but in a collective and synergistic manner. Individual features of oscillatory activity may be only weakly informative about behavior because of their apparent randomness. However, multiple features taken together may still carry relevant information that individual features do not (Wibral et al., 2017). Such a situation may occur if the observed oscillatory events do not arise in all theoretically possible configurations of features but are sampled on a low-dimensional manifold in state space (Chaudhuri and Fiete, 2016). This representation would constrain dynamic trajectories, creating interdependencies between them, possibly modulated by context. In such a view, there would not be discrete classes

of oscillatory events but a lower-dimensional space of possible modes of oscillation that the system can smoothly explore along time, possibly under the biasing influence of the exogenous or endogenous input drive. Machine learning approaches could then be used to learn these manifolds without fully determining oscillatory modes and their relations to behavior so as to decode and extract the complex information hidden in the apparent stochasticity of the observed activity time-series.

AUTHOR CONTRIBUTIONS

MA, RG, and DB wrote the manuscript. VD provided critical inputs. All authors contributed to the article and approved the submitted version.

FUNDING

This work was supported by the Agence Nationale de la Recherche (ANR JCC: ANR-17-CE37-0002 to RG), the University of Strasbourg Institute for Advanced Study (USIAS 2020 fellowship to DB), the Fondation pour la Recherche Medicale (FRM, Ph.D. fellowship to MA), and the University of Strasbourg and the Centre National de la Recherche Scientifique (CNRS).

ACKNOWLEDGMENTS

The authors wish to thank all the intern students who worked on this project across the years. They are extremely grateful to Jesse Jackson for critical comments on this review.

REFERENCES

Bagur, S., and Benchenane, K. (2018). The Theta rhythm mixes and matches gamma oscillations cycle by cycle. *Neuron* 100, 768–771. doi: 10.1016/j.neuron.2018.11.008

Battaglia, D., Karagiannis, A., Gallopin, T., Gutch, H. W., and Cauli, B. (2013). Beyond the frontiers of neuronal types. *Front. Neural Circuits* 7:13. doi: 10.3389/fncir.2013.00013

Bieri, K. W., Bobbitt, K. N., and Colgin, L. L. (2014). Slow and fast gamma rhythms coordinate different spatial coding modes in hippocampal place cells. *Neuron* 82, 670–681. doi: 10.1016/j.neuron.2014.03.013

Bragin, A., Jando, G., Nadasdy, Z., Hetke, J., Wise, K., and Buzsaki, G. (1995). Gamma (40-100 Hz) oscillation in the hippocampus of the behaving rat. *J. Neurosci.* 15, 47–60. doi: 10.1523/jneurosci.15-01-00047.1995

Brun, V. H., Leutgeb, S., Wu, H.-Q., Schwarcz, R., Witter, M. P., Moser, E. I., et al. (2008). Impaired spatial representation in CA1 after lesion of direct input from entorhinal cortex. *Neuron* 57, 290–302. doi: 10.1016/j.neuron.2007.11.034

Brun, V. H., Otnæss, M. K., Molden, S., Steffenach, H. A., Witter, M. P., Moser, M. B., et al. (2002). Place cells and place recognition maintained by direct entorhinal-hippocampal circuitry. *Science* 296, 2243–2246. doi: 10.1126/science.1071089

Brunel, N., and Hansel, D. (2006). How noise affects the synchronization properties of recurrent networks of inhibitory neurons. *Neural Comput.* 18, 1066–1110. doi: 10.1162/neco.2006.18.5.1066

Brunel, N., and Wang, X. J. (2003). What determines the frequency of fast network oscillations with irregular neural discharges? I. Synaptic dynamics and excitation-inhibition balance. *J. Neurophysiol.* 90, 415–430. doi: 10.1152/jn.01095.2002

Burkhalter, A. (2008). Many specialists for suppressing cortical excitation. *Front. Neurosci.* 2:155–167. doi: 10.3389/neuro.01.026.2008

Buzsáki, G. (2002). Theta oscillations in the hippocampus. *Neuron* 33, 325–340. doi: 10.1016/S0896-6273(02)00586-X

Buzsáki, G. (2010). Neural syntax: cell assemblies, synapsembles, and readers. *Neuron* 68, 362–385. doi: 10.1016/j.neuron.2010.09.023

Buzśaki, G., and Wang, X. J. (2012). Mechanisms of gamma oscillations. *Annu. Rev. Neurosci.* 35, 203–225. doi: 10.1146/annurev-neuro-062111-150444

Chaudhuri, R., and Fiete, I. (2016). Computational principles of memory. *Nat. Neurosci.* 19, 394–403. doi: 10.1038/nn.4237

Colgin, L. L., and Moser, E. I. (2010). Gamma oscillations in the hippocampus. *Physiology* 25, 319–329. doi: 10.1152/physiol.00021.2010

Colgin, L. L., Denninger, T., Fyhn, M., Hafting, T., Bonnevie, T., Jensen, O., et al. (2009). Frequency of gamma oscillations routes flow of information in the hippocampus. *Nature* 462, 353–357. doi: 10.1038/nature08573

Dvorak, D., Radwan, B., Sparks, F., Talbot, Z. N., and Fenton, A. (2018). Control of recollection by slow gamma dominating mid-frequency gamma in hippocampus CA1. *PLoS Biol.* 16:e2003354. doi: 10.1371/journal.pbio.2003354

Etter, G., van der Veldt, S., Manseau, F., Zarrinkoub, I., Trillaud-Doppia, E., and Williams, S. (2019). Optogenetic gamma stimulation rescues memory impairments in an Alzheimer's disease mouse model. *Nat. Commun.* 10:5322. doi: 10.1038/s41467-019-13260-9

Fernández-Ruiz, A., and Herreras, O. (2013). Identifying the synaptic origin of ongoing neuronal oscillations through spatial discrimination of electric fields. *Front. Comput. Neurosci.* 7:5. doi: 10.3389/fncom.2013.00005

Fernández-Ruiz, A., Oliva, A., Soula, M., Rocha-Almeida, F., Nagy, G. A., Martin-Vazquez, G., et al. (2021). Gamma rhythm communication between entorhinal cortex and dentate gyrus neuronal assemblies. *Science* 372:eabf3119. doi: 10.1126/science.abf3119

Fries, P. (2009). Neuronal gamma-band synchronization as a fundamental process in cortical computation. *Annu. Rev. Neurosci.* 32, 209–224. doi: 10.1146/annurev.neuro.051508.135603

Fyhn, M., Molden, S., Witter, M. P., Moser, E. I., and Moser, M. B. (2004). Spatial representation in the entorhinal cortex. *Science* 305, 1258–1264. doi: 10.1126/science.1099901

Gillespie, A. K., Jones, E. A., Lin, Y. H., Karlsson, M. P., Kay, K., Yoon, S. Y., et al. (2016). Apolipoprotein E4 causes age-dependent disruption of slow gamma oscillations during hippocampal sharp-wave ripples. *Neuron* 90, 740–751. doi: 10.1016/j.neuron.2016.04.009

Hafting, T., Fyhn, M., Molden, S., Moser, M. B., and Moser, E. I. (2005). Microstructure of a spatial map in the entorhinal cortex. *Nature* 436, 801–806. doi: 10.1038/nature03721

Hasselmo, M. E., Bodelón, C., and Wyble, B. P. (2002). A proposed function for hippocampal theta rhythm: separate phases of encoding and retrieval enhance reversal of prior learning. *Neural Comput.* 14, 793–817. doi: 10.1162/089976602317318965

Iaccarino, H. F., Singer, A. C., Martorell, A. J., Rudenko, A., Gao, F., Gillingham, T. Z., et al. (2016). Gamma frequency entrainment attenuates amyloid load and modifies microglia. *Nature* 540, 230–235. doi: 10.1038/nature20587

Lisman, J. (2005). The theta/gamma discrete phase code occuring during the hippocampal phase precession may be a more general brain coding scheme. *Hippocampus* 15, 913–922. doi: 10.1002/hipo.20121

Lisman, J., and Buzsáki, G. (2008). A neural coding scheme formed by the combined function of gamma and theta oscillations. *Schizophr. Bull.* 34, 974–980. doi: 10.1093/schbul/sbn060

Lopes-dos-Santos, V., van de Ven, G. M., Morley, A., Trouche, S., Campo-Urriza, N., and Dupret, D. (2018). Parsing hippocampal theta oscillations by nested spectral components during spatial exploration and memory-guided behavior. *Neuron* 100, 940–952.e7. doi: 10.1016/j.neuron.2018.09.031

López-Madrona, V. J., Pérez-Montoyo, E., Álvarez-Salvado, E., Moratal, D., Herreras, O., Pereda, E., et al. (2020). Different theta frameworks coexist in the rat hippocampus and are coordinated during memory-guided and novelty tasks. *Elife* 9:e57313. doi: 10.7554/eLife.57313

Mably, A. J., and Colgin, L. L. (2018). Gamma oscillations in cognitive disorders. *Curr. Opin. Neurobiol.* 52, 182–187. doi: 10.1016/j.conb.2018.07.009

Mably, A. J., Gereke, B. J., Jones, D. T., and Colgin, L. L. (2017). Impairments in spatial representations and rhythmic coordination of place cells in the 3xTg mouse model of Alzheimer's disease. *Hippocampus* 27, 378–392. doi: 10.1002/hipo.22697

Markram, H., Toledo-Rodriguez, M., Wang, Y., Gupta, A., Silberberg, G., and Wu, C. (2004). Interneurons of the neocortical inhibitory system. *Nat. Rev. Neurosci.* 5, 793–807. doi: 10.1038/nrn1519

Palmigiano, A., Geisel, T., Wolf, F., and Battaglia, D. (2017). Flexible information routing by transient synchrony. *Nat. Neurosci.* 20, 1014–1022. doi: 10.1038/nn.4569

Parra, P., Gulyás, A. I., and Miles, R. (1998). How many subtypes of inhibitory cells in the hippocampus? *Neuron* 20, 983–993. doi: 10.1016/S0896-6273(00)80479-1

Rolls, E. T. (2018). The storage and recall of memories in the hippocampo-cortical system. *Cell Tissue Res.* 373, 577–604. doi: 10.1007/s00441-017-2744-3

Schomburg, E. W., Fernández-Ruiz, A., Mizuseki, K., Berényi, A., Anastassiou, C. A., Koch, C., et al. (2014). Theta phase segregation of input-specific gamma patterns in entorhinal-hippocampal networks. *Neuron* 84, 470–485. doi: 10.1016/j.neuron.2014.08.051

Wang, X. J. (2010). Neurophysiological and computational principles of cortical rhythms in cognition. *Physiol. Rev.* 90, 1195–1268. doi: 10.1152/physrev.00035.2008

Wibral, M., Priesemann, V., Kay, J. W., Lizier, J. T., and Phillips, W. A. (2017). Partial information decomposition as a unified approach to the specification of neural goal functions. *Brain Cogn.* 112, 25–38. doi: 10.1016/j.bandc.2015.09.004

Zhang, L., Lee, J., Rozell, C., and Singer, A. C. (2019). Sub-second dynamics of theta-gamma coupling in hippocampal CA1. *Elife* 8:e44320. doi: 10.7554/eLife.44320

Zhou, Y., Sheremet, A., Qin, Y., Kennedy, J. P., DiCola, N. M., Burke, S. N., et al. (2019). Methodological considerations on the use of different spectral decomposition algorithms to study hippocampal rhythms. *eNeuro* 6, ENEURO.142–ENEURO.119. doi: 10.1523/ENEURO.0142-19.2019

Conflict of Interest: The authors declare that the research was conducted in the absence of any commercial or financial relationships that could be construed as a potential conflict of interest.

frontiers in Neural Circuits

REVIEW
published: 04 March 2022
doi: 10.3389/fncir.2022.846905

Breaking Down a Rhythm: Dissecting the Mechanisms Underlying Task-Related Neural Oscillations

Inés Ibarra-Lecue[1,2], Saskia Haegens[1,2,3] and Alexander Z. Harris[1,2]**

[1] Department of Psychiatry, College of Physicians and Surgeons, Columbia University, New York, NY, United States, [2] New York State Psychiatric Institute, New York, NY, United States, [3] Donders Centre for Cognitive Neuroimaging, Donders Institute for Brain, Cognition and Behaviour, Radboud University, Nijmegen, Netherlands

A century worth of research has linked multiple cognitive, perceptual and behavioral states to various brain oscillations. However, the mechanistic roles and circuit underpinnings of these oscillations remain an area of active study. In this review, we argue that the advent of optogenetic and related systems neuroscience techniques has shifted the field from correlational to causal observations regarding the role of oscillations in brain function. As a result, studying brain rhythms associated with behavior can provide insight at different levels, such as decoding task-relevant information, mapping relevant circuits or determining key proteins involved in rhythmicity. We summarize recent advances in this field, highlighting the methods that are being used for this purpose, and discussing their relative strengths and limitations. We conclude with promising future approaches that will help unravel the functional role of brain rhythms in orchestrating the repertoire of complex behavior.

Keywords: electrophysiology, optogenetic stimulation, optogenetic inhibition, alpha oscillations, beta oscillations, theta oscillations, delta oscillations, gamma oscillations

OPEN ACCESS

Edited by:
Sanja Mikulovic, Leibniz Institute for Neurobiology (LG), Germany

Reviewed by:
Vikaas Singh Sohal, University of California, San Francisco, United States
Julia Veit, University of Freiburg, Germany

****Correspondence:***
Saskia Haegens
shaegens@gmail.com
Alexander Z. Harris
ah2835@cumc.columbia.edu

Received: *31 December 2021*
Accepted: *10 February 2022*
Published: *04 March 2022*

Citation:
Ibarra-Lecue I, Haegens S and Harris AZ (2022) Breaking Down a Rhythm: Dissecting the Mechanisms Underlying Task-Related Neural Oscillations. Front. Neural Circuits 16:846905. doi: 10.3389/fncir.2022.846905

INTRODUCTION

History

In the early 20th century, Berger (1929) discovered that the electrical activity of neurons can be recorded from electrodes placed on the scalp. These electrical recordings, known as electroencephalography (EEG), reflect the summed synaptic activity of large neuronal populations (Buzsaki et al., 2012) and reveal that brain activity is highly rhythmic. Berger (1929) reported that activity at approximately 10 Hz – the so-called alpha rhythm – is strongest during eye closure and rest, and reduced by visual stimulation (Mazaheri et al., 2014). Subsequent research using not only EEG, but also other non-invasive techniques such as magnetoencephalography (MEG), and invasive recordings of the local field potential (LFP), has associated different behavioral and cognitive processes with particular brain regions and oscillatory dynamics. For example, hippocampal theta oscillations (4–8 Hz) have been linked with episodic memory and navigation (McNaughton et al., 2006; Buzsáki and Moser, 2013), alpha oscillations (8–14 Hz) with sensory processing and attention (Haegens et al., 2011a; Mazaheri et al., 2014; Samaha et al., 2020; Zhou et al., 2021), cortical beta (15–30 Hz) with working memory and perceptual decision making (Haegens et al., 2011b; Herding et al., 2016; Spitzer and Haegens, 2017), and gamma (30–90 Hz) in a variety of different brain regions with sensory processing, cognition, memory, and

attention (Cardin et al., 2009; Lundqvist et al., 2018; Kanta et al., 2019; Zielinski et al., 2019). Recently, the field has moved away from simply correlating oscillations with behavior. Instead, new theoretical frameworks propose that different rhythms reflect distinct lower-level functions (such as modulating gain or facilitating synchrony) that are flexibly employed to change specific neuronal population dynamics, based on the information processing required for the behavioral context. Defining these lower-level functions involves an ongoing challenge that represents one main approach to studying oscillations in behavior. Another fruitful approach involves using oscillations as a window into the dynamic activity of neuronal circuits that mediate specific behaviors, by determining the contribution of neural subpopulations to the oscillations that emerge during behavior. We will summarize these two approaches which, while having different scientific goals, can unravel complementary questions about brain processing.

Toward Understanding the Fundamental Role of Oscillations

Neural oscillations emerge from synchronized synaptic activity, resulting in periodic collective shifts between higher and lower intracellular voltage or excitability states (Bishop, 1932). Neural oscillations have been proposed to facilitate neural communication (Fries, 2015; Harris and Gordon, 2015), either by synchronizing distant brain regions to align inter-regional information transfer (Varela et al., 2001; Jones and Wilson, 2005a; Adhikari et al., 2010), by facilitating the perception of disparate features as a unified object (Gray, 1999; Engel and Singer, 2001), or by organizing the neural activity of local ensembles (O'keefe and Recce, 1993; Csicsvari et al., 2000; Fries, 2001; Dejean et al., 2016). Ongoing efforts aim to uncover the underlying principles by which different rhythms support brain operation.

A recent proposal suggests that different rhythms cooperate to change the dynamics of neuronal populations, thereby preparing the system for the ongoing task (see **Figure 1**). In this scheme, oscillations in different frequency bands may serve distinct functions. Slow (<8 Hz) oscillations seem to provide the temporal framework for sensory selection and encoding (Lakatos et al., 2008; Schroeder and Lakatos, 2009). Slow coherent oscillations between networks are thought to enhance effective communication between regions, as coherence increases in behaviorally relevant periods and predicts learning (Decoteau et al., 2007). During sleep, different low frequencies dominate during different phases (theta oscillations in the rapid-eye-movement (REM) phase, and slow waves in the delta (1–4 Hz) range in the non-REM phase), and seem to play complementary roles in memory consolidation (Diekelmann and Born, 2010; Buzsáki and Moser, 2013; Jacobs, 2014). Moreover, hippocampal theta phase coding, known as phase precession, has been suggested to organize the spike timing of individual neurons both locally and in distant brain regions (O'keefe and Recce, 1993; Jones and Wilson, 2005a; Van Der Meer and Redish, 2011). In addition, slow oscillations organize faster rhythms, reflected in phase-amplitude coupling, where each cycle of the slower rhythm provides a window-of-opportunity for faster beta/gamma oscillations. These rhythmic interactions have been implicated in spatial working memory performance and memory processing during sleep (Jones and Wilson, 2005a,b; Decoteau et al., 2007; Axmacher et al., 2010; Arnal et al., 2015; Antony et al., 2019). Alpha oscillations have been proposed to reflect suppression of irrelevant inputs (Klimesch et al., 2007), as pre-stimulus alpha power inversely correlates with firing rates and lower alpha in task-relevant regions predicts enhanced sensory perception (Thut, 2006; Haegens et al., 2011c; Van Kerkoerle et al., 2014), while concurrently, alpha power increases in task-irrelevant regions (Klimesch et al., 1999; Jensen et al., 2002). We recently suggested that beta oscillations reflect reactivation of neural ensembles when previously encoded information is required for subsequent processing steps such as decision making (Spitzer and Haegens, 2017). This model is in agreement with evidence of content-specific beta power modulations in multiple areas including the prefrontal cortex, which reflect task-relevant stimulus features maintained in working memory, and predict subsequent decision outcomes (Spitzer and Blankenburg, 2012; Haegens et al., 2017). Finally, gamma oscillations are suggested to reflect neural excitation, circuit engagement, and consequent amplification of input, given that sensory stimulation evokes gamma rhythms in sensory areas, and attending to different sensory stimuli increases evoked gamma power (Tiitinen et al., 1993; Fries, 2001; Bentley et al., 2016; Kim et al., 2016), predicts faster visual perception (Womelsdorf et al., 2006) and successful memory formation (Sederberg et al., 2006), and usually correlates with increased neural firing rates (Ray et al., 2008; Manning et al., 2009). This rhythm may also support precise inter-area communication, as gamma-synchronization increases during visual processing and cognitive tasks, and may support enhanced cognitive flexibility (Fries, 2009; Igarashi et al., 2014; Yamamoto et al., 2014; Cho et al., 2020; Fernández-Ruiz et al., 2021).

Thus, an important goal of studying oscillations is to understand their fundamental functional roles. Indeed, one of the main challenges of this endeavor is to identify the crucial parameters that define (or the level at which one could define) these roles. To do so, collecting evidence from different behavioral paradigms, brain regions, and species is crucial. In this regard, interesting evidence indicates that slower hippocampal oscillations organize faster rhythms and PFC cell assemblies, and predict memory consolidation across species (Louie and Wilson, 2001; Benchenane et al., 2010; Boyce et al., 2016; Schreiner et al., 2021). However, functionally equivalent oscillations can cross the traditional frequency boundaries, depending on the species, strain, or even individuals (Haegens et al., 2014; Tort et al., 2018a; Halgren et al., 2019). For example, while rodent hippocampal theta rhythms represent one of the most well-understood oscillations (Hasselmo, 2005), human hippocampal "theta" rhythms may actually fall in the delta range (Watrous et al., 2013; Jacobs, 2014). In mice, we recently found that the same stressor induced nucleus accumbens oscillations in the delta or the theta range depending on the strain, suggesting genetic differences play a role in frequency boundaries (Lowes et al., 2021). Similarly, some individuals, have beta oscillations that function the way alpha rhythms do in other individuals (Haegens et al., 2014). These examples argue that strictly adhering

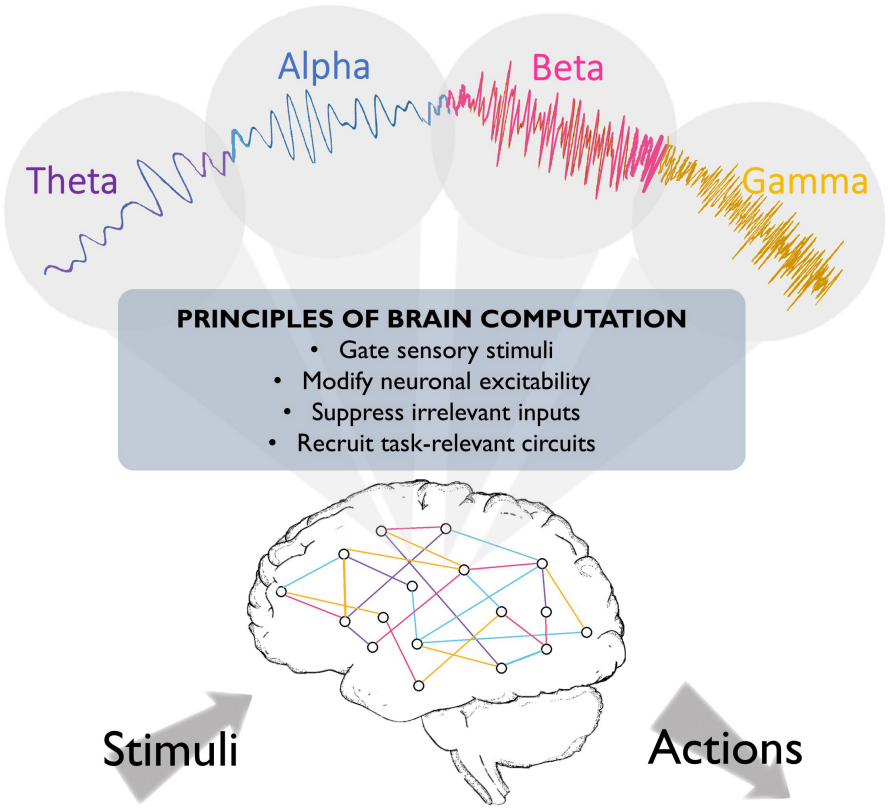

FIGURE 1 | Fundamental roles that oscillations may play in brain function. Brain oscillations have been implicated in crucial aspects of neural circuit activity, such as stimulus perception. They have also been suggested to play a role in top-down processing, such that different oscillations might emerge to engage task-relevant circuits and silence irrelevant information, thereby optimizing brain processing and behavioral performance.

to traditional frequency-based nomenclatures to describe brain rhythms may hinder efforts to address their functional role. Instead, rhythms arising from the same circuit and neuronal subpopulations may play a similar functional role across species while differing in their frequency, as has been suggested for hippocampal theta (Jacobs, 2014). Thus, we suggest that, when possible, studies should refer to oscillations by the circuit and conditions that elicit them, rather than simply by strict frequency ranges.

Developing this circuit-based taxonomy of oscillations requires better understanding of the underlying neural activity, but may help resolve seemingly contradictory functional consequences of oscillations (Shin et al., 2017; Lundqvist et al., 2018). For example, beta oscillations have been proposed to serve as an inhibitory mechanism in the sensorimotor system (Donner et al., 2009; Pogosyan et al., 2009). However, during working memory, beta oscillations in other regions including prefrontal cortex seem to reflect formation and endogenous reactivation of specific neuronal ensembles for subsequent processing, with conflicting evidence about whether it provides local inhibition or excitation (Haegens et al., 2011b; Spitzer and Haegens, 2017; Miller et al., 2018). Determining the neural populations that produce these respective beta oscillations may explain this apparent discrepancy. Prior efforts to dissect simultaneous rhythms using pharmacological interventions have helped unravel decades-lasting debates, such as the existence of at least two different hippocampal oscillations that emerge from different cell types during anesthesia and active exploration (Kramis et al., 1975), and are still used for dissecting the functional role of different hippocampal theta rhythms (Park et al., 2021).

These results highlight the utility of invasive, intracortical recordings, which provide better spatial resolution of the rhythmic activity (since they are less confounded by volume conduction) as well as measures of individual neuronal activity. Evaluating action potentials can reveal local influences of oscillations on the timing of neuronal spikes, which provides further evidence that the pertinent oscillation is not simply volume conducted (Shin et al., 2017; Lundqvist et al., 2018). Furthermore, this analysis can help address open questions such as the impact of beta oscillations on neuronal activity (Spitzer and Haegens, 2017; Lundqvist et al., 2018), or how the actual information is encoded (Romo et al., 1999; Barak et al., 2010; Vergara et al., 2016). Analysis of the relationship between firing rates and oscillations extended to long-range circuits can also provide strong evidence regarding the source of oscillatory activity, by identifying the neuronal populations that spontaneously fire at specific frequencies, thereby driving synchrony and generating oscillatory activity under different

circumstances. Some examples of successfully exploiting this relationship include the discovery of a subset of thalamocortical neurons with intrinsic burst firing that are implicated in the generation of alpha rhythms (Lorincz et al., 2008), the role of GABA neurons within the medial septum in generating hippocampal theta (Hangya et al., 2009), and of inhibitory interneurons in gamma oscillations (Whittington et al., 1995; Cardin et al., 2009; Sohal et al., 2009; Kim et al., 2016).

Ultimately, causal interventions manipulating neural populations can definitively demonstrate the neural origins of specific oscillations. This approach has the additional advantage of providing insight into the functional relevance of oscillations. As we will discuss below, such causal interventions are ushering in an exciting new era of neural oscillations research. These experiments require rodents – species that allows invasive experiments – and rest on two assumptions: (1) that the same behavioral tasks require similar neuronal circuits across different species; and (2) that involved neuronal circuits show similar oscillatory activity between species, when engaged in similar tasks. The first assumption has some long-standing evidence, such as the studies of the primary visual cortex and its role in visual processing across different species, pioneered in the early 19th century by anatomist Bartolomeo Panizza (Mazzarello and Sala, 1993). More recent studies include demonstrations that V1 neuronal activity is similarly modulated in visual perception tasks in humans (Tootell et al., 1998), rodents (Cone et al., 2020), and cats (Hua et al., 2010). However, the second assumption remains more controversial, as evidenced by the previously mentioned differences between hippocampal rhythms in mice and humans (Lisman and Idiart, 1995; Lisman and Jensen, 2013; Jacobs, 2014; Boyce et al., 2016; Vass et al., 2016). Given the inter-species [and inter-individual (Haegens et al., 2014)] variation in frequency discussed earlier, we propose that oscillation studies should be grounded in which behavioral conditions, neural circuits, neural subpopulations, or even ion channels (Kalmbach et al., 2018; Stagkourakis et al., 2018), elicit the oscillation. To do so, it will be critical to conduct carefully designed parallel human-murine studies which use equivalent tasks (Cavanagh et al., 2021), identify the human EEG source with sophisticated source localization algorithms (Michel and Brunet, 2019; Seeber et al., 2019) and/or functional imaging, and confirm similar neural population involvement with pharmacology when possible.

In summary, disentangling exactly how and where these rhythms are generated in the brain may provide more definitive evidence of what oscillations mean for brain processing, as well as how different circuits encode and route the information that is needed for specific behaviors and, in general, for an efficient interaction with the world.

Rhythms as a Window to Understand the Neuronal Circuits Underlying Behavior

A complementary approach to studying brain rhythms views the oscillations that accompany behavior as a tool that yields insight into the underlying neurons and circuits. The main goal of this approach is to understand the specific neuronal circuits and cellular populations that are necessary for different behaviors. As a result, state-induced oscillatory activity helps track activated areas and synchronized brain regions (Hultman et al., 2018; Schneider et al., 2021), to evaluate which neuronal populations drive the activity, and their impact on behavior (Harris and Gordon, 2015). Unlike the approach described above, these investigations are not driven by specific hypotheses about general functional roles of specific rhythms. Instead, what is key for this approach is tightly linking the oscillation to the specific behavior on the one hand, and to underlying neurons and circuits, on the other. Once there is evidence that oscillatory activity is related to a particular behavior, a key aspect of this approach is to evaluate the effect of the ongoing oscillatory activity in the firing rates of local or distant areas, to find the neural populations that are synchronized, i.e., phase locked, and/or modulated by the oscillations. This analysis makes it possible to identify the key circuit nodes within a larger network that underlie a given behavior as well as to determine which neurons mediate the neural activity that supports that behavior.

To illustrate this approach, recent studies using intracortical recordings have observed that low-frequency (2–7 Hz) oscillations emerge during stressful and anxiety-like conditions in many limbic areas such as the ventral tegmental area (VTA), nucleus accumbens (NAc), amygdala and prelimbic cortex (Kumar et al., 2014; Karalis et al., 2016; Lowes et al., 2021). These brain areas play crucial roles in mediating such disparate consequences of stress as decreased reward seeking and fear-induced freezing. Investigating the circuit basis of these rhythms in different behavioral contexts reveals that the low-frequency rhythm that accompanies stress-induced deficits in reward seeking reflects VTA to NAc circuit activity (Lowes et al., 2021). By contrast, freezing behavior co-occurs with a synchronization of prelimbic cortex and amygdala (Lesting et al., 2011; Likhtik et al., 2014; Stujenske et al., 2014; Karalis et al., 2016). Interestingly, this cortico-amygdala synchrony may arise from respiration-induced activity in the olfactory bulb (Ito et al., 2014; Tort et al., 2018a; Bagur et al., 2021), while the VTA-NAc does not correlate with respiration (Lowes et al., 2021). These examples illustrate how oscillations can help identify the unique circuits relevant to particular behaviors. As can be seen from these examples, the same frequency range may reflect different circuit activity with different behavioral consequences. Indeed, different researchers have published competing interpretations of which circuits produce this frequency range activity (Roy et al., 2017; Tort et al., 2018b). Fortunately, spatially precise manipulations allow us to dissect the different circuits that yield similar frequency oscillations and determine different aspects of behavior.

USING CAUSAL INTERVENTIONS TO INTERROGATE THE ROLE OF NEURAL OSCILLATIONS

While current efforts provide a better insight into how different oscillations may function together to tune different task-relevant

BOX 1 | Optogenetics refers to a combination of biological techniques that makes it possible to use light to control cell physiology (Fenno et al., 2011). Using genetic engineering methods, transmembrane light-sensitive proteins (known as opsins) are artificially expressed in the cells of interest. Opsins covalently bind a specific molecule – chromophore – which, upon photon absorption, transiently changes its conformation and allows ions to pass through the plasma membrane, thereby regulating the electrical activity of the cell. This technique can be applied to nearly every cell type, either by a viral delivery of the opsin gene, or by generating transgenic lines that express the opsin with the promoter of a gene of interest. The major role that electrical activity plays in generating action potentials has made optogenetics especially applicable for neuronal activity manipulation. Optogenetics pioneer Karl Deisseroth and colleagues first generated light-evoked neuronal spikes *ex vivo* in 2005, by (1) modifying a lentivirus to contain a opsin gene, originally from unicellular algae, (2) infecting a rat hippocampal cell culture with the virus, and (3) inducing rapid depolarizing currents that trigger action potentials with blue light pulses (Boyden et al., 2005). The first successful *in vivo* study with a mouse line expressing opsins in the central nervous system came a few years later, showing that this technique can reliably generate firing rates as high as 40 Hz in individual neurons of the olfactory bulb (Arenkiel et al., 2007). Since then, this technique has become very powerful, as it can be implemented in awake, behaving rodents, and combined with electrophysiology probes or neurotransmitter sensors (Cardin et al., 2010; Kim et al., 2017). Opsins modulate neural activity with high temporal and spatial resolution, which ultimately depend on the opsin type, light source, and tissue characteristics. See Boyden (2011) for an in-depth historical overview on the field, and (Yizhar et al., 2011) for a comprehensive technical review of this rapidly developing field and its main challenges.

Briefly, optogenetic stimulation involves the expression of an ion channel that in response to light opens and lets multiple cations diffuse into the cytosol, evoking neuronal depolarization and triggering action potentials. The most used excitatory opsin is the channelrhodopsin, which responds to blue light. Currently, there are multiple excitatory opsins that display different photocurrent amplitudes and kinetics and can be activated with different light wavelengths. For example, stable step-function or bi-stable opsins have an increased open-state lifetime of several minutes, allowing long periods of a higher-rate spontaneous spiking pattern of defined neurons (Yizhar et al., 2011). Other examples are Chronos, with faster kinetic parameters; and Chrimson, which activation spectrum is substantially red-shifted (Klapoetke et al., 2014).

Optogenetic inhibition, in contrast, is used to hyperpolarize the neurons and silence them with light. This hyperpolarization is attained through the expression of ion pumps that respond to green-yellow light, either pumping chloride anions inside the cell (halorhodopsins) or pumping protons out (archaerhodopsins) (Zhang et al., 2007). Similarly to the stimulation approach, these opsins have been engineered to achieve enhanced performance, such as eNpHR, which has increased photocurrent amplitudes (Gradinaru et al., 2008).

Crucially, the expression of the opsins can be restricted to different cell populations by using gene-targeting technology such as specialized mouse lines. These mice lines have been engineered to express a gene-editing enzyme (Cre recombinase) under cell-specific promoters [such as glutamate transporter or choline acetyltransferase (Borgius et al., 2010; Rossi et al., 2011)]. This enzyme binds specific gene sequences, called loxP sites, and rearranges any DNA fragments that are flanked between two loxP sites. This technology allows a viral vector to deliver active opsins selectively to the cells with the promoter of interest, allowing regional and cell subtype specific manipulation of neuronal activity.

brain circuits underlying the complex computations that guide behavior, several outstanding questions remain. First, are these oscillations necessary for the proposed neural function? Second, does the oscillatory activity cause the behavioral effect? Third, which neural elements underlie an oscillation in a given behavioral condition? As different oscillations seem to have opposite effects on neuronal activity, suggesting that they might differ in their underlying neuronal circuits, it is crucial to identify their neurophysiological underpinnings. In the following section, we will highlight new approaches to tackle these questions using optogenetics (see **Box 1**), which makes it possible to manipulate specific local oscillatory dynamics with high temporal and spatial precision (Boyden et al., 2005; Adamantidis et al., 2007; Zhang et al., 2007). We aim to provide a roadmap for evaluating the theories regarding functional/mechanistic roles of oscillations in awake-behaving animal models.

Addressing Oscillations With Optogenetics

Whether certain oscillations are required for behavioral output is a topic that still generates strong debate (Doelling and Assaneo, 2021). For many decades, lesion and pharmacological experiments in rodents, as well as observational studies of neurological and psychiatric patients, provided indirect evidence for the potential causal role of oscillations (Mitchell et al., 1982; Schnitzler and Gross, 2005; Haenschel et al., 2009; Mccarthy et al., 2011; Buzsáki and Moser, 2013). Now, with the emergence of optogenetic tools, we can inhibit or activate the neuronal population underlying a particular oscillatory activity with sufficient temporal precision to assess direct impact on behavior. Combined with electrophysiological measures of summed (LFP) and individual (single unit) neuronal activity, this approach provides an ideal framework to test whether these oscillatory dynamics are causally related to ongoing behavior, and whether functional accounts of specific rhythms hold up (see **Box 2**). A search of the literature reveals that since the introduction of optogenetic methods for manipulating neurons in 2005, 271 papers have been published applying this approach to investigating oscillations, which are split between 85% dissections of the neural circuitry underlying oscillations and 15% investigations of the function of oscillations (**Figure 2**).

To illustrate using optogenetics to link behaviorally relevant oscillations with the neural circuitry underlying them, we will describe the approach we recently took to unravel a slow oscillatory activity associated with stress in mice. The power of low-frequency rhythms increase in multiple brain regions during fear-inducing and stressful situations (Kumar et al., 2014; Karalis et al., 2016). We recently found that acute stress-induced low oscillations in the nucleus accumbens (NAc) predict subsequent deficits in reward seeking, and that NAc neurons whose firing rates decrease during the stressor are tightly synchronized with the oscillation, suggesting that the oscillation reflects a net inhibitory input to the area (Lowes et al., 2021). Subsequent coherence and directionality analyses demonstrate that the ventral tegmental area (VTA), a key component of reward processing circuitry, synchronizes at 2–7 Hz with the NAc during stress. Ultimately, optogenetic inhibition demonstrated the necessity of VTA activity for both the stress-induced oscillation and subsequent blunted reward seeking. Interestingly, this approach revealed that VTA

BOX 2 | Illustrative example of an experimental design and data analysis for dissecting the circuit underlying a behaviorally relevant oscillation.

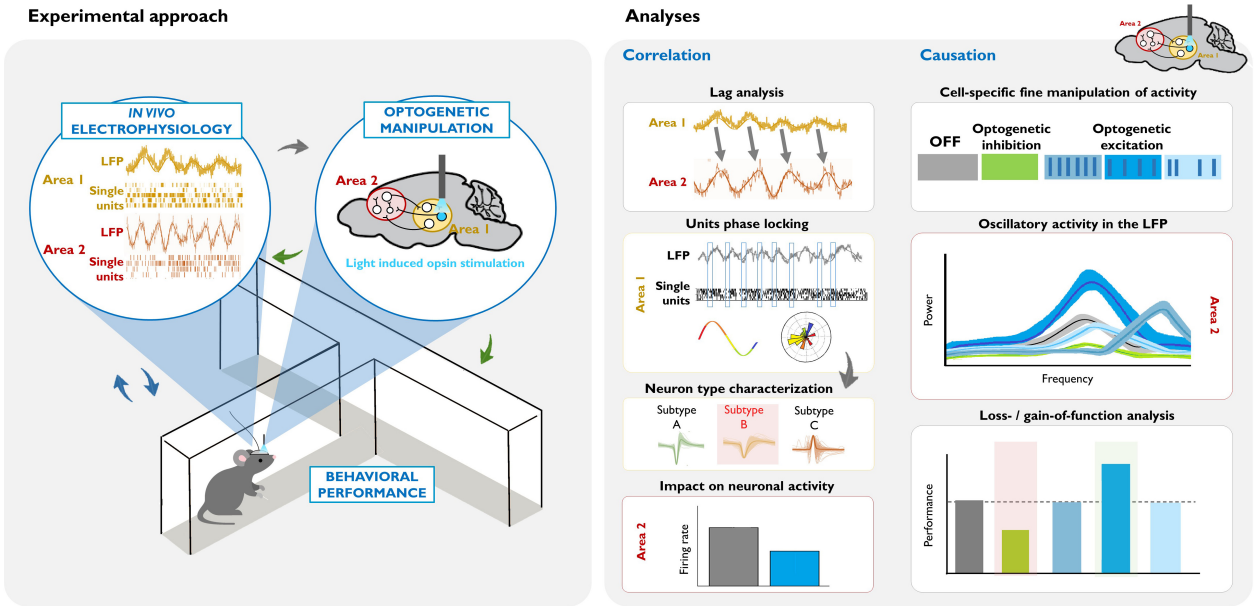

Left: Combining *in vivo* invasive electrophysiological recordings in awake-behaving rodents with cell-type specific optogenetic manipulation. Oscillatory activity (in the LFP or single unit recordings) is correlated with particular behaviors or states (blue arrows). The virus, opsin type, mouse model, area, and pattern of the optogenetic manipulation are chosen based on this neural activity and the goals of the study (gray arrow). Crucially, the consequences of these causal manipulations of neuronal activity are evaluated, in terms of electrophysiological measurements in the area(s) of interest, and their behavioral correlates (green arrows).

Right: Summary of commonly used analyses for dissecting the circuits and neuronal populations underlying a task-relevant oscillation. *Correlation studies:* In this example, lag analysis of the LFP of two areas shows that past oscillatory activity in Area 1 predicts the future oscillatory activity of Area 2 (see the shift in the phase, and that the frequency of the LFP signal is similar). Phase locking analysis of Area 1 activity demonstrates that there is entrainment of local single units, such that they fire at a specific phase of the oscillation. Subsequent analysis of different action potential parameters within the phase-locked neurons (gray arrow) can help identify a putative neuronal subtype that drives the oscillation. Measuring net firing rates in Area 2 can help identify whether the oscillation reflects global excitatory or inhibitory input. *Causation studies:* Once there is evidence suggesting that a specific cell subtype causes the oscillation, different optogenetic approaches can be used in order to demonstrate the necessity and/or sufficiency of that cell type for the oscillation, and in turn, for the particular behavior. In this example, optogenetic inhibition of the cell inhibits the naturally occurring oscillatory activity in Area 2, and decreases behavioral performance (see green vs. gray data in the graphics). Optogenetic excitation allows for precise control of the neuronal activity. Here, we illustrate three patterns of stimulation: higher frequency rhythmic, lower frequency rhythmic, and arrhythmic. In this example, lower frequency rhythmic is the only pattern that produces an oscillation of a similar frequency (see the similar position of the bright blue and gray peaks at the frequency axis), and evokes a behavioral output.

inhibitory GABA neurons—and not dopaminergic neurons—decreased NAc stress-induced 2–7 Hz oscillatory power and restored reward-seeking behavior. This work provides an example of how optogenetic experiments can demonstrate the neural populations necessary for generating oscillations, and the impact of those neural populations on behavior. Demonstrating that the 2–7 Hz rhythm itself causes decreased reward-seeking behavior requires stimulation experiments (discussed below and in **Box 2**).

Notably, this example of stress-induced slow rhythms falls into the general category of supporting long-range network interactions. Slow oscillations have been suggested to synchronize distant areas (Jiang et al., 2017), and to organize the spiking of neurons across long-range circuits (Lisman and Idiart, 1995; Buzsáki, 2005; Benchenane et al., 2010; Reddy et al., 2021). Interestingly, in the case of VTA-NAc stress-induced oscillations, the synchronization reflects a net inhibitory influence. By contrast, low frequency oscillations in the low theta range are also observed in the prefrontal cortex (PFC) and ventral hippocampus (vHip) during anxiogenic conditions (Adhikari et al., 2010). In that situation, however, vHip theta oscillations do not affect the net firing rates within the PFC. Instead, optogenetic inhibition revealed that excitatory neurons from vHip that project to the PFC are necessary for theta synchrony, reorganizing PFC neuronal firing in order to modulate anxiety-like behavior (Padilla-Coreano et al., 2016).

These examples illustrate how optogenetic inhibition studies can identify the neural substrates of oscillatory activity underlying different aspects of behavior. These experiments also reveal the impact of the oscillation on local firing (e.g., modulating firing *rate* versus *timing*) as well as the specific neural subpopulation necessary for generating the oscillation. This approach has recently been exploited to show that different subpopulations of GABA interneurons in the primary visual cortex, such as parvalbumin- and somatostatin- containing neurons, are needed for spontaneous and visually induced gamma oscillations, respectively (Chen et al., 2017; Veit et al., 2017). In fact, optogenetic dissection of the neural basis of oscillations underlying behavior has become increasingly sophisticated, identifying the ion channels that confer

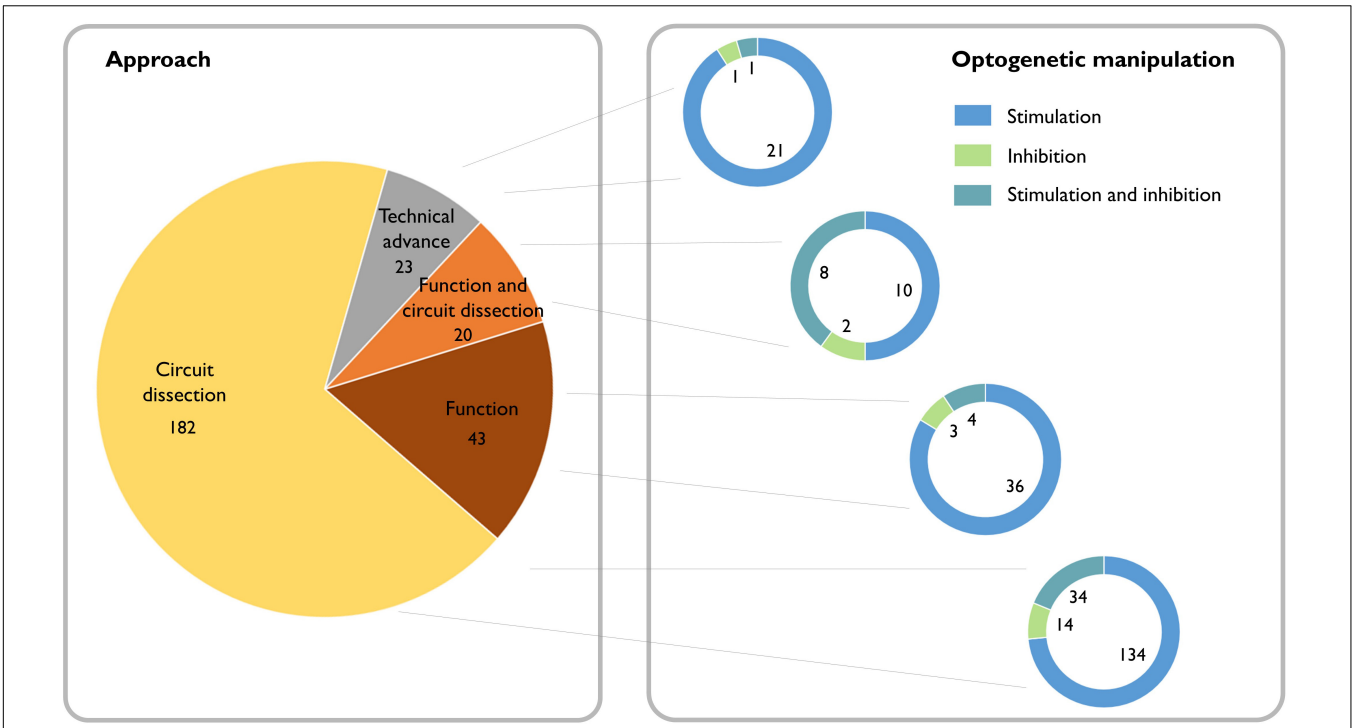

FIGURE 2 | Literature review of the causal role of neuronal oscillations. Left: Searching PubMed with the terms "(oscillation OR oscillations) AND (optogenetics OR halorhodopsin OR archaerhodopsin OR channelrhodopsin)" from 2004 to the present yielded 377 papers. Of these, 49 did not address neural oscillations, 37 were review articles, 17 were computational/modeling-based, five did not make use of optogenetics, and one was a corrigendum. We classified the remaining 268 scientific articles containing experimental data based on whether the experiments addressed dissecting circuits, the function of oscillations, or neither (purely technical). Right: We further classified the papers based on whether they used optogenetic stimulation or inhibition and found that independent of the scientific question, optogenetic stimulation is the most broadly used technique.

rhythmicity (Ludwig et al., 1998; Varga et al., 2008; Vesuna et al., 2020), and impact specific behaviors (Vesuna et al., 2020).

While optogenetic inhibition is an ideal approach to determine the necessity of specific neurons and circuits for different behavioral outputs, it leaves open the question of whether the oscillations are sufficient to cause the behavior. Moreover, inhibition experiments often modulate multiple frequency bands at once, making it difficult to demonstrate that a particular rhythm is necessary for a given task. Along similar lines, it is difficult to disentangle whether behavioral changes result from decreased rhythmic activity *per se*, as opposed to a frequency-independent decrease of neuronal activity. For these reasons, optogenetic activation is a more appropriate technique to determine whether certain rhythms affect performance in a frequency-specific manner.

With optogenetic stimulation one can manipulate neuronal firing in a frequency-specific manner to create artificial oscillatory activity and evaluate the impact on behavior. For example, 4-Hz periodic stimulation of NAc-projecting VTA neurons was sufficient to recapitulate the low frequency NAc oscillations and subsequent reward seeking deficits observed in animals subjected to stress, whereas stimulating the same neurons at a faster rhythm (20 Hz) did not reproduce this phenotype (Lowes et al., 2021). Similarly, stimulating hippocampal terminals in the PFC with sinusoidal 8-Hz, but not 2- or 20-Hz, stimulation increased anxiety-like behavior (Padilla-Coreano et al., 2019). An important additional experiment to demonstrate that the rhythm causes the behavior would be to assess the effect of non-rhythmic stimulation of the same cells (see **Box 2**). These examples highlight the importance of recording the rhythmic circuit activity associated with a given behavior before using optogenetic manipulations to determine if that circuit is necessary for the behavior.

Nonetheless, optogenetic stimulation also has its limitations. Even when stimulating at a physiological frequency, it remains unclear whether optogenetic stimulation recapitulates the natural activity of neurons, or whether it elicits an artificial activity pattern that the neurons would otherwise never engage in. For example, while sinusoidal 8-Hz stimulation of vHip-PFC projections increased anxiety-like behavior, stimulating at the same frequency with pulses of light did not (Padilla-Coreano et al., 2019). Similarly, optogenetic activation of cells that encoded a shock-paired context within the dentate gyrus of the hippocampus elicited fear responses in a novel context, demonstrating a false memory recall (Ramirez et al., 2013). However, non-specific stimulation of the same area disrupts the fear memory encoding and recall (Kheirbek et al., 2013). When reconciling findings across optogenetic studies, it is important to consider technical aspects such as suboptimal

expression of opsins or poor light penetration (see Yizhar et al., 2011 for review). However, it is likely that gain-of-function experiments can be best achieved by faithfully replicating the activity of circuits and neuronal downstream machinery of the naturally occurring oscillations. In fact, recent studies took advantage of this need for coordinated rhythmic activity across a long-range circuit to demonstrate that uncoordinated gamma-frequency stimulation disrupted behavioral performance (Fernández-Ruiz et al., 2021), whereas gamma synchrony between hemispheres is needed for tasks that require updating strategies (Cho et al., 2020). Crucially, optogenetic stimulation studies usually modify the firing rates of the stimulated neurons, thus failing to unequivocally prove that the generated rhythm rather than the altered firing is sufficient to modify behavior. While these two phenomena are difficult to disentangle, recent *in vitro* work has shown how distinct neuronal subtypes differently encode rate and rhythm information (Prince et al., 2021). Similar *in vivo* experiments assessing the effects of non-rhythmic, matched-rate, optogenetic stimulation on behavior can further help disentangle these factors (**Box 2**).

It is worth noting that oscillation-induced changes in behavior may not necessarily occur during the rhythmic activity. For example, we found that stress-induced oscillations led to changes in reward-seeking behavior for as long as 1 h after the activity had stopped (Lowes et al., 2021). This finding raises the intriguing possibility that some oscillations may represent network/circuit implementations of changes in synaptic plasticity, which are crucial for memory and learning (see Neves et al., 2008 for a review). Indeed, we recently showed that exposing mice to a novel environment induces a theta rhythm in the ventral hippocampus that weakens synaptic strength between the ventral hippocampus and medial prefrontal cortex, but facilitates both learning and optogenetic induction of long-term potentiation, a form of synaptic plasticity (Park et al., 2021). Interestingly, delta oscillations during sleep have been proposed as a homeostatic mechanism to rescale the potentiation in synaptic strength that occurs with prolonged wakefulness (Tononi and Cirelli, 2003). This mechanism is disrupted in patients with depressive disorders, possibly leading to the cognitive impairments seen in this population (Goldschmied and Gehrman, 2019). Optogenetic manipulations of delta rhythms during sleep and subsequent tests of synaptic plasticity (both *in vitro* and *in vivo*) provide exciting opportunities to test these hypotheses (Durkin et al., 2017).

Testing the hypothesis that slow wave oscillations during sleep modulate plasticity represents an example of using optogenetic manipulations to test the functional, rather than circuit-specific, role of oscillations. The application of optogenetics to understanding the functions of oscillations has lagged behind circuit-dissection approaches (see **Figure 2**) but has recently produced some exciting results. Of clinical interest, disruptions in gamma rhythms have been linked to cognitive disorders (Mably and Colgin, 2018) and gamma-frequency stimulation has been shown to improve cognitive impairments in genetic animal models of mental diseases (Cho et al., 2015, 2020; Iaccarino et al., 2016; Cao et al., 2018; Etter et al., 2019). From a more conceptual perspective, a recent study provided evidence that gamma coherence supports inter-area communication by showing that selectively perturbing gamma, but not theta oscillations, in different entorhinal cortical inputs to the hippocampus disrupts the information provided by the respective input (Fernández-Ruiz et al., 2021). Similarly, recent work demonstrated that simultaneous bilateral gamma stimulation, but not asynchronous or non-gamma frequency stimulation, increased gamma synchrony and restored cognitive flexibility (Cho et al., 2020). In contrast, another recent study used optogenetic manipulations and modeling to argue that long-range coherence simply reflects, but does not directly contribute to, communication between brain areas (Schneider et al., 2021). While these studies are unlikely to resolve this long-standing debate (Singer, 2018), they lay the groundwork for future experiments that interrogate the role of oscillations in circuit communication during behavior with optogenetic interventions. More broadly, these studies point the way for future research testing other hypotheses about the role of oscillations. For example, one could test the hypothesis that the alpha rhythm functionally inhibits irrelevant input by designing a task where one set of cues (e.g., visual stimuli) predict reward, while another set of cues (e.g., auditory stimuli) act as distractors. This experimental setup should show increased alpha oscillations in the distractor-cue sensory cortex, with corresponding decreases in firing rates. Crucially, optogenetically inhibiting the neural elements that generate alpha in the distractor-cue sensory cortex, or imposing a non-rhythmic firing pattern, would reveal its role in the task performance. Experiments using optogenetic manipulations during gamma oscillations have provided evidence that gamma oscillations enhance the processing of otherwise less salient stimuli (Siegle et al., 2014; Li et al., 2015; Ni et al., 2016). A similar approach can help resolve the functional role of beta oscillations during working memory, by revealing whether disrupting beta oscillations disinhibits the circuit or prevents the reactivation of information-encoding ensembles. A crucial consideration that is often neglected when using optogenetics to investigate the role of an oscillation in behavior, is that any intervention that changes the behavior may alter the oscillation indirectly (i.e., the optogenetic manipulation puts the animal into a new behavioral state that in turn impacts the oscillation). An important control for this confound is to conduct optogenetic manipulations that impact the oscillation without changing behavior (for example, unilateral inhibition in behavior that requires both hemispheres).

METHODOLOGICAL ADVANCES

As previously noted, human oscillation research has largely relied on M/EEG recordings, which may mostly reflect cortical activity. By contrast, invasive recordings in rodents have revealed subcortical rhythms. Moreover, cell-type specific optogenetic manipulations have demonstrated multiple overlapping sources for oscillations. While intracranial recordings have provided

important insights regarding the relationship between different oscillatory frequencies and firing rates (Manning et al., 2009) or the influence of oscillations on single-neuron spike timing (Jacobs et al., 2007), there is a critical need for simultaneous EEG and intracranial recordings, preferably incorporating optogenetic interventions to help identify the circuits associated with oscillations observed extracranially. This data could in turn inform analytic efforts to improve source localization (Michel and Brunet, 2019; Seeber et al., 2019).

The recognition that oscillatory frequency can vary across subjects has also prompted advances in analytic methods. Historically, oscillations have been identified by decomposing the recorded signal into sinusoids of different frequencies and then computing their amplitude and frequency properties. Power tends to decrease with frequency (following a 1/f pattern), so to distinguish between true oscillations versus aperiodic changes in power, oscillations are typically identified as narrowband peaks in power above the non-oscillatory 1/f activity. However, changes in 1/f activity across development, species, or pathological conditions (Voytek et al., 2015; Peterson et al., 2017; Dave et al., 2018), frequency peak shifts with aging, clinical conditions, and GABA concentrations (Muthukumaraswamy et al., 2009; Haegens et al., 2014; Furman et al., 2018; Bódizs et al., 2021), changes in the rate of transient oscillatory events (Shin et al., 2017), or non-sinusoidal rhythms (Cole and Voytek, 2017), all can affect the estimation of oscillatory power. Ongoing efforts focused on improving current analytical methods for studying brain oscillations (Donoghue et al., 2020) show promise in developing estimates of neural activity frequency that account for individual differences.

Finally, as noted above, optogenetic stimulation can induce synaptic plasticity (Zhang and Oertner, 2007). Thus, an important consideration to take into account when incorporating optogenetic interventions into dissecting the function of oscillations, is that optogenetic interventions might themselves modulate circuit connectivity and impact behavior for this reason.

FUTURE DIRECTIONS

In conclusion, optogenetic interventions show great promise in determining the functional consequence of oscillations. Here we suggest experimental advances to improve investigations of the necessity and sufficiency of rhythmic activity.

First, naturally occurring oscillations are often short-lived. Even when the pacemaker neurons that drive the rhythm are found, finding the temporal window(s) during which they set the pace and evoke a behavioral output can be difficult. "Closed-loop" optogenetic control of neurons based on ongoing activity was suggested several years ago (Grosenick et al., 2015), and has proven efficient at controlling seizures in rodents (Sorokin et al., 2017; Hristova et al., 2021). This approach could be used for manipulating neuronal activity selectively during relevant periods, such as when a specific oscillatory power exceeds or goes below a critical value (Van De Ven et al., 2016; Nicholson et al., 2018). This approach effectively impacts memory consolidation when applied to ongoing gamma oscillations in the amygdala region (Kanta et al., 2019), but studies on other frequencies are lacking. This technique is particularly suitable for addressing the role of oscillations, as it tightens the causal relationship between the neural activity and behavior-associated oscillations by minimizing non-specific stimulation.

Second, optogenetic studies comparing arrhythmic versus rhythmic stimulation patterns can provide useful information about whether increased neuronal activity is sufficient to impact behavior, or whether rhythmicity is required instead. This comparison would also be useful to assess how asynchronous activity of specific neurons impact broadband spectral power, and whether specific frequency bands are preferentially affected by changes in firing rate.

Third, as previously discussed, coherent oscillations between distant areas arise during different brain processes. A recent framework postulates that coherence mainly appears because spiking activity in the sending area causes post-synaptic potentials in other areas, reflecting anatomical connectivity (Schneider et al., 2021). Experiments examining the impact of synchronous vs. asynchronous optogenetic stimulation in two areas on neural coherence and task performance can provide evidence for the role of rhythmic activity in supporting inter-area communication, and the functional relevance of this connectivity. This approach has been successfully exploited to demonstrate the key role of prefrontal gamma coherence in rule updating tasks (Cho et al., 2020). Future studies using this approach with other task-relevant rhythms would advance the field.

Lastly, parallel studies comparing observations in rodents and humans are crucial for advancing the field. Specially, the combination of human non-invasive EEG or intracranial EEG, and invasive recordings with optogenetic manipulations in rodents can provide comprehensive information of relevant oscillations from the macro- to the micro-level, i.e., identifying the physiological properties, principal neurons, and proteins implicated in the generation of specific rhythms. A recently published study, which investigated the role of posteromedial 1–3 Hz rhythm in eliciting dissociative states (Vesuna et al., 2020), demonstrates with an unprecedented level of detail, the biophysical basis of a clinically relevant rhythm. Taking a similar approach to other brain oscillations will allow us to systematically resolve important outstanding questions such as how different oscillations are generated within different brain regions (Buzsaki and Wang, 2012; Colgin, 2013), how local is the LFP (Kajikawa and Schroeder, 2011; Herreras, 2016), and what function do oscillations play at the neurocomputational and behavioral levels. Doing so could additionally help disentangle rhythms implicated in pathological states, providing the basis for future treatments or new approaches to brain-related diseases.

AUTHOR CONTRIBUTIONS

II-L, SH, and AZH wrote the manuscript. SH and AZH provided funding. All authors contributed to the article and approved the submitted version.

FUNDING

This work was supported by grant from the NIMH to AZH (R01 MH124998-01A1) and SH (R01 MH123679).

ACKNOWLEDGMENTS

We would like to thank Jennifer Goldschmied, Nancy Padilla-Coreano, and Joseph Stujenske for their helpful feedback.

REFERENCES

Adamantidis, A. R., Zhang, F., Aravanis, A. M., Deisseroth, K., and De Lecea, L. (2007). Neural substrates of awakening probed with optogenetic control of hypocretin neurons. *Nature* 450, 420–424. doi: 10.1038/nature06310

Adhikari, A., Topiwala, M. A., and Gordon, J. A. (2010). Synchronized activity between the ventral hippocampus and the medial prefrontal cortex during anxiety. *Neuron* 65, 257–269. doi: 10.1016/j.neuron.2009.12.002

Antony, J. W., Schönauer, M., Staresina, B. P., and Cairney, S. A. (2019). Sleep Spindles and Memory Reprocessing. *Trends Neurosci.* 42, 1–3. doi: 10.1016/j.tins.2018.09.012

Arenkiel, B. R., Peca, J., Davison, I. G., Feliciano, C., Deisseroth, K., Augustine, G. J., et al. (2007). In Vivo Light-Induced Activation of Neural Circuitry in Transgenic Mice Expressing Channelrhodopsin-2. *Neuron* 54, 205–218. doi: 10.1016/j.neuron.2007.03.005

Arnal, L. H., Doelling, K. B., and Poeppel, D. (2015). Delta-Beta Coupled Oscillations Underlie Temporal Prediction Accuracy. *Cereb. Cortex* 25, 3077–3085. doi: 10.1093/cercor/bhu103

Axmacher, N., Henseler, M. M., Jensen, O., Weinreich, I., Elger, C. E., and Fell, J. (2010). Cross-frequency coupling supports multi-item working memory in the human hippocampus. *Proc. Natl. Acad. Sci.* 107, 3228–3233. doi: 10.1073/pnas.0911531107

Bagur, S., Lefort, J. M., Lacroix, M. M., De Lavilléon, G., Herry, C., Chouvaeff, M., et al. (2021). Breathing-driven prefrontal oscillations regulate maintenance of conditioned-fear evoked freezing independently of initiation. *Nat. Commun.* 12:2605. doi: 10.1038/s41467-021-22798-6

Barak, O., Tsodyks, M., and Romo, R. (2010). Neuronal Population Coding of Parametric Working Memory. *J. Neurosci.* 30, 9424–9430. doi: 10.1523/JNEUROSCI.1875-10.2010

Benchenane, K., Peyrache, A., Khamassi, M., Tierney, P. L., Gioanni, Y., Battaglia, F. P., et al. (2010). Coherent Theta Oscillations and Reorganization of Spike Timing in the Hippocampal- Prefrontal Network upon Learning. *Neuron* 66, 921–936. doi: 10.1016/j.neuron.2010.05.013

Bentley, W. J., Li, J. M., Snyder, A. Z., Raichle, M. E., and Snyder, L. H. (2016). Oxygen Level and LFP in Task-Positive and Task-Negative Areas: Bridging BOLD fMRI and Electrophysiology. *Cereb. Cortex* 26, 346–357. doi: 10.1093/cercor/bhu260

Berger, H. (1929). Über das Elektrenkephalogramm des Menschen. *Archiv für Psychiatrie Nervenkrankheiten* 87, 527–570.

Bishop, G. H. (1932). CYCLIC CHANGES IN EXCITABILITY OF THE OPTIC PATHWAY OF THE RABBIT. *Am. J. Physiol. Legacy Content* 103, 213–224. doi: 10.1152/ajplegacy.1932.103.1.213

Bódizs, R., Szalárdy, O., Horváth, C., Ujma, P. P., Gombos, F., Simor, P., et al. (2021). A set of composite, non-redundant EEG measures of NREM sleep based on the power law scaling of the Fourier spectrum. *Sci. Rep.* 11, 2041–2041. doi: 10.1038/s41598-021-81230-7

Borgius, L., Restrepo, C. E., Leao, R. N., Saleh, N., and Kiehn, O. (2010). A transgenic mouse line for molecular genetic analysis of excitatory glutamatergic neurons. *Mol. Cell. Neurosci.* 45, 245–257. doi: 10.1016/j.mcn.2010.06.016

Boyce, R., Glasgow, S. D., Williams, S., and Adamantidis, A. (2016). Causal evidence for the role of REM sleep theta rhythm in contextual memory consolidation. *Science* 352, 812–816. doi: 10.1126/science.aad5252

Boyden, E. S. (2011). A history of optogenetics: the development of tools for controlling brain circuits with light. *F1000 Biol. Rep.* 3:11. doi: 10.3410/B3-11

Boyden, E. S., Zhang, F., Bamberg, E., Nagel, G., and Deisseroth, K. (2005). Millisecond-timescale, genetically targeted optical control of neural activity. *Nat. Neurosci.* 8, 1263–1268. doi: 10.1038/nn1525

Buzsáki, G. (2005). Theta rhythm of navigation: Link between path integration and landmark navigation, episodic and semantic memory. *Hippocampus* 15, 827–840. doi: 10.1002/hipo.20113

Buzsaki, G., Anastassiou, C. A., and Koch, C. (2012). The origin of extracellular fields and currents–EEG, ECoG, LFP and spikes. *Nat. Rev. Neurosci.* 13, 407–420. doi: 10.1038/nrn3241

Buzsáki, G., and Moser, E. I. (2013). Memory, navigation and theta rhythm in the hippocampal-entorhinal system. *Nat. Neurosci.* 16, 130–138. doi: 10.1038/nn.3304

Buzsaki, G., and Wang, X. J. (2012). Mechanisms of gamma oscillations. *Annu. Rev. Neurosci.* 35, 203–225.

Cao, W., Lin, S., Xia, Q.-Q., Du, Y.-L., Yang, Q., Zhang, M.-Y., et al. (2018). Gamma Oscillation Dysfunction in mPFC Leads to Social Deficits in Neuroligin 3 R451C Knockin Mice. *Neuron* 97, 1253.e–1260.e.

Cardin, J. A., Carlén, M., Meletis, K., Knoblich, U., Zhang, F., Deisseroth, K., et al. (2009). Driving fast-spiking cells induces gamma rhythm and controls sensory responses. *Nature* 459, 663–667. doi: 10.1038/nature08002

Cardin, J. A., Carlén, M., Meletis, K., Knoblich, U., Zhang, F., Deisseroth, K., et al. (2010). Targeted optogenetic stimulation and recording of neurons in vivo using cell-type-specific expression of Channelrhodopsin-2. *Nat. Protoc.* 5, 247–254. doi: 10.1038/nprot.2009.228

Cavanagh, J. F., Gregg, D., Light, G. A., Olguin, S. L., Sharp, R. F., Bismark, A. W., et al. (2021). Electrophysiological biomarkers of behavioral dimensions from cross-species paradigms. *Translat. Psychiat.* 11:482. doi: 10.1038/s41398-021-01562-w

Chen, G., Zhang, Y., Li, X., Zhao, X., Ye, Q., Lin, Y., et al. (2017). Distinct Inhibitory Circuits Orchestrate Cortical beta and gamma Band Oscillations. *Neuron* 96, 1403.e–1418.e. doi: 10.1016/j.neuron.2017.11.033

Cho, K. K. A., Davidson, T. J., Bouvier, G., Marshall, J. D., Schnitzer, M. J., and Sohal, V. S. (2020). Cross-hemispheric gamma synchrony between prefrontal parvalbumin interneurons supports behavioral adaptation during rule shift learning. *Nat. Neurosci.* 23, 892–902. doi: 10.1038/s41593-020-0647-1

Cho, K. K. A., Hoch, R., Lee, A. T., Patel, T., Rubenstein, J. I. R., and Sohal, V. S. (2015). Gamma Rhythms Link Prefrontal Interneuron Dysfunction with Cognitive Inflexibility in Dlx5/6+/−Mice. *Neuron* 85, 1332–1343. doi: 10.1016/j.neuron.2015.02.019

Cole, S. R., and Voytek, B. (2017). Brain Oscillations and the Importance of Waveform Shape. *Trends Cognit. Sci.* 21, 137–149. doi: 10.1016/j.tics.2016.12.008

Colgin, L. L. (2013). Mechanisms and functions of theta rhythms. *Annu. Rev. Neurosci.* 36, 295–312. doi: 10.1146/annurev-neuro-062012-170330

Cone, J. J., Bade, M. L., Masse, N. Y., Page, E. A., Freedman, D. J., and Maunsell, J. H. R. (2020). Mice Preferentially Use Increases in Cerebral Cortex Spiking to Detect Changes in Visual Stimuli. *J. Neurosci.* 40, 7902–7920. doi: 10.1523/JNEUROSCI.1124-20.2020

Csicsvari, J., Hirase, H., Mamiya, A., and Buzsáki, G. (2000). Ensemble patterns of hippocampal CA3-CA1 neurons during sharp wave–associated population events. *Neuron* 28, 585–594. doi: 10.1016/s0896-6273(00)00135-5

Dave, S., Brothers, T. A., and Swaab, T. Y. (2018). 1/ f neural noise and electrophysiological indices of contextual prediction in aging. *Brain Res.* 1691, 34–43. doi: 10.1016/j.brainres.2018.04.007

Decoteau, W. E., Thorn, C., Gibson, D. J., Courtemanche, R., Mitra, P., Kubota, Y., et al. (2007). Learning-related coordination of striatal and hippocampal theta rhythms during acquisition of a procedural maze task. *Proc. Natl. Acad. Sci.* 104, 5644–5649. doi: 10.1073/pnas.0700818104

Dejean, C., Courtin, J., Karalis, N., Chaudun, F., Wurtz, H., Bienvenu, T. C., et al. (2016). Prefrontal neuronal assemblies temporally control fear behaviour. *Nature* 535, 420–424. doi: 10.1038/nature18630

Diekelmann, S., and Born, J. (2010). The memory function of sleep. *Nat. Rev. Neurosci.* 11, 114–126.

Doelling, K. B., and Assaneo, M. F. (2021). Neural oscillations are a start toward understanding brain activity rather than the end. *PLoS Biol.* 19:e3001234. doi: 10.1371/journal.pbio.3001234

Donner, T. H., Siegel, M., Fries, P., and Engel, A. K. (2009). Buildup of Choice-Predictive Activity in Human Motor Cortex during Perceptual Decision Making. *Curr. Biol.* 19, 1581–1585. doi: 10.1016/j.cub.2009.07.066

Donoghue, T., Haller, M., Peterson, E. J., Varma, P., Sebastian, P., Gao, R., et al. (2020). Parameterizing neural power spectra into periodic and aperiodic components. *Nat. Neurosci.* 23, 1655–1665. doi: 10.1038/s41593-020-00744-x

Durkin, J., Suresh, A. K., Colbath, J., Broussard, C., Wu, J., Zochowski, M., et al. (2017). Cortically coordinated NREM thalamocortical oscillations play an essential, instructive role in visual system plasticity. *Proc. Natl. Acad. Sci.* 114, 10485–10490. doi: 10.1073/pnas.1710613114

Engel, A. K., and Singer, W. (2001). Temporal binding and the neural correlates of sensory awareness. *Trends Cognit. Sci.* 5, 16–25. doi: 10.1016/s1364-6613(00)01568-0

Etter, G., Van Der Veldt, S., Manseau, F., Zarrinkoub, I., Trillaud-Doppia, E., and Williams, S. (2019). Optogenetic gamma stimulation rescues memory impairments in an Alzheimer's disease mouse model. *Nat. Commun.* 10:5322. doi: 10.1038/s41467-019-13260-9

Fenno, L., Yizhar, O., and Deisseroth, K. (2011). The Development and Application of Optogenetics. *Annu. Rev. Neurosci.* 34, 389–412.

Fernández-Ruiz, A., Oliva, A., Soula, M., Rocha-Almeida, F., Nagy, G. A., Martin-Vazquez, G., et al. (2021). Gamma rhythm communication between entorhinal cortex and dentate gyrus neuronal assemblies. *Science* 372:eabf3119. doi: 10.1126/science.abf3119

Fries, P. (2001). Modulation of Oscillatory Neuronal Synchronization by Selective Visual Attention. *Science* 291, 1560–1563. doi: 10.1126/science.1055465

Fries, P. (2009). Neuronal Gamma-Band Synchronization as a Fundamental Process in Cortical Computation. *Annu. Rev. Neurosci.* 32, 209–224. doi: 10.1146/annurev.neuro.051508.135603

Fries, P. (2015). Rhythms for Cognition: Communication through Coherence. *Neuron* 88, 220–235. doi: 10.1016/j.neuron.2015.09.034

Furman, A. J., Meeker, T. J., Rietschel, J. C., Yoo, S., Muthulingam, J., Prokhorenko, M., et al. (2018). Cerebral peak alpha frequency predicts individual differences in pain sensitivity. *NeuroImage* 167, 203–210. doi: 10.1016/j.neuroimage.2017.11.042

Goldschmied, J. R., and Gehrman, P. (2019). An Integrated Model of Slow-Wave Activity and Neuroplasticity Impairments in Major Depressive Disorder. *Curr. Psychiat. Rep.* 21:30. doi: 10.1007/s11920-019-1013-4

Gradinaru, V., Thompson, K. R., and Deisseroth, K. (2008). eNpHR: a Natronomonas halorhodopsin enhanced for optogenetic applications. *Brain Cell Biol.* 36, 129–139. doi: 10.1007/s11068-008-9027-6

Gray, C. M. (1999). The temporal correlation hypothesis of visual feature integration: still alive and well. *Neuron* 24, 111–125. doi: 10.1016/s0896-6273(00)80820-x

Grosenick, L., Marshel, J. H., and Deisseroth, K. (2015). Closed-Loop and Activity-Guided Optogenetic Control. *Neuron* 86, 106–139. doi: 10.1016/j.neuron.2015.03.034

Haegens, S., Cousijn, H., Wallis, G., Harrison, P. J., and Nobre, A. C. (2014). Inter- and intra-individual variability in alpha peak frequency. *NeuroImage* 92, 46–55. doi: 10.1016/j.neuroimage.2014.01.049

Haegens, S., Händel, B. F., and Jensen, O. (2011a). Top-down controlled alpha band activity in somatosensory areas determines behavioral performance in a discrimination task. *J. Neurosci.* 31, 5197–5204. doi: 10.1523/JNEUROSCI.5199-10.2011

Haegens, S., Nácher, V., Hernández, A., Luna, R., Jensen, O., and Romo, R. (2011b). Beta oscillations in the monkey sensorimotor network reflect somatosensory decision making. *Proc. Natl. Acad. Sci.* 108, 10708–10713. doi: 10.1073/pnas.1107297108

Haegens, S., Nacher, V., Luna, R., Romo, R., and Jensen, O. (2011c). α-Oscillations in the monkey sensorimotor network influence discrimination performance by rhythmical inhibition of neuronal spiking. *Proc. Natl. Acad. Sci.* 108, 19377–19382. doi: 10.1073/pnas.1117190108

Haegens, S., Vergara, J., Rossi-Pool, R., Lemus, L., and Romo, R. (2017). Beta oscillations reflect supramodal information during perceptual judgment. *Proc. Natl. Acad. Sci.* 114, 13810–13815. doi: 10.1073/pnas.1714633115

Haenschel, C., Bittner, R. A., Waltz, J., Haertling, F., Wibral, M., Singer, W., et al. (2009). Cortical Oscillatory Activity Is Critical for Working Memory as Revealed by Deficits in Early-Onset Schizophrenia. *J. Neurosci.* 29, 9481–9489. doi: 10.1523/JNEUROSCI.1428-09.2009

Halgren, M., Ulbert, I., Bastuji, H., Fabó, D., Erőss, L., Rey, M., et al. (2019). The generation and propagation of the human alpha rhythm. *Proc. Natl. Acad. Sci.* 116, 23772–23782. doi: 10.1073/pnas.1913092116

Hangya, B., Borhegyi, Z., Szilagyi, N., Freund, T. F., and Varga, V. (2009). GABAergic Neurons of the Medial Septum Lead the Hippocampal Network during Theta Activity. *J. Neurosci.* 29, 8094–8102. doi: 10.1523/JNEUROSCI.5665-08.2009

Harris, A. Z., and Gordon, J. A. (2015). Long-Range Neural Synchrony in Behavior. *Annu. Rev. Neurosci.* 38, 171–194. doi: 10.1146/annurev-neuro-071714-034111

Hasselmo, M. E. (2005). What is the function of hippocampal theta rhythm?—Linking behavioral data to phasic properties of field potential and unit recording data. *Hippocampus* 15, 936–949. doi: 10.1002/hipo.20116

Herding, J., Spitzer, B., and Blankenburg, F. (2016). Upper Beta Band Oscillations in Human Premotor Cortex Encode Subjective Choices in a Vibrotactile Comparison Task. *J. Cognit. Neurosci.* 28, 668–679. doi: 10.1162/jocn_a_00932

Herreras, O. (2016). Local Field Potentials: Myths and Misunderstandings. *Front. Neural Circuits* 10, 101. doi: 10.3389/fncir.2016.00101

Hristova, K., Martinez-Gonzalez, C., Watson, T. C., Codadu, N. K., Hashemi, K., Kind, P. C., et al. (2021). Medial septal GABAergic neurons reduce seizure duration upon optogenetic closed-loop stimulation. *Brain* 144, 1576–1589.

Hua, T., Bao, P., Huang, C.-B., Wang, Z., Xu, J., Zhou, Y., et al. (2010). Perceptual Learning Improves Contrast Sensitivity of V1 Neurons in Cats. *Curr. Biol.* 20, 887–894. doi: 10.1016/j.cub.2010.03.066

Hultman, R., Ulrich, K., Sachs, B. D., Blount, C., Carlson, D. E., Ndubuizu, N., et al. (2018). Brain-wide Electrical Spatiotemporal Dynamics Encode Depression Vulnerability. *Cell* 173, 166–180e114. doi: 10.1016/j.cell.2018.02.012

Iaccarino, H. F., Singer, A. C., Martorell, A. J., Rudenko, A., Gao, F., Gillingham, T. Z., et al. (2016). Gamma frequency entrainment attenuates amyloid load and modifies microglia. *Nature* 540, 230–235.

Igarashi, K. M., Lu, L., Colgin, L. L., Moser, M.-B., and Moser, E. I. (2014). Coordination of entorhinal–hippocampal ensemble activity during associative learning. *Nature* 510, 143–147. doi: 10.1038/nature13162

Ito, J., Roy, S., Liu, Y., Cao, Y., Fletcher, M., Lu, L., et al. (2014). Whisker barrel cortex delta oscillations and gamma power in the awake mouse are linked to respiration. *Nat. Commun.* 5:3572. doi: 10.1038/ncomms4572

Jacobs, J. (2014). Hippocampal theta oscillations are slower in humans than in rodents: implications for models of spatial navigation and memory. *Philosop. Transact. R. Soc. B Biol. Sci.* 369:20130304. doi: 10.1098/rstb.2013.0304

Jacobs, J., Kahana, M. J., Ekstrom, A. D., and Fried, I. (2007). Brain Oscillations Control Timing of Single-Neuron Activity in Humans. *J. Neurosci.* 27, 3839–3844. doi: 10.1523/JNEUROSCI.4636-06.2007

Jensen, O., Gelfand, J., Kounios, J., and Lisman, J. E. (2002). Oscillations in the alpha band (9-12 Hz) increase with memory load during retention in a short-term memory task. *Cereb. Cortex* 12, 877–882. doi: 10.1093/cercor/12.8.877

Jiang, H., Schuele, S., Rosenow, J., Zelano, C., Parvizi, J., Tao, J. X., et al. (2017). Theta Oscillations Rapidly Convey Odor-Specific Content in Human Piriform Cortex. *Neuron* 94, 207.e–219.e. doi: 10.1016/j.neuron.2017.03.021

Jones, M. W., and Wilson, M. A. (2005a). Phase precession of medial prefrontal cortical activity relative to the hippocampal theta rhythm. *Hippocampus* 15, 867–873. doi: 10.1002/hipo.20119

Jones, M. W., and Wilson, M. A. (2005b). Theta Rhythms Coordinate Hippocampal–Prefrontal Interactions in a Spatial Memory Task. *PLoS Biol.* 3, e402–e402. doi: 10.1371/journal.pbio.0030402

Kajikawa, Y., and Schroeder, C. E. (2011). How local is the local field potential? *Neuron* 72, 847–858. doi: 10.1016/j.neuron.2011.09.029

Kalmbach, B. E., Buchin, A., Long, B., Close, J., Nandi, A., Miller, J. A., et al. (2018). h-Channels Contribute to Divergent Intrinsic Membrane Properties of Supragranular Pyramidal Neurons in Human versus Mouse Cerebral Cortex. *Neuron* 100, 1194.e–1208.e. doi: 10.1016/j.neuron.2018.10.012

Kanta, V., Pare, D., and Headley, D. B. (2019). Closed-loop control of gamma oscillations in the amygdala demonstrates their role in spatial memory consolidation. *Nat. Commun.* 10, 3970–3970. doi: 10.1038/s41467-019-11938-8

Karalis, N., Dejean, C., Chaudun, F., Khoder, S., Rozeske, R. R., Wurtz, H., et al. (2016). 4-Hz oscillations synchronize prefrontal–amygdala circuits during fear behavior. *Nat. Neurosci.* 19, 605–612. doi: 10.1038/nn.4251

Kheirbek, M. A., Drew, L. J., Burghardt, N. S., Costantini, D. O., Tannenholz, L., Ahmari, S. E., et al. (2013). Differential control of learning and anxiety along the dorsoventral axis of the dentate gyrus. *Neuron* 77, 955–968. doi: 10.1016/j.neuron.2012.12.038

Kim, C. K., Adhikari, A., and Deisseroth, K. (2017). Integration of optogenetics with complementary methodologies in systems neuroscience. *Nat. Rev. Neurosci.* 18, 222–235. doi: 10.1038/nrn.2017.15

Kim, H., Ährlund-Richter, S., Wang, X., Deisseroth, K., and Carlén, M. (2016). Prefrontal Parvalbumin Neurons in Control of Attention. *Cell* 164, 208–218. doi: 10.1016/j.cell.2015.11.038

Klapoetke, N. C., Murata, Y., Kim, S. S., Pulver, S. R., Birdsey-Benson, A., Cho, Y. K., et al. (2014). Independent optical excitation of distinct neural populations. *Nat. Methods* 11, 338–346.

Klimesch, W., Doppelmayr, M., Schwaiger, J., Auinger, P., and Winkler, T. (1999). 'Paradoxical' alpha synchronization in a memory task. *Cognit. Brain Res.* 7, 493–501. doi: 10.1016/s0926-6410(98)00056-1

Klimesch, W., Sauseng, P., and Hanslmayr, S. (2007). EEG alpha oscillations: The inhibition–timing hypothesis. *Brain Res. Rev.* 53, 63–88. doi: 10.1016/j.brainresrev.2006.06.003

Kramis, R., Vanderwolf, C. H., and Bland, B. H. (1975). Two types of hippocampal rhythmical slow activity in both the rabbit and the rat: Relations to behavior and effects of atropine, diethyl ether, urethane, and pentobarbital. *Exp. Neurol.* 49, 58–85. doi: 10.1016/0014-4886(75)90195-8

Kumar, S., Hultman, R., Hughes, D., Michel, N., Katz, B. M., and Dzirasa, K. (2014). Prefrontal cortex reactivity underlies trait vulnerability to chronic social defeat stress. *Nat. Commun.* 5:4537. doi: 10.1038/ncomms5537

Lakatos, P., Karmos, G., Mehta, A. D., Ulbert, I., and Schroeder, C. E. (2008). Entrainment of Neuronal Oscillations as a Mechanism of Attentional Selection. *Science* 320, 110–113. doi: 10.1126/science.1154735

Lesting, J., Narayanan, R. T., Kluge, C., Sangha, S., Seidenbecher, T., and Pape, H. C. (2011). Patterns of coupled theta activity in amygdala-hippocampal-prefrontal cortical circuits during fear extinction. *PLoS One* 6:e21714. doi: 10.1371/journal.pone.0021714

Li, A., Gire, D. H., and Restrepo, D. (2015). Upsilon spike-field coherence in a population of olfactory bulb neurons differentiates between odors irrespective of associated outcome. *J. Neurosci.* 35, 5808–5822. doi: 10.1523/JNEUROSCI.4003-14.2015

Likhtik, E., Stujenske, J. M., Topiwala, M. A., Harris, A. Z., and Gordon, J. A. (2014). Prefrontal entrainment of amygdala activity signals safety in learned fear and innate anxiety. *Nat. Neurosci.* 17, 106–113. doi: 10.1038/nn.3582

Lisman, J. E., and Jensen, O. (2013). The Theta-Gamma Neural Code. *Neuron* 77, 1002–1016. doi: 10.1016/j.neuron.2013.03.007

Lisman, J., and Idiart, M. (1995). Storage of 7 +/- 2 short-term memories in oscillatory subcycles. *Science* 267, 1512–1515. doi: 10.1126/science.7878473

Lorincz, M. L., Crunelli, V., and Hughes, S. W. (2008). Cellular Dynamics of Cholinergically Induced (8 13 Hz) Rhythms in Sensory Thalamic Nuclei In Vitro. *J. Neurosci.* 28, 660–671. doi: 10.1523/JNEUROSCI.4468-07.2008

Louie, K., and Wilson, M. A. (2001). Temporally Structured Replay of Awake Hippocampal Ensemble Activity during Rapid Eye Movement Sleep. *Neuron* 29, 145–156. doi: 10.1016/s0896-6273(01)00186-6

Lowes, D. C., Chamberlin, L. A., Kretsge, L. N., Holt, E. S., Abbas, A. I., Park, A. J., et al. (2021). Ventral tegmental area GABA neurons mediate stress-induced blunted reward-seeking in mice. *Nat. Commun.* 12:3539. doi: 10.1038/s41467-021-23906-2

Ludwig, A., Zong, X., Jeglitsch, M., Hofmann, F., and Biel, M. (1998). A family of hyperpolarization-activated mammalian cation channels. *Nature* 393, 587–591. doi: 10.1038/31255

Lundqvist, M., Herman, P., Warden, M. R., Brincat, S. L., and Miller, E. K. (2018). Gamma and beta bursts during working memory readout suggest roles in its volitional control. *Nat. Commun.* 9:394. doi: 10.1038/s41467-017-02791-8

Mably, A. J., and Colgin, L. L. (2018). Gamma oscillations in cognitive disorders. *Curr. Opin. Neurobiol.* 52, 182–187. doi: 10.1016/j.conb.2018.07.009

Manning, J. R., Jacobs, J., Fried, I., and Kahana, M. J. (2009). Broadband Shifts in Local Field Potential Power Spectra Are Correlated with Single-Neuron Spiking in Humans. *J. Neurosci.* 29, 13613–13620. doi: 10.1523/JNEUROSCI.2041-09.2009

Mazaheri, A., Van Schouwenburg, M. R., Dimitrijevic, A., Denys, D., Cools, R., and Jensen, O. (2014). Region-specific modulations in oscillatory alpha activity serve to facilitate processing in the visual and auditory modalities. *NeuroImage* 87, 356–362. doi: 10.1016/j.neuroimage.2013.10.052

Mazzarello, P., and Sala, S. D. (1993). The demonstration of the visual area by means of the atrophic degeneration method in the work of Bartolomeo Panizza (1855). *J. Hist. Neurosci.* 2, 315–322. doi: 10.1080/09647049309525579

Mccarthy, M. M., Moore-Kochlacs, C., Gu, X., Boyden, E. S., Han, X., and Kopell, N. (2011). Striatal origin of the pathologic beta oscillations in Parkinson's disease. *Proc. Natl. Acad. Sci.* 108, 11620–11625. doi: 10.1073/pnas.1107748108

McNaughton, B. L., Battaglia, F. P., Jensen, O., Moser, E. I., and Moser, M.-B. (2006). Path integration and the neural basis of the 'cognitive map'. *Nat. Rev. Neurosci.* 7, 663–678. doi: 10.1038/nrn1932

Michel, C. M., and Brunet, D. (2019). EEG Source Imaging: A Practical Review of the Analysis Steps. *Front. Neurol.* 10:325. doi: 10.3389/fneur.2019.00325

Miller, E. K., Lundqvist, M., and Bastos, A. M. (2018). Working Memory 2.0. *Neuron* 100, 463–475.

Mitchell, S. J., Rawlins, J. N., Steward, O., and Olton, D. S. (1982). Medial septal area lesions disrupt theta rhythm and cholinergic staining in medial entorhinal cortex and produce impaired radial arm maze behavior in rats. *J. Neurosci.* 2, 292–302. doi: 10.1523/JNEUROSCI.02-03-00292.1982

Muthukumaraswamy, S. D., Edden, R. A. E., Jones, D. K., Swettenham, J. B., and Singh, K. D. (2009). Resting GABA concentration predicts peak gamma frequency and fMRI amplitude in response to visual stimulation in humans. *Proc. Natl. Acad. Sci.* 106, 8356–8361. doi: 10.1073/pnas.0900728106

Neves, G., Cooke, S. F., and Bliss, T. V. P. (2008). Synaptic plasticity, memory and the hippocampus: a neural network approach to causality. *Nat. Rev. Neurosci.* 9, 65–75. doi: 10.1038/nrn2303

Ni, J., Wunderle, T., Lewis, C. M., Desimone, R., Diester, I., and Fries, P. (2016). Gamma-Rhythmic Gain Modulation. *Neuron* 92, 240–251.

Nicholson, E., Kuzmin, D. A., Leite, M., Akam, T. E., and Kullmann, D. M. (2018). Analogue closed-loop optogenetic modulation of hippocampal pyramidal cells dissociates gamma frequency and amplitude. *Elife* 7:38346. doi: 10.7554/eLife.38346

O'keefe, J., and Recce, M. L. (1993). Phase relationship between hippocampal place units and the EEG theta rhythm. *Hippocampus* 3, 317–330. doi: 10.1002/hipo.450030307

Padilla-Coreano, N., Bolkan, S. S., Pierce, G. M., Blackman, D. R., Hardin, W. D., Garcia-Garcia, A. L., et al. (2016). Direct Ventral Hippocampal-Prefrontal Input Is Required for Anxiety-Related Neural Activity and Behavior. *Neuron* 89, 857–866. doi: 10.1016/j.neuron.2016.01.011

Padilla-Coreano, N., Canetta, S., Mikofsky, R. M., Alway, E., Passecker, J., Myroshnychenko, M. V., et al. (2019). Hippocampal-Prefrontal Theta Transmission Regulates Avoidance Behavior. *Neuron* 104, 601.e–610.e. doi: 10.1016/j.neuron.2019.08.006

Park, A. J., Harris, A. Z., Martyniuk, K. M., Chang, C.-Y., Abbas, A. I., Lowes, D. C., et al. (2021). Reset of hippocampal-prefrontal circuitry facilitates learning. *Nature* 591, 615–619. doi: 10.1038/s41586-021-03272-1

Peterson, E. J., Rosen, B. Q., Campbell, A. M., Belger, A., and Voytek, B. (2017). 1/f neural noise is a better predictor of schizophrenia than neural oscillations. *bioRxiv*. [Preprint].

Pogosyan, A., Gaynor, L. D., Eusebio, A., and Brown, P. (2009). Boosting Cortical Activity at Beta-Band Frequencies Slows Movement in Humans. *Curr. Biol.* 19, 1637–1641. doi: 10.1016/j.cub.2009.07.074

Prince, L. Y., Tran, M. M., Grey, D., Saad, L., Chasiotis, H., Kwag, J., et al. (2021). Neocortical inhibitory interneuron subtypes are differentially attuned to synchrony- and rate-coded information. *Commun. Biol.* 4:935. doi: 10.1038/s42003-021-02437-y

Ramirez, S., Liu, X., Lin, P.-A., Suh, J., Pignatelli, M., Redondo, R. L., et al. (2013). Creating a False Memory in the Hippocampus. *Science* 341:6. doi: 10.1126/science.1239073

Ray, S., Crone, N. E., Niebur, E., Franaszczuk, P. J., and Hsiao, S. S. (2008). Neural Correlates of High-Gamma Oscillations (60-200 Hz) in Macaque Local Field Potentials and Their Potential Implications in Electrocorticography. *J. Neurosci.* 28, 11526–11536. doi: 10.1523/JNEUROSCI.2848-08.2008

Reddy, L., Self, M. W., Zoefel, B., Poncet, M., Possel, J. K., Peters, J. C., et al. (2021). Theta-phase dependent neuronal coding during sequence learning in human single neurons. *Nat. Commun.* 12:4839. doi: 10.1038/s41467-021-25150-0

Romo, R., Brody, C. D., Hernández, A., and Lemus, L. (1999). Neuronal correlates of parametric working memory in the prefrontal cortex. *Nature* 399, 470–473. doi: 10.1038/20939

Rossi, J., Balthasar, N., Olson, D., Scott, M., Berglund, E., Lee, C. E., et al. (2011). Melanocortin-4 Receptors Expressed by Cholinergic Neurons Regulate Energy Balance and Glucose Homeostasis. *Cell Metabol.* 13, 195–204. doi: 10.1016/j.cmet.2011.01.010

Roy, A., Svensson, F. P., Mazeh, A., and Kocsis, B. (2017). Prefrontal-hippocampal coupling by theta rhythm and by 2–5 Hz oscillation in the delta band: The role of the nucleus reuniens of the thalamus. *Brain Struct. Funct.* 222, 2819–2830. doi: 10.1007/s00429-017-1374-6

Samaha, J., Iemi, L., Haegens, S., and Busch, N. A. (2020). Spontaneous Brain Oscillations and Perceptual Decision-Making. *Trends Cognit. Sci.* 24, 639–653. doi: 10.1016/j.tics.2020.05.004

Schneider, M., Broggini, A. C., Dann, B., Tzanou, A., Uran, C., Sheshadri, S., et al. (2021). A mechanism for inter-areal coherence through communication based on connectivity and oscillatory power. *Neuron* 2021:S0896627321007108. doi: 10.1016/j.neuron.2021.09.037

Schnitzler, A., and Gross, J. (2005). Normal and pathological oscillatory communication in the brain. *Nat. Rev. Neurosci.* 6, 285–296. doi: 10.1038/nrn1650

Schreiner, T., Petzka, M., Staudigl, T., and Staresina, B. P. (2021). Endogenous memory reactivation during sleep in humans is clocked by slow oscillation-spindle complexes. *Nat. Commun.* 12:3112. doi: 10.1038/s41467-021-23520-2

Schroeder, C. E., and Lakatos, P. (2009). Low-frequency neuronal oscillations as instruments of sensory selection. *Trends Neurosci.* 32, 9–18. doi: 10.1016/j.tins.2008.09.012

Sederberg, P. B., Schulze-Bonhage, A., Madsen, J. R., Bromfield, E. B., Mccarthy, D. C., Brandt, A., et al. (2006). Hippocampal and Neocortical Gamma Oscillations Predict Memory Formation in Humans. *Cereb. Cortex* 17, 1190–1196. doi: 10.1093/cercor/bhl030

Seeber, M., Cantonas, L.-M., Hoevels, M., Sesia, T., Visser-Vandewalle, V., and Michel, C. M. (2019). Subcortical electrophysiological activity is detectable with high-density EEG source imaging. *Nat. Commun.* 10, 753–753. doi: 10.1038/s41467-019-08725-w

Shin, H., Law, R., Tsutsui, S., Moore, C. I., and Jones, S. R. (2017). The rate of transient beta frequency events predicts behavior across tasks and species. *eLife* 6:e29086. doi: 10.7554/eLife.29086

Siegle, J. H., Pritchett, D. L., and Moore, C. I. (2014). Gamma-range synchronization of fast-spiking interneurons can enhance detection of tactile stimuli. *Nat. Neurosci.* 17, 1371–1379. doi: 10.1038/nn.3797

Singer, W. (2018). Neuronal oscillations: unavoidable and useful? *Eur. J. Neurosci.* 48, 2389–2398. doi: 10.1111/ejn.13796

Sohal, V. S., Zhang, F., Yizhar, O., and Deisseroth, K. (2009). Parvalbumin neurons and gamma rhythms enhance cortical circuit performance. *Nature* 459, 698–702. doi: 10.1038/nature07991

Sorokin, J. M., Davidson, T. J., Frechette, E., Abramian, A. M., Deisseroth, K., Huguenard, J. R., et al. (2017). Bidirectional Control of Generalized Epilepsy Networks via Rapid Real-Time Switching of Firing Mode. *Neuron* 93, 194–210. doi: 10.1016/j.neuron.2016.11.026

Spitzer, B., and Blankenburg, F. (2012). Supramodal Parametric Working Memory Processing in Humans. *J. Neurosci.* 32, 3287–3295. doi: 10.1523/JNEUROSCI.5280-11.2012

Spitzer, B., and Haegens, S. (2017). Beyond the Status Quo: A Role for Beta Oscillations in Endogenous Content (Re)Activation. *eneuro* 4, ENEURO.170–ENEURO.117. doi: 10.1523/ENEURO.0170-17.2017

Stagkourakis, S., Pérez, C. T., Hellysaz, A., Ammari, R., and Broberger, C. (2018). Network oscillation rules imposed by species-specific electrical coupling. *eLife* 7:e33144. doi: 10.7554/eLife.33144

Stujenske, J. M., Likhtik, E., Topiwala, M. A., and Gordon, J. A. (2014). Fear and safety engage competing patterns of theta-gamma coupling in the basolateral amygdala. *Neuron* 83, 919–933. doi: 10.1016/j.neuron.2014.07.026

Thut, G. (2006). a-Band Electroencephalographic Activity over Occipital Cortex Indexes Visuospatial Attention Bias and Predicts Visual Target Detection. *J. Neurosci.* 26, 9494–9502. doi: 10.1523/JNEUROSCI.0875-06.2006

Tiitinen, H. T., Sinkkonen, J., Reinikainen, K., Alho, K., Lavikainen, J., and Näätänen, R. (1993). Selective attention enhances the auditory 40-Hz transient response in humans. *Nature* 364, 59–60. doi: 10.1038/364059a0

Tononi, G., and Cirelli, C. (2003). Sleep and synaptic homeostasis: a hypothesis. *Brain Res. Bull.* 62, 143–150. doi: 10.1016/j.brainresbull.2003.09.004

Tootell, R. B. H., Hadjikhani, N. K., Vanduffel, W., Liu, A. K., Mendola, J. D., Sereno, M. I., et al. (1998). Functional analysis of primary visual cortex (V1) in humans. *Proc. Natl. Acad. Sci.* 95, 811–817. doi: 10.1073/pnas.95.3.811

Tort, A. B. L., Brankačk, J., and Draguhn, A. (2018b). Respiration-Entrained Brain Rhythms Are Global but Often Overlooked. *Trends Neurosci.* 41, 186–197.

Tort, A. B. L., Ponsel, S., Jessberger, J., Yanovsky, Y., Brankačk, J., and Draguhn, A. (2018a). Parallel detection of theta and respiration-coupled oscillations throughout the mouse brain. *Sci. Rep.* 8:6432. doi: 10.1038/s41598-018-24629-z

Van De Ven, G. M., Trouche, S., Mcnamara, C. G., Allen, K., and Dupret, D. (2016). Hippocampal Offline Reactivation Consolidates Recently Formed Cell Assembly Patterns during Sharp Wave-Ripples. *Neuron* 92, 968–974.

Van Der Meer, M. A. A., and Redish, A. D. (2011). Theta Phase Precession in Rat Ventral Striatum Links Place and Reward Information. *J. Neurosci.* 31, 2843–2854. doi: 10.1523/JNEUROSCI.4869-10.2011

Van Kerkoerle, T., Self, M. W., Dagnino, B., Gariel-Mathis, M.-A., Poort, J., Van Der Togt, C., et al. (2014). Alpha and gamma oscillations characterize feedback and feedforward processing in monkey visual cortex. *Proc. Natl. Acad. Sci.* 111, 14332–14341. doi: 10.1073/pnas.1402773111

Varela, F., Lachaux, J. P., Rodriguez, E., and Martinerie, J. (2001). The brainweb: phase synchronization and large-scale integration. *Nat. Rev. Neurosci.* 2, 229–239. doi: 10.1038/35067550

Varga, V., Hangya, B., Kránitz, K., Ludányi, A., Zemankovics, R., Katona, I., et al. (2008). The presence of pacemaker HCN channels identifies theta rhythmic GABAergic neurons in the medial septum. *J. Physiol.* 586, 3893–3915. doi: 10.1113/jphysiol.2008.155242

Vass, L. K., Copara, M. S., Seyal, M., Shahlaie, K., Farias, S. T., Shen, P. Y., et al. (2016). Oscillations Go the Distance: Low-Frequency Human Hippocampal Oscillations Code Spatial Distance in the Absence of Sensory Cues during Teleportation. *Neuron* 89, 1180–1186. doi: 10.1016/j.neuron.2016.01.045

Veit, J., Hakim, R., Jadi, M. P., Sejnowski, T. J., and Adesnik, H. (2017). Cortical gamma band synchronization through somatostatin interneurons. *Nat. Neurosci.* 20, 951–959. doi: 10.1038/nn.4562

Vergara, J., Rivera, N., Rossi-Pool, R., and Romo, R. (2016). A Neural Parametric Code for Storing Information of More than One Sensory Modality in Working Memory. *Neuron* 89, 54–62. doi: 10.1016/j.neuron.2015.11.026

Vesuna, S., Kauvar, I. V., Richman, E., Gore, F., Oskotsky, T., Sava-Segal, C., et al. (2020). Deep posteromedial cortical rhythm in dissociation. *Nature* 586, 87–94. doi: 10.1038/s41586-020-2731-9

Voytek, B., Kramer, M. A., Case, J., Lepage, K. Q., Tempesta, Z. R., Knight, R. T., et al. (2015). Age-Related Changes in 1/f Neural Electrophysiological Noise. *J. Neurosci.* 35, 13257–13265. doi: 10.1523/JNEUROSCI.2332-14.2015

Watrous, A. J., Lee, D. J., Izadi, A., Gurkoff, G. G., Shahlaie, K., and Ekstrom, A. D. (2013). A comparative study of human and rat hippocampal low-frequency oscillations during spatial navigation: Comparison of Human and Rodent Theta. *Hippocampus* 23, 656–661. doi: 10.1002/hipo.22124

Whittington, M. A., Traub, R. D., and Jefferys, J. G. R. (1995). Synchronized oscillations in interneuron networks driven by metabotropic glutamate receptor activation. *Nature* 373, 612–615. doi: 10.1038/373612a0

Womelsdorf, T., Fries, P., Mitra, P. P., and Desimone, R. (2006). Gamma-band synchronization in visual cortex predicts speed of change detection. *Nature* 439, 733–736. doi: 10.1038/nature04258

Yamamoto, J., Suh, J., Takeuchi, D., and Tonegawa, S. (2014). Successful Execution of Working Memory Linked to Synchronized High-Frequency Gamma Oscillations. *Cell* 157, 845–857. doi: 10.1016/j.cell.2014.04.009

Yizhar, O., Fenno, L. E., Davidson, T. J., Mogri, M., and Deisseroth, K. (2011). Optogenetics in Neural Systems. *Neuron* 71, 9–34. doi: 10.1016/j.neuron.2011.06.004

Zhang, F., Wang, L.-P., Brauner, M., Liewald, J. F., Kay, K., Watzke, N., et al. (2007). Multimodal fast optical interrogation of neural circuitry. *Nature* 446, 633–639. doi: 10.1038/nature05744

Zhang, Y.-P., and Oertner, T. G. (2007). Optical induction of synaptic plasticity using a light-sensitive channel. *Nat. Methods* 4, 139–141. doi: 10.1038/nmeth988

Zhou, Y. J., Iemi, L., Schoffelen, J.-M., De Lange, F. P., and Haegens, S. (2021). Alpha Oscillations Shape Sensory Representation and Perceptual Sensitivity. *J. Neurosci.* 41, 9581–9592. doi: 10.1523/JNEUROSCI.1114-21.2021

Zielinski, M. C., Shin, J. D., and Jadhav, S. P. (2019). Coherent Coding of Spatial Position Mediated by Theta Oscillations in the Hippocampus and Prefrontal Cortex. *J. Neurosci.* 39, 4550–4565. doi: 10.1523/JNEUROSCI.0106-19.2019

Conflict of Interest: The authors declare that the research was conducted in the absence of any commercial or financial relationships that could be construed as a potential conflict of interest.

Publisher's Note: All claims expressed in this article are solely those of the authors and do not necessarily represent those of their affiliated organizations, or those of the publisher, the editors and the reviewers. Any product that may be evaluated in this article, or claim that may be made by its manufacturer, is not guaranteed or endorsed by the publisher.

frontiers in Neural Circuits

METHODS
published: 24 March 2022
doi: 10.3389/fncir.2022.783768

Discriminating Sleep From Freezing With Cortical Spindle Oscillations

Marco N. Pompili[1]* *and Ralitsa Todorova*[2]*

[1] Aix Marseille University, INSERM, Institut de Neurosciences des Systèmes (INS), Marseille, France, [2] Department of Neurobiology and Behavior, Cornell University, Ithaca, NY, United States

In-vivo longitudinal recordings require reliable means to automatically discriminate between distinct behavioral states, in particular between awake and sleep epochs. The typical approach is to use some measure of motor activity together with extracellular electrophysiological signals, namely the relative contribution of theta and delta frequency bands to the Local Field Potential (LFP). However, these bands can partially overlap with oscillations characterizing other behaviors such as the 4 Hz accompanying rodent freezing. Here, we first demonstrate how standard methods fail to discriminate between sleep and freezing in protocols where both behaviors are observed. Then, as an alternative, we propose to use the smoothed cortical spindle power to detect sleep epochs. Finally, we show the effectiveness of this method in discriminating between sleep and freezing in our recordings.

Keywords: sleep spindles, behavioral state classification, freezing, sleep, cortical oscillations, local field potential oscillations

OPEN ACCESS

Edited by:
Gabrielle Girardeau, INSERM U839 Institut du Fer à Moulin (IFM), France

Reviewed by:
Thomas C. Watson, University of Edinburgh, United Kingdom
Ross Purple, University of Bristol, United Kingdom

***Correspondence:**
Marco N. Pompili
marco.pompili@normalesup.org
Ralitsa Todorova
rt428@cornell.edu

Received: *26 September 2021*
Accepted: *31 January 2022*
Published: *24 March 2022*

Citation:
Pompili MN and Todorova R (2022) Discriminating Sleep From Freezing With Cortical Spindle Oscillations. Front. Neural Circuits 16:783768. doi: 10.3389/fncir.2022.783768

1. INTRODUCTION

One of the main ambitions of systems neuroscience is to understand the relationship between the activity of the nervous system and animal behavior. To this end, a fruitful approach is to record neural activity as animals perform specific tasks as well as during natural behavior. Indeed, monitoring brain activity across a wide range of training-dependent and spontaneous behavioral states is crucial in the study of potential mappings between neural activity and behavior (Krakauer et al., 2017). Moreover, contrasting the neurophysiology of active vs. inactive states (such as rest), helps disentangle the neural activity underpinning cognitive functions such as learning from those controlling motor behavior and perception. In particular, the neurophysiology of sleep examines endogenous activity taking place when the brain is disengaged from the external world and self-organized computation emerges (Buzsáki et al., 2014).

In electrophysiological studies, neural activity can be recorded for many hours, and in some cases days or weeks, across many behavioral states (e.g., Wilson and McNaughton, 1994; Hirase et al., 2001; Lin et al., 2006; Benchenane et al., 2010; Hengen et al., 2016; Dhawale et al., 2017; Girardeau et al., 2017; Chung et al., 2019; Todorova and Zugaro, 2019). Matching specific neural processes to particular behaviors requires reliable automated means to distinguish between different behavioral states, such as wakefulness vs. sleep, but also between rapid eye movement (REM) sleep and non-REM sleep, also known as slow-wave sleep (SWS).

State of the art automated brain state scoring techniques rely on motor activity as well as neural recordings, taking advantage of the fact that active awake behavior and REM are characterized by oscillations in the theta frequency band (7–8.5 Hz), while SWS is dominated by slower rhythms in the delta range (1–4 Hz). The most common approach for classifying sleep stages consists of sampling animal movement (using video recordings, inertial sensors, or electromyography) to

detect immobility periods, and then dividing the resulting epochs into REM and SWS based on the relative power of theta vs. delta oscillations in the electroencephalography or local field potential (LFP) recordings. This technique has been used for more than 40 years (Gottesmann et al., 1971; Kohn et al., 1974; Johns et al., 1977) and is still very popular today (e.g., Todorova and Zugaro, 2019; Sosa et al., 2020; Wang et al., 2020; Tingley et al., 2021).

A limitation of this approach is the assumption that all immobility corresponds to rest, uniquely composed of its sub-states: quiet wakefulness, SWS, and REM. However, certain behavioral paradigms may involve immobility which should not be equated to resting. In particular, immobility is also the main feature of freezing behavior (Blanchard and Blanchard, 1969), a widely used index of fear typically employed to probe for learning in fear conditioning (Fanselow and Poulos, 2005), a very popular paradigm in rodent behavioral research. This presents a problem for studies addressing the role of sleep in emotional regulation and fear memory consolidation, a research focus likely to become more and more popular since sleep neurophysiology is finally crossing paths with the investigation of emotional learning (Trouche et al., 2020).

In order to correctly discriminate between sleep and freezing in a behavioral protocol involving both behaviors, we developed a method based on spindle oscillations in cortical recordings. Spindle oscillations are characteristic of SWS (Steriade et al., 1993; Fernandez and Lüthi, 2020), which constitutes 90% or rodents sleep (Brankack et al., 2010). Here, after illustrating how standard approaches, by construction, cannot discriminate between freezing and sleep/rest states, we show how these can be disentangled by the smoothed spindle power. Finally, we validate that this approach was effective in detecting sleep and freezing epochs interspersed in a fear conditioning and extinction paradigm. The algorithm we propose requires solely the LFP from a single neocortical channel and a readout of the animal motor activity and is therefore a simple and effective solution to determine behavioral states in freely moving animal recordings.

2. RESULTS

2.1. Standard Approach Fails to Distinguish Sleep From Freezing

As a case study, we analyzed data recorded from rats performing both freezing and sleeping behaviors. The rats underwent a multi-day fear conditioning and extinction protocol, and rest sessions were recorded in a familiar non-anxiogenic environment before and after each training session (**Figure 1A**).

We first used standard methods to detect freezing and sleep. Freezing is typically defined as all immobility periods longer than a particular threshold (0.5–2 s; e.g., Bagur et al., 2018; Moberly et al., 2018; Gründemann et al., 2019; Jercog et al., 2021; Ressler et al., 2021). Nonetheless, standard sleep-scoring algorithms assume that all such immobility corresponds to rest states. Therefore, these techniques label most immobility periods as both sleep and freezing. Indeed, while in some cases immobility periods correspond to sleep (see the left part of **Figure 1B**; **Supplementary Video 1**), a freezing period may also last for long periods of time (right part of **Figure 1B**; **Supplementary Video 2**). This makes the standard approach to sleep detection unsuitable for data involving freezing.

Our recordings included the local field potential (LFP) from the hippocampus (HPC) and medial prefrontal cortex (mPFC). As expected, theta and delta oscillations displayed a marked difference between REM and SWS epochs (**Figure 2C**). However, the theta/delta ratio did not help separate SWS from freezing, because in both of these epochs delta power dominated over theta power (**Figure 1B**). This is likely due to the overlap between the delta frequency band and the frequency band of the respiratory-driven cortical oscillation around 4 Hz associated with freezing (Ciatipis et al., 2014; Karalis et al., 2016; Lockmann et al., 2016; Biskamp et al., 2017; Moberly et al., 2018; Bagur et al., 2021; Karalis and Sirota, 2022). On the other hand, power in the spindle band (9–17 Hz) was high in sleep epochs and low in freezing (**Figure 1B**), suggesting that spindle power may be an exclusive marker for SWS.

2.2. Smoothed Cortical Spindle Power to Detect SWS

To develop a method to separate freezing and sleep, we took advantage of the lack of overlap between the spindle frequency and the slower 4 Hz oscillation associated with freezing. On the fine timescale, spindle power increases particularly during individual spindles, which are distinct thalamocortical events occurring in SWS. However, spindle events are common in SWS, and therefore the *smoothed* spindle power is relatively constant as it joins multiple spindle events (**Supplementary Figure 1**). Indeed, the smoothed spindle power during immobility periods follows a bimodal distribution (**Supplementary Figure 2**), allowing the separation between SWS and non-SWS immobility periods as they are characterized by high and low smoothed spindle power, respectively.

The pipeline we developed (see Section 4 for details) starts by detecting all periods of immobility (**Figure 2A**). We then classify immobility periods with high spindle power as SWS (**Figure 2B**). Since REM periods do not occur in isolation but are nested within SWS cycles (McCarley, 2007), we label as REM sleep those epochs where HPC theta power is higher than HPC delta power, on the condition that they closely follow SWS (**Figure 2C**). In the absence of HPC recordings the algorithm can detect REM using the theta/delta ratio of the cortical LFP used to detect SWS (**Supplementary Figure 3**).

The remaining immobility periods are considered non-sleep immobility states (**Figure 2D**). These include the periods of quiet wakefulness prior to falling asleep, which must be disentangled from freezing. We therefore classify these SWS-preceding immobility periods as quiet wakefulness epochs, and the remaining immobility is labeled as freezing (**Figure 2D**). Contrary to a compounded use of the standard approaches for sleep and freezing detection, this method is designed to guarantee

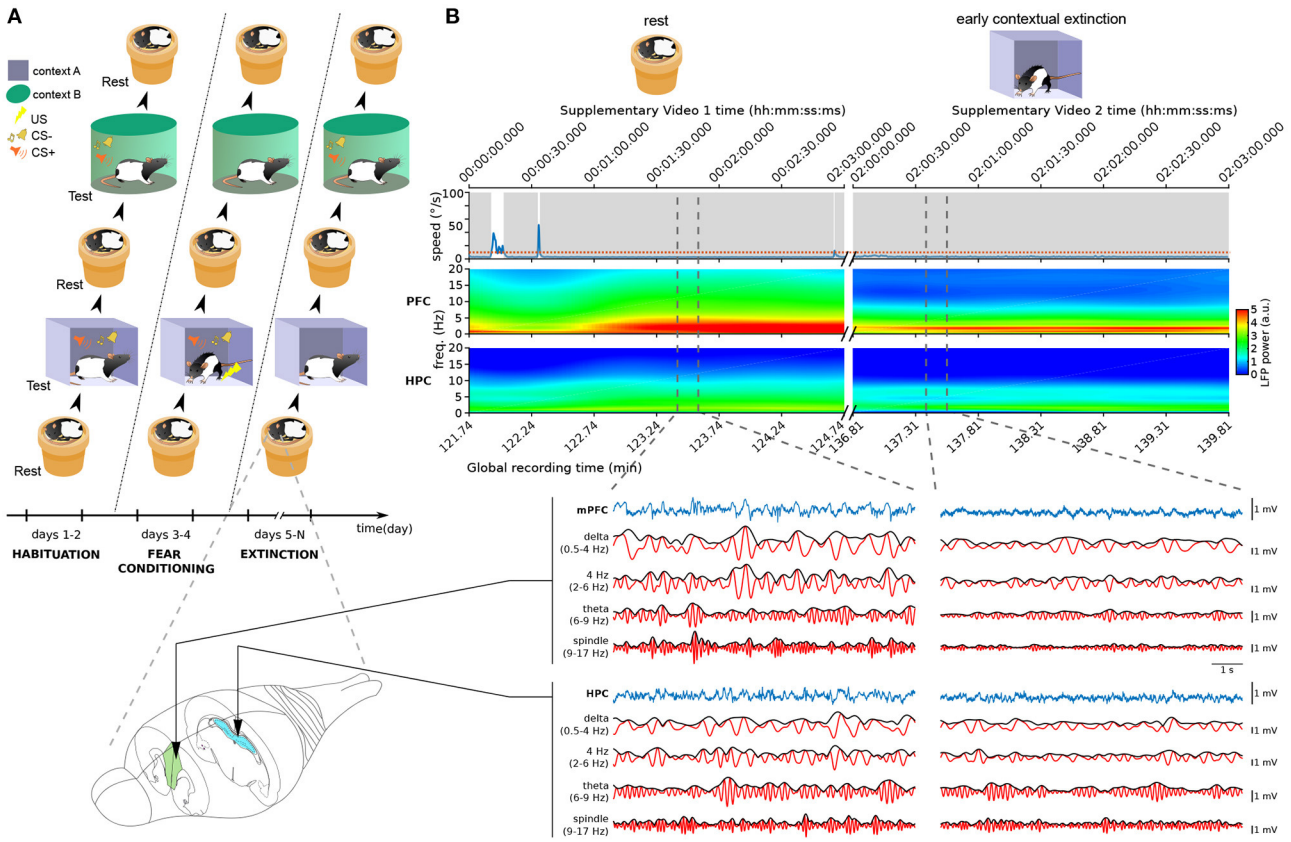

FIGURE 1 | Neural and behavioral activity during rest vs. freezing **(A)** Overview of the behavioral protocol. Each day, animals were exposed to a resting environment (a familiar non-anxiogenic flowerpot) and to two testing environments **(A,B)**. In habituation sessions (2 days, left), animals were exposed to context A and context B and to the auditory stimuli employed in the protocol. This was followed by fear conditioning (2 days, middle) where the presentations of the conditioned stimulus (CS+) in context A were coupled with the delivery of aversive footshocks. In the following days of the protocol (6–12 days, right), the animals underwent contextual fear extinction in context A as well as cued fear extinction in context B (see Section 4). **(B)** Example neural activity recorded during sleep in the resting environment (left, see **Supplementary Video 1**) and during freezing in context A (right, **Supplementary Video 2**) in the first day of extinction training. Time stamps corresponding to those overlaid in **Supplementary Video** frames are shown on top. (Top) Animal speed as measured by head movements; red dotted line: threshold used to detect immobility; gray shadings: immobility periods. (Middle) Spectrograms of the LFP recorded in the medial prefrontal cortex (mPFC) and hippocampus (HPC). Vertical dashed lines: The boundaries of example intervals represented on the bottom. (Bottom) mPFC and HPC LFP signal recorded in the intervals marked above. Blue: raw recorded LFP; red: filtered LFP in the delta, 4 Hz, theta, and spindle frequency bands; black: instantaneous amplitude of the filtered LFPs.

zero overlap between different behavioral states, in particular between freezing and sleep.

2.3. Effective Detection of Sleep and Freezing

To validate our scoring pipeline, we analyzed data from a multi-day fear conditioning and extinction dataset. The results of the algorithm were consistent with behavior to be expected in our protocol. Regardless of the day, in rest sessions animals spent most of the time sleeping, and freezing levels were low (**Figures 3A,D**). In habituation sessions, in the first 3 min (baseline) of being placed in context A, animals tended to actively explore the environment (**Supplementary Video 3**), and freezing and sleep were mostly absent (**Figure 3B**). Conversely, in the last 3 min of these sessions, after the animal had remained there for some time (each training session lasted 35 min), sleep was not uncommon (**Figure 3C**; **Supplementary Video 4**). Following fear conditioning in context A, animals tended to freeze there during baseline (**Supplementary Video 2**). Unlike habituation training sessions, they did not sleep at the end of conditioning ones (**Figure 3C**). Both of these tendencies (to freeze during baseline and to remain awake until the end of the session) gradually decreased over extinction (**Figures 3B,C**). Indeed, an animal's tendency to sleep in training sessions appeared to be a good indicator of global fear levels in our task (**Figures 3C,E**; **Supplementary Figure 4**). The epochs detected by our approach are therefore consistent with: (1) contextual freezing emerging only after conditioning and decreasing over extinction training and (2) animals sleeping (and therefore being calm) in the conditioning context only at low fear stages of the protocol (before conditioning and in late extinction).

The need for a method separating between sleep and freezing is most pronounced in cases when it's possible to

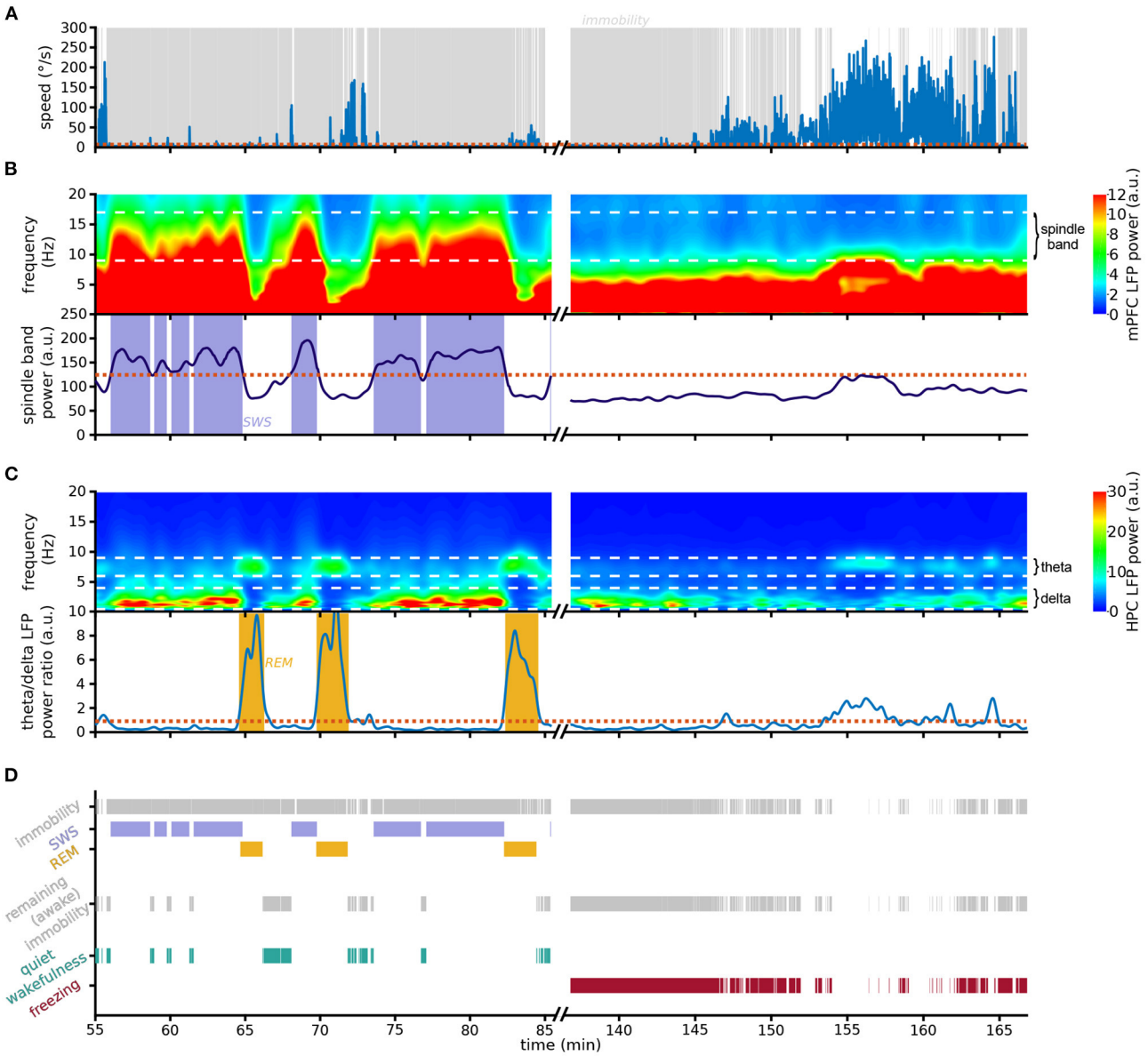

FIGURE 2 | Scoring pipeline. Left: An example 30 min recording in the resting environment; right: an example 30 min recording in context A during the first day of extinction. **(A)** Animal speed as measured by head movements. **(B)** (Top) Spectrogram of mPFC LFP activity; white dashed horizontal lines: boundaries of spindle frequency band. Note the prominent spindle band activity recorded in the rest epoch but absent in the conditioning environment. (Bottom) Smoothed spindle band power. Red dotted line: threshold used to detect SWS; blue shading: detected SWS periods. **(C)** (Top) Spectrogram of HPC LFP activity; white dashed horizontal lines: boundaries of delta and theta frequency bands. Note that in the resting session theta-dominating periods immediately follow the high-spindle power SWS periods depicted above. (Bottom) Theta/delta ratio; red dotted line: threshold used to detect REM sleep; yellow shading: detected REM sleep periods. **(D)** Detection chart. (Top) All detected immobility, SWS and REM periods. (Middle) Immobility periods not identified as either SWS or REM sleep are labeled awake immobility behaviors. (Bottom) Awake immobility periods immediately preceding SWS are classified as quiet wakefulness (green), and the remaining immobility is scored as freezing (red). Note that freezing was the dominating behavior detected during the first 10 min of exposure to the conditioning context A.

observe both of these behaviors in the same sessions, which can sometimes involve abrupt transitions between states. To test the performance of our method in such a scenario, we analyzed the moments when an animal slept when a CS+ was being presented in cued fear extinction sessions. Indeed, the unanticipated presentations of a strong sound can wake up the sleeping animal. In the example in **Figure 3F**; **Supplementary Video 5**, the first couple of CS+ presentations induced freezing behavior, which was detected by our method because smoothed spindle power remained low during these immobility periods. After some minutes, the animal fell asleep, which was accompanied by increased smoothed spindle power.

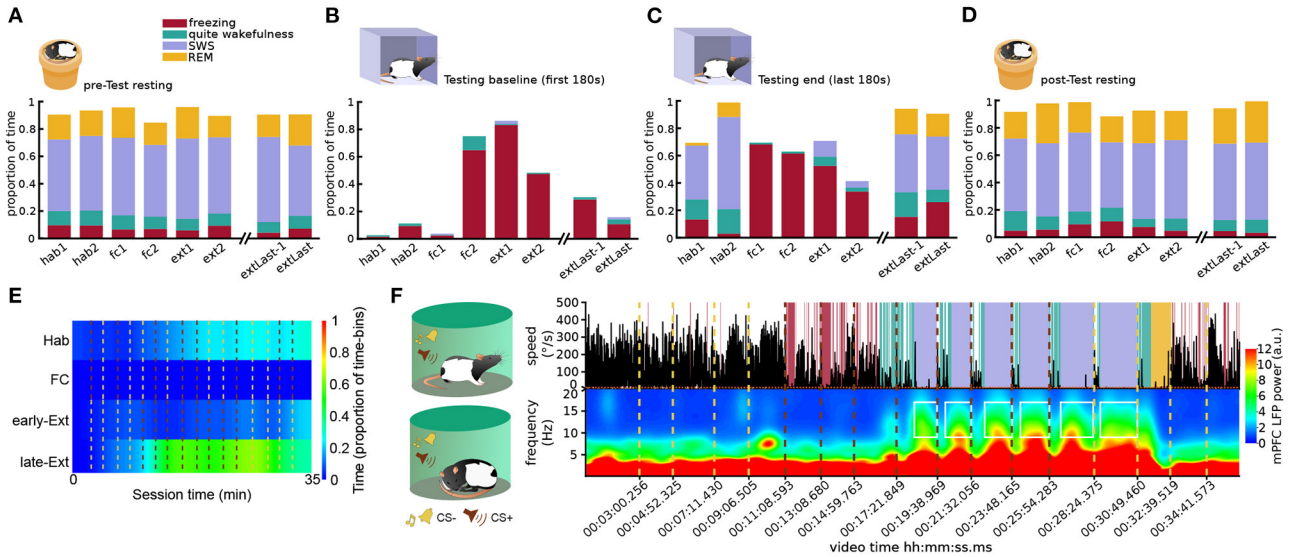

FIGURE 3 | Scoring pipeline performance on a multi-day fear conditioning and extinction protocol. **(A)** Average time classified SWS, REM, quiet wakefulness, and freezing during the rest sessions before exposure to the testing environments for each day of the behavioral protocol. **(B)** Same as **(A)** but for the first 3 min in the conditioning context A. **(C)** Same as **(A)** but for the last 3 min in the conditioning context A. **(D)** Same as **(A)** but for rest sessions following exposure to the testing environments. **(E)** Average time spent sleeping across auditory cued extinction training sessions in context B for all animals; red dashed vertical lines: CS+ onsets; ochre dashed vertical lines: CS− onsets. **(F)** State scoring in a representative session of late extinction of cued fear involving both sleep and freezing (see **Supplementary Video 5**). (Top) Animal speed as measured by head movements; red dashed vertical lines: CS+ onsets; ochre dashed vertical lines: CS− onsets. Time stamps of CSs presentations corresponding to those overlaid in **Supplementary Video 5** frames are indicated below the plots. Shaded area: periods classified as freezing (red), quiet wakefulness (green), SWS (blue), and REM (yellow). Note how the animal did not freeze during CS− presentations, but the onsets of the first three CS+ triggered freezing responses. (Bottom) Spectrogram of mPFC LFP activity; white squares: intervals of elevated sleep spindle power scored as SWS. The rat started to sleep after the fourth CS+ presentation and from then on, every CS+ presentation woke him up, but he fell asleep again within 30–40 s.

Each subsequent CS presentation briefly woke the animal up, resulting in sleep-wake-sleep transitions detected by our method. The smoothed spindle power can therefore serve as a precise tag for SWS.

Finally, while ground truth data for the internal state of the animal is impossible to obtain, we compared the results of the algorithm to the scoring by an expert observer, blind to the algorithm results, who manually labeled 2 s video snippets ($n = 600$) classified as either freezing or sleep by the algorithm across five recording sessions from three different animals. The freezing vs. sleep separation by this manual scoring agreed with the algorithm classification 92% of the time.

3. DISCUSSION

Discriminating between freezing and resting states can be critical in longitudinal recordings of emotional behavior. However, traditionally, these behaviors have been studied separately, and standard scoring methods using immobility and theta/delta ratio cannot disambiguate between them. Unlike delta band power, the smoothed spindle power in cortical LFP recordings can correctly identify SWS epochs and separate them from freezing. The remaining immobility periods can be scored as REM sleep, quiet wakefulness, or freezing, depending on the theta/delta ratio and their timing to detected SWS epochs. We applied this approach to recordings of rats involving both freezing and sleep as part of a fear conditioning and extinction protocol, and our results are consistent with correct scoring of freezing and sleep states.

The key advantage of the smoothed spindle power is that while it is high in SWS, it remains low during freezing. Basing the SWS detection on this signal alone thus avoids confounding SWS and freezing, when other signals such as delta power can respond strongly to both behaviors due to the overlap between the delta band and the 4 Hz oscillation (2–5 Hz respiratory-driven rhythmic activity; Moberly et al., 2018). While the spindle band power is used by many sleep classification algorithms (e.g., Gottesmann et al., 1977; Louis et al., 2004; Liang et al., 2012; Supratak et al., 2017), its contribution is often secondary to slow oscillations in the delta band. Therefore, these algorithms can be used to score sleep stages only after freezing has already been excluded, but they were not designed to separate between sleep and freezing, especially given their assumption that all immobility corresponds to resting states.

Recently, Bagur et al. (2018) showed that sleeping and freezing states can be disambiguated using oscillations recorded in the olfactory bulb. This is a powerful method which resolves the sleeping/freezing ambiguity. Using the neocortical smoothed spindle power as proposed here can be an alternative in the absence of such recordings from the olfactory bulb.

Here, we introduced a technique to detect SWS periods based solely upon the smoothed spindle band oscillatory activity and we demonstrated its effectiveness in our data. To our knowledge, this is the only automated approach discriminating between freezing and resting immobility in the absence of olfactory bulb recordings. Our algorithm is straightforward to implement as it only requires recording from a single neocortical electrode, and it could be of use for future systems neuroscience research involving both fear and rest behavioral states. Moreover, the lack of overlap between the spindle band and breathing frequencies observed in immobility (Herent et al., 2020) can help separate sleep from other awake behaviors beyond freezing, permitting the smoothed spindle power to serve as a simple method to detect SWS in general.

4. MATERIALS AND METHODS

4.1. Recording of Neural Activity During a Multi-Day Fear Conditioning and Extinction Training Protocol and Peri-Training Rest

4.1.1. Animals

Five male Long-Evans rats (350–400 g at the time of the surgery, 2–5 months old) were housed individually in monitored conditions (21°C and 45% humidity) and maintained on a 12 h light–12 h dark cycle. In order to avoid obesity, feeding was restricted to 13–16 g chow per day, with water available *ad libitum*. To habituate the rats to human manipulation, they were handled each workday. All experiments conformed to the approved protocols and regulations of the local ethics committee and the French ministry of agriculture and the French ministry of higher education and research.

4.1.2. Surgery

Rats were deeply anesthetized using a ketamine-xylazine mixture (Imalgene and Rompun, 180 and 10 mg/kg, respectively) and anesthesia was maintained with isoflurane (0.1–1.5% in oxygen). Analgesia was assured by subcutaneous injection of buprenorphine (Buprecaire, 0.025 mg/kg) and meloxicam (Metacam, 3 mg/kg). The animals were implanted bilaterally with a custom built microdrive with 24–42 bundles of independently movable twisted electrodes (12 μm tungsten wires twisted in groups of either six or eight wires and gold-plated to 200 kΩ) 0.5 mm above the target brain regions. Electrode bundle placement varied between rats. Nevertheless, in all animals there were electrodes implanted in the medial prefrontal cortex (sterotaxic coordinates: ±0.3–0.6 mm mediolateral and +2.5–4.8 mm anterioposterior from bregma) and dorsal hippocampus (±3.8–5 mm mediolateral and −5 mm anterioposterior from bregma). During recovery after surgery (minimum 7 days), the rats received antibiotic (Marbofloxacine, 2 mg/kg) and analgesic (Meloxicam, 3 mg/kg) treatments via subcutaneous injections, and were provided with food and water *ad libitum*. The recording electrodes were then progressively lowered until they reached their targets.

4.1.3. Behavioral Apparatus

After full recovery, rats were exposed to two testing environments (context A and context B), and one resting environment. Context A was a cubicle conditioning chamber (40×40×40 cm) with gray plexiglass walls lined with ribbed black rubber sheets and a floor composed of nineteen stainless steel rods [0.48 cm diameter with 1.6 cm spacing connected to a scrambled shock generator (ENV-414S, Med Associates, USA)]. It was mildly scented daily with mint-perfumed cleaning solution (Simple Green, Sunshine Makers). Context B was a stadium-shaped PVC enclosure (30 cm side and 15 cm radius) with a black wooden floor and walls lined with light brown pieces of rope rug. It was mildly scented daily with a vanilla extract solution. The resting environment was a cloth-lined plastic flowerpot (30 cm upper diameter, 20 cm lower diameter, 25 cm high). Auditory stimuli (conditioned stimuli, CSs) were delivered in either of the two testing environments via a custom-made electronic system. The stimuli were white noise (CS+) or 8 kHz pure tone (CS−) 250 ms long pips repeated at 1 Hz for the duration of 20 s at 80 dB.

4.1.4. Behavioral Protocol

Habituation took place on days 1 and 2. On day 1, CSs were presented in one context and on day 2 they were presented in the other (context order presentation was switched every day and was counterbalanced across animals), habituating the animals to the stimuli. On days 3 and 4, the animals were fear conditioned in context A, where CS+ presentations were coupled with foot shocks (1 s, 0.6 mA, co-terminating with CS+ presentations). Extinction training began on day 5, with CS presentations in context B and context exposure (no CS presentations) in context A. Extinction training was repeated every day until the rat was seen sleeping throughout CS+ presentations.

Every day of the experimental protocol consisted of one 35 min session in each context. When introduced in the contexts the animals were either presented with the auditory CSs (after a baseline period of 3 min, the animals were presented to 16 CSs, 8 CS+, and 8 CS−, separated by inter-trial intervals of random duration, range 120–240 s) or received no auditory stimuli (context exposure sessions). During habituation and fear conditioning, CS+ and CS− were presented in pseudorandom order (no more than 2 consecutive presentations of the same-type CS), while in extinction training, 4 CS− were presented first, followed by 8 CS+ and then 4 CS−. Before and after each session the animals were left undisturbed for at least 2 h in the resting environment to record sleep activity.

4.1.5. Data Acquisition and Processing

An inertial measurement unit (IMU, non wireless version of the one described in Pasquet et al., 2016) recorded 3D angular velocity and linear acceleration of the animals' heads (sampled at 300 Hz). Animal behavior was also recorded by lateral video

cameras (50 Hz sampling rate) in contexts A and B (acA25000, Basler). Brain activity was recorded wideband at 20,000 Hz using a KJE-1001 data acquisition system (Amplipex, Szeged, Hungary). Neurophysiological and behavioral data were explored with NeuroScope (Hazan et al., 2006). LFPs were derived from wideband signals by downsampling all channels to 1,250 Hz. At the end of the experiments, recording sites were marked with small electrolytic lesions (∼20 μA for 20 s, one lesion per bundle). After a delay of at least 3 days to permit glial scarring, rats were deeply anesthetized with a lethal dose of pentobarbital and intracardially perfused with saline (0.9%) followed by paraformaldehyde (4%). Coronal slices (35 μm) were stained with cresyl-violet and imaged with conventional transmission light microscopy (**Supplementary Figure 5**). Recording sites were reconstructed by comparing the images with the stereotaxic atlas of Paxinos and Watson (2013).

4.2. Data Analysis and Statistics

Data were analyzed using FMAToolbox (http://fmatoolbox.sourceforge.net), Chronux (http://chronux.org/), and custom written programs in Matlab (MathWorks, Natick, MA).

4.2.1. Scoring of Behavioral States With Standard Approaches

In order to compare our proposed approach with standard sleep and freezing detection protocols, we performed standard behavioral scoring as follows. Automatic detection of immobility was performed by applying a threshold detection routine to the angular speed calculated from gyroscopic data as we described previously (Pasquet et al., 2016).

4.2.1.1. Freezing Detection

Typically, the minimum duration of immobility to be classified as freezing ranges between 0.5 and 2 s, and brief movements of 0.1–0.2 s are ignored (e.g., Courtin et al., 2014; Jercog et al., 2021). We therefore defined freezing as moments where the animals remained immobile for more than 1.5 s, ignoring brief movements of <0.2 s.

4.2.1.2. Sleep Detection

To identify sleep stages (NREM and REM), LFP data was visualized using Neuroscope (Hazan et al., 2006) and a hippocampal channel with clear theta oscillations during exploration was identified. The signal from this channel was filtered in the theta (6–9 Hz) and delta (0.5–4 Hz) bands. Typically, only periods longer than 30–120 s are retained as sleep and periods around brief movements of 0.5–1 s are merged together (e.g., Drieu et al., 2018; Todorova and Zugaro, 2019). Therefore, here, only the periods of immobility lasting longer than 60 s were considered, and brief movements shorter than 1 s were ignored. The time bins of theta/delta ratio of these periods were clustered in two groups with k-means.

4.2.2. Scoring of Behavioral States With Spindle Power

4.2.2.1. Slow Wave Sleep Detection

Immobility was detected as above. LFP data was visualized using Neuroscope (Hazan et al., 2006) and a channel with distinct spindles during sleep (mPFC) was selected. The LFP signal was filtered in the spindle band (9–17 Hz), and the instantaneous amplitude was estimated using the Hilbert transform. This amplitude was then smoothed (Gaussian window of 14 s), and immobility periods where the smoothed amplitude exceeded a k-means identified threshold (**Supplementary Figure 2**) were classified as SWS. The minimum duration allowed for sleep bouts and the maximum duration of small movements are parameters that users are free to select. For the results presented here these parameters were set to 30 and 1 s, respectively.

4.2.2.2. REM Sleep Detection

The remaining immobility periods where the ratio between the theta (6–9 Hz) and delta (0.5–4 Hz) power of the HPC LFP signal exceeded 1 and followed a SWS period were classified as REM. The maximum delay by which REM periods can follow SWS is a parameter set by the user. However, since SWS to REM transitions are known to last up to 30 s (Datta and Hobson, 2000), we recommend allowing for at least 30 s.

In the absence of hippocampal LFP the algorithm can detect REM periods using the theta/delta ratio of the cortical LFP used to detect SWS, with the following adjustments. First, the cortical theta/delta ratio is smoothed by Gaussian smoothing window, with a window width of 8 s maximizing the correspondence to the results obtained using HPC recordings. Then, because the theta/delta ratio tends to be lower in the mPFC than in the hippocampus, the threshold to detect REM epochs is determined using the Otsu method (Otsu, 1979; which divides the theta/delta values into two groups maximizing inter-class variance) rather than the hard-coded threshold of 1 used for HPC recordings. The resulting REM periods thus obtained by PFC recordings matched the ones estimated by HPC recordings 93.45% of the time (**Supplementary Figure 3**).

4.2.2.3. Quiet Wakefulness Detection

Animals don't fall asleep in their freezing posture: at the minimum, they would always readjust their heads and more typically also curl up their bodies. This means that freezing and pre-sleep immobility are interrupted by movement. Therefore, other periods of immobility which preceded SWS by <2 min were classified as immobile wakefulness. This duration is a parameter free to user selection, and reasonable choices would fall within a range of 30 s to a few minutes.

4.2.2.4. Freezing Detection

All the remaining immobility was classified as freezing with a minimum duration of freezing bouts and minimal interruptions set respectively to 2 and 0.2 s. These parameters are free to user selection in our code.

4.2.3. Analyses of Scoring Performance and Data Visualization

To assess the optimal smoothing window of the spindle power, we computed the effectiveness metric m of the k-means separation

of the smoothed spindle power in two groups, as defined by the proportion of inter-group variance and computed as $m = 1 - \frac{\sigma_i}{\sigma_{tot}}$, where σ_i is the intra-group variance σ_{tot} is the total variance of the smoothed spindle power.

To compute spectrograms, we employed an adapted version of the wavelet transform code from http://paos.colorado.edu/research/wavelets/.

CODE AVAILABILITY STATEMENT

A Matlab function to apply the scoring pipeline presented here is freely available on github (https://github.com/mnpompili/behavioralStates.git).

DATA AVAILABILITY STATEMENT

The data supporting the conclusions of this article will be made available by the authors upon request.

ETHICS STATEMENT

The animal protocol was reviewed and approved by Comité d'Ethique en Matière d'Expérimentation Animale N°59.

AUTHOR CONTRIBUTIONS

MP and RT: research project conception and design and data analysis. MP: funding gathering and project management. RT: algorithm conception and implementation. MP with contributions from RT: manuscript. Both authors contributed to the article and approved the submitted version.

FUNDING

MP was supported by the Agence Nationale de la Recherche (ANR-20-NEUC-0005-01) and RT by Cornell University.

ACKNOWLEDGMENTS

We thank Sidney Wiener, Michaël Zugaro, and Christophe Bernard for help hosting and financing this work.

SUPPLEMENTARY MATERIAL

The Supplementary Material for this article can be found online at: https://www.frontiersin.org/articles/10.3389/fncir.2022.783768/full#supplementary-material

Supplementary Video 1 | Representative video of a rat sleeping in the resting environment. The video corresponds to the time interval shown on the left side of **Figure 1B**, part of the resting session immediately preceding the first contextual extinction session. Note how the animal sleeps almost all the time with small movements to adjust its posture.

Supplementary Video 2 | Representative video of a rat freezing in the conditioning environment. The video corresponds to the time interval shown on the right side of **Figure 1B**, that is the baseline period of the first contextual extinction session. These are the first moments the animal enters this environment since conditioning. Note how the animal freezes all the time in a stiff position and only the movements associated to a deep respiration are visible.

Supplementary Video 3 | Representative video of an animal exploring the conditioning environment. This corresponds to the first 30 seconds of exposure to the conditioning environment on the fourth day of extinction. This is the same rat of **Supplementary Video 2** but after 3 sessions of contextual fear extinction. Note how the animal does not freeze any more and explores the environment as the contextual fear has been extinguished.

Supplementary Video 4 | Representative video of an animal sleeping in the conditioning environment. This corresponds to 30 seconds in the conditioning environment on the fourth day of extinction. Namely, the same session of **Supplementary Video 3** 15 minutes later. Note how the animal sleeps, although uncomfortably, on the rods of the floor. The reclined head adjusted on the fore-paws is a good sleep marker.

Supplementary Video 5 | Video corresponding to the example session of **Figure 3F** where both freezing and sleeping were detected. The timestamp overlaid on video frames are on the same time scale of the x axis of the figure. Note how the animal explores the environment during baseline, freezes after the onsets of the first two CS+ presentations, but then gradually falls asleep. This rest is systematically interrupted by CS+ presentations (only two episodes shown in this video). All these transitions were captured by our technique as shown in **Figure 3F**.

REFERENCES

Bagur, S., Lacroix, M. M., de Lavilléon, G., Lefort, J. M., Geoffroy, H., and Benchenane, K. (2018). Harnessing olfactory bulb oscillations to perform fully brain-based sleep-scoring and real-time monitoring of anaesthesia depth. *PLoS Biol.* 16:e2005458. doi: 10.1371/journal.pbio.2005458

Bagur, S., Lefort, J. M., Lacroix, M. M., de Lavilléon, G., Herry, C., Chouvaeff, M., et al. (2021). Breathing-driven prefrontal oscillations regulate maintenance of conditioned-fear evoked freezing independently of initiation. *Nat. Commun.* 12, 1–15. doi: 10.1038/s41467-021-22798-6

Benchenane, K., Peyrache, A., Khamassi, M., Tierney, P. L., Gioanni, Y., Battaglia, F. P., et al. (2010). Coherent theta oscillations and reorganization of spike timing in the hippocampal- prefrontal network upon learning. *Neuron* 66, 921–936. doi: 10.1016/j.neuron.2010.05.013

Biskamp, J., Bartos, M., and Sauer, J. F. (2017). Organization of prefrontal network activity by respiration-related oscillations. *Sci. Rep.* 7, 1–11. doi: 10.1038/srep45508

Blanchard, R. J., and Blanchard, D. C. (1969). Crouching as an index of fear. *J. Compar. Physiol. Psychol.* 67, 370–375. doi: 10.1037/h0026779

Brankack, J., Kukushka, V. I., Vyssotski, A. L., and Draguhn, A. (2010). EEG gamma frequency and sleep-wake scoring in mice: comparing two types of supervised classifiers. *Brain Res.* 1322, 59–71. doi: 10.1016/j.brainres.2010.01.069

Buzsáki, G., Peyrache, A., and Kubie, J. (2014). Emergence of cognition from action. *Cold Spring Harb. Symp. Quant. Biol.* 79, 41–50. doi: 10.1101/sqb.2014.79.024679

Chung, J. E., Joo, H. R., Fan, J. L., Liu, D. F., Barnett, A. H., Chen, S., et al. (2019). High-density, long-lasting, and multi-region electrophysiological recordings using polymer electrode arrays. *Neuron* 101, 21–31.e5. doi: 10.1016/j.neuron.2018.11.002

Ciatipis, M., Branka, K, J., Draguhn, A., Tort, A. B. L., and Yanovsky, Y. (2014). Slow oscillations in the mouse hippocampus entrained by nasal respiration. *J. Neurosci.* 34, 5949–5964. doi: 10.1523/JNEUROSCI.5287-13.2014

Courtin, J., Chaudun, F., Rozeske, R. R., Karalis, N., Gonzalez-Campo, C., Wurtz, H., et al. (2014). Prefrontal parvalbumin interneurons shape neuronal activity to drive fear expression. *Nature* 505, 92–96. doi: 10.1038/nature12755

Datta, S., and Hobson, J. A. (2000). The rat as an experimental model for sleep neurophysiology. *Behav. Neurosci.* 114, 1239–1244. doi: 10.1037/0735-7044.114.6.1239

Dhawale, A. K., Poddar, R., Wolff, S. B., Normand, V. A., Kopelowitz, E., and Ölveczky, B. P. (2017). Automated long-term recording and analysis of neural activity in behaving animals. *eLife* 6, 1–40. doi: 10.7554/eLife.27702

Drieu, C., Todorova, R., and Zugaro, M. (2018). Nested sequences of hippocampal assemblies during behavior support subsequent sleep replay. *Science* 362, 675–679. doi: 10.1126/science.aat2952

Fanselow, M. S., and Poulos, A. M. (2005). The neuroscience of mammalian associative learning. *Annu. Rev. Psychol.* 56, 207–234. doi: 10.1146/annurev.psych.56.091103.070213

Fernandez, L. M., and Lüthi, A. (2020). Sleep spindles: mechanisms and functions. *Physiol. Rev.* 100, 805–868. doi: 10.1152/physrev.00042.2018

Girardeau, G., Inema, I., and Buzsáki, G. (2017). Reactivations of emotional memory in the hippocampusamygdala system during sleep. *Nat. Neurosci.* 20:1634. doi: 10.1038/nn.4637

Gottesmann, C., de Mendoza, J. L. J., Lacoste, G., Lallement, B., Rodrigues, L., and Tasset, M. (1971). Etude sur l'analyse et la quantification automatiques del différents états de veille et de sommeil chez le Rat. *CR Acad. Sci.* 272, 301–302.

Gottesmann, C., Kirkham, P. A., Lacoste, G., Rodrigues, L., and Arnaud, C. (1977). Automatic analysis of the sleep-waking cycle in the rat recorded by miniature telemetry. *Brain Res.* 132, 562–568. doi: 10.1016/0006-8993(77)90205-0

Gründemann, J., Bitterman, Y., Lu, T., Krabbe, S., Grewe, B. F., Schnitzer, M. J., et al. (2019). Amygdala ensembles encode behavioral states. *Science* 364:aav8736. doi: 10.1126/science.aav8736

Hazan, L., Zugaro, M., and Buzsáki, G. (2006). Klusters, NeuroScope, NDManager: a free software suite for neurophysiological data processing and visualization. *J. Neurosci. Methods* 155, 207–216. doi: 10.1016/j.jneumeth.2006.01.017

Hengen, K. B., Torrado Pacheco, A., McGregor, J. N., Van Hooser, S. D., and Turrigiano, G. G. (2016). Neuronal firing rate homeostasis is inhibited by sleep and promoted by wake. *Cell* 165, 180–191. doi: 10.1016/j.cell.2016.01.046

Herent, C., Diem, S., Fortin, G., and Bouvier, J. (2020). Absent phasing of respiratory and locomotor rhythms in running mice. *eLife* 9, 1–21. doi: 10.7554/eLife.61919

Hirase, H., Leinekugel, X., Czurkó, A., Csicsvari, J., and Buzsáki, G. (2001). Firing rates of hippocampal neurons are preserved during subsequent sleep episodes and modified by novel awake experience. *Proc. Natl. Acad. Sci. U.S.A.* 98, 9386–9390. doi: 10.1073/pnas.161274398

Jercog, D., Winke, N., Sung, K., Fernandez, M. M., Francioni, C., Rajot, D., et al. (2021). Dynamical prefrontal population coding during defensive behaviours. *Nature* 595, 690–694. doi: 10.1038/s41586-021-03726-6

Johns, T. G., Piper, D. C., James, G. W., Birtley, R. D., and Fischer, M. (1977). Automated analysis of sleep in the rat. *Electroencephalogr. Clin. Neurophysiol.* 43, 103–105. doi: 10.1016/0013-4694(77)90201-2

Karalis, N., Dejean, C., Chaudun, F., Khoder, S., Rozeske, R. R., Wurtz, H. H. H. H. H., et al. (2016). 4-Hz oscillations synchronize prefrontal-amygdala circuits during fear behavior. *Nat. Neurosci.* 19, 605–612. doi: 10.1038/nn.4251

Karalis, N., and Sirota, A. (2022). Breathing coordinates cortico-hippocampal dynamics in mice during offline states. *Nat. Commun.* 13, 1–20. doi: 10.1038/s41467-022-28090-5

Kohn, M., Litchfield, D., Branchey, M., and Brebbia, D. R. (1974). An automatic hybrid analyzer of sleep stages in the rat. *Electroencephalogr. Clin. Neurophysiol.* 37, 518–520. doi: 10.1016/0013-4694(74)90095-9

Krakauer, J. W., Ghazanfar, A. A., Gomez-Marin, A., MacIver, M. A., and Poeppel, D. (2017). Neuroscience needs behavior: correcting a reductionist bias. *Neuron* 93, 480–490. doi: 10.1016/j.neuron.2016.12.041

Liang, S. -F., Kuo, C. -E., Hu, Y. -H., and Cheng, Y. -S. (2012). A rule-based automatic sleep staging method. *J. NeuroSci. Methods* 205, 169–176. doi: 10.1016/j.jneumeth.2011.12.022

Lin, S. C., Gervasoni, D., and Nicolelis, M. A. (2006). Fast modulation of prefrontal cortex activity by basal forebrain noncholinergic neuronal ensembles. *J. Neurophysiol.* 96, 3209–3219. doi: 10.1152/jn.00524.2006

Lockmann, A. L. V., Laplagne, D. A., Le ao, R. N., and Tort, A. B. L. (2016). A respiration-coupled rhythm in the rat hippocampus independent of theta and slow oscillations. *J. Neurosci.* 36, 5338–5352. doi: 10.1523/JNEUROSCI.3452-15.2016

Louis, R. P., Lee, J., and Stephenson, R. (2004). Design and validation of a computer-based sleep-scoring algorithm. *J. Neurosci. Methods* 133, 71–80. doi: 10.1016/j.jneumeth.2003.09.025

McCarley, R. W. (2007). Neurobiology of REM and NREM sleep. *Sleep Med.* 8, 302–330. doi: 10.1016/j.sleep.2007.03.005

Moberly, A. H., Schreck, M., Bhattarai, J. P., Zweifel, L. S., Luo, W., and Ma, M. (2018). Olfactory inputs modulate respiration-related rhythmic activity in the prefrontal cortex and freezing behavior. *Nat. Commun.* 9, 1528. doi: 10.1038/s41467-018-03988-1

Otsu, N. (1979). A threshold selection method from gray-level histograms. *IEEE Trans. Syst. Man Cybern.* 9, 62–66. doi: 10.1109/TSMC.1979.4310076

Pasquet, M. O., Tihy, M., Gourgeon, A., Pompili, M. N., Godsil, B. P., Léna, C., et al. (2016). Wireless inertial measurement of head kinematics in freely-moving rats. *Sci. Rep.* 6:35689. doi: 10.1038/srep35689

Paxinos, G., and Watson, C. (2013). *The Rat Brain in Stereotaxic Coordinate, 7th Edn*. New York, NY: Academic Press.

Ressler, R. L., Goode, T. D., Kim, S., Ramanathan, K. R., and Maren, S. (2021). Covert capture and attenuation of a hippocampus-dependent fear memory. *Nat. Neurosci.* 24, 677–684. doi: 10.1038/s41593-021-00825-5

Sosa, M., Joo, H. R., and Frank, L. M. (2020). Dorsal and ventral hippocampal sharp-wave ripples activate distinct nucleus accumbens networks. *Neuron* 105, 725–741.e8. doi: 10.1016/j.neuron.2019.11.022

Steriade, M., McCormick, D. A., and Sejnowski, T. J. (1993). Thalamocortical oscillations in the sleeping and aroused brain. *Science* 262, 679–685. doi: 10.1126/science.8235588

Supratak, A., Dong, H., Wu, C., and Guo, Y. (2017). DeepSleepNet: a model for automatic sleep stage scoring based on raw single-channel EEG. *IEEE Trans. Neural Syst. Rehabil. Eng.* 25, 1998–2008. doi: 10.1109/TNSRE.2017.2721116

Tingley, D., McClain, K., Kaya, E., Carpenter, J., and Buzsáki, G. (2021). A metabolic function of the hippocampal sharp wave-ripple. *Nature* 597, 82–86. doi: 10.1038/s41586-021-03811-w

Todorova, R., and Zugaro, M. B. (2019). Isolated cortical computations during delta waves. *Science*. 366, 377–381. doi: 10.1126/science.aay0616

Trouche, S., Pompili, M. N., and Girardeau, G. (2020). The role of sleep in emotional processing: insights and unknowns from rodent research. *Curr. Opin. Physiol.* 15, 230–237. doi: 10.1016/j.cophys.2020.04.003

Wang, M., Foster, D. J., and Pfeiffer, B. E. (2020). Alternating sequences of future and past behavior encoded within hippocampal theta oscillations. *Science* 370, 247–250. doi: 10.1126/science.abb4151

Wilson, M. A., and McNaughton, B. L. (1994). Reactivation of hippocampal ensemble memories during sleep. *Science* 265, 676–679. doi: 10.1126/science.8036517

Conflict of Interest: The authors declare that the research was conducted in the absence of any commercial or financial relationships that could be construed as a potential conflict of interest.

The handling editor declared past co-authorships with both authors.

frontiers | Frontiers in Neural Circuits

PERSPECTIVE
published: 01 April 2022
doi: 10.3389/fncir.2022.885684

Rhythmic Memory Consolidation in the Hippocampus

Miriam S. Nokia[1,2]* *and Markku Penttonen*[1,2]

[1]*Department of Psychology, University of Jyväskylä, Jyväskylä, Finland,* [2]*Centre for Interdisciplinary Brain Research, University of Jyväskylä, Jyväskylä, Finland*

Functions of the brain and body are oscillatory in nature and organized according to a logarithmic scale. Brain oscillations and bodily functions such as respiration and heartbeat appear nested within each other and coupled together either based on phase or based on phase and amplitude. This facilitates communication in wide-spread neuronal networks and probably also between the body and the brain. It is a widely accepted view, that nested electrophysiological brain oscillations involving the neocortex, thalamus, and the hippocampus form the basis of memory consolidation. This applies especially to declarative memories, that is, memories of life events, for example. Here, we present our view of hippocampal contribution to the process of memory consolidation based on the general ideas stated above and on some recent findings on the topic by us and by other research groups. We propose that in addition to the interplay between neocortical slow oscillations, spindles, and hippocampal sharp-wave ripples during sleep, there are also additional mechanisms available in the hippocampus to control memory consolidation: a rather non-oscillatory hippocampal electrophysiological phenomenon called the dentate spike might provide a means to not only consolidate but to also modify the neural representation of declarative memories. Further, we suggest that memory consolidation in the hippocampus might be in part paced by breathing. These considerations might open new possibilities for regulating memory consolidation in rest and sleep.

Keywords: electrophysiology, respiration, brain oscillations, sleep, neuronal circuits

OPEN ACCESS

Edited by:
Gabrielle Girardeau, INSERM U839 Institut du Fer à Moulin (IFM), France

Reviewed by:
Lisa Genzel, University of Edinburgh, United Kingdom

***Correspondence:**
Miriam S. Nokia
miriam.nokia@jyu.fi

Received: *28 February 2022*
Accepted: *15 March 2022*
Published: *01 April 2022*

Citation:
Nokia MS and Penttonen M (2022) Rhythmic Memory Consolidation in the Hippocampus. Front. Neural Circuits 16:885684. doi: 10.3389/fncir.2022.885684

INTRODUCTION

Constant fluctuations in membrane potential of cells in the brain, especially synaptic activity of neurons, produce voltage fluctuations in the extracellular space that can be detected by means of local-field potential (LFP) or electrocorticogram (ECoG) recordings invasively or electroencephalogram (EEG) and magnetoencephalogram (MEG) recordings noninvasively (Buzsaki et al., 2012). When monitoring these measures, it is obvious that the electrophysiological activity of the brain is rhythmic: slow oscillations tend to involve large neural networks and span multiple brain structures whereas fast oscillations confine to smaller neural assemblies and are limited to specific regions. The oscillations are often categorized into specific frequency bands according to the following: <0.5 Hz (ultra-slow oscillations), 0.5–1 Hz (slow oscillations), 1–3.5 Hz (delta), 3.5–8 Hz (theta), 8–12 Hz (alpha), 13–30 Hz (beta), 30–80 Hz (gamma), >80 Hz (fast oscillations).

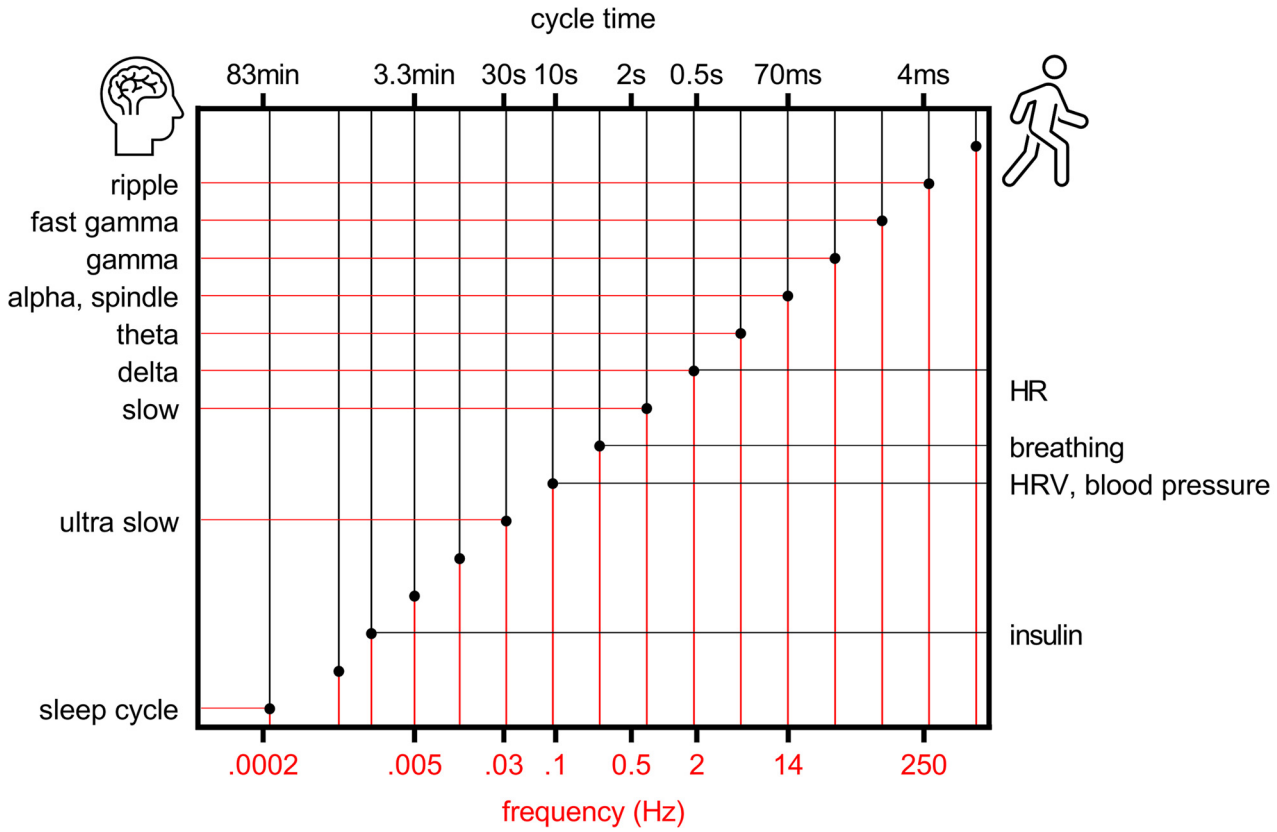

FIGURE 1 | Rhythms of the brain and body follow a logarithmic scale. Organization of brain (left y-axis) and bodily (right y-axis) rhythms on a logarithmic scale, modified from Penttonen and Buzsaki (2003). HR, heart rate; HRV, heart rate variability.

Some 20 years ago it was proposed that to allow efficient and reliable communication at different temporal and spatial scales, the center frequencies of brain oscillations follow a logarithmic scale where the distance between neighboring bands is close to Neper's number e, a real and irrational number approaching ∼2.72 (Penttonen and Buzsaki, 2003; **Figure 1**). This ensures that signaling at neighboring frequency bands does not interfere with each other. It was further suggested that the electrophysiological oscillations of distinct frequencies are produced by separate, independent biological mechanisms in the brain and also serve distinct physiological functions (Penttonen and Buzsaki, 2003). The idea has since been further discussed and developed, demonstrating for example how similar the frequency bands of brain oscillations are in mammals from mice to humans despite the differences in the size of the nervous system (Buzsáki and Draguhn, 2004; Buzsáki et al., 2013) and by incorporating also rhythms of the body into the system of interrelated oscillations [(Klimesch, 2018), golden mean approaching ∼1.62 as the base].

As explained above, brain electrophysiological oscillations are organized into separate frequency bands to avoid interference. However, oscillations at different frequency bands interact by means of phase-amplitude coupling or by phase-phase coupling, usually so that the phase of the slower oscillation modulates the amplitude or phase of the faster oscillation with n:m ratios where n and m are integer numbers. Phase-phase coupling is thought to facilitate communication by aligning the duty cycles of two oscillating neural assemblies while suppressing information flow between assemblies in which duty cycles do not overlap (Fries, 2005). An example would be the phase synchrony between distant neocortical regions in humans demonstrated in various studies and at various frequencies (Palva and Palva, 2018). A well-known example of phase-amplitude coupling in the hippocampus is that between theta phase and gamma amplitude (Lisman and Jensen, 2013; Colgin, 2015; **Figure 2A**). Another is the ultra-slow (0.025 Hz, cycle duration ∼40 s) variation in neuronal excitability and the amplitude of beta (8–22 Hz) oscillation (Penttonen et al., 1999; see also Achermann and Borbély, 1997). This kind of link between oscillations is generally referred to as nesting, and it has been suggested to facilitate communication in neural networks (Bonnefond et al., 2017) much like the direct phase-phase coupling.

Brain oscillations emerge spontaneously but can also be entrained (**Figure 2B**). In humans, entrainment can be obtained by rhythmic sensory stimulation (Henao et al., 2020) or by using non-invasive methods such as transcranial magnetic stimulation (Thut et al., 2011). A straightforward means in animal models is to electrically stimulate the brain at a certain frequency to induce rhythmic fluctuations in neuronal

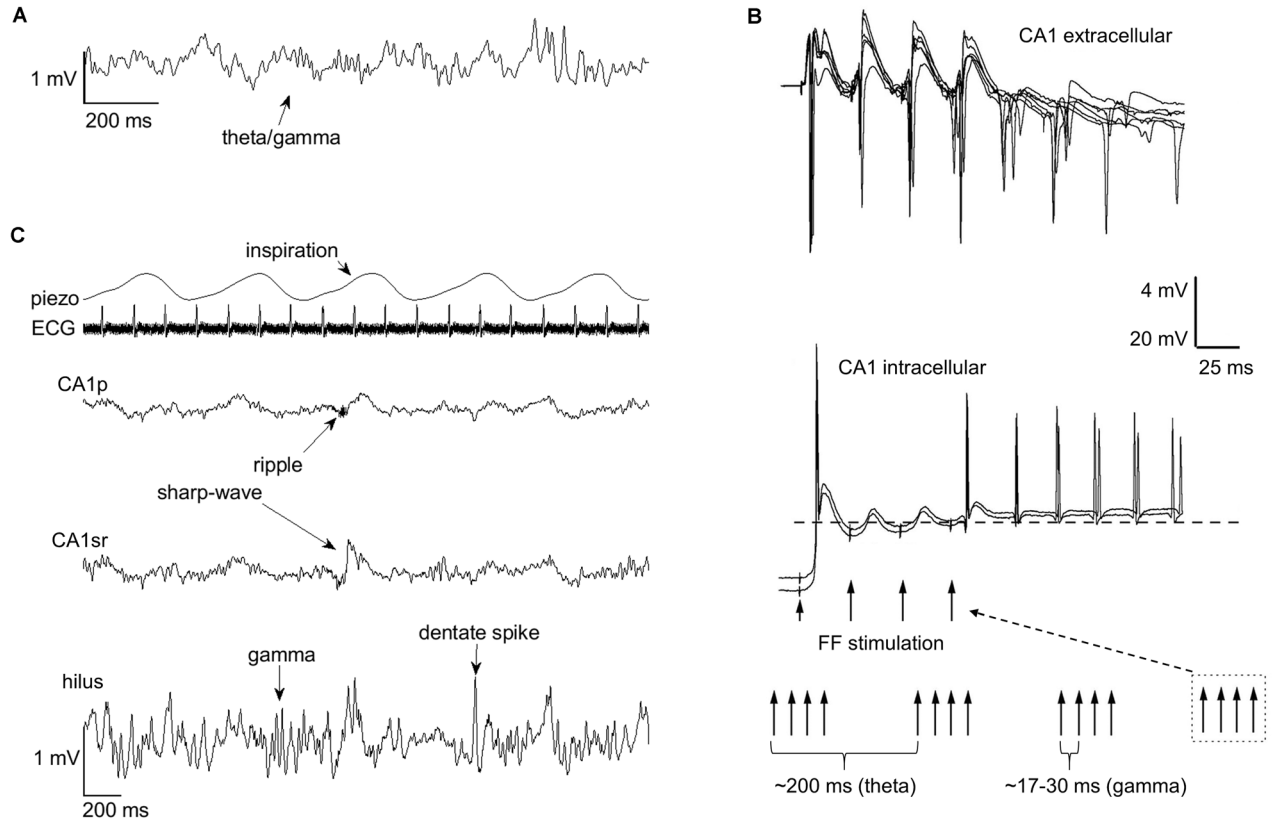

FIGURE 2 | Rhythms of the brain nest within each other and within the rhythmic fluctuations of bodily states. Nesting facilitates entrainment of oscillatory activity within the hippocampus. **(A)** Phase-amplitude coupling of theta and gamma band oscillations (respectively) in the hippocampus is a well-known example of endogenous nesting of rhythmic brain activity. **(B)** The graph is modified from Mikkonen et al. (2002). Rhythmic stimulation of the fimbria fornix (FF) in urethane anesthetized Wistar rats produced entrainment of CA1 activity at the stimulation frequency, but this effect was only evident if trains of gamma-band (30–60 Hz) stimulations were conducted at theta (3–7.5 Hz) frequency, mimicking the naturally occurring theta-gamma nested oscillations in the hippocampus. In addition to entrainment, a sustained rhythmic response retaining the stimulation gamma frequency, probably dependent on the resonant properties of CA1 interneurons and pyramidal cells, is also evident. **(C)** Rhythms of the brain also seem to nest within the rhythms of the body. The occurrence of hippocampal sharp-wave ripples, gamma bursts, and dentate spikes are paced by breathing (piezo). The example traces in **(A,C)** are from a urethane-anesthetized adult male Sprague-Dawley rat. ECG, electrocardiogram; CA1p, CA1 pyramidal cell layer; CA1sr, CA1 stratum radiatum.

excitability. Interestingly, stimulation of the fimbria fornix at a pattern mimicking endogenous theta/gamma-coupling entrains persistent oscillatory responses in the hippocampal CA1 (Mikkonen et al., 2002) while neither gamma nor theta stimulation alone has such an outcome. Remarkably, stimulation of just one pyramidal neuron in the CA3 is able to entrain the firing of neurons in the CA1 taken that this stimulation is timed to occur in synchrony with extracellular stimulation at the nested theta and slow frequencies (Mikkonen et al., 2006). This is to demonstrate the influence of even single neurons on the network activity of the brain, an effect that seems to directly depend on synchrony.

Entrainment can also take place in the brain endogenously, that is, without external stimulation. This might be especially prominent during non-rapid eye movement (NREM) sleep, when the brain is at a state of low synchronization: Epileptic seizures are most likely during this state in human Alzheimer's disease (AD) patients (Horváth et al., 2017) as well as in transgenic mouse models of AD (Gureviciene et al., 2019). On the other hand, in a healthy brain, endogenous entrainment of nested oscillatory activity during sleep might facilitate memory consolidation by allowing recurrent activation of neural assemblies in wide-spread networks formed during the previous wake period.

SLOW OSCILLATIONS, SPINDLES, AND SHARP-WAVE RIPPLES ALIGN TO SUPPORT MEMORY CONSOLIDATION

Hippocampal CA1 pyramidal cells fire in sequences during awake behavior and presumably form neural representations of the experiences. During subsequent sleep, the CA1 firing sequences are replayed in condensed form (Buzsaki, 2015; Liu et al., 2019). This replay of the neural representations is evident in hippocampal LFPs as so-called sharp-wave ripples (SPW-Rs; Buzsaki, 2015). They are set forth within the hippocampus as a result of an interplay of inhibitory interneurons and

excitatory pyramidal neurons of the CA2 and CA3 subregions (Csicsvari et al., 2000; Oliva et al., 2016) as well as perhaps the subiculum (Imbrosci et al., 2021). As a result, thousands of CA1 hippocampal pyramidal cells fire in synchrony which is manifested in the LFP as a burst (∼100 ms) of fast oscillations (∼150–250 Hz, ripple). Within the hippocampus, SPW-Rs lead to sustained synaptic facilitation between groups of CA3 and CA1 pyramidal cells potentiated during experience (Sadowski et al., 2016; see also Norimoto et al., 2018). Further, SPW-Rs are associated with signaling from the hippocampus to the neocortex *via* the subiculum (Böhm et al., 2015) and the reactivation of neocortical neural assemblies also formed during the experience (Ji and Wilson, 2007). Importantly, disrupting brain activity associated with awake (Nokia et al., 2012) or sleep (Girardeau et al., 2009) SPW-Rs hampers learning while facilitating it improves learning (Maingret et al., 2016).

SPW-Rs are most common during non-rapid eye movement sleep and occur nested to spindles (9–15 Hz) and neocortical slow oscillations (SOs, <1 Hz; Siapas and Wilson, 1998; Maingret et al., 2016; Jiang et al., 2019; Varela and Wilson, 2020). Neocortical SOs might actually drive the occurrence of spindles that then regulate the emergence of hippocampal SPW-Rs (Oyanedel et al., 2020; Peyrache and Seibt, 2020; Varela and Wilson, 2020). A study in humans recently reported directional information flow from the neocortex to the hippocampus during spindles and preceding the associated hippocampal SPW-Rs (Ngo et al., 2020). Further, neocortical SOs and spindle density correlate with memory performance (Hanert et al., 2017), and sleep spindle-contingent targeted memory reactivation by presenting auditory cues can enhance memory in humans (Antony et al., 2018). To summarize, SOs, spindles, and SPW-Rs seem to support the consolidation of memories into long-term storage (Klinzing et al., 2019).

The interplay between SOs, spindles, and SPW-Rs seems to be a textbook example of hierarchically ordered electrophysiological brain oscillations that have a distinct mechanism of generation, occur nested to each other, and that contribute to specific physiological functions (Penttonen and Buzsaki, 2003). However, some events within the brain are less oscillatory in nature, yet they still seem to have a specific mechanism of generation and a distinct physiological function. Regarding hippocampal memory consolidation, the dentate spike makes a good example.

DENTATE SPIKES POSSIBLY ENABLE MEMORY MODULATION WITHIN THE HIPPOCAMPUS

Dentate spikes are fast (∼20–80 ms), high-amplitude (∼1–2.5 mV) events evident in LFPs recorded from the hilus of the hippocampal dentate gyrus (DG) in rodents (Bragin et al., 1995; Penttonen et al., 1997; Headley et al., 2017). During dentate spikes, entorhinal neocortical activation stemming from both lateral and medial parts arrives at the DG *via* the perforant path and evokes a rapid increase in the firing rate of granule cells and interneurons (Bragin et al., 1995; Senzai and Buzsaki, 2017). This is noteworthy because granule cells fire seldom overall and are the cells that supposedly form the initial hippocampal engram (Kitamura et al., 2017) supporting reliable, orthogonal encoding of unique but similar experiences (Rolls, 2018). At the same time, dentate spikes seem to have a feed-forward inhibitory effect on CA3 (Bragin et al., 1995; Sanchez-Aguilera et al., 2021) and CA1 (Penttonen et al., 1997) pyramidal cells as they hyperpolarize and decrease firing concomitant with dentate spikes. That is, whereas SPW-Rs reflect increased firing of neurons projecting from the hippocampus to the neocortex, dentate spikes have an opposite effect resulting in a pause in hippocampal output.

Much like SPW-Rs, dentate spikes take place, especially during quiet rest and sleep. Their likelihood is increased during neocortical SO excitatory (UP) states and within a narrow time-period (∼50 ms) following SPW-Rs (Headley et al., 2017) but dentate spikes mostly emerge in the absence of SPW-Rs (Bragin et al., 1995). As dentate spikes seem to exert a suppressive effect on the firing of CA1 pyramidal cells (Penttonen et al., 1997) it is not surprising that when they co-occur with SPW-Rs, the ripples are smaller in amplitude than in the absence of dentate spikes (Headley et al., 2017). In fact, dentate spikes seem to suppress the occurrence of SPW-Rs at least for a duration of 200 ms (Bragin et al., 1995). This is rather interesting as, on the other hand, input from DG granule cells *via* the mossy fibers is reported necessary for learning-related increases in CA3 awake SPW-Rs (Sasaki et al., 2018). That is, input from DG granule cells might in fact contribute to initiating SPW-Rs, except during dentate spikes, when the effect would be opposite.

Interestingly, unlike SPW-Rs, dentate spikes are not oscillatory in themselves. However, they are sometimes surrounded by a few gamma cycles in the DG [type 1 dentate spikes (Bragin et al., 1995)]. It is not entirely clear how hippocampal theta/gamma synchronization (Lisman and Jensen, 2013) relates to dentate spikes but dentate spikes are accompanied by interregional synchronization of neocortical gamma (35–100 Hz; Headley et al., 2017). Gamma-band synchronization in the hippocampo-neocortical system has long been suggested to play a role in memory formation (Axmacher et al., 2006) and might thus also involve the hippocampal dentate spike. It could be that the hippocampal gamma oscillation aids in recruiting specific granule cells to fire (de Almeida et al., 2009; Lisman and Jensen, 2013) during a (type 1) dentate spike. Together with the evidence suggesting that the DG controls SPW-R generation in the CA3/CA1 (see the end of the previous paragraph), this hints at a possible link between dentate spikes and pattern separation/completion in the DG (Leutgeb et al., 2007; Neunuebel and Knierim, 2014).

We suggest a specific function of dentate spikes in memory consolidation could be to selectively reorganize neural representations within the hippocampus, based on input from the entorhinal neocortex. Our own findings (Nokia et al., 2017; Lensu et al., 2019) imply dentate spikes as a likely candidate for merging together discrete but related neural representations during rest and sleep: Specifically, disrupting dentate spikes after training in classical conditioning of the eyeblink response hindered learning suggesting that normally dentate spikes are

needed for making associations between temporally separate events, in this case, the conditioned and the unconditioned stimulus (Nokia et al., 2017). On the contrary, the same dentate spike-contingent disruption conducted after a context-object discrimination task promoted later performance, that is, memory for the two similar context-object configurations was more accurate (Lensu et al., 2019). This implies that, in our latter study, disrupting dentate spikes prevented the merging of representations of recent similar experiences. Further, promoting DG to CA3 feed-forward inhibition (also evident during dentate spikes, see above) can prevent spontaneous generalization of fear in mice over time (Guo et al., 2018). In sum, dentate spikes clearly have the potential to regulate the spontaneous reorganization of newly acquired neural representations within the hippocampus during rest. More studies are needed to better characterize the significance of dentate spikes in terms of memory consolidation.

RESPIRATION MIGHT PACE MEMORY CONSOLIDATION IN THE HIPPOCAMPUS AND BEYOND

Another angle to the organized oscillatory activity of the brain is the fact that the brain is a functionally inseparable part of the body. It has been suggested that bodily functions might organize according to a hierarchical system similar to brain oscillations (Klimesch, 2018; **Figure 1**). That is, the principles of facilitating communication within the brain as well as across the brain and body would essentially be scale-free, applying to oscillations differing in frequency by an order of magnitude. An interesting question is whether, during evolution, synchrony between oscillations first emerged within the bodily functions (for example respiratory-sinus arrhythmia) or within the brain or perhaps within and across the brain and body at once.

Possibly the most studied bodily rhythms affecting the brain is respiration (see for example Heck et al., 2019). In humans, MEG signals at awake, eyes-open resting state are amplitude-modulated according to the phase of breathing: Signal amplitude at delta (∼2 Hz), gamma (∼75 Hz), and fast (∼130 Hz) frequency bands is larger near the inspiration peak and at beta (∼30 Hz) band the signal amplitude is greatest during inspiration onset (Kluger and Gross, 2021). In mice, it seems that many of the hippocampal oscillations related to memory consolidation phase-lock to respiration: Specifically, a recent quite extensive report suggests SPW-Rs and dentate spikes are more likely during or right after inspiration than during expiration (Karalis and Sirota, 2022; but see also Liu et al., 2017). Our own preliminary results suggest dentate spikes, as well as dentate gyrus gamma bursts, are more abundant during inspiration than expiration also in urethane anesthetized rats (Nokia et al. under preparation) (**Figure 2C**). In addition to hippocampal oscillations, in mice, breathing also seems to pace prefrontal cortical activity and the interplay between the cortex and the hippocampus during sleep (Karalis and Sirota, 2022). Further, in rats, the greatest drive from respiration to wide-scale brain oscillations is obtained during awake rest by long and deep inspirations (Girin et al., 2021). To summarize, breathing might set the stage for effective memory consolidation during rest and sleep by synchronizing the oscillatory activity of the brain at large.

Further studies are needed to validate the findings reviewed above, using different species and under varying brain and bodily states. It would be interesting to know if the brain oscillations believed to support memory consolidation are governed by respiration in humans. Indeed, in awake healthy humans, nasal respiration (as opposed to oral respiration) seems to drive limbic system activity (Zelano et al., 2016) and to support memory consolidation (Arshamian et al., 2018). Specifically, when adult participants rehearsed an odor recognition memory task and then, during a 1-h delay, were forced to breathe only through the nose or the mouth, participants breathing through the nose recognized the memorized odors better compared to those breathing through the mouth (Arshamian et al., 2018). Perhaps an effective way to facilitate memory consolidation *via* breathing would be to take long and deep inspirations (Karalis and Sirota, 2022) through the nose (Girin et al., 2021).

DISCUSSION

To summarize, we suggest that while memory consolidation in the hippocampus is convincingly demonstrated to revolve around SPW-Rs, also dentate spikes might play a specific and perhaps complementary role (Nokia et al., 2017; Lensu et al., 2019). Further, we propose that respiration might govern memory consolidation in the hippocampus by pacing the occurrence of oscillatory phenomena (Karalis and Sirota, 2022). While there is ample evidence for the hippocampal neuronal activity related to SPW-Rs, the difficulty in recording single-unit activity from granule cells has impeded the study of dentate spike-related processing in the DG (Senzai and Buzsaki, 2017; Sanchez-Aguilera et al., 2021). However, some recent reports utilizing calcium imaging of the DG granule cells during memory tasks have yielded promising results (Pofahl et al., 2021). In the future it would be most interesting to accompany DG calcium imaging with both electrophysiology from the hippocampus as well as physiological signals from the body (respiration and heartbeat) in conjunction with a declarative memory task and subsequent sleep in freely moving rodents, to further probe the mechanisms of memory consolidation in the hippocampus.

DATA AVAILABILITY STATEMENT

The raw data supporting the conclusions of this article will be made available by the authors, without undue reservation.

ETHICS STATEMENT

The animal study was reviewed and approved by Project Authorisation Board, Regional State Administrative Agency (licence number ESAVI/24666/2018).

AUTHOR CONTRIBUTIONS

MN and MP wrote the article. All authors contributed to the article and approved the submitted version.

FUNDING

This work was funded by the Academy of Finland (grant nr. 316966 to MP and grant nr. 321522 to MN).

REFERENCES

Achermann, P., and Borbély, A. A. (1997). Low-frequency (<1 Hz) oscillations in the human sleep electroencephalogram. *Neuroscience* 81, 213–222. doi: 10.1016/s0306-4522(97)00186-3

Antony, J. W., Piloto, L., Wang, M., Pacheco, P., Norman, K. A., and Paller, K. A. (2018). Sleep spindle refractoriness segregates periods of memory reactivation. *Curr. Biol.* 28, 1736–1743.e4. doi: 10.1016/j.cub.2018.04.020

Arshamian, A., Iravani, B., Majid, A., and Lundström, J. N. (2018). Respiration modulates olfactory memory consolidation in humans. *J. Neurosci.* 38, 10286–10294. doi: 10.1523/JNEUROSCI.3360-17.2018

Axmacher, N., Mormann, F., Fernandez, G., Elger, C. E., and Fell, J. (2006). Memory formation by neuronal synchronization. *Brain Res. Rev.* 52, 170–182. doi: 10.1016/j.brainresrev.2006.01.007

Böhm, C., Peng, Y., Maier, N., Winterer, J., Poulet, J. F. A., Geiger, J. R. P., et al. (2015). Functional diversity of subicular principal cells during hippocampal ripples. *J. Neurosci.* 35, 13608–13618. doi: 10.1523/JNEUROSCI.5034-14.2015

Bonnefond, M., Kastner, S., and Jensen, O. (2017). Communication between brain areas based on nested oscillations. *eNeuro* 4:ENEURO.0153-16.2017. doi: 10.1523/ENEURO.0153-16.2017

Bragin, A., Jando, G., Nadasdy, Z., van Landeghem, M., and Buzsaki, G. (1995). Dentate EEG spikes and associated interneuronal population bursts in the hippocampal hilar region of the rat. *J. Neurophysiol.* 73, 1691–1705. doi: 10.1152/jn.1995.73.4.1691

Buzsaki, G. (2015). Hippocampal sharp wave-ripple: a cognitive biomarker for episodic memory and planning. *Hippocampus* 25, 1073–1188. doi: 10.1002/hipo.22488

Buzsaki, G., Anastassiou, C. A., and Koch, C. (2012). The origin of extracellular fields and currents-EEG, ECoG, LFP and spikes. *Nat. Rev. Neurosci.* 13, 407–420. doi: 10.1038/nrn3241

Buzsáki, G., and Draguhn, A. (2004). Neuronal oscillations in cortical networks. *Science* 304, 1926–1929. doi: 10.1126/science.1099745

Buzsáki, G., Logothetis, N., and Singer, W. (2013). Scaling brain size, keeping timing: evolutionary preservation of brain rhythms. *Neuron* 80, 751–764. doi: 10.1016/j.neuron.2013.10.002

Colgin, L. L. (2015). Theta-gamma coupling in the entorhinal-hippocampal system. *Curr. Opin. Neurobiol.* 31, 45–50. doi: 10.1016/j.conb.2014.08.001

Csicsvari, J., Hirase, H., Mamiya, A., and Buzsaki, G. (2000). Ensemble patterns of hippocampal CA3-CA1 neurons during sharp wave-associated population events. *Neuron* 28, 585–594. doi: 10.1016/s0896-6273(00)00135-5

de Almeida, L., Idiart, M., and Lisman, J. E. (2009). A second function of gamma frequency oscillations: an E%-Max winner-take-all mechanism selects which cells fire. *J. Neurosci.* 29, 7497–7503. doi: 10.1523/JNEUROSCI.6044-08.2009

Fries, P. (2005). A mechanism for cognitive dynamics: neuronal communication through neuronal coherence. *Trends Cogn. Sci.* 9, 474–480. doi: 10.1016/j.tics.2005.08.011

Girardeau, G., Benchenane, K., Wiener, S. I., Buzsaki, G., and Zugaro, M. B. (2009). Selective suppression of hippocampal ripples impairs spatial memory. *Nat. Neurosci.* 12, 1222–1223. doi: 10.1038/nn.2384

Girin, B., Juventin, M., Garcia, S., Lefèvre, L., Amat, C., Fourcaud-Trocmé, N., et al. (2021). The deep and slow breathing characterizing rest favors brain respiratory-drive. *Sci. Rep.* 11:7044. doi: 10.1038/s41598-021-86525-3

Guo, N., Soden, M. E., Herber, C., Kim, M. T., Besnard, A., Lin, P., et al. (2018). Dentate granule cell recruitment of feedforward inhibition governs engram maintenance and remote memory generalization. *Nat. Med.* 24, 438–449. doi: 10.1038/nm.4491

Gureviciene, I., Ishchenko, I., Ziyatdinova, S., Jin, N., Lipponen, A., Gurevicius, K., et al. (2019). Characterization of epileptic spiking associated with brain amyloidosis in APP/PS1 Mice. *Front. Neurol.* 10:1151. doi: 10.3389/fneur.2019.01151

Hanert, A., Weber, F. D., Pedersen, A., Born, J., and Bartsch, T. (2017). Sleep in humans stabilizes pattern separation performance. *J. Neurosci.* 37, 12238–12246. doi: 10.1523/JNEUROSCI.1189-17.2017

Headley, D. B., Kanta, V., and Pare, D. (2017). Intra- and interregional cortical interactions related to sharp-wave ripples and dentate spikes. *J. Neurophysiol.* 117, 556–565. doi: 10.1152/jn.00644.2016

Heck, D. H., Kozma, R., and Kay, L. M. (2019). The rhythm of memory: how breathing shapes memory function. *J. Neurophysiol.* 122, 563–571. doi: 10.1152/jn.00200.2019

Henao, D., Navarrete, M., Valderrama, M., and Le Van Quyen, M. (2020). Entrainment and synchronization of brain oscillations to auditory stimulations. *Neurosci. Res.* 156, 271–278. doi: 10.1016/j.neures.2020.03.004

Horváth, A., Szúcs, A., Barcs, G., and Kamondi, A. (2017). Sleep EEG detects epileptiform activity in Alzheimer's disease with high sensitivity. *J. Alzheimers Dis.* 56, 1175–1183. doi: 10.3233/JAD-160994

Imbrosci, B., Nitzan, N., McKenzie, S., Donoso, J. R., Swaminathan, A., Böhm, C., et al. (2021). Subiculum as a generator of sharp wave-ripples in the rodent hippocampus. *Cell Rep.* 35:109021. doi: 10.1016/j.celrep.2021.109021

Ji, D., and Wilson, M. A. (2007). Coordinated memory replay in the visual cortex and hippocampus during sleep. *Nat. Neurosci.* 10, 100–107. doi: 10.1038/nn1825

Jiang, X., Gonzalez-Martinez, J., and Halgren, E. (2019). Coordination of human hippocampal sharpwave ripples during NREM sleep with cortical theta bursts, spindles, downstates and upstates. *J. Neurosci.* 39, 8744–8761. doi: 10.1523/JNEUROSCI.2857-18.2019

Karalis, N., and Sirota, A. (2022). Breathing coordinates cortico-hippocampal dynamics in mice during offline states. *Nat. Commun.* 13:467. doi: 10.1038/s41467-022-28090-5

Kitamura, T., Ogawa, S. K., Roy, D. S., Okuyama, T., Morrissey, M. D., Smith, L. M., et al. (2017). Engrams and circuits crucial for systems consolidation of a memory. *Science* 356, 73–78. doi: 10.1126/science.aam6808

Klimesch, W. (2018). The frequency architecture of brain and brain body oscillations: an analysis. *Eur. J. Neurosci.* 48, 2431–2453. doi: 10.1111/ejn.14192

Klinzing, J. G., Niethard, N., and Born, J. (2019). Mechanisms of systems memory consolidation during sleep. *Nat. Neurosci.* 22, 1598–1610. doi: 10.1038/s41593-019-0467-3

Kluger, D. S., and Gross, J. (2021). Respiration modulates oscillatory neural network activity at rest. *PLoS Biol.* 19:e3001457. doi: 10.1371/journal.pbio.3001457

Lensu, S., Waselius, T., Penttonen, M., and Nokia, M. S. (2019). Dentate spikes and learning: disrupting hippocampal function during memory consolidation can improve pattern separation. *J. Neurophysiol.* 121, 131–139. doi: 10.1152/jn.00696.2018

Leutgeb, J. K., Leutgeb, S., Moser, M.-B., and Moser, E. I. (2007). Pattern separation in the dentate gyrus and CA3 of the hippocampus. *Science* 315, 961–966. doi: 10.1126/science.1135801

Lisman, J., and Jensen, O. (2013). The theta-gamma neural code. *Neuron* 77, 1002–1016. doi: 10.1016/j.neuron.2013.03.007

Liu, Y., Dolan, R. J., Kurth-Nelson, Z., and Behrens, T. E. J. (2019). Human replay spontaneously reorganizes experience. *Cell* 178, 640–652.e14. doi: 10.1016/j.cell.2019.06.012

Liu, Y., McAfee, S. S., and Heck, D. H. (2017). Hippocampal sharp-wave ripples in awake mice are entrained by respiration. *Sci. Rep.* 7:8950. doi: 10.1038/s41598-017-09511-8

Maingret, N., Girardeau, G., Todorova, R., Goutierre, M., and Zugaro, M. (2016). Hippocampo-cortical coupling mediates memory consolidation during sleep. *Nat. Neurosci.* 19, 959–964. doi: 10.1038/nn.4304

Mikkonen, J. E., Grönfors, T., Chrobak, J. J., and Penttonen, M. (2002). Hippocampus retains the periodicity of gamma stimulation *in vivo*. *J. Neurophysiol.* 88, 2349–2354. doi: 10.1152/jn.00591.2002

Mikkonen, J. E., Huttunen, J., and Penttonen, M. (2006). Contribution of a single CA3 neuron to network synchrony. *Neuroimage* 31, 1222–1227. doi: 10.1016/j.neuroimage.2006.01.007

Neunuebel, J. P., and Knierim, J. J. (2014). CA3 retrieves coherent representations from degraded input: direct evidence for CA3 pattern completion and dentate gyrus pattern separation. *Neuron* 81, 416–427. doi: 10.1016/j.neuron.2013.11.017

Ngo, H.-V., Fell, J., and Staresina, B. (2020). Sleep spindles mediate hippocampal-neocortical coupling during long-duration ripples. *eLife* 9:e57011. doi: 10.7554/eLife.57011

Nokia, M. S., Gureviciene, I., Waselius, T., Tanila, H., and Penttonen, M. (2017). Hippocampal electrical stimulation disrupts associative learning when targeted at dentate spikes. *J. Physiol.* 595, 4961–4971. doi: 10.1113/JP274023

Nokia, M. S., Mikkonen, J. E., Penttonen, M., and Wikgren, J. (2012). Disrupting neural activity related to awake-state sharp wave-ripple complexes prevents hippocampal learning. *Front. Behav. Neurosci.* 6:84. doi: 10.3389/fnbeh.2012.00084

Norimoto, H., Makino, K., Gao, M., Shikano, Y., Okamoto, K., Ishikawa, T., et al. (2018). Hippocampal ripples down-regulate synapses. *Science* 359, 1524–1527. doi: 10.1126/science.aao0702

Oliva, A., Fernández-Ruiz, A., Buzsáki, G., and Berényi, A. (2016). Role of hippocampal CA2 region in triggering sharp-wave ripples. *Neuron* 91, 1342–1355. doi: 10.1016/j.neuron.2016.08.008

Oyanedel, C. N., Durán, E., Niethard, N., Inostroza, M., and Born, J. (2020). Temporal associations between sleep slow oscillations, spindles and ripples. *Eur. J. Neurosci.* 52, 4762–4778. doi: 10.1111/ejn.14906

Palva, J. M., and Palva, S. (2018). Functional integration across oscillation frequencies by cross-frequency phase synchronization. *Eur. J. Neurosci.* 48, 2399–2406. doi: 10.1111/ejn.13767

Penttonen, M., and Buzsaki, G. (2003). Natural logarithmic relationship between brain oscillators. *Thalamus Related Sys.* 2, 145–152. doi: 10.1017/S1472928803000074

Penttonen, M., Kamondi, A., Sik, A., Acsady, L., and Buzsaki, G. (1997). Feed-forward and feed-back activation of the dentate gyrus *in vivo* during dentate spikes and sharp wave bursts. *Hippocampus* 7, 437–450. doi: 10.1002/(SICI)1098-1063(1997)7:4<437::AID-HIPO9>3.0.CO;2-F

Penttonen, M., Nurminen, N., Miettinen, R., Sirvio, J., Henze, D. A., Csicsvari, J., et al. (1999). Ultra-slow oscillation (0.025 Hz) triggers hippocampal afterdischarges in wistar rats. *Neuroscience* 94, 735–743. doi: 10.1016/s0306-4522(99)00367-x

Peyrache, A., and Seibt, J. (2020). A mechanism for learning with sleep spindles. *Philos. Trans. R. Soc. Lond. B Biol. Sci.* 375:20190230. doi: 10.1098/rstb.2019.0230

Pofahl, M., Nikbakht, N., Haubrich, A. N., Nguyen, T., Masala, N., Distler, F., et al. (2021). Synchronous activity patterns in the dentate gyrus during immobility. *eLife* 10:e65786. doi: 10.7554/eLife.65786

Rolls, E. T. (2018). The storage and recall of memories in the hippocampo-cortical system. *Cell Tissue Res.* 373, 577–604. doi: 10.1007/s00441-017-2744-3

Sadowski, J. H. L. P., Jones, M. W., and Mellor, J. R. (2016). Sharp-wave ripples orchestrate the induction of synaptic plasticity during reactivation of place cell firing patterns in the hippocampus. *Cell Rep.* 14, 1916–1929. doi: 10.1016/j.celrep.2016.01.061

Sanchez-Aguilera, A., Wheeler, D. W., Jurado-Parras, T., Valero, M., Nokia, M. S., Cid, E., et al. (2021). An update to Hippocampome.org by integrating single-cell phenotypes with circuit function *in vivo*. *PLoS Biol.* 19:e3001213. doi: 10.1371/journal.pbio.3001213

Sasaki, T., Piatti, V. C., Hwaun, E., Ahmadi, S., Lisman, J. E., Leutgeb, S., et al. (2018). Dentate network activity is necessary for spatial working memory by supporting CA3 sharp-wave ripple generation and prospective firing of CA3 neurons. *Nat. Neurosci.* 21, 258–269. doi: 10.1038/s41593-017-0061-5

Senzai, Y., and Buzsaki, G. (2017). Physiological properties and behavioral correlates of hippocampal granule cells and mossy cells. *Neuron* 93, 691–704.e5. doi: 10.1016/j.neuron.2016.12.011

Siapas, A. G., and Wilson, M. A. (1998). Coordinated interactions between hippocampal ripples and cortical spindles during slow-wave sleep. *Neuron* 21, 1123–1128. doi: 10.1016/s0896-6273(00)80629-7

Thut, G., Schyns, P. G., and Gross, J. (2011). Entrainment of perceptually relevant brain oscillations by non-invasive rhythmic stimulation of the human brain. *Front. Psychol.* 2:170. doi: 10.3389/fpsyg.2011.00170

Varela, C., and Wilson, M. A. (2020). MPFC spindle cycles organize sparse thalamic activation and recently active CA1 cells during non-REM sleep. *eLife* 9:e48881. doi: 10.7554/eLife.48881

Zelano, C., Jiang, H., Zhou, G., Arora, N., Schuele, S., Rosenow, J., et al. (2016). Nasal respiration entrains human limbic oscillations and modulates cognitive function. *J. Neurosci.* 36, 12448–12467. doi: 10.1523/JNEUROSCI.2586-16.2016

Conflict of Interest: The authors declare that the research was conducted in the absence of any commercial or financial relationships that could be construed as a potential conflict of interest.

Publisher's Note: All claims expressed in this article are solely those of the authors and do not necessarily represent those of their affiliated organizations, or those of the publisher, the editors and the reviewers. Any product that may be evaluated in this article, or claim that may be made by its manufacturer, is not guaranteed or endorsed by the publisher.

Advantages of publishing in Frontiers

OPEN ACCESS
Articles are free to read for greatest visibility and readership

FAST PUBLICATION
Around 90 days from submission to decision

HIGH QUALITY PEER-REVIEW
Rigorous, collaborative, and constructive peer-review

TRANSPARENT PEER-REVIEW
Editors and reviewers acknowledged by name on published articles

Frontiers
Avenue du Tribunal-Fédéral 34
1005 Lausanne | Switzerland

Visit us: www.frontiersin.org
Contact us: frontiersin.org/about/contact

REPRODUCIBILITY OF RESEARCH
Support open data and methods to enhance research reproducibility

DIGITAL PUBLISHING
Articles designed for optimal readership across devices

FOLLOW US
@frontiersin

IMPACT METRICS
Advanced article metrics track visibility across digital media

EXTENSIVE PROMOTION
Marketing and promotion of impactful research

LOOP RESEARCH NETWORK
Our network increases your article's readership